

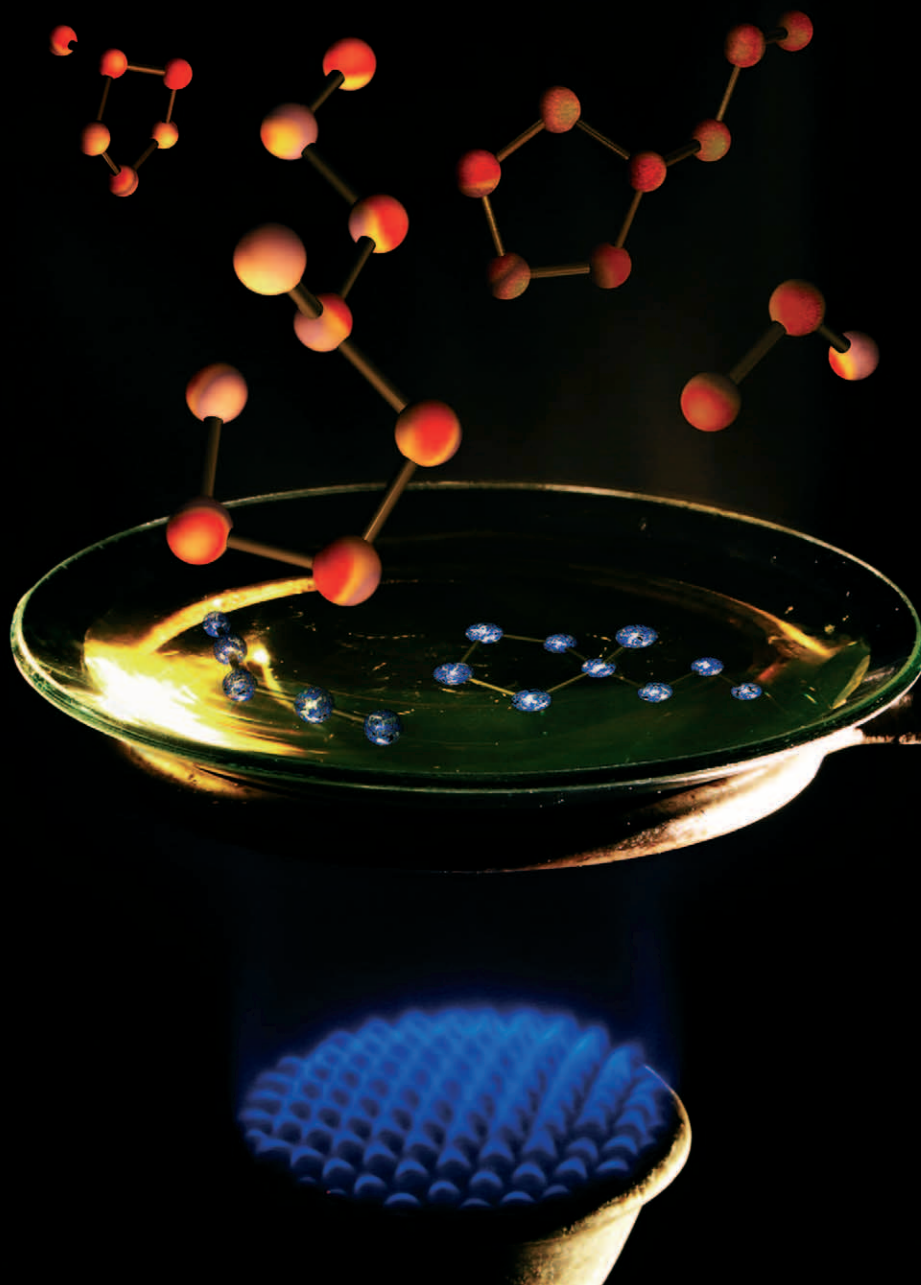
Green Chemistry

Cutting-edge research for a greener sustainable future

www.rsc.org/greenchem

Volume 8 | Number 8 | August 2006 | Pages 665–752

Downloaded on 07 November 2010
Published on 01 August 2006 on http://pubs.rsc.org | doi:10.1039/B610133J



ISSN 1463-9262

RSC Publishing

Wooster *et al.*
Thermal degradation of cyano
containing ionic liquids

Anastas *et al.*
Ten years of green chemistry at the
Gordon Research Conferences

Sloboda-Rozner and Neumann
Aqueous biphasic catalysis with
polyoxometalates

Guo *et al.*
L-Proline in an ionic liquid as an
efficient and reusable catalyst



1463-9262 (2006) 8:8;1-6



 Cambridge Healthtech Institute's Second Annual

PROCESS R&D SUMMIT

October 3-6, 2006

The Loews Philadelphia Hotel • Philadelphia, Pennsylvania

"Improving the Process"

Pre-Conference-Accelerated Tutorial

The Bu\$iness Value of Green Chemistry

October 3, 2006 • 1 - 5 PM

Co-Directed by



Presentations:

Green Chemistry: Designing Sustainability in at the Molecular Level

John C. Warner, Ph.D., Professor of Plastics Engineering and Community Health and Sustainability, Director, UML Center for Green Chemistry, University of Massachusetts Lowell

Development of a "Green" Manufacturing Process for Januvia

Feng Xu, Ph.D., Senior Investigator, Process Research, Merck & Co., Inc.

Interactive Participation

The Grass is Always Greener: Selecting Green Alternatives to Current Practices

Julie B. Manley, MPH, CHMM, Senior Industrial Coordinator, ACS Green Chemistry Institute

Green Chemistry is Good Bu\$iness: A Vice President's Perspective

Berkeley W. Cue, Jr., Ph.D., Private Consultant; Pfizer, Inc., Retired

Panel Discussion

Integrating Green Chemistry into the Bu\$iness of Process R&D

Conference Sessions

- ➔ Improving the Process
- ➔ Process Intensification
- ➔ Moving Toward a Greener Future
- ➔ Global Methodology and Sourcing
- ➔ Process Analytical Technology

Thursday, October 5, 2006

MOVING TOWARD A GREENER FUTURE SESSION Presentations Include:

Abbott's Green Scorecard Report

Christa A. Moster, B.S., Environmental Specialist, GPRD Environmental, Health and Safety, Abbott

Green Process Principles in Action: Taking a Complex Process and Making it Simpler through the Partnership between a Chemist and an Engineer: Part I

Alan Christensen, B.S., Chemist, Associate Research Chemist, Dept. R450, Abbott Labs

Green Process Principles in Action: Taking a Complex Process and Making it Simpler through a Partnership between a Chemist and an Engineer: Part II

Kimberley Allen, Ph.D., Chemical Engineer, Associate Research Investigator, Abbott Labs

Bristol-Myers Squibb - Process Greenness Scorecard

Stephan P. B. Taylor, Ph.D., Director - Learning, Training & Knowledge Systems, Process Research and Development, Bristol-Myers Squibb Pharmaceutical Research Institute

Assessing the "Greenness" of Processes: the GSK Experience

Concepcion 'Conchita' Jimenez-Gonzalez, Ph.D., Manager, Sustainable Processing and New Product Support; Environmental, Health & Safety Product Stewardship, GlaxoSmithKline

**Reference
Keycode U02A
when registering online**

www.ProcessSummit.com

Green Chemistry

Cutting-edge research for a greener sustainable future

www.rsc.org/greenchem

RSC Publishing is a not-for-profit publisher and a division of the Royal Society of Chemistry. Any surplus made is used to support charitable activities aimed at advancing the chemical sciences. Full details are available from www.rsc.org

IN THIS ISSUE

ISSN 1463-9262 CODEN GRCHFJ 8(8) 665–752 (2006)



Cover

Ionic liquids decompose, releasing volatile degradants, at lower temperatures than often implied and those containing dicyanamide anions form polymers during this process. Image reproduced by permission of Michael Clarke, Centre for Green Chemistry, Monash University, Australia, from *Green Chem.*, 2006, **8**(8), 691.

CHEMICAL TECHNOLOGY

T29

Chemical Technology highlights the latest applications and technological aspects of research across the chemical sciences.

Chemical Technology

August 2006/Volume 3/Issue 8

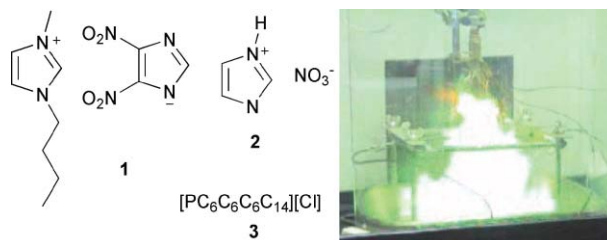
www.rsc.org/chemicaltechnology

HIGHLIGHT

675

Highlights

Markus Hölscher reviews some of the recent literature in green chemistry.



EDITORIAL STAFF

Editor

Sarah Ruthven

News writer

Markus Hölscher

Publishing assistant

Emma Hacking

Team leader, serials production

Stephen Wilkes

Administration coordinator

Sonya Spring

Editorial secretaries

Lynne Braybrook, Jill Segev, Julie Thompson

Publisher

Adrian Kybett

Green Chemistry (print: ISSN 1463-9262; electronic: ISSN 1463-9270) is published 12 times a year by the Royal Society of Chemistry, Thomas Graham House, Science Park, Milton Road, Cambridge, UK CB4 0WF.

All orders, with cheques made payable to the Royal Society of Chemistry, should be sent to RSC Distribution Services, c/o Portland Customer Services, Commerce Way, Colchester, Essex, UK CO2 8HP. Tel +44 (0) 1206 226050; E-mail sales@rscdistribution.org

2006 Annual (print + electronic) subscription price: £859; US\$1571. 2006 Annual (electronic) subscription price: £773; US\$1414. Customers in Canada will be subject to a surcharge to cover GST. Customers in the EU subscribing to the electronic version only will be charged VAT.

If you take an institutional subscription to any RSC journal you are entitled to free, site-wide web access to that journal. You can arrange access via Internet Protocol (IP) address at www.rsc.org/ip. Customers should make payments by cheque in sterling payable on a UK clearing bank or in US dollars payable on a US clearing bank. Periodicals postage paid at Rahway, NJ, USA and at additional mailing offices. Airfreight and mailing in the USA by Mercury Airfreight International Ltd., 365 Blair Road, Avenel, NJ 07001, USA.

US Postmaster: send address changes to Green Chemistry, c/o Mercury Airfreight International Ltd., 365 Blair Road, Avenel, NJ 07001. All despatches outside the UK by Consolidated Airfreight.

PRINTED IN THE UK

Advertisement sales: Tel +44 (0) 1223 432246; Fax +44 (0) 1223 426017; E-mail advertising@rsc.org

Green Chemistry

Cutting-edge research for a greener sustainable future

www.rsc.org/greenchem

Green Chemistry focuses on cutting-edge research that attempts to reduce the environmental impact of the chemical enterprise by developing a technology base that is inherently non-toxic to living things and the environment.

EDITORIAL BOARD

Chair

Professor Colin Raston,
Department of Chemistry
University of Western Australia
Perth, Australia
E-mail clraston@chem.uwa.edu.au

Dr Janet Scott, Centre for Green
Chemistry, Monash University,
Australia

Dr A Michael Warhurst,
University of Massachusetts,
USA
E-mail michael-warhurst@uml.edu

Professor Buxing Han, Chinese
Academy of Sciences
E-mail hanbx@iccas.ac.cn

Scientific editor

Professor Walter Leitner,
RWTH-Aachen, Germany
E-mail leitner@itmc.rwth-aachen.de

Professor Tom Welton,
Imperial College, UK

E-mail t.welton@ic.ac.uk
Professor Roshan Jachuck,
Clarkson University, USA

Associate editors

Professor C. J. Li, McGill
University, Canada
E-mail cj.li@mcgill.ca
Professor Kyoko Nozaki
Kyoto University, Japan
E-mail nozaki@chembio.tu-tokyo.ac.jp

E-mail rjachuck@clarkson.edu
Dr Paul Anastas, Green Chemistry
Institute, USA
E-mail p_anastas@acs.org

Members

Professor Joan Brennecke,
University of Notre Dame, USA
Professor Steve Howdle, University
of Nottingham, UK

INTERNATIONAL ADVISORY EDITORIAL BOARD

James Clark, York, UK
Avelino Corma, Universidad
Politécnica de Valencia, Spain
Mark Harmer, DuPont Central
R&D, USA
Herbert Hugl, Lanxess Fine
Chemicals, Germany
Makato Misono, Kogakuin
University, Japan
Robin D. Rogers, Centre for Green
Manufacturing, USA

Kenneth Seddon, Queen's
University, Belfast, UK
Roger Sheldon, Delft University of
Technology, The Netherlands
Gary Sheldrake, Queen's
University, Belfast, UK
Pietro Tundo, Università ca
Foscari di Venezia, Italy
Tracy Williamson, Environmental
Protection Agency, USA

INFORMATION FOR AUTHORS

Full details of how to submit material for publication in Green Chemistry are given in the Instructions for Authors (available from <http://www.rsc.org/authors>). Submissions should be sent via ReSource: <http://www.rsc.org/resource>.

Authors may reproduce/republish portions of their published contribution without seeking permission from the RSC, provided that any such republication is accompanied by an acknowledgement in the form: (Original citation) – Reproduced by permission of the Royal Society of Chemistry.

© The Royal Society of Chemistry 2006. Apart from fair dealing for the purposes of research or private study for non-commercial purposes, or criticism or review, as permitted under the Copyright, Designs and Patents Act 1988 and the Copyright and Related Rights Regulations 2003, this publication may only be reproduced, stored or transmitted, in any form or by any means, with the prior permission in writing of the Publishers or in the case of reprographic reproduction in accordance with the terms of

licences issued by the Copyright Licensing Agency in the UK. US copyright law is applicable to users in the USA.

The Royal Society of Chemistry takes reasonable care in the preparation of this publication but does not accept liability for the consequences of any errors or omissions.

Ⓢ The paper used in this publication meets the requirements of ANSI/NISO Z39.48-1992 (Permanence of Paper).

Royal Society of Chemistry: Registered Charity No. 207890

677

Ten years of green chemistry at the Gordon Research Conferences: frontiers of science

Paul Anastas, Romas Kazlauskas and Gary Sheldrake

Paul Anastas, Romas Kazlauskas and Gary Sheldrake look back at ten years of Green Chemistry Gordon Research Conferences, and look forward to this year's conference.



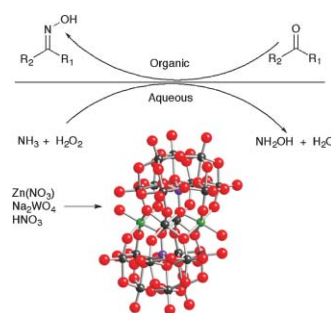
COMMUNICATIONS

679

Aqueous biphasic catalysis with polyoxometalates: Oximation of ketones and aldehydes with aqueous ammonia and hydrogen peroxide

Dorit Sloboda-Rozner and Ronny Neumann*

$\text{Na}_{12}[\text{WZn}_3(\text{H}_2\text{O})_2[\text{ZnW}_9\text{O}_{34}]_2]$, easily self assembled from Na_2WO_4 and $\text{Zn}(\text{NO}_3)_2$, catalyses the *in situ* oxidation of ammonia with hydrogen peroxide to hydroxylamine, which further reacts with ketones and aromatic aldehydes in an aqueous biphasic medium to yield oximes.

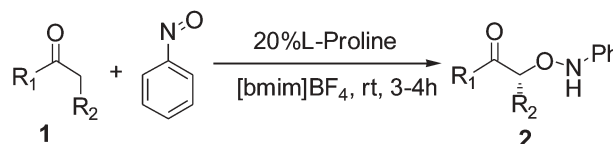


682

L-Proline in an ionic liquid as an efficient and reusable catalyst for direct asymmetric α -aminoxylation of aldehydes and ketones

Hai-Ming Guo, Hong-Ying Niu, Meng-Xia Xue, Qi-Xiang Guo, Lin-Feng Cun, Ai-Qiao Mi, Yao-Zhong Jiang* and Jian-Ji Wang*

Proline-catalyzed direct asymmetric α -aminoxylation of aldehydes and ketones in the room temperature ionic liquid 1-*n*-butyl-3-methylimidazolium tetrafluoroborate achieved high yields and high enantioselectivities.

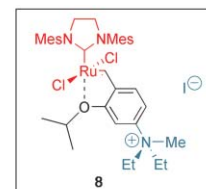
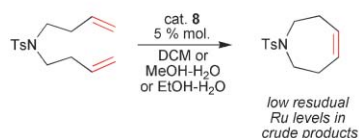


685

A green catalyst for green chemistry: Synthesis and application of an olefin metathesis catalyst bearing a quaternary ammonium group

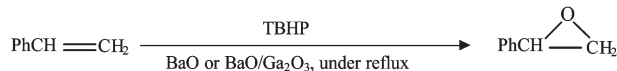
Anna Michrowska, Łukasz Gułajski, Zuzanna Kaczmarek, Klaas Mennecke, Andreas Kirschning and Karol Grela*

The novel catalyst **8**, bearing a polar quaternary ammonium group, is very stable, can be easily prepared from commercially available reagents, and can be efficiently used for olefin metathesis in both traditional and aqueous media.



COMMUNICATIONS

689



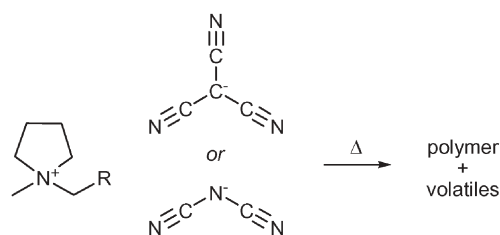
Epoxidation of styrene by TBHP to styrene oxide using barium oxide as a highly active/selective and reusable solid catalyst

Vasant R. Choudhary,* Rani Jha and Prabhas Jana

Styrene oxide can be produced in high yields by the epoxidation of styrene by tertiary butylhydroperoxide using a simple, inexpensive and environmentally friendly (easily separable, reusable and non-toxic) BaO catalyst.

PAPERS

691

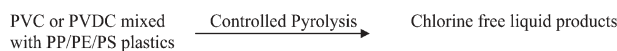


Thermal degradation of cyano containing ionic liquids

Tim J. Wooster, Katarina M. Johanson, Kevin J. Fraser, Douglas R. MacFarlane and Janet L. Scott*

The long term thermal stability of ionic liquids containing dicyanamide or tricyanomethide anions is significantly lower than might be expected from temperature ramped TGA studies, and these anions, combined with N-based cations, yield polymeric products during thermal decomposition.

697

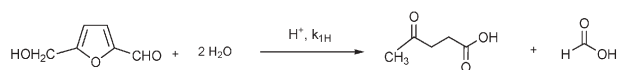


Prevention of chlorinated hydrocarbons formation during pyrolysis of PVC or PVDC mixed plastics

Thallada Bhaskar,* Rie Negoro, Akinori Muto and Yusaku Sakata

We report for the first time, the controlled pyrolysis of PVC or PVDC plastics mixed with PP/PE/PS to produce chlorine free liquid products in the absence of dechlorination catalyst/sorbent.

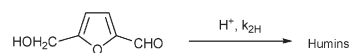
701



A kinetic study on the decomposition of 5-hydroxymethylfurfural into levulinic acid

B. Girisuta, L. P. B. M. Janssen and H. J. Heeres*

This study describes an in-depth experimental and modelling study on the acid catalysed decomposition of 5-hydroxymethylfurfural into levulinic acid. The results are applied to gain insights into the optimum process conditions for this conversion.

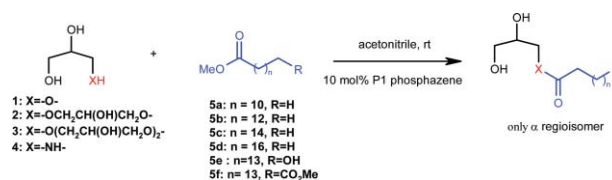


710

Facile and regioselective mono- or diesterification of glycerol derivatives over recyclable phosphazene organocatalyst

Ghizlane Kharchafi, François Jérôme,* Jean-Paul Douliez and Joël Barrault

A facile and selective method for the mono- and diesterification of glycerol and its derivatives using a recyclable phosphazene catalyst is presented.

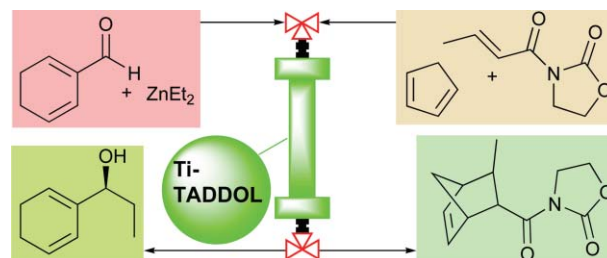


717

Functional monolithic resins for the development of enantioselective versatile catalytic minireactors with long-term stability: TADDOL supported systems

Belen Altava,* M. Isabel Burguete,* Eduardo García-Verdugo, Santiago V. Luis* and Maria J. Vicent

Polymeric Ti-TADDOLates prepared as monoliths show remarkable long-term stability and can be used sequentially for different reactions.

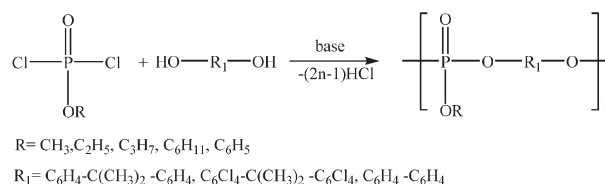


727

Solvent and catalyst-free synthesis of polyphosphates

Smaranda Iliescu, Gheorghe Iliu,* Nicoleta Plesu, Adriana Popa and Aurelia Pascariu

Polyphosphates were synthesised using a solvent and catalyst-free gas-liquid interfacial polycondensation between alkyl(aryl)phosphoric dichlorides and aromatic diols.

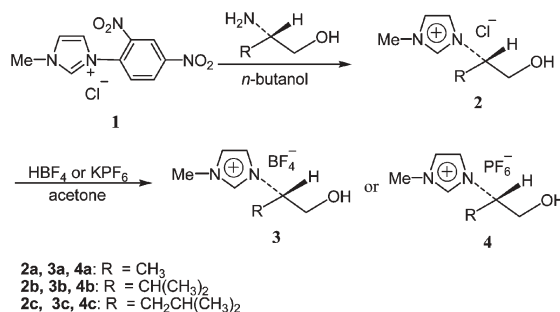


731

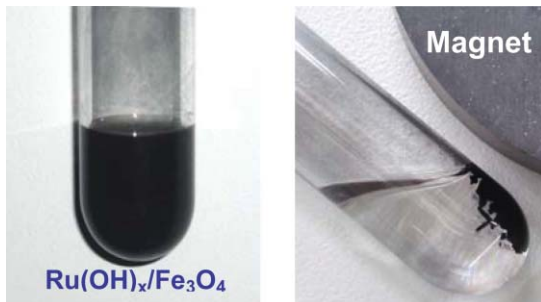
An efficient and practical synthesis of chiral imidazolium ionic liquids and their application in an enantioselective Michael reaction

Wen-Hua Ou and Zhi-Zhen Huang*

We have developed a practical and efficient synthesis of chiral imidazolium ionic liquids by only two or three steps from cheap *N*-methyl imidazole with 67–81% overall yields.



735

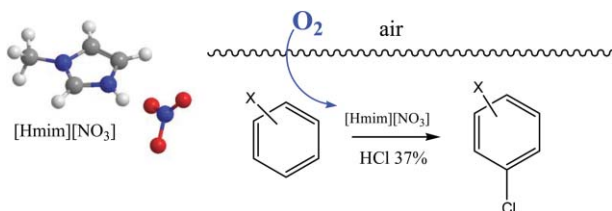


Ruthenium hydroxide on magnetite as a magnetically separable heterogeneous catalyst for liquid-phase oxidation and reduction

Miyuki Kotani, Takeshi Koike, Kazuya Yamaguchi and Noritaka Mizuno*

Ruthenium hydroxide on magnetite ($\text{Ru}(\text{OH})_x/\text{Fe}_3\text{O}_4$) could act as a magnetically separable heterogeneous catalyst for the aerobic oxidation of alcohols and amines, and reduction of carbonyl compounds with 2-propanol.

742

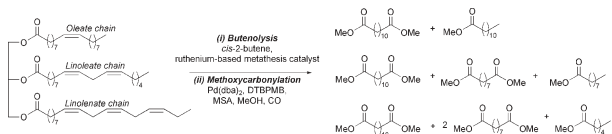


[Hmim][NO₃]*—*an efficient solvent and promoter in the oxidative aromatic chlorination

Cinzia Chiappe,* Elsa Leandri and Marianna Tebano

Brønsted acidic ionic liquid [Hmim][NO₃] has been used as a cosolvent and “promoter” for oxidative halogenation of aromatic compounds with aqueous halohydric acids.

746



Preparation of terminal oxygenates from renewable natural oils by a one-pot metathesis–isomerisation–methoxycarbonylation–transesterification reaction sequence

Yulei Zhu, Jim Patel, Selma Mujcinovic, W. Roy Jackson* and Andrea J. Robinson

Renewable natural oils can be converted into potentially high value terminal oxygenates by a single-pot, high yielding one-pot metathesis–isomerisation–methoxycarbonylation–transesterification reaction sequence.

AUTHOR INDEX

- Altava, Belen, 717
 Anastas, Paul, 677
 Barrault, Joël, 710
 Bhaskar, Thallada, 697
 Burguete, M. Isabel, 717
 Chiappe, Cinzia, 742
 Choudhary, Vasant R., 689
 Cun, Lin-Feng, 682
 Douliez, Jean-Paul, 710
 Fraser, Kevin J., 691
 Garcia-Verdugo, Eduardo, 717
 Girisuta, B., 701
 Grell, Karol, 685
 Gułajski, Lukasz, 685
 Guo, Hai-Ming, 682
 Guo, Qi-Xiang, 682
- Heeres, H. J., 701
 Huang, Zhi-Zhen, 731
 Ilija, Gheorghe, 727
 Iliescu, Smaranda, 727
 Jackson, W. Roy, 746
 Jana, Prabhas, 689
 Janssen, L. P. B. M., 701
 Jérôme, François, 710
 Jha, Rani, 689
 Jiang, Yao-Zhong, 682
 Johanson, Katarina M., 691
 Kaczmarek, Zuzanna, 685
 Kazlauskas, Romas, 677
 Kharchafi, Ghizlane, 710
 Kirschning, Andreas, 685
 Koike, Takeshi, 735
- Kotani, Miyuki, 735
 Leandri, Elsa, 742
 Luis, Santiago V., 717
 MacFarlane, Douglas R., 691
 Mennecke, Klaas, 685
 Mi, Ai-Qiao, 682
 Michrowska, Anna, 685
 Mizuno, Noritaka, 735
 Mujcinovic, Selma, 746
 Muto, Akinori, 697
 Negoro, Rie, 697
 Neumann, Ronny, 679
 Niu, Hong-Ying, 682
 Ou, Wen-Hua, 731
 Pascariu, Aurelia, 727
 Patel, Jim, 746
- Plesu, Nicoleta, 727
 Popa, Adriana, 727
 Robinson, Andrea J., 746
 Sakata, Yusaku, 697
 Scott, Janet L., 691
 Sheldrake, Gary, 677
 Sloboda-Rozner, Dorit, 679
 Tebano, Marianna, 742
 Vicent, Maria J., 717
 Wang, Jian-Ji, 682
 Wooster, Tim J., 691
 Xue, Meng-Xia, 682
 Yamaguchi, Kazuya, 735
 Zhu, Yulei, 746

FREE E-MAIL ALERTS AND RSS FEEDS


Contents lists in advance of publication are available on the web via www.rsc.org/greenchem - or take advantage of our free e-mail alerting service (www.rsc.org/ej_alert) to receive notification each time a new list becomes available.

RSS Try our RSS feeds for up-to-the-minute news of the latest research. By setting up RSS feeds, preferably using feed reader software, you can be alerted to the latest Advance Articles published on the RSC web site. Visit www.rsc.org/publishing/technology/rss.asp for details.

ADVANCE ARTICLES AND ELECTRONIC JOURNAL

Free site-wide access to Advance Articles and the electronic form of this journal is provided with a full-rate institutional subscription. See www.rsc.org/ejs for more information.

* Indicates the author for correspondence: see article for details.

 Electronic supplementary information (ESI) is available via the online article (see <http://www.rsc.org/esi> for general information about ESI).

RENEWABLE RESOURCES & BIOREFINERIES CONFERENCE

6th-8th SEPTEMBER, 2006

THE UNIVERSITY of York

www.rrbconference.net

A major international conference at the University of York, focusing on renewable energy and chemicals from biomass.

CONFIRMED KEYNOTE SPEAKERS:

**Right Honourable
Michael Meacher MP**
Former Environment Minister

Dr Gerhard Isenberg
former Head of Energy Strategy
for Daimler Chrysler

Dr Wiktor Raldow
Head of the New and Renewable
Energy Sources Unit for
the European Commission

Dr John Pierce
Director of Biochemical Sciences
and Engineering, Dupont, USA

Dr Uma Shaanker
University of Agricultural Sciences,
Bangalore, India

Dr Hosein Shapouri
USDA

Professor Charles Perrings
Arizona State University

Dr-Ing Andreas Schutte
Agency for Renewable
Resources (FNR) Germany



"What sets this conference apart is the wide-ranging but cohesive blend of experts it will bring together, encompassing the disciplines of chemistry, engineering, biology, environmental studies, economics and social policy.

It is an opportunity to discover more about the latest innovations and the capabilities of science needed to switch to renewable resources."

Professor James Clark, University of York Green Chemistry Centre

Conference Themes:

- Biofuels & Bio-energy
 - Green Chemistry / Platform Molecules
 - Biopolymers / Biomaterials
 - Investment & End Users Perspective
 - European Policy & Socio-Economic Issues
 - Biocatalysis
 - Bioresources
 - Fermentation & Metabolic Engineering
 - Chemical Products
- Extensive opportunities for poster and exhibition viewing
 - Informal discussion and networking, including a gala conference dinner



WHO SHOULD ATTEND?

Senior academics, industrialists and policy makers with an interest in the latest developments in Green Chemistry innovation.

Register now www.rrbconference.net



In association with
University of Ghent

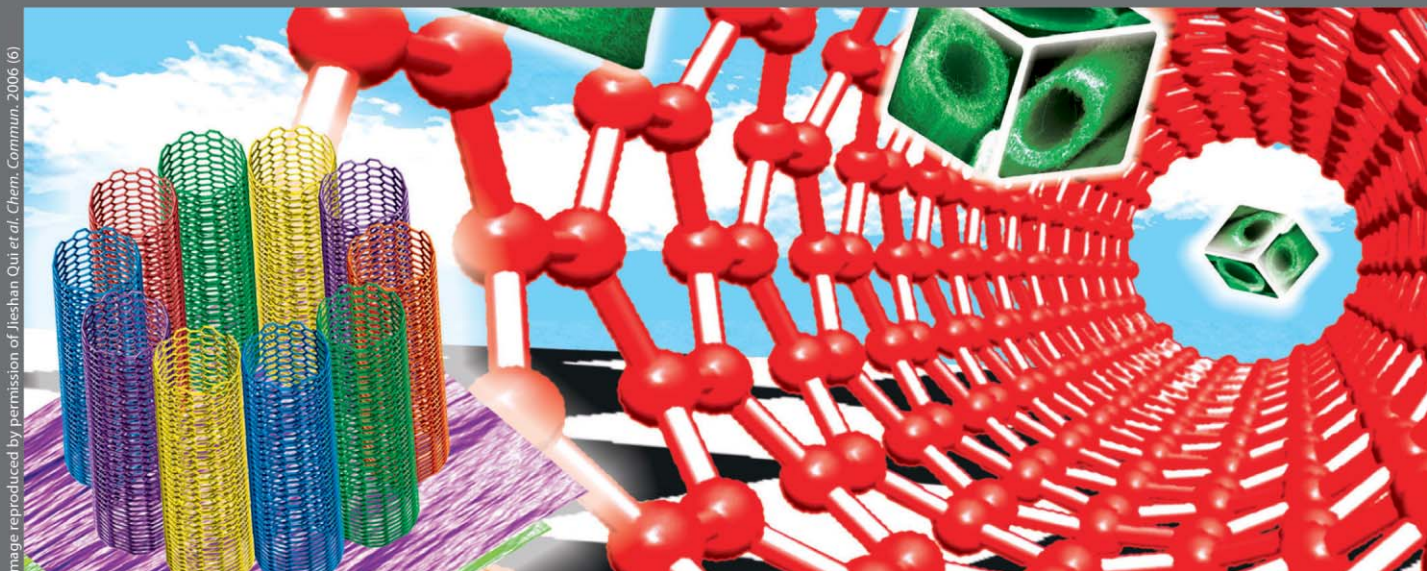


Image reproduced by permission of Jiehan Qui et al., Chem. Commun., 2006 (6)

08060512

ChemComm

A leading international journal for the publication of communications on important new developments in the chemical sciences.

- Weekly publication
- Impact factor: 4.426
- Rapid publication – typically 60 days
- 3 page communications – providing authors with the flexibility to develop their results and discussion
- More than 40 years publishing excellent research
- High visibility – indexed in MEDLINE



RSC Publishing

www.rsc.org/chemcomm

Highlights

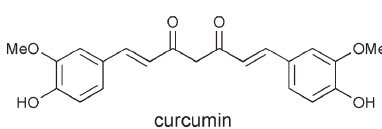
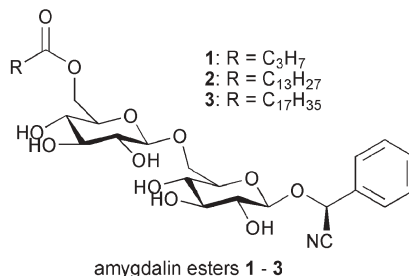
DOI: 10.1039/b609430a

Markus Hölscher reviews some of the recent literature in green chemistry.

Novel hydrogelators for controlled, enzyme-catalyzed drug release

The usage of renewable resources in white biotechnology contributes increasingly to a sustainable economy, and nano-engineering is an important field in this context, as new building blocks can be generated for a multitude of purposes. John *et al.* (City College of New York and The City University of New York) presented an interesting approach for novel drug carriers which are put together by self assembly processes and are later degraded by enzyme catalysis.¹ The authors reasoned that D-amygdalin, which is a natural glycoside, could be a building block in novel hydrogelators for the formation of nanoaggregates thermally and chemically stable enough to be useful for the encapsulation of drugs. For the formation of self assembled hydrogels the introduction of long fatty acid chains is necessary, which was accomplished by esterification of the primary hydroxy group of amygdalin generating compounds **1–3**. These were found to form hydrogels by intra- and intermolecular hydrogen bonding and π -stacking in numerous solvents with gel-to-solution temperatures between 40 and 85 °C. In the second step of the study, curcumin, which is a strong anti-oxidative and anti-inflammatory drug, was encapsulated into the hydrogels and drug release was studied by degrading the hydrogel by enzyme catalysis.

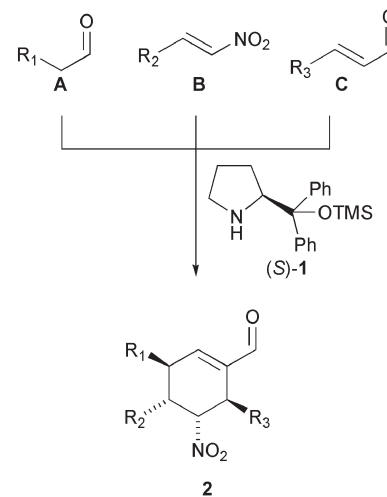
The release of curcumin was studied by UV spectroscopy and unequivocally showed that hydrolase (Lipolase 100 L, type EX) broke the ester linkage and thus destroyed the hydrogel. As a result the drug was released into the solution. These findings open new routes for designed drug encapsulation and transportation followed by controlled drug release, and as such should stimulate material and medicinal sciences.



Three new C–C bonds and four stereocenters in one organocatalytic reaction cascade

C–C bond forming reactions are among the most important and challenging chemical transformations, especially with regard to diastereoselectivity and enantioselectivity. While the typical procedure for creating molecules consists of a stepwise build up with one chemical transformation at a time, cascade reactions generating a multitude of bond forming events mediated by only one catalyst are both extremely efficient and challenging, as many different stereoisomers become available. The careful choice of reactants, catalyst and reaction conditions can aid in setting up highly selective processes, which was successfully demonstrated very recently by Enders *et al.* from RWTH Aachen university.²

The authors reasoned that a chiral secondary amine would be a useful catalyst for enamine and iminium catalysis. If reactants with the appropriate reactivity were chosen, a reaction cascade should be initiated in which C–C bonds are formed in the correct sequence and in selective manner. Indeed, it was possible to observe this reaction sequence experimentally. By reacting a linear aldehyde (**A**) with a nitroalkene (**B**) followed by



reaction with an α,β -unsaturated aldehyde (**C**) in the presence of chiral secondary amine catalyst (*S*)-**1**, product **2** was obtained enantioselectively. Usage of catalyst (*R*)-**1** accordingly generated *ent*-**2**. Only 2 of the 16 theoretically possible stereoisomers were generated, rendering this reaction cascade highly stereoselective. This is an excellent proof that chemists can imitate the complexity of nature's way of synthesizing molecules.

Increased hydrogen storage capacity in metal-organic frameworks by designed use of spillover

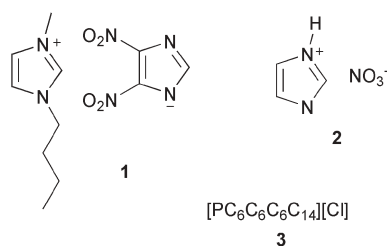
Researchers are trying to meet the targets for hydrogen storage capacity set up by the U.S. Department of Energy. The anticipated figures for onboard storage systems are 4.5 wt% by 2007, 6 wt% by 2010 and 9 wt% by 2015. The reasons are clear: clean burning processes generate only water as the end product, making the combustion of H₂ a lot more sustainable than the use of carbon based fuels. Though many efforts have already been made, hydrogen storage capacities of different kinds of materials have not really been convincing. However, a novel strategy, developed by Yang *et al.* from the University of Michigan, comes

significantly closer to the desired values.³ The underlying concept is the idea that secondary spillover in hydrogen storage materials consisting of a metal and a support can be used to increase the storage capacity. Spillover is the dissociative chemisorption of hydrogen on the metal and the subsequent migration of atomic hydrogen onto the surface of the support. Secondary spillover is the migration to a secondary material. If different materials were used and physical linkages between them were made, the secondary spillover should be accomplished more easily, and secondary materials should be usable which themselves would not induce spillover. Accordingly the authors used metal-organic frameworks (MOF) and combined them with a metal on activated carbon as the matrix. Simple mixing is good, but even better is the establishment of carbon bridges between the materials by carbonizing sucrose. At first the mixture is heated to 473 K to melt the sucrose, ensuring a thorough distribution of the carbohydrate and filling of the interstitial space. Subsequently the mixture was heated to 523 K resulting in the carbonization of sucrose leaving a material in which the metal-activated carbon material is physically linked to the MOF. Adsorption experiments with materials obtained from different $[\text{Zn}_4\text{O}]^{6+}$ -cluster based MOFs showed remarkably enhanced hydrogen storage capacity, reaching values as high as 4 wt% at a temperature of 298 K and a pressure of 10 MPa. According to detailed structural analyses, the estimated capacity at 15 MPa should be in the range of 6 wt%, which would meet the requirements fairly well, as pressures in the range of 15 MPa are viable for practical automotive applications.

Laboratory safety of ionic liquids

Due to their unique physicochemical properties ionic liquids (ILs) have gained an enormous interest over the past years for a variety of applications. In chemistry the most important field is the usage of ILs as non volatile solvents, which—as conventional wisdom suggests—are safe solvents with comparatively low

tendency to ignite and burn. Rogers *et al.* from the University of Alabama and Wilkes from the United States Air Force Academy inspected the behaviour of 20 ILs with respect to combustibility, and undertook calorimetric measurements as well as ignition experiments.⁴ As a first trial, all 20 ILs were heated with a torch flame for 5 to 7 s and every single IL ignited under these conditions. Some ILs burned only shortly while others burned to complete or nearly complete combustion. Nitro groups seem to enhance burning rates, with IL **1** burning most rapidly. In a set of calorimetric experiments it was found that IL **2**, and others, develop explosive potential when they were heated above a certain temperature. Interestingly commercially available IL **3** (Cyphos[®]), which was not thought to be energetic, can be ignited when present as a spray in air.



When a fine spray of **3** got in contact with an electrically heated nickel-chromium wire this IL, and others, ignite readily. In the case of Cyphos[®], the authors suspect the impurities (5 to 7%) to be responsible for the ignition. Furthermore, caution was especially recommended when ILs are dried to completeness, as the condition of dryness may influence their shock and friction sensitivities. As a result, the ignition and combustion behaviour of ILs should be carefully evaluated from case to case.

2006 Presidential Green Chemistry Challenge Award

The U.S. Environmental Protection Agency (EPA) awarded the 2006 Presidential Green Chemistry Challenge Award in Washington D.C. on June 26, 2006 to selected individuals and organizations that have made innovative science contributions with identifiable applications that result in less pollution

or waste. Five categories were recognized this year: Academic Award, Small Business Award, Greener Synthetic Pathways Award, Greener Reaction Conditions Award and Designing Greener Chemicals Award. Galen J. Suppes from the Department of Chemical Engineering, University of Missouri–Columbia won the Academic Award for the development of an inexpensive method for the conversion of glycerine to propylene glycol, which can be used as a replacement for ethylene glycol in automotive antifreezers. The Small Business Award went to Arkon Consultants and NuPro Technologies, Inc. for the development of a safer chemical processing system for flexographic printing, in which the millions of gallons of hazardous solvents are avoided. The Greener Synthetic Pathways Award was presented to Merck & Co., Inc. for the discovery of a highly innovative and efficient synthesis of sitagliptin, which is the active ingredient in Januvia[™], the company's new treatment for type 2 diabetes. The new synthesis route generates 220 pounds less waste per pound of product, while the overall chemical yield is increased to 50%. In the product's lifetime Merck estimates an avoidance of 330 million pounds of waste, including 110 million pounds of aqueous waste. The Greener Reaction Conditions award was given to Codexis, Inc. for a novel enzyme-based process which significantly improves the manufacture of the key building block for Lipitor[®], which is a best-selling cholesterol lowering drug. The Designing Greener Chemicals Award was awarded to S. C. Johnson & Son, Inc. for Greenlist[™], which is a system that rates the environmental and health effects of S. C. Johnson's products.

References

- 1 P. K. Vemula, J. Li and G. John, *J. Am. Chem. Soc.*, 2006, DOI: 10.1021/ja062650u.
- 2 D. Enders, M. R. M. Hüttl, C. Grondal and G. Raabe, *Nature*, 2006, **441**, 861–863.
- 3 Y. Li and R. T. Yang, *J. Am. Chem. Soc.*, 2006, **128**, 8136–8137.
- 4 M. Smiglak, W. M. Reichert, J. D. Holbrey, J. S. Wilkes, L. Sun, J. S. Thrasher, K. Kirichenko, S. Singh, A. R. Katritzky and R. D. Rogers, *Chem. Commun.*, 2006, 2554–2556.

Ten years of green chemistry at the Gordon Research Conferences: frontiers of science

Paul Anastas,^a Romas Kazlauskas^b and Gary Sheldrake^c

DOI: 10.1039/b608918f

The 2006 Green Chemistry Gordon Research Conference will mark the 10th anniversary of Green Chemistry GRCs. The GRC format, with its strong emphasis on discussion and interaction, has been especially suited to green chemistry which, more than most areas of chemistry research, depends on true interdisciplinarity for success. The ingenuity and innovation displayed by the green chemistry community in developing solutions to real manufacturing problems has been breathtaking. This success has been mirrored in the ten years of the Green Chemistry GRCs, and the 2006 conference will provide a glimpse at how green chemistry will develop over the next ten years.

Gordon Research Conferences (GRCs) differ from most other scientific conferences in three key ways: their informal environment, their emphasis on discussion and their focus on the cutting edge of science. The GRC format, with its strong emphasis on discussion and interaction, has been especially suited to green chemistry which, more than most areas of chemistry research, depends on true interdisciplinarity for success. At no other GRC would you find participants including synthetic, physical and theoretical chemists, chemical engineers, microbiologists and biochemists, all with equal contributions to one field of research and enthused by new opportunities to apply their expertise.

Green chemistry has its roots in the feelings of environmental responsibility that arose in both the industrial and academic chemical communities in the 1980s following the high public profile of human and environmental tragedies, such as Minamata Bay, Love Canal, Seveso and Bhopal. The discovery that materials produced “by chemists” could deplete the ozone layer and affect the global environment started the decline in public confidence in chemistry. The first response was techniques for the analysis

and remediation of chemical contamination and end-of-pipe waste treatment strategies for containing pollution. The second and only acceptable long term solution for sustainable chemical manufacturing was pollution prevention, which sowed the seeds of the green chemistry community.

The Green Chemistry Gordon Conference was a natural next step in the growth of green chemistry in 1996. There had been numerous symposia and seminars in green chemistry since the inception of the Green Chemistry Program at the U.S. EPA in 1991 in venues such as the American Chemical Society's National Meetings. The founding chair of the conference Paul Anastas recognized that a meeting focused on the cutting edge science of green chemistry, rather than the more general discussions that often blend the science, technology, application, and implementation of green chemistry, was necessary and submitted a proposal to the Gordon Research Conferences in 1994 which was accepted to be held in 1996. At the conclusion of the first conference in 1996, it was deemed to be so successful that the Gordon Research Conferences approached the organizers about doing one of the first Gordon Conferences in the new site at Oxford University the following year. Vice-Chair Stephen DeVito agreed to chair the second, equally successful, Green Chemistry Gordon Conference.

A sample of the speakers at the inaugural conference reads like a *Who's Who* of green chemistry over the last

decade: Barry Trost, Ronald Breslow, Terry Collins, John Frost, John Warner, Barry Sharpless, Pietro Tundo were all there. Over the ten years almost every major international name in green chemistry has presented at the Green Chemistry GRCs. The topics covered in the 1996 conference focused on organic chemistry and featured the topics of atom economy, cleaner oxidations, water-based organic transformations, heterogeneous catalysis and biocatalysis. Most presentations focused on improving existing processes by the development of catalysts with improved selectivity, movement from stoichiometric to catalytic procedures, the elimination of toxic reagents and transfer of processes from organic solvents to water.

Later Green Chemistry GRCs continued some of these topics, and new areas were developed. For example, cleaner oxidation has received much attention and generated individual successes, but remains one the most challenging problems for large scale processes. Solid phase chemistry has developed from a handful of polymer- and clay-supported reagents and catalysts in the early 1990s to a wide availability of organic, inorganic and composite supports, leading to automated syntheses and combinatorial libraries. The field of ionic liquids, notwithstanding the ongoing debate about their “green credentials”, has developed from a laboratory curiosity to one of the most intensely studied class of materials, which offer almost limitless

^aGreen Chemistry Institute, Washington D.C., USA

^bDepartment of Biochemistry, Molecular Biology and Biophysics, University of Minnesota, Twin Cities, St. Paul, MN, USA

^cThe Queen's University of Belfast, School of Chemistry, David Keir Building, Belfast, Northern Ireland, United Kingdom BT9 5AG

potential for novel and cleaner chemical processes. There has been a similar explosion in interest in supercritical fluids, which have found applications as diverse as fine chemical manufacture, chromatography, biomedical science, mineralization of waste and even dry cleaning.

Key events that have raised the profile of green chemistry over this last decade have included the launch of Green Chemistry journal in 1999; the establishment of the Green Chemistry Institute in the US, the Green Chemistry Network in the UK and many similar organizations around the globe; the Presidential Green Chemistry Challenge Awards (US), the Green Chemical Technology Awards in the UK, and equivalent schemes elsewhere. Apart from the exponential growth in international green chemistry conferences, the community has also established many workshops and produced text books and educational material suitable for all ages, to spread the message to the next generation of chemists and engineers.

One of the more remarkable aspects of the Green Chemistry Gordon Conference is the frequency with which cross-disciplinary collaborations have been built over the past decade. Because green chemistry cuts across the many sub-disciplines of chemistry, it is not unusual for a polymer chemist at the Green Chemistry Gordon Conference to discuss with a catalysis chemist, also there, how a catalyst might be modified so it can be used in the supercritical carbon dioxide

medium just described by a third chemist at the conference; or for interactions between biochemists working with enzymes to discover the possibility of using ionic liquids for their transformations, and other numerous interactions like this. The ingenuity and innovation displayed by the green chemistry community in developing solutions to real manufacturing problems has been breathtaking. Anyone doubting the scale of what has been achieved needs to look no further than the list of Presidential Green Chemistry Challenge Award winners, the successful implementation of industrial processes using supercritical fluids and ionic liquids or the vast array of new heterogeneous, homogeneous and bio-catalysts now available to the manufacturing community. The rate at which these ideas have been transferred from laboratory to plant is a testament to the interdisciplinary nature of green chemistry research. It is one of the few branches of genuine “blue skies” chemical research, where process chemists and engineers are often involved from the beginning and “invention” moves seamlessly into “application”.

How will green chemistry develop over the next ten years? The 2006 Green Chemistry GRC will provide a glimpse. The theme of the conference—Cradle to Grave—will focus on the multifaceted nature of any environmental assessment. The current global threats posed by rising greenhouse gas emissions and dwindling fossil fuel resources will set

the agenda for radically new approaches to sustainability in energy generation, product design and manufacturing processes. As green chemistry looks to the future the fundamental scientific challenges facing the field could include:

- the design protocol for molecular structures that are inherently less hazardous to human health and the environment;
- the integration of material and energy systems for the synthesis and isolation of new molecules;
- a molecular level understanding of the nature of chemical synergism in the body and the biosphere;
- a deep and rigorous investigation of the manifestation of chemical endocrine disruption;
- design of chemical systems that possess the intrinsic ability to resist perturbations that could cause accidents, performance failure or toxicity (resilience);
- using weak intermolecular forces able to impart performance;
- design of solvents and systems in which external stimuli (*e.g.* heat, light) can change physical properties.

The 2006 Green Chemistry GRC will be at Magdalen College, Oxford from 27th August to 1st September. To find out more, see the programme at <http://kazlauskas.cbs.umn.edu/GreenChem06.html>, and follow the links to the GRC application and registration pages to participate in the debate on the current and future direction of Green Chemistry.

Aqueous biphasic catalysis with polyoxometalates: Oximation of ketones and aldehydes with aqueous ammonia and hydrogen peroxide†

Dorit Sloboda-Rozner and Ronny Neumann*

Received 4th April 2006, Accepted 19th June 2006

First published as an Advance Article on the web 26th June 2006

DOI: 10.1039/b604837d

$\text{Na}_{12}[\text{WZn}_3(\text{H}_2\text{O})_2[\text{ZnW}_9\text{O}_{34}]_2]$, easily self assembled from Na_2WO_4 and $\text{Zn}(\text{NO}_3)_2$, catalyses the *in situ* oxidation of ammonia with hydrogen peroxide to hydroxylamine, which further reacts with ketones and aromatic aldehydes in an aqueous biphasic medium without organic solvent to yield oximes as valuable intermediates.

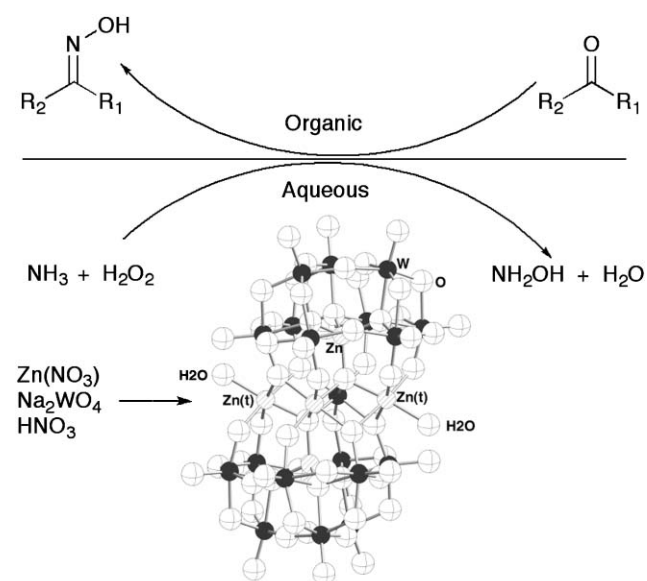
The reaction of ketones and aldehydes with hydroxylamine to obtain oximes as intermediates, that can be either dehydrated to nitriles or undergo an acid catalyzed Beckmann rearrangement to obtain amides, is a valuable synthetic tool. This methodology is also applied industrially on a large scale for the production of ϵ -caprolactam from cyclohexanone. From a safety point of view the use of hydroxylamine appears to be quite dangerous; two severe accidents, both involving loss of life, have occurred during the last decade.¹ In order to reduce safety hazards, hydroxylamine is often used as a salt, $(\text{NH}_2\text{OH})_x \cdot \text{H}_x\text{B}$ where B = sulfate, phosphate, nitrate, chloride and so forth, or as $\text{NH}_2\text{OSO}_3\text{H}$ by reaction of hydroxylamine with chlorosulfonic acid. Thus, the use of hydroxylamine in the form of $(\text{NH}_2\text{OH})_x \cdot \text{H}_x\text{B}$ or $\text{NH}_2\text{OSO}_3\text{H}$ introduces salts as by-products into oximation reactions. Note also that HCl is formed in the synthesis of $\text{NH}_2\text{OSO}_3\text{H}$. The formation of unneeded salts and safety concerns, especially at higher concentrations in processes involving the use of hydroxylamine, raises the need for waste free and *in situ* synthesis of NH_2OH . Oxidation of ammonia with dioxygen is one option, however, the selectivity observed in such reactions has been limited.² On the other hand the use of titanium oxide incorporated in silica based heterogeneous catalysts for formation of hydroxylamine from ammonia and aqueous hydrogen peroxide and further *in situ* oximation have been quite successful.³ Recently there have also been reports on the integration of the hydrogen peroxide synthesis step into the ammonia oxidation to hydroxylamine.⁴

Recently we have realized the concept of aqueous biphasic catalysis with a self-assembled water soluble polyoxometalate.⁵ Thus, the $\text{Na}_{12}[\text{WZn}_3(\text{H}_2\text{O})_2[\text{ZnW}_9\text{O}_{34}]_2]$ polyoxometalate in water has been shown to catalyse the aqueous biphasic oxidation of various substrates, such as secondary alcohols to ketones, primary alcohols to carboxylic acids, pyridine derivatives to the corresponding *N*-oxides and the carbon-carbon bond cleavage of vicinal diols.⁵ These aqueous biphasic reactions have the advantage of allowing *in situ* synthesis of the catalyst from simple starting

materials, easy separation of the water insoluble product from the aqueous catalyst mixture by phase separation and finally advantageous reuse of the catalyst containing aqueous phase for additional catalytic cycles.

In this paper we extend the concept of aqueous biphasic catalysis with a self-assembled $\text{Na}_{12}[\text{WZn}_3(\text{H}_2\text{O})_2[\text{ZnW}_9\text{O}_{34}]_2]$ polyoxometalate catalyst to an oximation reaction, Scheme 1. An aqueous solution of ammonia and hydrogen peroxide reacts in the presence of $\text{Na}_{12}[\text{WZn}_3(\text{H}_2\text{O})_2[\text{ZnW}_9\text{O}_{34}]_2]$ to yield hydroxylamine. Hydroxylamine then further reacts *in situ* by nucleophilic substitution with the water insoluble ketone or aldehyde at the water/substrate interphase to yield the corresponding oxime.⁶ Further acid catalyzed reactions include Beckmann rearrangement to the amide or dehydration of the (primary) oxime to yield nitriles, Scheme 2.

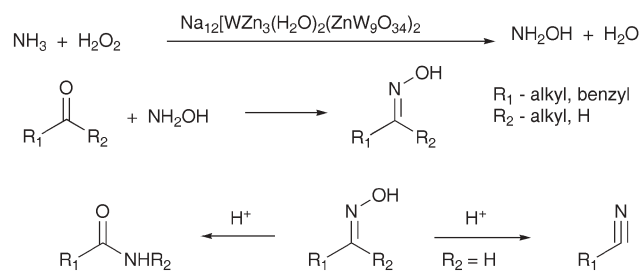
The results for ammoxidation of some exemplary substrates are presented in Table 1. Several trends may be noted. First, ketones reacted to give only oximes as products, with no further Beckmann rearrangement to yield amides. The reactivity of the ketones was more or less as expected, with the reactivity of cyclic aliphatic ketones > acyclic aliphatic ketones > aromatic ketones. Similar to what was observed previously in alcohol oxidation in biphasic media, the more hydrophobic substrates tended to react less efficiently,⁵ presumably due to poorer contact at the interface



Scheme 1 Generalized picture for the aqueous biphasic oxidation of organic substrates with H_2O_2 catalyzed by $\text{Na}_{12}[(\text{WZn}_3(\text{H}_2\text{O})_2)[(\text{ZnW}_9\text{O}_{34})_2]]$.

Department of Organic Chemistry, Weizmann Institute of Science, Rehovot, 76100, Israel. E-mail: Ronny.Neumann@weizmann.ac.il; Fax: +972-8-934335; Tel: +972-8-9344142

† Electronic supplementary information (ESI) available: Description of experimental methods. See DOI: 10.1039/b604837d



Scheme 2 Reaction pathway for oximation and further Beckmann rearrangement or dehydration.

Table 1 Oxidation of ketones/aldehydes using ammonia and H_2O_2 solutions catalyzed by $\text{Na}_{12}[\text{WZn}_3(\text{H}_2\text{O})_2(\text{ZnW}_9\text{O}_{34})_2]$. Reaction conditions: 5 mmol substrate, 14 mmol H_2O_2 (~27%), 0.01 mmol $\text{Na}_{12}[\text{WZn}_3(\text{H}_2\text{O})_2(\text{ZnW}_9\text{O}_{34})_2]$ dissolved in 1 ml water, 16 mmol NH_3 solution (25%) was added drop wise. The reactions were carried out at room temperature, 6 h.

Substrate	Conversion/ mol%	Oxime/ mol%	Amide/ mol% ^a	Nitrile/ mol% ^b
benzaldehyde	95	>99.9	0	0
benzaldehyde ^c	93	>99.9	0	0
3-nitrobenzaldehyde	95	30	2	68
4-nitrobenzaldehyde	94	57	0	43
3-bromobenzaldehyde	95	32	38	26
4-bromobenzaldehyde	66	95	0	5
3-chlorobenzaldehyde	85	62	13	25
2,4-fluorobenzaldehyde	66	84	3	13
4-methylbenzaldehyde	98	82	0	18
4-hydroxy-acetophenone	30	>99.9	0	0
4-methoxybenzaldehyde	97 ^d	30	0	0
3-pyridine carboxaldehyde	100	52	38	6
2-thiophene carboxaldehyde	94	55	13	32
2-butanone	85	>99.9	0	0
2-pentanone	80	>99.9	0	0
cyclohexanone	90	>99.9	0	0
cyclohexanone ^c	91	>99.9	0	0
cycloheptanone	90	>99.9	0	0
cyclooctane	70	>99.9	0	0
acetophenone	15	>99.9	0	0

^a Beckmann rearrangement product. ^b Dehydration product. ^c 0.01 mmol $\text{Na}_{12}[\text{WZn}_3(\text{H}_2\text{O})_2(\text{ZnW}_9\text{O}_{34})_2]$ was formed *in situ* prior to the addition of H_2O_2 and NH_3 . ^d 70% 4-Methoxybenzoic acid formed.

between the water-soluble hydroxylamine and the ketone substrate. Second, the reaction of some aromatic aldehydes tended to be less selective, with formation of mostly nitriles and amides (less frequently) in further acid catalyzed reaction, as presented in Scheme 2. This reduced selectivity, observed in aromatic aldehydes with both electron withdrawing and electron donating moieties is not necessarily undesirable since the final synthesis of nitriles from aldehydes is often desirable. For more reactive 4-methoxybenzaldehyde, the competitive oxidation of the aldehyde with hydrogen peroxide to the corresponding benzoic acid became considerable (70% 4-methoxybenzoic acid). This effect was exacerbated in the case of aliphatic aldehyde substrates, where only the corresponding carboxylic acid products were observed. Finally, the results of reactions with self assembled $\text{Na}_{12}[\text{WZn}_3(\text{H}_2\text{O})_2(\text{ZnW}_9\text{O}_{34})_2]$ were identical to those with purified $\text{Na}_{12}[\text{WZn}_3(\text{H}_2\text{O})_2(\text{ZnW}_9\text{O}_{34})_2]$. In the past, there have been some reports that ammonoxidation could be catalyzed by simple Na_2WO_4 .⁷ In order compare our results with $\text{Na}_{12}[\text{WZn}_3(\text{H}_2\text{O})_2(\text{ZnW}_9\text{O}_{34})_2]$ to the results published in the

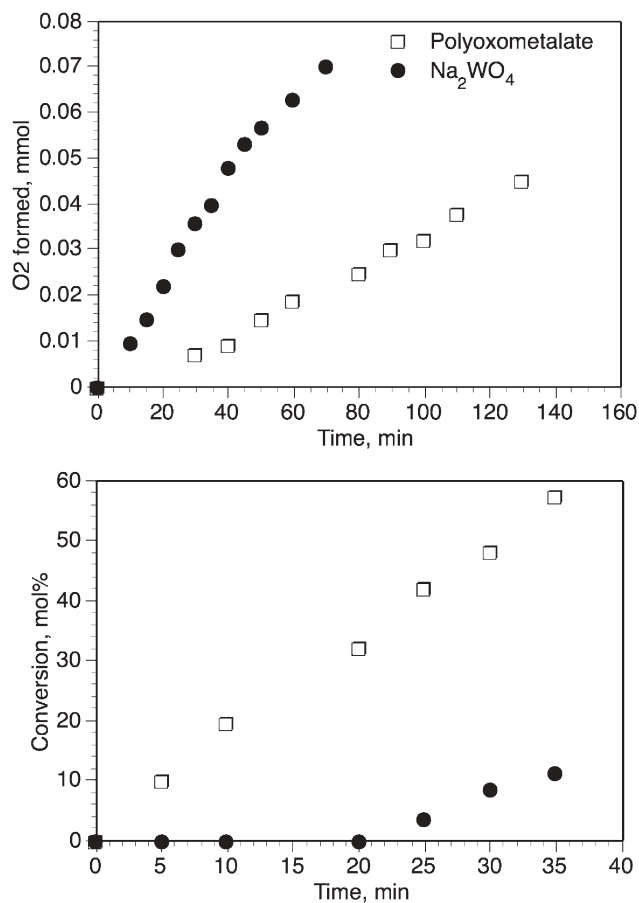


Fig. 1 Decomposition of H_2O_2 (top) and kinetic profile for cyclohexanone oximation (bottom). Reaction conditions: (top) 14 mmol H_2O_2 , 16 mmol NH_3 , 0.01 mmol catalyst. (bottom) 5 mmol cyclohexanone, 14 mmol H_2O_2 (~27%), 0.1 meq W. dissolved in 1 ml water, 16 mmol NH_3 solution (25%) was added drop wise.

literature, the systems were compared using two parameters for comparison: (i) efficiency in the utilization of the oxidant and ammonia and (ii) the kinetic profile of product formation based on equivalents of tungsten (not mols of catalyst). As one can see from the profiles shown in Fig. 1 (top), the $\text{Na}_{12}[\text{WZn}_3(\text{H}_2\text{O})_2(\text{ZnW}_9\text{O}_{34})_2]$ polyoxometalate decomposed hydrogen peroxide much more slowly than Na_2WO_4 , even with an equimolar amount of catalyst. Furthermore at equivalent amounts of tungsten the polyoxometalate showed significantly higher oxidation efficiency and no induction period for the reaction, Fig. 1 (bottom).

In order to check the stability of the catalyst in the reaction mixture, a catalyst recycling experiment, in which cyclohexanone was oximated (reaction conditions as in Table 1), was carried out. The catalyst in the aqueous phase was recovered simply by separating off the organic phase and the recycling was carried out by re-addition of cyclohexanone and 30% aqueous hydrogen peroxide and dropwise addition of 25% aqueous ammonia over 6 h at room temperature. The results showed essentially no change in activity (90 ± 2 mol% conversion) or selectivity to cyclohexanoneoxime (>99.9%) for six cycles.

The $\text{Na}_{12}[\text{WZn}_3(\text{H}_2\text{O})_2(\text{ZnW}_9\text{O}_{34})_2]$ polyoxometalate, which can be easily synthesized from Na_2WO_4 and $\text{Zn}(\text{NO}_3)_2$ in the

presence of HNO_3 without purification steps, is an efficient catalyst for the oximation of ketones and aromatic aldehydes in aqueous biphasic media, and does not require an organic solvent.

Acknowledgements

This research was supported by the Israel Science Foundation, the European Commission (GIRD-CT-2000-00347) SUSTOX program and the Helen and Martin Kimmel Center for Molecular Design. R.N. is the Rebecca and Israel Sieff Professor of Organic Chemistry.

Notes and references

- 1 See: http://psc.tamu.edu/research/reactivechem_lab/research/hydroxylamine.htm.
- 2 (a) R. Raja, G. Sankar and J. M. Thomas, *J. Am. Chem. Soc.*, 2001, **123**, 8153–8154; (b) G. Fornasari and F. Trifiro, *Catal. Today*, 1998, **41**, 443–455; (c) J. N. Armor, *J. Am. Chem. Soc.*, 1980, **102**, 1453–1454.
- 3 (a) A. Cesana, M. A. Mantegazza and M. Pastori, *J. Mol. Catal. A: Chem.*, 1997, **117**, 367–373; (b) L. Dal Pozzo, G. Fornasari and T. Monti, *Catal. Commun.*, 2002, **3**, 369–375; (c) H. Ichihashi and H. Sato, *Appl. Catal., A*, 2001, **221**, 359–366; (d) P. Wu, T. Komatsu and T. Yashima, *J. Catal.*, 1997, **168**, 400–411; (e) J. Le Bars, J. Dakka and R. A. Sheldon, *Appl. Catal., A*, 1996, **136**, 69–80; (f) A. Bhaumik, S. Samanta and N. K. Mal, *Microporous Mesoporous Mater.*, 2004, **68**, 29–35.
- 4 (a) T. Liu, X. Meng, Y. Wang, X. Liang, Z. Mi, X. Qi, S. Li, W. Wu, E. Min and S. Fu, *Ind. Eng. Chem. Res.*, 2004, **43**, 166–172; (b) X. Liang, Z. Mi, Y. Wang, L. Wang, X. Zhang and T. Liu, *Chem. Eng. Technol.*, 2004, **27**, 176–180.
- 5 (a) D. Sloboda-Rozner, P. L. Alsters and R. Neumann, *J. Am. Chem. Soc.*, 2003, **125**, 5280–5281; D. Sloboda-Rozner, P. Witte, P. L. Alsters and R. Neumann, *Adv. Synth. Catal.*, 2004, **346**, 339–345.
- 6 In this way the aqueous concentrations of both hydrogen peroxide (<30%) and hydroxylamine (<5%) are kept low, thus providing a safe reaction medium.
- 7 O. L. Lebedev and S. N. Kazarnovskii, *Zh. Obshch. Khim.*, 1960, **30**, 1631–1635.

ReSource

Lighting your way through the publication process

A website designed to provide user-friendly, rapid access to an extensive range of online services for authors and referees.

ReSource enables authors to:

- Submit manuscripts electronically
- Track their manuscript through the peer review and publication process
- Collect their free PDF reprints
- View the history of articles previously submitted

ReSource enables referees to:

- Download and report on articles
- Monitor outcome of articles previously reviewed
- Check and update their research profile

Register today!

RSC Publishing

www.rsc.org/resource

02030508

L-Proline in an ionic liquid as an efficient and reusable catalyst for direct asymmetric α -aminoxylation of aldehydes and ketones

Hai-Ming Guo,^{abc} Hong-Ying Niu,^{bc} Meng-Xia Xue,^{bc} Qi-Xiang Guo,^{bc} Lin-Feng Cun,^b Ai-Qiao Mi,^b Yao-Zhong Jiang^{*b} and Jian-Ji Wang^{*a}

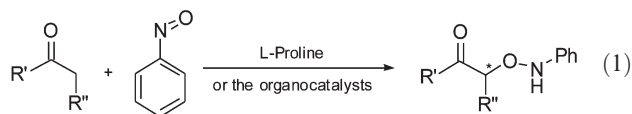
Received 21st March 2006, Accepted 19th June 2006

First published as an Advance Article on the web 27th June 2006

DOI: 10.1039/b604191d

Proline-catalyzed direct asymmetric α -aminoxylation of aldehydes and ketones in the room temperature ionic liquid 1-*n*-butyl-3-methylimidazolium tetrafluoroborate achieved high yields and high enantioselectivities, even when just 1–5% of proline was used as the catalyst; immobilisation of the catalyst in an ionic liquid phase offers simple product isolation and the reuse of the catalytic system at least four times in subsequent reactions.

The stereoselective synthesis of α -hydroxycarbonyl compounds is a topic of interest, as these structures represent fundamental building blocks for the construction of complex natural products and other important bioactive molecules; this importance has motivated the investigation of a wide variety of reactions for diastereoselective and enantioselective synthesis.¹ Momiyama and Yamamoto have reported an excellent catalytic asymmetric nitroso-aldol reaction, in which the tin enolate of a ketone reacts with nitrosobenzene in the presence of a catalytic amount of BINAP–AgOTf complex, affording an α -aminoxyketone in high enantioselectivity, which can be easily converted into the corresponding α -hydroxyketone.² Just recently, inspired by the notion that nitrosobenzene acts as an electrophilic aminoxylation reagent, organocatalyzed reactions of α -aminoxylation of aldehydes and ketones with nitrosobenzene in the presence of L-proline and its derivatives have also been actively investigated (eqn (1)).³



Ionic liquids⁴ have been widely used as environmentally benign solvents to replace the common organic reaction media.⁵ Moreover, they are reusable, allow for simple isolation of products and enable the easy recovery of catalysts.⁶ L-Proline in combination with ionic liquids has proved to be an efficient system for direct asymmetric aldol reactions,⁷ cross-aldol reactions,⁸ Michael additions,⁹ α -aminations of aldehydes and ketones,¹⁰ Ullmann-type reactions,¹¹ as well as Mannich reactions.¹² As a part of our

ongoing research in the field of ionic liquids,¹³ we are highly interested in studying the influence of ionic liquids on L-proline-catalyzed direct asymmetric α -aminoxylation of aldehydes and ketones in an ionic liquid, and in comparing the results with the published data in more common organic solvents. The next important aspect was the examination of the catalyst recovery and the possibility of the reuse of the catalyst in subsequent reactions.

At first, several aldehydes and ketones (**1**) and nitrosobenzene as substrates were investigated in ionic liquid [bmim]BF₄ (ee values in CHCl₃ have been reported in the literature^{3a,3b}). To a dried vial charged with L-proline (20 mol%, 23 mg) and nitrosobenzene (1 mmol, 107.1 mg) was added the ionic liquid [bmim]BF₄ (2 ml), followed by the appropriate aldehyde or ketone (2 mmol) in one portion at room temperature. After the resulting solution was stirred for 3–4 h, the reaction mixture was extracted with ether (6 × 10 ml) to leave the ionic liquid containing L-proline. The achieved results are summarized in Table 1. It can be seen that ionic liquid gave the desired α -aminoxylation products. In all cases, the expected α -aminoxylation products were obtained with comparable or better yield and ee in [bmim]BF₄ than in CHCl₃.^{3a,3b}

The effect of catalyst loading on the reaction efficiency was evaluated next, using isovaleraldehyde and nitrosobenzene as substrates (Table 2). No reaction took place in the absence of proline (entry 1). The same result was obtained for the reaction catalyzed by 10 mol% of proline as the reaction catalyzed by 20 mol% of proline (entry 2 and entry 3). With 5 mol% of proline, the product yield remained at a comparable level, but with 1 mol% of proline, a significant loss of yield was observed (entry 4 and entry 5). In all cases the enantioselectivity was not affected (98% ee).

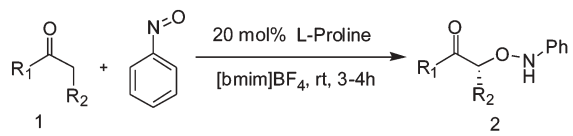
Finally, the possibility to reuse or recycle the ionic liquid [bmim]BF₄ containing L-proline was examined by employing the direct α -aminoxylation reaction of cyclohexanone with nitrosobenzene as a model. After the reaction was completed, the reaction mixture was extracted with ether (6 × 10 ml) to give the ionic liquid residue containing L-proline. The ionic liquid containing L-proline phase was dried *in vacuo* at 40 °C for 3–4 h and was used directly for the subsequent reaction. The data shown in Table 3 illustrate that the ionic liquid [bmim]BF₄ containing L-proline can be reused at least four times without sacrificing the yield and enantioselectivity (>99% ee) (entries 2, 3 and 4).

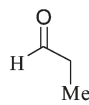
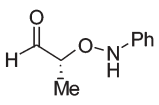
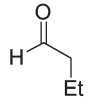
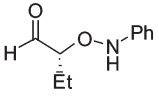
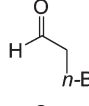
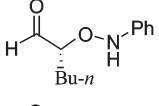
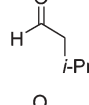
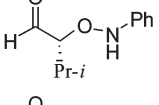
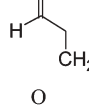
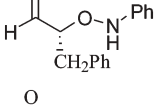
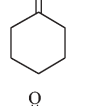
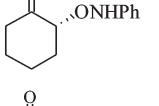
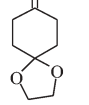
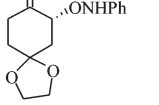
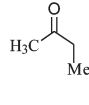
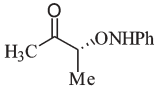
In conclusion, we have demonstrated that the room temperature ionic liquid [bmim]BF₄ is a suitable solvent for proline catalyzed asymmetric α -aminoxylation reactions of aldehydes and ketones

^aDepartment of Chemistry, Henan Normal University, Xinxiang, Henan, 453002, People's Republic of China. E-mail: guohm518@hotmail.com

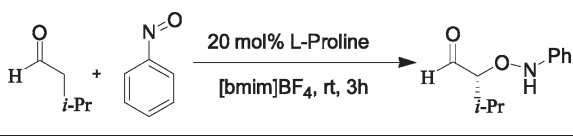
^bKey Laboratory for Asymmetric Synthesis and Chirotechnology of Sichuan Province and Union Laboratory of Asymmetric Synthesis, Chengdu Institute of Organic Chemistry, Chinese Academy of Sciences, Chengdu, 610041, China

^cGraduate School of Chinese Academy of Sciences, Beijing, China

Table 1 Proline-catalyzed α -aminoxylation of aldehydes and ketones in ionic liquid [bmim]BF₄^a


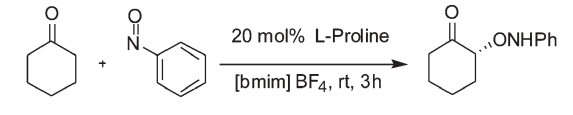
Entry	Substrate	Product	Yield (%)	ee (%) ^b
1			89 ^c	97
2			98 ^c	99
3			76 ^c	99
4			91 ^c	98
5			93 ^c	97
6			74 ^d	>99
7			70 ^d	>99
8			67 ^d	>99

^a The reaction was conducted with 0.2 equiv L-proline, 3 equiv aldehyde or ketone and 1.0 equiv nitrosobenzene in ionic liquid [bmim]BF₄ at room temperature. ^b Determined by HPLC. ^c Isolated yield of the alcohol (2 steps). ^d Isolated yield.

Table 2 Effect of catalyst loading on the reaction yield and enantioselectivity in the α -aminoxylation of isovaleraldehyde with nitrosobenzene


Entry	L-proline/mol%	Yield (%) ^a	ee (%) ^b
1	0	0	—
2	20	91	98
3	10	91	98
4	5	87	98
5	1	64	98

^a Isolated yield of the alcohol (2 steps). ^b Determined by HPLC (Chiralpak AD-H column).

Table 3 Studies on catalyst recycling


Run	Yield (%) ^a	ee (%) ^b
1	74	>99%
2	74	>99%
3	73	>99%
4	73	>99%
5	50	>99%

^a Isolated yield. ^b Determined by HPLC (Chiralpak AD-H column).

with nitrosobenzene. The catalyst immobilised in [bmim]BF₄ could be reused at least four times, and the product yield and enantiopurity remained at a comparable level to the case with the fresh catalyst.

Acknowledgements

We are grateful for financial support from the National Natural Science Foundation of China (grants 20472082, 203900505 and 20273019).

Notes and references

- (a) F. A. Davis and B. C. Chen, *Methods of Organic Chemistry*, ed. G. Helmchen, R. W. Hoffmann, J. Mulzer, E. Schaumann, Houben-Weyl, Thieme, Stuttgart, 1995, vol. E21, p. 4497; (b) D. Enders and U. Reinhold, *Liebigs Ann.*, 1996, 11; (c) D. Enders and U. Reinhold, *Synlett*, 1994, 792. For reviews, see: (d) J. M. Janey, *Angew. Chem., Int. Ed.*, 2005, **44**, 4292; (e) P. Merino and T. Tejero, *Angew. Chem., Int. Ed.*, 2004, **43**, 2995.
- (a) N. Momiyama and H. Yamamoto, *J. Am. Chem. Soc.*, 2003, **125**, 6038; (b) N. Momiyama and H. Yamamoto, *J. Am. Chem. Soc.*, 2004, **126**, 6498 [corrections].
- (a) G. Zhong, *Angew. Chem., Int. Ed.*, 2003, **42**, 4247; (b) S. P. Brown, M. P. Brochu, C. J. Sinz and D. W. C. MacMillan, *J. Am. Chem. Soc.*, 2003, **125**, 10808; (c) Y. Hayashi, J. Yamaguchi, K. Hibino and M. Shoji, *Tetrahedron Lett.*, 2003, **44**, 8293; (d) A. Bøgevig, H. Sundén and A. Córdova, *Angew. Chem., Int. Ed.*, 2004, **43**, 1109; (e) W. Wang, J. Wang, H. Li and L. Liao, *Tetrahedron Lett.*, 2004, **45**, 7235; (f) Y. Hayashi, J. Yamaguchi, T. Sumiya, K. Hibino and M. Shoji, *J. Org. Chem.*, 2004, **69**, 5966; (g) H. Sundén, N. Dahlin, I. Ibrahim, H. Adolfsson and A. Córdova, *Tetrahedron Lett.*, 2005, **46**, 3385; (h) A. Córdova, H. Sundén, A. Bøgevig, M. Johansson and F. Himo, *Chem.-Eur. J.*, 2004, **10**, 3673; (i) Y. Hayashi, J. Yamaguchi, K. Hibino and M. Shoji, *Angew. Chem., Int. Ed.*, 2004, **43**, 1112.
- Synthesis of ionic liquids see: P. Bonhôte, A.-P. Dias, N. Papageorgiou, K. Kalyanasundaram and M. Grätzel, *Inorg. Chem.*, 1996, **35**, 1168.
- For a review, see: (a) J. Dupont, R. F. de Souza and P. A. Z. Suarez, *Chem. Rev.*, 2002, **102**, 3667; (b) D. Zhao, M. Wu, Y. Kou and E. Min, *Catal. Today*, 2002, **74**, 157; (c) J. S. Wilkes, *J. Mol. Catal. A: Chem.*, 2004, **214**, 11; (d) T. Welton, *Coord. Chem. Rev.*, 2004, **248**, 2459.
- (a) C. E. Song, W. H. Shim, E. J. Roh, S.-G. Lee and J. H. Choi, *Chem. Commun.*, 2001, 1122; (b) S.-G. Lee, J. H. Park, J. Kang and J. K. Lee, *Chem. Commun.*, 2001, 1698.
- (a) T.-P. Loh, L.-C. Feng, H.-Y. Yang and J.-Y. Yang, *Tetrahedron Lett.*, 2002, **43**, 8741; (b) P. Kotrusz, I. Kmentova, B. Gotov, S. Toma and E. Solcaniova, *Chem. Commun.*, 2002, 2510; (c) M. Gruttadauria, S. Rielu, P.-L. Meo, F. D'Anna and R. Noto, *Tetrahedron Lett.*, 2004, **45**, 6113; (d) A. M. Salaheldin, Z. Yi and T. Kitazume, *J. Fluorine Chem.*, 2004, **125**, 1105.
- A. Córdova, *Tetrahedron Lett.*, 2004, **45**, 3949.
- (a) M. S. Rasalkar, M. K. Potdar, S. S. Mohile and M. M. Salunkhe, *J. Mol. Catal. A: Chem.*, 2005, **235**, 267; (b) H. Hagiwara, T. Okabe, T. Hoshi and T. Suzuki, *J. Mol. Catal. A: Chem.*, 2004, **214**, 167; (c)

- T. Kitazume, Z. J. Jiang, K. Kasai, Y. Mihara and M. Suzuki, *J. Fluorine Chem.*, 2003, **121**, 205; (d) P. Kotrusz, S. Toma, H. G. Schmalz and A. Adler, *Eur. J. Org. Chem.*, 2004, 1577.
- 10 P. Kotrusz, S. Alemayehu, S. Toma, H. G. Schmalz and A. Adler, *Eur. J. Org. Chem.*, 2005, 4094.
- 11 Z. M. Wang, W. L. Bao and Y. Jiang, *Chem. Commun.*, 2005, 2849.
- 12 N. S. Chowdari, D. B. Ramchary and C. F. Barbas, III, *Synlett*, 2003, 1906.
- 13 H.-M. Guo, L.-F. Cun, L.-Z. Gong, A.-Q. Mi and Y.-Z. Jiang, *Chem. Commun.*, 2005, 1450.

Chemical Biology

An exciting news supplement providing a snapshot of the latest developments in chemical biology



Free online and in print issues of selected RSC journals!*

Research Highlights – newsworthy articles and significant scientific advances

Essential Elements – latest developments from RSC publications

Free links to the full research paper from every online article during month of publication

*A separately issued print subscription is also available

RSC Publishing

www.rsc.org/chemicalbiology

30110553

A green catalyst for green chemistry: Synthesis and application of an olefin metathesis catalyst bearing a quaternary ammonium group†

Anna Michrowska,^a Łukasz Gułajski,^{ab} Zuzanna Kaczmarska,^{ac} Klaas Mennecke,^d Andreas Kirschning^d and Karol Grela^{*a}

Received 10th April 2006, Accepted 15th June 2006

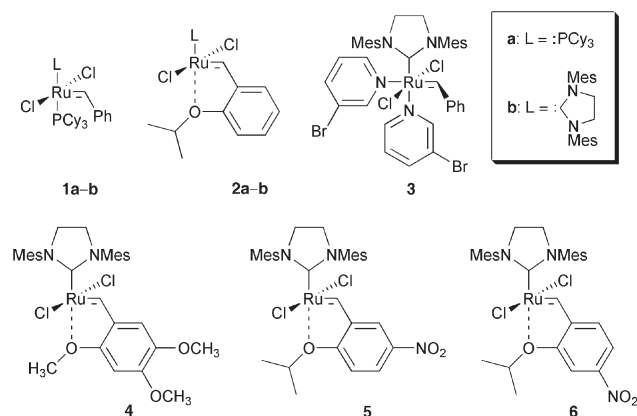
First published as an Advance Article on the web 28th June 2006

DOI: 10.1039/b605138c

The novel catalyst **8**, bearing a polar quaternary ammonium group, is very stable and can be easily prepared from commercially available reagents. Catalyst **8** can be efficiently used for olefin metathesis not only in traditional but also in aqueous media. Various ring closing-, cross- and enyne-metathesis reactions were conducted in water-methanol mixtures in air. The electron withdrawing quaternary ammonium group not only activates the catalyst chemically, but at the same time allows its efficient separation after reaction. Application of **8** leads to organic products of high purity, which exhibit very low ruthenium contamination levels (12–68 ppm) after filtering through a pad of silica gel.

Introduction

Despite the general superiority offered by modern *homogeneous* Grubbs and Hoveyda–Grubbs catalysts **1–3** (Scheme 1),¹ they



Scheme 1 Selected ruthenium precatalysts for alkene metathesis. Cy = cyclohexyl; Mes = 2,4,6-trimethylphenyl.

^aInstitute of Organic Chemistry, Polish Academy of Sciences, Kasprzaka 44/52, Warsaw, 01-224, Poland. E-mail: grela@icho.edu.pl

^bFaculty of Chemistry, Warsaw University of Technology (Politechnika), Noakowskiego 3, Warsaw, 00-664, Poland

^cDepartment of Chemistry, Warsaw University, Pasteura 1, Warsaw, 02-093, Poland

^dInstitut für Organische Chemie, Universität Hannover, Schneiderberg 1b, Hannover, 30167, Germany

† Electronic supplementary information (ESI) available: Experimental procedures for ligand and catalyst syntheses, including characterization data of metathesis products. See DOI: 10.1039/b605138c

share some disadvantages. Since olefin metathesis reaction is expected to be used in pharmaceutical processes, the most undesirable feature of these complexes is that during the reaction they form ruthenium byproducts, which are difficult to remove from the reaction products.² In many cases, ruthenium levels of >2000 ppm remain after chromatography of products prepared by RCM with 5 mol% of Grubbs catalysts.³ The ruthenium has to be removed prior to further processing.⁴

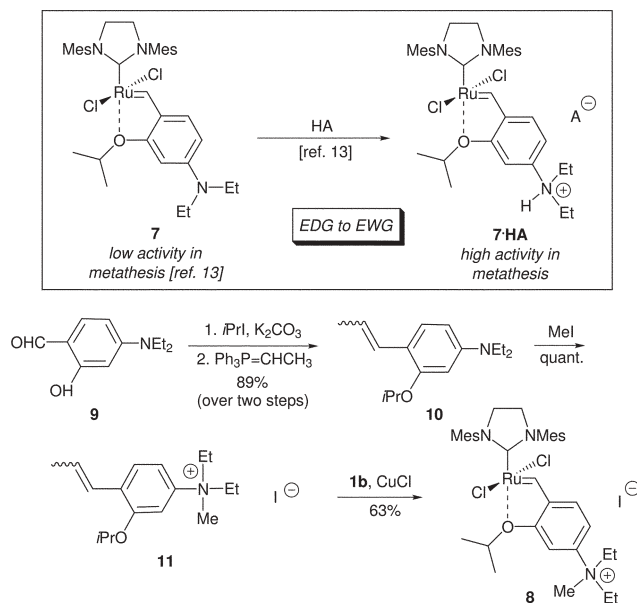
Several protocols to solve problems associated with Ru contamination arising during pharmaceutical or fine chemical processing, from R&D scale through to manufacture, have been proposed.³ Use of biphasic aqueous extraction,⁵ various scavengers, such as lead tetraacetate,⁶ DMSO,⁷ triphenylphosphine oxide,⁷ and supported phosphines⁸ were reported to reduce the ruthenium content to between 200–1200 ppm. Alternatively, two cycles of chromatography, followed by 12 h incubation with activated charcoal, resulted in <100 ppm.⁹ Recently, special functional polymers—QuadraPure[™] resins—were intended for heavy metal (including Ru) removal in both batch and continuous processes.¹⁰ Complex **4**, introduced by our group,¹¹ exhibits catalytic activity comparable to the parent Hoveyda–Grubbs carbene **2b**, but shows much higher affinity for silica gel when CH₂Cl₂ is used as eluent, which enables its efficient removal. We have recently developed a new efficient strategy for phase-separation and recovery of **4**, which provides crude products containing up to 400 ppm of ruthenium.¹²

In continuation of our program to develop a ‘green’ metathesis catalyst,^{12,13} herein we report on a new, airstable ruthenium homogeneous catalyst, that exhibits an increased activity in metathesis reactions and allows us to obtain crude products with low residual ruthenium levels.

Results and discussion

Catalyst design

We demonstrated that the 5- and 4-nitro-substituted complexes **5** and **6** initiate olefin metathesis dramatically faster than the parent Hoveyda–Grubbs catalyst **2b**.¹⁴ We proposed that the electron-withdrawing (EWG) nitro-group in the benzylidene fragment of **5** and **6** weakens the O→Ru chelation and facilitates faster initiation of the catalytic cycle.¹⁴ In accordance with this assumption, we observed that complex **7** (Scheme 2), bearing the electron-donating (EDG) diethylamino group shows little or no activity in olefin metathesis.^{13,15} However, in a striking contrast, the *in situ* formed salts obtained by treatment of aniline **7** with Brønsted acids (Scheme 2) are of high activity, surpassing the parent



Scheme 2 The concept of 'EWG-to-EDG activity switch' and preparation of complex **8**.

Hoveyda–Grubbs complex **2b** in terms of initiation speed (*electron donating to electron withdrawing activity switch*).¹³

Exploring further the concept of activating a catalyst using EDG to EWG activity switch, we have attempted to prepare complex **8**, bearing a quaternary ammonium group.¹⁶ As illustrated on Scheme 2, we used commercially available aldehyde **10** as a starting material for the preparation of the corresponding quaternary salt **11**.¹⁷ Complex **8** was obtained in the reaction of **11** (1.1 equiv.) with **1b** (1.0 equiv.) and CuCl (1.4 equiv.). Washing of the crude product with ethyl acetate and methanol afforded pure complex **8** as an air-stable, green micro-crystalline solid, soluble in acetonitrile, dichloromethane, methanol, methanol–water and ethanol–water 5 : 2 (v/v), respectively.

Catalytic performance of **8**

To compare the relative activities of catalysts **2b**, **7** and **8**, the ring-closing metathesis of diethyl 2-allyl-2-methylmalonate (**12a**) (Table 1, entry 1) was investigated under identical conditions. The results show that the initial rate of metathesis was markedly enhanced in the case of the EWG-substituted **8**. After 20 and 40 min the yields of **13a** were 51% and 81% respectively (96% after 1.5 h), as opposed to 20% and 46% obtained with **2b** (81% after 1.5 h). This demonstrates again^{14,13} that the activity of ruthenium metathesis catalyst **2b** can be enhanced by introduction of electron-withdrawing groups without detriment to the catalyst stability. An analogous experiment was conducted with free-amine catalyst **7**. As expected,¹³ practically no reaction was observed during the first 2 hours (<1% conversion after 1.5 h and 8% after 24 h).

We supposed that the introduction of a polar quaternary ammonium group can be used not only to increase the catalyst activity, but also to alter its physical–chemical properties, such as affinity to silica gel, which should facilitate its separation after the reaction. To reduce this assumption to reality, a spectrum of various substrates for RCM and enyne-cycloisomerisation were tested (Table 1, entries 2–7). The data compiled in Table 1 show

that complex **8** is a superb catalyst in CH₂Cl₂. In addition, we observed that simple silica-gel filtration of the reaction mixture through a short pad of silica gel (20–40 × weight of the product) allows almost complete removal of ruthenium byproducts. Inductively coupled plasma mass spectrometry (ICP-MS) analysis of the selected crude products (**13**) indicated 12–68 ppm Ru, which is much lower than contamination levels obtained in reactions with catalyst **1a**³ and **4**.¹²

Metathesis reactions are usually carried out in nonpolar organic solvents under inert and anhydrous conditions.¹ From an economic and environmental standpoint, water or aqueous solutions represent very attractive media for organic reactions,¹⁸ and recently some efforts have been directed to the application of water or aqueous solutions in metathesis reactions.¹⁹

We were pleased to see that complex **8** efficiently catalysed the metathesis of various substrates in *non-distilled, non-degassed protic media in air* (Table 1, entries 4–5 and 8–9). Again, in one selected case we checked that the crude organic product (**13h**) contained a very low level of residual ruthenium (37 ppm).

In conclusion, we have reported the first example of a homogenous Hoveyda–Grubbs catalyst containing a quaternary ammonium group. Catalyst **8** initiates various types of metathesis reaction in both dichloromethane and methanol–water mixtures. Furthermore, the very low levels of residual ruthenium impurities in crude organic products make **8** particularly suitable for use in pharmaceutical applications. The application of this catalyst in the synthesis of biologically important molecules in aqueous solvent mixtures is currently being pursued.

Experimental

Representative procedure of metathesis in CH₂Cl₂

A reaction tube equipped with a magnetic stirring bar was charged with CH₂Cl₂ (10 mL), catalyst **8** (1–5 mol%) and substrate **12** (0.2 mmol). The reaction mixture was stirred at 25 °C. After complete conversion (TLC), the reaction mixture was passed through a cartridge containing silica gel (1–2 g). The cartridge was washed with an additional portion of CH₂Cl₂ (10–20 mL). The CH₂Cl₂ fraction was concentrated under reduced pressure to yield crude product **13**.

Representative procedure of metathesis in a mixture of MeOH–H₂O or EtOH–H₂O, 5 : 2 v/v

A reaction tube equipped with a magnetic stirring bar was charged with catalyst **8** (6 mg, 0.007 mmol, 5 mol%) and non-degassed water (2 mL). To the resulting suspension a solution of substrate **12** (0.14 mmol) in MeOH or EtOH (5 mL) was added. The reaction mixture was stirred at 25 °C. After complete conversion (TLC), the reaction mixture was evaporated to dryness, dissolved in CH₂Cl₂ (5 mL) and passed through a cartridge containing silica gel (1–2 g). The cartridge was washed with an additional portion of CH₂Cl₂ (15–25 mL). The CH₂Cl₂ fraction was concentrated under reduced pressure to yield crude product **13**.

Acknowledgements

We thank Prof. C. Vogt and S. Gruhl (Institute of Inorganic Chemistry, University of Hannover) for conducting the

Table 1 Metathesis reactions catalyzed by **8**^a

Entry	Substrate 12	Product 13	Solvent	Catalyst (mol%)	Time/h	Conversion (%) ^b	Ru/ppm ^c
1			CH ₂ Cl ₂	2b (5)	0.3	20	
		2b (5)		0.6	46		
		2b (5)		1.5	81		
		7 (5)		1.5	<1		
		8 (5)		0.3	51		
		8 (5)		0.6	81		
		8 (5)		1.5	96		
2			CH ₂ Cl ₂	8 (5)	0.5	99	68
3			CH ₂ Cl ₂	8 (5)	1	99	12
				8 (1)	3.5	99	
4			CH ₂ Cl ₂ MeOH/H ₂ O	8 (5) 8 (5)	1 0.5	97 99	33
5			CH ₂ Cl ₂ MeOH/H ₂ O EtOH/H ₂ O	8 (5) 8 (5) 8 (5)	0.5 0.5 0.5	98 92 99	
6			CH ₂ Cl ₂	8 (2.5)	0.5	99	
7			CH ₂ Cl ₂	8 (3)	2	91	21
8			MeOH/H ₂ O EtOH/H ₂ O	8 (5) 8 (5)	0.5 0.5	99 83	37
9			MeOH/H ₂ O	8 (10)	24	99 ^d	

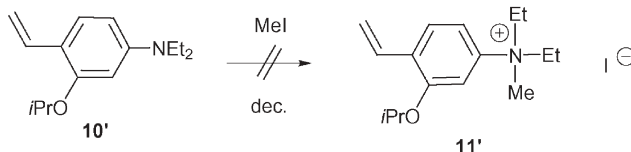
^a Conditions: 1–5 mol% of catalyst, CH₂Cl₂ or MeOH/H₂O; *c* = 0.02 mol L⁻¹, 25 °C. ^b Conversions were determined by analysis of ¹H NMR or GC-MS of the crude reaction mixture. ^c Level of Ru impurity in crude products determined by ICP-MS and shown as parts per million (ppm). ^d Reaction with 10 mol% of **8** at 40 °C.

ICP-MS analyses, and the Institute of Organic Chemistry, Polish Academy of Sciences for support (stipend for L.G.). Preparation of this manuscript would not have been possible without the help of the Alexander von Humboldt Foundation (travel allowance to K.G.), which is gratefully acknowledged.

Notes and references

- Pertinent reviews: (a) R. H. Grubbs, *Handbook of Metathesis*, Wiley-VCH, Weinheim, 2003, vol. 1–3; (b) T. M. Trnka and R. H. Grubbs, *Acc. Chem. Res.*, 2001, **34**, 18; (c) A. Fürstner, *Angew. Chem.*, 2000, **112**, 3140, *Angew. Chem., Int. Ed.*, 2000, **39**, 3012; (d) R. H. Grubbs and S. Chang, *Tetrahedron*, 1998, **54**, 4413; (e) M. Schuster and S. Blechert, *Angew. Chem.*, 1997, **109**, 2124.
- T. Nicola, M. Brenner, K. Donsbach and P. Kreye, *Org. Process Res. Dev.*, 2005, **9**, 513.
- (a) J. C. Conrad, H. H. Parnas, J. L. Snelgrove and D. E. Fogg, *J. Am. Chem. Soc.*, 2005, **127**, 11882; (b) For example, in a crude untreated product of diethyl diallylmalonate (**12c**) RCM catalysed by 5 mol% of Grubbs I-generation catalyst the theoretical amount of Ru is 90 µg per 5 mg of product (18 000 ppm, see Ref. 7). After filtration of the crude reaction mixture, the Ru level was reduced to 59.7 ± 0.50 µg per 5 mg (12 000 ppm). Further purification of such crude metathesis products usually reduces ruthenium levels below 2000 ppm, see *ibid.*, and K. McEleney, D. P. Allen, A. E. Holliday and C. M. Crudden, *Org. Lett.*, 2006, **8**, 2663.
- Another solution to this problem might be based on the immobilisation of a metathesis catalysts in a separate liquid or solid phase. For recent reviews, see: (a) A. H. Hoveyda, D. G. Gillingham, J. J. Van Veldhuizen, O. Kataoka, S. B. Garber, J. S. Kingsbury and J. P. A. Harrity,

- Org. Biomol. Chem.*, 2004, **2**, 1; (b) R. M. Buchmeiser, *New J. Chem.*, 2004, **28**, 549. For related systems developed in our laboratories, see: (c) K. Grela, K. Mennecke, U. Kunz and A. Kirschning, *Synlett*, 2005, 2948; (d) K. Grela, M. Tryznowski and M. Bieniek, *Tetrahedron Lett.*, 2002, **43**, 6425.
- 5 Boehringer Ingelheim International GmbH, *World Pat.* WO 2004/089974 A1, 2004.
- 6 L. A. Paquette, J. D. Schloss, I. Efremov, F. Fabris, F. Gallou, J. Mendez-Andino and J. Yang, *Org. Lett.*, 2000, **2**, 1259.
- 7 Y. M. Ahn, K. Yang and G. I. Georg, *Org. Lett.*, 2001, **3**, 1411.
- 8 (a) H. Maynard and R. H. Grubbs, *Tetrahedron Lett.*, 1999, **40**, 4137; (b) M. Westhus, E. Gonthier, D. Brohm and R. Breinbauer, *Tetrahedron Lett.*, 2004, **45**, 3141.
- 9 J. H. Cho and B. M. Kim, *Org. Lett.*, 2003, **5**, 531.
- 10 For a technical data sheet on the application of QuadraPure[™] resins, see: Avecia Pharmaceuticals, <http://www.quadrapure.com>.
- 11 K. Grela and M. Kim, *Eur. J. Org. Chem.*, 2003, 963.
- 12 A. Michrowska, L. Gulajski and K. Grela, *Chem. Commun.*, 2006, 841.
- 13 (a) A. Michrowska, *PhD Thesis*, Institute of Organic Chemistry, Polish Academy of Sciences, Warsaw, Poland, 2006. For a preliminary study on the activation of **7** and other complexes, see: (b) L. Gulajski, A. Michrowska, R. Bujok and K. Grela, *J. Mol. Catal. A: Chem.*, in print.
- 14 (a) K. Grela, S. Harutyunyan and A. Michrowska, *Angew. Chem., Int. Ed.*, 2002, **41**, 4038–4040; (b) A. Michrowska, R. Bujok, S. Harutyunyan, V. Sashuk, G. Dolgonos and K. Grela, *J. Am. Chem. Soc.*, 2004, **126**, 9318–9325; (c) S. Harutyunyan, A. Michrowska and K. Grela, in *Catalysts for Fine Chemical Synthesis*; ed. S. M. Roberts, J. Whittall, P. Mather, P. McCormack, Wiley-Interscience, New York, 2004, vol. 3, ch. 9.1, pp. 169–173.
- 15 For an example of a catalytically active ruthenium allenylidene complex bearing a Me₂N group, see: A. Fürstner, M. Liebl, C. Lehmann, M. Piquet, R. Kunz, C. Bruneau, D. Touchard and P. H. Dixneuf, *Chem.–Eur. J.*, 2000, **6**, 10, 1847.
- 16 For Grubbs-type ruthenium alkylidenes bearing a quarternary ammonium group, see: D. M. Lynn, B. Mohr, R. H. Grubbs, L. M. Henling and M. W. Day, *J. Am. Chem. Soc.*, 2000, **122**, 6601.
- 17 Attempts to carry out the quaternisation of another easily available precursor **10'** [ref.13b] proved unsuccessful.



- 18 (a) C.-J. Li, *Chem. Rev.*, 1993, **93**, 2023; (b) C.-J. Li and T.-H. Chen, *Organic Reaction in Aqueous Media*, Wiley, New York, 1997; (c) P. A. Grieco, *Organic Synthesis in Water*, Blackie Academic & Professional, London, 1998; (d) S. Kobayashi and K. Manabe, *Pure Appl. Chem.*, 2000, **72**, 1373.
- 19 For ruthenium complexes that catalyse olefin metathesis reactions in water and protic organic solvents, see: (a) ref. 16; (b) B. Mohr, D. M. Lynn and R. H. Grubbs, *Organometallics*, 1996, **15**, 4317; (c) S. J. Connon and S. Blechert, *Bioorg. Med. Chem. Lett.*, 2002, **12**, 1873; (d) S. J. Connon, M. Rivard, M. Zaja and S. Blechert, *Adv. Synth. Catal.*, 2003, **345**, 572; (e) T. Rölle and R. H. Grubbs, *Chem. Commun.*, 2002, 1070.

Epoxidation of styrene by TBHP to styrene oxide using barium oxide as a highly active/selective and reusable solid catalyst

Vasant R. Choudhary,* Rani Jha and Prabhas Jana

Received 5th April 2006, Accepted 23rd June 2006

First published as an Advance Article on the web 30th June 2006

DOI: 10.1039/b604937k

Styrene can be oxidised by TBHP to styrene oxide with high selectivity/yield using barium oxide (with or without gallium oxide support) as a simple, inexpensive and reusable solid catalyst; compared to the other alkaline and rare earth metal oxides, barium oxide showed a much better performance in the styrene epoxidation.

Styrene oxide (which is an important organic intermediate in the synthesis of fine chemicals and pharmaceuticals) is conventionally produced by epoxidation of styrene using stoichiometric amounts of peracid as an oxidizing agent.¹ However, peracids are very expensive, corrosive, hazardous to handle, non-selective for the epoxide formation and also lead to formation of undesirable products, creating voluminous waste. In order to overcome these limitations, a number of studies have reported on the epoxidation of styrene over easily separable solid catalysts, containing Ti,²⁻⁷ Fe or V⁴ or nanosize-gold,⁸ using safer oxidizing agent, such as TBHP (tertiary butylhydroperoxide)^{2,8} or H₂O₂.³⁻⁷ With H₂O₂ as an oxidizing agent, although the styrene conversion was high, the selectivity for styrene oxide was very poor. Recently Choudhary and coworkers⁹ used bohemite or alumina as a catalyst for the selective epoxidation of styrene by anhydrous H₂O₂ with a continuous removal of the reaction water. It is, therefore, interesting to know whether other simple metal oxides, such as alkaline and rare earth oxides have activity in the selective epoxidation of styrene. The present work was undertaken for this purpose. In this communication, we report, for the first time, the use of a simple, inexpensive and reusable metal oxide, such as BaO, for the selective epoxidation of styrene by TBHP with a very good selectivity/yield for styrene oxide. However, the other alkaline earth oxides and also rare earth oxides show a much lower performance in the epoxidation.

The styrene epoxidation by anhydrous TBHP over commercial BaO and other alkaline and rare earth metal oxides and supported BaO [prepared by impregnating barium nitrate (2 mmol g⁻¹(support)) on different supports (*viz.* SiO₂, Ga₂O₃, Al₂O₃, In₂O₃ and Si-MCM-41) by incipient wetness technique, drying and calcining at 500 °C for 4 h] was carried out under reflux, using a reaction mixture containing 10 mmol styrene, 15 mmol TBHP and 0.1 g of catalyst, by procedures described earlier.⁸ Results of the epoxidation over the different catalysts are presented in Tables 1 and 2.

Chemical Engineering & Process Development Division, National Chemical Laboratory, Pune, 411 008, India.
E-mail: vr.choudhary@ncl.res.in; Fax: +91 20 25902612;
Tel: +91 20 25902318

Table 1 Performance of different alkaline and rare earth metal oxides for the epoxidation of styrene to styrene oxide by anhydrous TBHP (SO = styrene oxide, PA = phenylacetaldehyde, Bzh = benzaldehyde, OP = other products)

Catalyst	Conversion (%)		Selectivity (%)				SO Yield (%)	TOF ^b
	Styrene	TBHP	SO	PA	Bzh	OP ^a		
Nil	7.5	16.5	11.0	7.7	1.7	81.7	0.8	—
MgO	15.9	28.0	19.8	7.0	4.9	68.2	3.2	1.1
CaO	0.9	45.3	—	—	—	100	≅0.0	0.0
SrO	15.2	24.2	60.2	8.0	0.0	31.8	9.2	3.1
BaO	40.7	32.1	78.7	8.9	1.1	11.2	32.0	10.7
BaO ^c	33.1	26.0	78.5	9.0	1.0	11.5	26.0	10.8
La ₂ O ₃	3.2	19.5	69.0	4.7	0.0	26.3	2.2	0.7
CeO ₂	28.7	52.4	38.9	6.0	4.2	50.7	11.2	3.7
Nd ₂ O ₃	20.0	23.2	62.8	8.0	1.1	28.0	12.6	4.2
Sm ₂ O ₃	9.8	14.2	48.6	5.2	0.0	46.1	4.8	1.6
Eu ₂ O ₃	9.8	12.1	50.2	5.3	0.0	44.4	4.9	1.6
Gd ₂ O ₃	15.7	16.0	60.0	10.8	0.0	29.0	9.4	3.1
Tb ₂ O ₃	9.8	10.5	48.3	8.2	0.0	43.5	4.7	1.5
Er ₂ O ₃	7.4	13.0	60.0	3.6	0.5	35.8	4.4	1.5
Yb ₂ O ₃	10.9	21.7	4.1	2.9	0.0	88.3	0.4	0.1

^a Benzoic acid and phenylacetic acid. ^b Defined as mmols of styrene oxide formed per gram of catalyst per hour. ^c For its 5th reuse (amount of catalyst used was 0.08 g).

The results in Table 1 reveal the following important information:

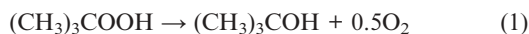
(1) Among the alkaline earth metal oxides, the BaO catalyst showed the best performance, *i.e.* the highest styrene oxide selectivity (79%) and yield (32%) in the epoxidation.

Table 2 Performance of different supported BaO catalysts for the epoxidation of styrene by anhydrous or aqueous TBHP

Catalyst	Conversion (%)		Selectivity (%)				SO Yield (%)	TOF ^a
	Styrene	TBHP	SO	PA	Bzh	OP		
Epoxidation using anhydrous TBHP								
BaO/SiO ₂	25.0	29.0	18.0	0.2	0.6	79.2	4.5	4.9
BaO/In ₂ O ₃	23.6	28.6	36.2	3.8	2.0	58.0	8.5	9.2
BaO/Ga ₂ O ₃	49.3	45.3	58.0	1.2	6.0	34.9	28.6	30.9
BaO/Ga ₂ O ₃ ^b	42.2	38.9	58.3	1.1	55.8	34.8	24.6	31.8
BaO/Al ₂ O ₃	25.5	40.2	30.0	8.7	1.3	60.0	7.7	8.3
BaO/Si-MCM-41	27.4	45.6	30.0	5.6	4.4	60.0	8.2	8.9
Epoxidation using aqueous TBHP								
BaO/In ₂ O ₃	31.0	38.3	40.2	6.8	0.3	52.7	12.5	13.5
BaO/Ga ₂ O ₃	40.1	58.6	56.1	0.6	2.3	41.1	22.5	24.3
BaO/Al ₂ O ₃	20.4	32.4	41.0	6.5	2.5	50.0	8.4	9.1
BaO/Si-MCM-41	30.8	48.0	36.2	3.1	2.7	58.0	11.1	12.0

^a Defined as mmols of styrene oxide formed per gram of BaO deposited on the support per hour. ^b For its 4th reuse (amount of catalyst used was 0.085 g).

(2) The CaO showed the lowest performance (high conversion of TBHP but <1% conversion of styrene). The observed high conversion of TBHP is due to its decomposition over the catalyst (with the evolution of oxygen) according to the reaction:



This catalyst in fact inhibits the styrene oxidation; even in the absence of any catalyst, the styrene conversion is much higher than that obtained in the presence of the CaO catalyst.

(3) The SrO catalyst also showed a good styrene oxide selectivity (60.2%) but at a low conversion of styrene (15.2%).

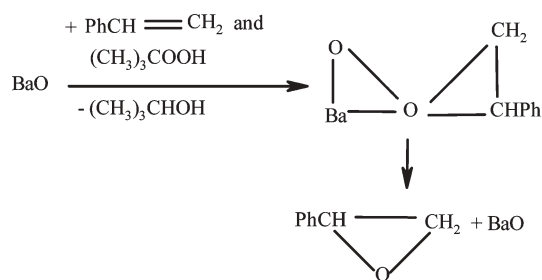
(4) Among the rare earth metal oxides, the CeO₂, Nd₂O₃ and Gd₂O₃ catalysts showed a good performance in the epoxidation of styrene. When comparing the styrene oxide yield, the three catalysts showed a somewhat comparable performance. However, they differed in their styrene conversion activity and epoxide selectivity; the CeO₂ catalyst was more active but less selective for the epoxidation. Also, the Nd₂O₃ and Gd₂O₃ showed higher styrene oxide selectivity (62.8 and 60%, respectively) but at a low styrene conversion (20 and 15.7%, respectively).

(5) The Er₂O₃ and La₂O₃ also showed high epoxide selectivity (60 and 69%, respectively) but at a very low conversion of styrene (7.4 and 3.2%, respectively). The Yb₂O₃ showed very poor epoxide selectivity and also low styrene conversion activity. The other rare earth oxides Tb₂O₃, Sm₂O₃ and Eu₂O₃ catalysts showed good epoxide selectivity (about 50%) but low styrene conversion activity (<10% conversion).

The alkaline and rare earth metal oxides showed the following order for their performance in the epoxidation (the value in brackets shows the styrene oxide yield): BaO (32%) >> Nd₂O₃ (12.6%) > CeO₂ (11.2%) > Gd₂O₃ (9.4%) > Eu₂O₃, Sm₂O₃, Tb₂O₃ and Er₂O₃ (4.4–4.9%) > MgO (3.2%) > La₂O₃ (2.2%) > without catalyst (0.8%) > Yb₂O₃ (0.4%) > CaO (0.0%).

Among the supported BaO catalysts (Table 2), the BaO/Ga₂O₃ showed the best performance (28.6% styrene oxide yield). It may be noted that both the conversion and selectivity/yield were more when anhydrous TBHP was used instead of aqueous TBHP. However, in case of the other supported BaO catalysts, the selectivity/yield was better for aqueous TBHP. Among the different supports used for the supported BaO catalyst, Ga₂O₃ was found to be the best one, probably because of its redox properties. The TOF for the BaO/Ga₂O₃ catalyst was much higher [30.9 mmol g⁻¹(BaO) h⁻¹] than that observed for the BaO (without support) catalyst [10.7 mmol g⁻¹(BaO) h⁻¹]. This is expected most probably because of the finely dispersed BaO on the support.

Both the Ga₂O₃-supported and unsupported BaO catalysts showed excellent reusability in the epoxidation (Tables 1 and 2). It is also interesting to note that the TOF of the BaO (without support) catalyst (which is an inexpensive metal oxide) is quite comparable to that [11–12 mmol g⁻¹(cat.) h⁻¹] of the very expensive supported nanosize-gold,⁸ Ti/SiO₂³ and Ti-HMS¹⁰ catalysts, reported earlier for the styrene epoxidation by TBHP.



Scheme 1

The very high activity of BaO, as compared to other alkaline and rare earth metal oxides, may be attributed to the relatively easier formation of barium peroxide species by the reaction of barium oxide with TBHP, and its further reaction with styrene (Scheme 1). Further work is necessary to understand/confirm the reaction mechanism.

The epoxidation would be a totally green process if the oxidant TBHP is replaced by H₂O₂ (which after consumption leaves water as a side product) or, more preferably, by molecular oxygen. Unfortunately, barium oxide is a highly basic metal oxide and hence has high H₂O₂ decomposition activity. It showed almost no epoxidation activity when molecular oxygen was used as an oxidizing agent.

In summary, unsupported or Ga₂O₃-supported BaO is a highly active and environmentally friendly (easily separable, reusable and non-toxic) and also inexpensive catalyst for the difficult to accomplish epoxidation of terminal alkenes, such as styrene, with high conversion and selectivity/yield.

Notes and references

- 1 D. Swern in *Organic Peroxide*, ed. D. Swern, Wiley Interscience, New York, 1971, vol. 2.
- 2 R. Van Grieken, J. L. Sotelo, C. Martos, J. L. G. Fierro, M. Lopez-Granados and R. Mariscal, *Catal. Today*, 2000, **61**, 49.
- 3 Q. Yang, S. Wang, J. Lu, G. Xiong, Z. Feng, X. Xin and C. Li, *Appl. Catal., A*, 2000, **194**, 507.
- 4 Q. Yang, C. Li, J. L. Wang, P. Ying, X. Xin and W. Shi, *Stud. Surf. Sci. Catal.*, 2000, **130**, 221.
- 5 S. B. Kumar, S. P. Mirajkar, G. C. G. Pais, P. Kumar and R. Kumar, *J. Catal.*, 1995, **156**, 163.
- 6 W. Zhang, M. Froba, J. Wang, P. Tanev, J. Wong and T. J. Pinnavaia, *J. Am. Chem. Soc.*, 1996, **118**, 9164.
- 7 J. Fu, D. Yin, Q. Li, L. Zhang and Y. Zhang, *Microporous Mesoporous Mater.*, 1999, **29**, 351.
- 8 (a) N. S. Patil, B. S. Uphade, P. Jana, S. K. Bhargava and V. R. Choudhary, *J. Catal.*, 2004, **223**, 236; (b) N. S. Patil, B. S. Uphade, P. Jana, R. S. Sonawane, S. K. Bhargava and V. R. Choudhary, *Catal. Lett.*, 2004, **94**, 89; (c) N. S. Patil, R. Jha, S. K. Bhargava and V. R. Choudhary, *Appl. Catal., A*, 2004, **275**, 87; (d) N. S. Patil, B. S. Uphade, D. G. McCulloh, S. K. Bhargava and V. R. Choudhary, *Catal. Commun.*, 2004, **5**, 681; (e) N. S. Patil, B. S. Uphade, P. Jana, S. K. Bhargava and V. R. Choudhary, *Chem. Lett.*, 2004, **33**, 400.
- 9 (a) V. R. Choudhary, N. S. Patil and S. K. Bhargava, *Catal. Lett.*, 2003, **89**, 55; (b) V. R. Choudhary, N. S. Patil, N. K. Chaudhari and S. K. Bhargava, *J. Mol. Catal. A: Chem.*, 2005, **227**, 217.
- 10 J. L. Sotelo, R. Van Grieken and C. Martos, *Chem. Commun.*, 1999, 549.

Thermal degradation of cyano containing ionic liquids

Tim J. Wooster,^{†a} Katarina M. Johanson,^b Kevin J. Fraser,^b Douglas R. MacFarlane^b and Janet L. Scott^{*a}

Received 8th May 2006, Accepted 19th June 2006

First published as an Advance Article on the web 4th July 2006

DOI: 10.1039/b606395k

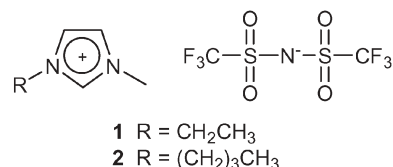
The long term thermal stability of ionic liquids containing dicyanamide or tricyanomethide anions is significantly lower than might be expected from temperature ramped TGA studies, and these anions, combined with N-based cations, yield polymeric products during thermal decomposition. Operational upper temperature limits for extended heating have been determined from isothermal decomposition measurements and extraction of $t_{0.99}$ values, and a simple relationship between onset of decomposition (determined by non-zero 1st derivative) and $T_{0.01/10}$ (the temperature at which 1% decomposition occurs in 10 h) is derived.

Introduction

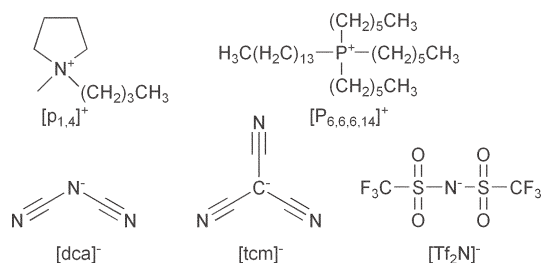
Ionic liquids (ILs) offer a number of unique possibilities to the green chemistry practitioner. The extraordinarily low vapour pressure^{1,2} (exhibited by many ILs), mitigates issues of VOC emission due to solvent evaporation and hazards associated with the use of high P equipment. The lack of vapours also renders the bulk ILs non-flammable³ and provides for product isolation by distillation of product rather than solvent.⁴ In addition, large liquid ranges obviate the need for solvent changes in multi-step processes with variable temperature regimes, and tunable miscibility and phase separation⁵ provide opportunities for new catalysts,⁶ catalyst immobilisation,⁷ reuse and recycling.⁸

Many ILs are reported to be resistant to thermal decomposition and thus suitable for high temperature applications⁹ yet, in most cases, thermal stability is inferred from measurement of weight loss by rising temperature thermogravimetric analysis (TGA). Such “thermal stability” is a useful comparative value, as the experiment to allow comparison of the decomposition temperature of a new IL is quick and easily reproduced. However, this is an overestimation of the operational upper temperature limit, at which an IL may be expected to retain its structural integrity during extended periods at elevated temperatures. For example, the widely used hydrophobic ILs [emim] bis(trifluoromethanesulfonyl)amide **1** and [bmim] bis(trifluoromethanesulfonyl)amide **2** are reported to decompose at temperatures ranging from 455¹⁰ to 234 °C¹¹ and 450¹² to 235 °C¹³ respectively. The higher values are derived from ‘step tangent’ analysis of temperature ramped TGA experiments and the lower from experiments designed to probe long term thermal stability. Each of these values is valid, as long as the method of analysis is reported, but do not serve

to answer the question “how hot and for how long can I heat my IL without it decomposing?”.



The huge range of possible combinations of cation and anion may provide ILs that are tailor-made solvents for specific applications and it is advantageous to consider how inclusion of a specific, apparently desirable, cation or anion might affect properties such as thermal stability and thus the longevity and recyclability of an IL. The effect of nucleophilicity of anions on the rate of the reverse Menschutkin reaction and the predisposition of particular side chains to Hofmann elimination has been described for ammonium and imidazolium cations,^{10,11,14} and herein we consider the effect of prolonged heating on ILs based on combinations of N,N -dialkylpyrrolidinium [P_{1,4}]⁺ and tetra-alkylphosphonium [P_{6,6,6,14}]⁺ cations, with dicyanamide [dca] and tricyanomethide [tcm] anions. Phosphonium cations are readily prepared at low cost,¹⁵ and ILs prepared from these tend to exhibit higher thermal stability than quaternary nitrogen based cations,¹⁶ while the pyrrolidinium cation is a cyclic analogue of an ammonium cation and yields ILs with low fusion



Scheme 1 Cations and anions used in this study: N -butyl, N -methylpyrrolidinium [P_{1,4}]⁺, trihexyltetradecylphosphonium [P_{6,6,6,14}]⁺, dicyanamide [dca]⁻, tricyanomethide [tcm]⁻ and bis(trifluoromethanesulfonyl)amide [Tf₂N]⁻.

^aARC Special Research Centre for Green Chemistry, Monash University, Clayton, 3800, Victoria, Australia.

E-mail: janet.scott@sci.monash.edu.au; Fax: +61 3 9905 4597; Tel: +61 3 9905 4600

^bSchool of Chemistry, Monash University, Clayton, 3800, Victoria, Australia

[†] Present address: Food Science Australia (CSIRO), Werribee, 3029, Victoria, Australia.

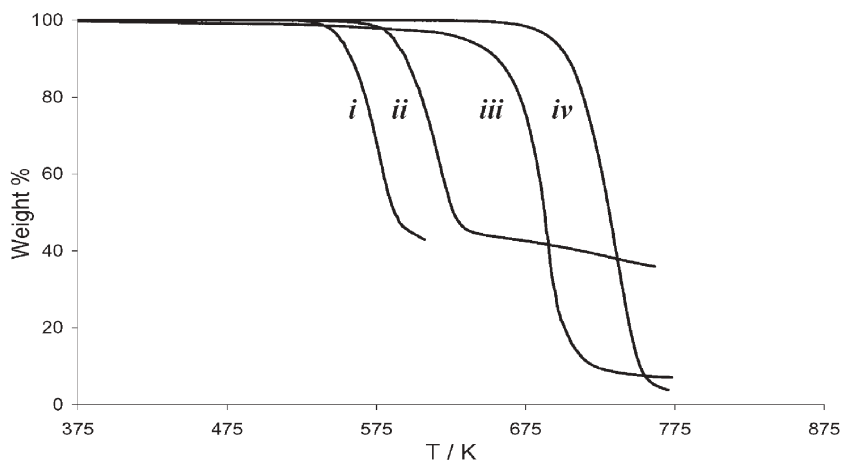


Fig. 1 Degradation measured by temperature ramped TGA (10 K min⁻¹, N₂ flow, Al pans); (i) [p_{1,4}][dca], (ii) [p_{1,4}][tcm], (iii) [P_{6,6,6,14}][dca] and (iv) [p_{1,4}][Tf₂N]. [p_{1,4}][dca] and [p_{1,4}][tcm] do not decompose completely to volatile products but yield a significant amount of charred material post analysis.

temperatures.¹⁷ Anions [dca] and [tcm] confer low viscosity on ILs¹⁸ and the bis(trifluoromethanesulfonyl)amide anion, [Tf₂N]⁻, is included for comparison with previous studies.¹¹ The combination of the cations and anions represented here allows comparison of modes of degradation.

Results and discussion

Thermal stability of the ILs was compared using both rising temperature TGA and an isothermal method. In the first case the order of thermal stability is found to be: [p_{1,4}][Tf₂N] > [P_{6,6,6,14}][dca] > [p_{1,4}][tcm] > [p_{1,4}][dca], as illustrated in Fig. 1. Although the estimation of first onset of weight loss is fraught with difficulties (leading some authors to conclude that this is not an appropriate technique for stability determination¹⁹) the determination of the temperature at which the first derivative of the weight loss vs. *T* curve is non-zero ($dw/dT \neq 0$) provides an estimate of the lowest *T* at which volatile products are evolved, under the conditions of the experiment. These values are significantly lower than those derived from step tangent analysis, Table 1, but are not an accurate measure of longer term stability at elevated temperatures.

We have previously described a method that allows determination of the temperature at which negligible decomposition occurs, even after extended heating.¹¹ This entails determination of the value *T*_{*z/y*}, the temperature at which a specific degree of composition (expressed as a fraction, *z*)

occurs in a designated period of time (*y*). This is achieved by: (a) measurement of decomposition curves under isothermal conditions at a series of temperatures; (b) extraction of rate constants, *k*, for decomposition (under the conditions of the experiment, the ILs exhibit zero order decomposition and *k* is thus simply the gradient of the linear decomposition 'curve'); (c) determination of *t*_{0.99}: the time taken for 1% decomposition to occur (analogous to *t*_{1/2}) at each temperature, from eqn (1); (d) a fit of an exponential equation (eqn (2)) to a plot of *t*_{0.99} vs. *T* and (e) extrapolation (or interpolation) to provide *T*_{*z/y*}, with acceptable degree of decomposition *z* in chosen time *y*.

We have chosen *T*_{0.01/10}, the temperature at which 1% degradation occurs in 10 h, as a good indicator of thermal stability. Depending on intended application, different degrees of degradation and/or time periods may be appropriate. (A caution: attempting to extrapolate to very lengthy periods of time is likely to lead to great loss of accuracy and it is preferable to consider treating a temperature 10 K lower than *T*_{0.01/10} as the maximum operating temperature.) Experimental data and fitted curves used in the determination of *T*_{0.01/10} for these ILs are provided in Fig. 2 and Table 1.

$$t_{1-x} = 100x/k_d \quad (1)$$

$$t_x = ae^{(-\frac{T_x}{T})} \quad (2)$$

Clearly, long-term thermal stability reflects the general trend of stability indicated in temperature ramped studies, but the ILs degrade at significantly lower temperatures than the latter imply. In the worst case, there is >200 K difference between the decomposition temperature arrived at by the step tangent method and the present one.

As determination of *T*_{*z/y*} by measurement and analysis of multiple isothermal TGA runs is experimentally onerous, it would be desirable to find a simple and direct relationship between *T*_{*z/y*} and decomposition temperature measurable by a simple rising temperature TGA experiment. Examination of the values for this small sample, reveals a linear relationship between the onset temperature of degradation (measured by

Table 1 Comparison of decomposition temperatures derived from rising temperature and isothermal TGA

IL	<i>T</i> _{decomp onset} ^a /°C ^{a,b}	<i>T</i> _{0.01/10} ^c /°C ^c	ΔT ^d /°C ^d
[p _{1,4}][dca]	283 (262)	170	149 (113)
[p _{1,4}][tcm]	319 (301)	192	174 (127)
[P _{6,6,6,14}][dca]	396 (355)	233	192 (163)
[p _{1,4}][Tf ₂ N]	435 (399)	271	235 (164)

^a Ramped TGA, step tangent analysis. ^b Numbers in brackets refer to the temperature at which $dw/dT \neq 0$. ^c From isothermal TGA, *T*_{0.01/10} is the temperature at which 1% decomposition occurs in 10 h. ^d $\Delta T = (T_{\text{decomp onset}} - T_{0.01/10})$.

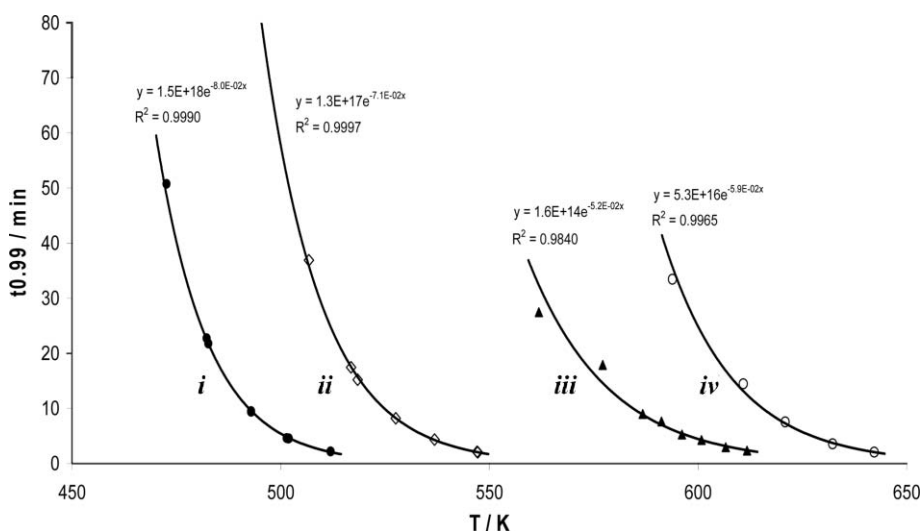


Fig. 2 $t_{0.99}$ vs. T for (i) $[p_{1,4}][dca]$, (ii) $[p_{1,4}][tcm]$, (iii) $[P_{6,6,6,14}][dca]$ and (iv) $[p_{1,4}][Tf_2N]$. Points are experimentally determined values and solid lines fitted curves.

rising temperature TGA) and isothermal TGA methods, as illustrated in Fig. 3. As a good first estimate of $T_{0.01/10}$, the decomposition T (expressed in Kelvin) $\times 0.82$ would fall on the dotted line (*i.e.* intercept = 0 rather than 12 K, the intercept of the best fit line). Thus, it is a relatively simple matter to arrive at a reasonable estimate of $T_{0.01/10}$ from a single temperature ramped TGA run, provided the first appreciable weight loss ($dw/dT \neq 0$) is used to estimate the temperature of degradation onset: $T_{0.01/10} \approx 0.82 \times T_{(dw/dT \neq 0)}$.

As might be expected, the anion $[Tf_2N]^-$ confers the greatest resistance to thermal degradation.¹⁰ While the dca anion, which has been demonstrated to provide an IL with basic character,²⁰ begins to decompose to volatile products at

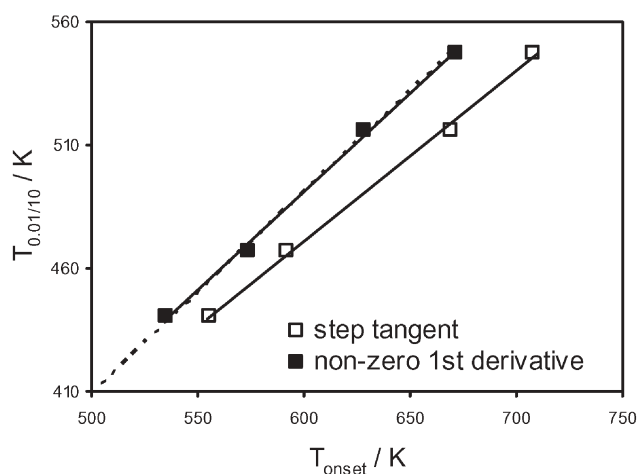
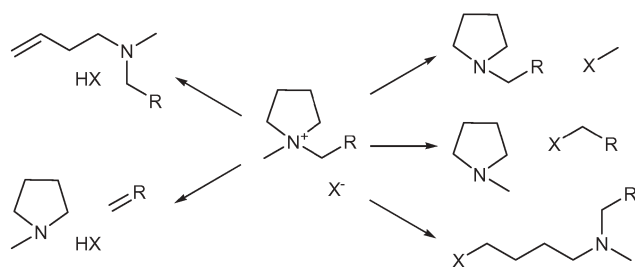


Fig. 3 Plot of $T_{0.01/10}$ vs. T_{onset} for decomposition, as measured by rising temperature TGA, using the step tangent and non-zero 1st derivative methods analysis methods. Expressions for each fitted line are: $y = 0.6902x + 56.829$ and $y = 0.798x + 11.924$, respectively. The dotted line represents the line of best fit to the non-zero 1st derivative data if the intercept is set to 0.

relatively low temperatures. Decomposition products of ILs containing the cation $[p_{1,4}]^+$, detected by pyrolysis mass spectrometry, include monoalkylated pyrroles and pyrrolidines confirming that decomposition proceeds in similar fashion to that previously reported for ILs with ammonium cations *i.e.* the Hofmann elimination and/or reverse Menshutkin reactions.^{10,11} Alkenes and trialkylphosphine degradation products emanating from the phosphonium IL indicate Hofmann elimination as the primary route for decomposition to volatile products, also in accordance with previous findings.²¹

Notably however, the *extent* of decomposition of the ILs tested differs, with anions dca, or tcm, paired with pyrrolidinium cations, yielding a large mass of charred residue post analysis. This char exhibits great resistance to further decomposition, requiring high temperatures and an oxidising atmosphere to effect removal from TGA pans. (Similar residues occur for TCM based salts with both imidazolium and pyrrolidinium cations.^{18a}) In contrast, $[P_{6,6,6,14}][dca]$ and $[p_{1,4}][Tf_2N]$ decompose completely to volatile products in a single step, leaving no significant residue. Thus, (a) both pyrrolidinium and phosphonium ILs yield some dealkylated cation residues and terminal alkenes, indicating Hofmann elimination processes and/or dealkylation reactions; (b) ILs with N containing cations and either dca or tcm anions do not decompose completely to volatile products, yielding an intractable char post degradation; (c) conversely, the IL comprising a P containing cation with dca anion decomposes completely and provides no char residue and (d) the N-containing cations yield no char when combined with non-cyano anions. Incomplete decomposition to volatile products and the occurrence of an intractable char is restricted to ILs composed of N-based cations and cyano containing anions.

Observation of incompletely decomposed samples of the char-yielding ILs reveals that a membrane forms on the surface of the sample at relatively low extents of decomposition (measured by TGA). Subsequent evolution of volatile decomposition products in the bulk of the sample results in



Scheme 2 Possible decomposition routes of pyrrolidinium ILs. Hoffman elimination (left) yields terminal alkenes and protonated anions, while the reverse of the alkylation reaction (right) provides alkylated anions.

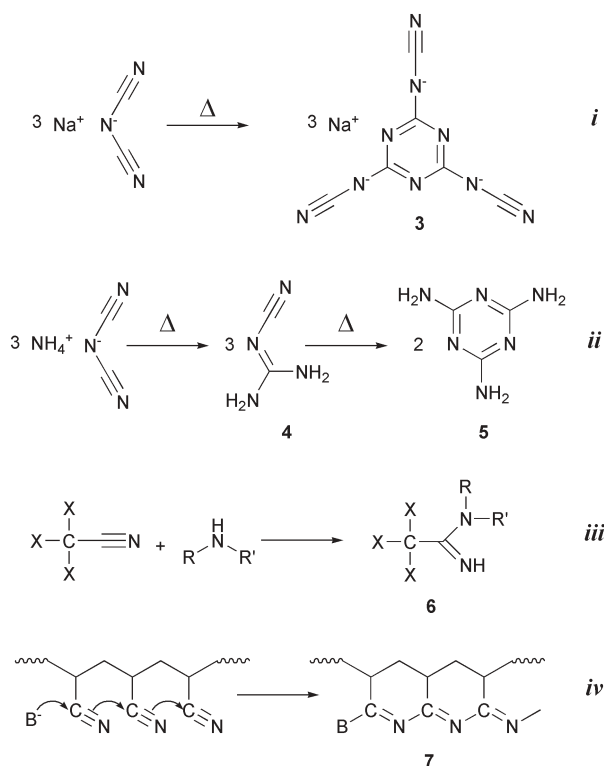
bubbling of this membranous layer. It is apparent that the sample is polymerising during decomposition.

As such polymerisation is only noted during decomposition of ILs with N-based cations and CN containing anions, possible combinations of decomposition products and cations/anions were considered. Possible decomposition products of pyrrolidinium ILs are illustrated in Scheme 2. *N*-Alkyl pyrrolidine products are detected in pyrolysis GC-MS experiments (along with pyrroles resulting from oxidation).

A number of transformations of dicyanamide salts at elevated temperatures have been described. Trimerisation of sodium dicyanamide salts, at elevated temperatures, yields tricyanomelaminates anions **3** (Scheme 3i),²² and thermally induced reaction of ammonium dicyanamide yields cyanoguanidine **4**, which on further heating transforms into melamine **5** (Scheme 3ii).²³ In addition, α -halogen substituted acetonitriles react with secondary amines, to form amidines **6** (Scheme 3iii)²⁴ and polyacrylonitrile may cyclise to a ladder polymer **7** (Scheme 3iv), either upon heating or induced by added base.²⁵

As amines are produced during decomposition of pyrrolidinium salts and have been implicated in reactions that might be expected to lead to cross-linked polymeric products, it is tempting to suggest that amine decomposition products act as initiators in a polymerisation reaction of cyano containing anions. To test this hypothesis, samples of [p_{1,3}][dca] (methylpropylpyrrolidinium dicyanamide) and [P_{6,6,6,14}][dca] were doped with *ca.* 10 mol% of either pyrrolidine or *N*-methylpyrrolidine and maintained at 50 and 100 °C for 1 week. All samples with added base show distinct colour changes on heating (Table 2), although the phosphonium IL is significantly less prone to discolouration than the pyrrolidinium IL, under these conditions.

TGA analysis of these samples after >1 week of heating in the presence of either added base, however, indicate that only the pyrrolidinium IL samples yield char, while [P_{6,6,6,14}][dca], with and without additives, decomposes completely to volatile products. Thus, the formation of the polymeric material requires the presence of both pyrrolidinium cation and CN containing anion, and is not the result of base initiated polymerisation of CN containing anions alone. A number of reaction sequences bearing similarity to Scheme 3ii and iii, possibly including attack on the products resembling **3** may be



Scheme 3 (i) Sodium and other group I metal dicyanamides trimerise to 3M⁺ tricyanomelaminates;²² (ii) ammonium dicyanamide on heating forms cyanoguanidine and thence melamine;²³ (iii) variously α -halogen substituted acetonitriles react with secondary amines, yielding amidines;²⁴ and (iv) base initiated cyclisation of polyacrylonitrile.²⁵

Table 2 Colour changes in base doped samples of dca ILs

IL	50 °C, 1 week	100 °C, 1 week
[p _{1,3}][dca]	No change	No change
[p _{1,4}][dca] + mpy ^b	Slightly red	Dark red/brown
[p _{1,4}][dca] + py ^c	Slightly red	Dark red/brown
[P _{6,6,6,14}][dca]	No change	Yellow
[P _{6,6,6,14}][dca] + mpy	No change	Orange
[P _{6,6,6,14}][dca] + py	No change	Orange

^a *N*-Methyl,*N*-propylpyrrolidinium. ^b *N*-Methylpyrrolidine.
^c Pyrrolidine.

invoked, but clarification of the route of polymerisation awaits further experiment.

Conclusions

Operational upper stability temperatures, $T_{0.01/10}$ values, for a group of ionic liquids are presented and demonstrated to be far lower than might be predicted from analysis of fast scan TGA curves by either step tangent analysis or use of the non-zero 1st differential as a measure of thermal stability. A means for estimating $T_{0.01/10}$ as simple factor applied to T_{onset} of decomposition, derived from the first onset of weight loss, is provided. Ionic liquids composed of anions containing cyano groups and N-based cations are prone to polymerisation during decomposition, but phosphonium based ionic liquids decompose completely to volatile products.

Experimental

Ionic liquids [p_{1,4}][dca], [p_{1,4}][tcm] and [p_{1,4}][Tf₂N] were synthesised as described previously.^{17,18} The phosphonium ionic liquid [P_{6,6,6,14}][dca] was used as supplied by Cytec industries.

Thermogravimetric analysis

An STA 1500 simultaneous thermal analyser (Rheometric Scientific) was used for thermal decomposition studies. The instrument was thermally calibrated using a five point melt series (indium, tin, lead, zinc and gold) and mass calibrated using a 100 mg certified mass standard. Experiments were performed in aluminium pans in a dry nitrogen atmosphere (50 ml min⁻¹). Rising temperature weight loss vs. *T* curves were obtained at heating rates of 10 °C min⁻¹ over the temperature range 25 to 500 °C. For isothermal studies, furnace PIDs were set such that there was no temperature overshoot and the following programme applied: e.g. isothermal temperature 260 °C, isothermal at 120 °C for 15 minutes then isothermal at 267 °C for *x* h. The PID configuration means that the “set temperature” is never reached, the change in temperature during the hours of isothermal heating was always less than 0.3 °C. Sample masses were typically 20–25 mg.

Weight loss vs. *t* isothermal decomposition curves were obtained for each IL in the *t*_{0.99} range 1 to 60 min. This correlated to a temperature range of: 240 to 199 °C for [p_{1,4}][dca], 274 to 215 °C for [p_{1,4}][tcm], 340 to 288 °C for [P_{6,6,6,14}][dca] and 370 to 320 °C for [p_{1,4}][Tf₂N].

In all cases kinetic analysis was restricted to a maximum mass loss of 15 weight% to avoid complications due to a change in decomposition mechanism. This is justified as it is the early stages of decomposition that are of interest. Kinetic analysis was conducted in the linear region of isothermal decomposition plots, and only after the sample had been subjected to at least 15 minutes at the nominal temperature. In all cases kinetic analysis was conducted over data collected over a minimum period of 1 h (over 120 data points), and in all cases linear fits provided *R*² values of greater than 0.995 (in most cases greater than 0.999). Linear fits involving eqn (1), eqn (2) and the Arrhenius equation were all conducted using at least 6 temperature points, and 8 points in most cases (except [p_{1,4}][Tf₂N]), most yielded *R*² values greater than 0.999 (0.995 for [p_{1,4}][Tf₂N]). All data analysis was conducted using Microsoft Excel 2000.

Pyrolysis mass spectrometry

Pyrolysis GC-MS was carried out using a Varian CP-3800 gas chromatograph, with a Varian Saturn 2200 GC/MS/MS unit. The capillary column used was a Varian factor four capillary column (VF-5 ms 30 m × 0.25 mm ID DF = 0.25). The pyrolysis probe was a CDS pyroprobe 1000 series and 2 μL of sample (diluted in CH₃Cl₂) was injected and held in the probe for 30 seconds at 500 °C. The sample was loaded onto the capillary column at 0 °C and then subjected to the following temperature ramp: heat at 8 °C min⁻¹ to 80 °C, heat from 80 °C to 200 °C at a rate of 10 °C min⁻¹, heat

from 200 °C to 325 °C at a rate of 15 °C min⁻¹ and hold isothermally for 5 min.

Acknowledgements

The authors would like to acknowledge the funding of the Australian Research Council and the gift of an ionic liquid from Cytec industries. The contributions of Vincent Verheyen, Frank Antolasic and Sally Duck for mass spectrometric data collection are also acknowledged.

References

- D. W. Armstrong, L. Zhang, L. He and M. L. Gross, *Anal. Chem.*, 2001, **73**, 3679.
- The non-distillability of ionic liquids has been widely propagated, but reports of distillation of common ionic liquids (albeit at very low pressures and slow distillation rates) are beginning to appear: M. J. Earle, J. S. S. Esperanca, M. A. Gilea, J. N. C. Lopez, L. P. N. Rebelo, J. W. Magee, K. R. Seddon and J. A. Widegren, *Nature*, 2006, **439**, 831.
- D. M. Fox, W. H. Awad, J. W. Gilman, P. H. Maupin, H. C. De Long and P. C. Trulove, *Green Chem.*, 2003, **5**, 724.
- Some recent examples include: (a) M. A. Klingshirn, R. D. Rogers and K. H. Shaughnessy, *J. Organomet. Chem.*, 2005, **690**, 3620; (b) E. Mizushima, T. Hayashi and M. Tanaka, *Green Chem.*, 2001, **3**, 76; (c) A. J. Carmichael, M. J. Earle, J. D. Holbrey, P. B. McCormac and K. R. Seddon, *Org. Lett.*, 1999, **1**, 997; (d) P. Wasserscheid and W. Keim, *Angew. Chem., Int. Ed.*, 2000, **39**, 3772.
- E. Gutowski, G. A. Broker, H. D. Willauer, J. G. Huddleston, R. P. Swatloski, J. D. Holbrey and R. D. Rogers, *J. Am. Chem. Soc.*, 2003, **125**, 6632.
- G. A. Olah, T. Mathew, A. Goeppert, B. Toeroek, I. Bucci, X.-Y. Li, Q. Wang, E. R. Martinez, P. Batamack, R. Aniszfeld and G. K. S. Prakash, *J. Am. Chem. Soc.*, 2005, **127**, 5964.
- Some recent examples include: (a) J. S. Yadav, B. V. S. Reddy, G. Baishya, K. V. Reddy and A. V. Narsaiah, *Tetrahedron*, 2005, **61**, 9541; (b) M. Johansson, A. A. Linden and J.-E. Baekkvall, *J. Organomet. Chem.*, 2005, **690**, 3614; (c) A. Serbanovic, L. C. Branco, M. Nunes da Ponte and C. A. M. Afonso, *J. Organomet. Chem.*, 2005, **690**, 3600.
- (a) M. Picquet, S. Stutzmann, I. Tkatchenko, I. Tommasi, J. Zimmermann and P. Wasserscheid, *Green Chem.*, 2003, **5**, 153; (b) S. A. Forsyth, H. Q. N. Gunaratne, C. Hardacre, A. McKeown, D. W. Rooney and K. R. Seddon, *J. Mol. Catal. A: Chem.*, 2005, **231**, 61; (c) M. T. Reetz, W. Wiesenhofer, G. Francio and W. Leitner, *Chem. Commun.*, 2002, 992.
- (a) J. L. Anderson and D. W. Armstrong, *Anal. Chem.*, 2005, **77**, 6453; (b) X. Han and D. W. Armstrong, *Org. Lett.*, 2005, **7**, 4205.
- H. L. Ngo, K. LeCompte, L. Hargens and A. B. McEwen, *Thermochim. Acta*, 2000, **357–358**, 97.
- K. Baranyai, G. B. Deacon, D. R. MacFarlane, J. M. Pringle and J. L. Scott, *Aust. J. Chem.*, 2004, **57**, 145.
- C. P. Fredlake, J. M. Crosthwaite, D. G. Hert, S. N. V. Aki and J. F. Brennecke, *J. Chem. Eng. Data*, 2004, **49**, 954.
- Z. Zhang and R. G. Reddy, *EPD Congress 2002, Fundamentals of Advanced Materials for Energy Conversion*, ed. P. R. Taylor, D. Chandra, R. G. Bautista, The Minerals, Metals & Materials Society, 2002, pp. 33.
- (a) J. E. Gordon, *J. Org. Chem.*, 1965, **30**, 2760; (b) J. O. Edwards, *J. Am. Chem. Soc.*, 1954, **76**, 1540; (c) J. R. Stuff, *Thermochim. Acta*, 1989, **152**, 421.
- C. J. Bradaric, A. Downard, C. Kennedy, A. J. Robertson and Y. Zhou, *Green Chem.*, 2003, **5**, 143.
- (a) W. Xie, R. Xie, W. Pan, D. Hunter, B. Koene, L. Tan and R. Vaia, *Chem. Mater.*, 2002, **14**, 4837; (b) S. J. Abraham and W. J. Criddle, *J. Anal. Appl. Pyrolysis*, 1985, **7**, 337.
- D. R. MacFarlane, P. Meakin, J. Sun, N. Amini and M. Forsyth, *J. Phys. Chem. B*, 1999, **103**, 4164.
- (a) S. A. Forsyth, S. R. Batten, Q. Dai and D. R. MacFarlane, *Aust. J. Chem.*, 2004, **57**, 121; (b) D. R. MacFarlane, S. A. Forsyth,

- J. Golding and G. B. Deacon, *Green Chem.*, 2002, **4**, 444; (c) D. R. MacFarlane, J. Golding, S. Forsyth, M. Forsyth and G. B. Deacon, *Chem. Commun.*, 2001, 1430.
- 19 J. Czarnecki and J. Šesták, *J. Therm. Anal. Calorim.*, 2000, **60**, 759.
- 20 (a) D. R. MacFarlane, J. M. Pringle, K. M. Johansson, S. A. Forsyth and M. Forsyth, *Chem. Commun.*, 2006, 1905; (b) S. A. Forsyth, D. R. MacFarlane, R. J. Thomson and M. von Itzstein, *Chem. Commun.*, 2002, 714.
- 21 W. Xie, R. Xie, W.-P. Pan, D. Hunter, B. Koene, L.-S. Tan and R. Vaia, *Chem. Mater.*, 2002, **14**, 4837.
- 22 E. Irran, B. Jürgens and W. Schnick, *Chem.–Eur. J.*, 2001, **7**, 5372.
- 23 B. Jürgens, H. A. Höpfe, E. Irran and W. Schnick, *Inorg. Chem.*, 2002, **41**, 4849.
- 24 J. C. Grivas and A. Taurins, *Can. J. Chem.*, 1961, **39**, 761.
- 25 (a) W. S. Batty and J. T. Guthrie, *Polymer*, 1978, **19**, 1145; (b) A. L. Endrey, *J. Polym. Sci.*, 1982, **20**, 2105.



90504090

Fast Publishing? Ahead of the field

To find out more about RSC Journals, visit

RSCPublishing

www.rsc.org/journals

Prevention of chlorinated hydrocarbons formation during pyrolysis of PVC or PVDC mixed plastics

Thallada Bhaskar,* Rie Negoro, Akinori Muto and Yusaku Sakata

Received 28th February 2006, Accepted 26th June 2006

First published as an Advance Article on the web 12th July 2006

DOI: 10.1039/b603037h

Pyrolysis of poly(vinyl chloride) (PVC) and poly(vinylidene chloride) (PVDC) mixed with poly(ethylene) (PE), poly(propylene) (PP), poly(styrene) (PS) [PE/PP/PS/PVC, and PE/PP/PS/PVDC (3 : 3 : 3 : 1)] were performed with a controlled temperature program (step I: room temperature to 330 °C; kept at 330 °C (for PVC), 300 °C (for PVDC) for 2 h; step II: 300 or 330 °C to final temperature 430 °C) and produced the chlorine free hydrocarbons in the absence of dechlorination catalyst/sorbent, which can be used as a chemical feedstock in a refinery. The temperature programs were selected based on the TGA analysis of individual plastic samples.

Introduction

The development of viable recycling technologies for waste plastics is becoming increasingly important. Feedstock recycling or liquefaction of waste plastics has more advantages than mechanical recycling or energy recovery, and the volume of harmful gases produced is much lower than that of the incineration process. Liquefaction of waste plastics is one of the best methods for preserving valuable petroleum resources. Municipal waste plastic (MWP) is a mixture of halogenated plastics (PVC and PVDC) and non-halogenated plastics (PP, PE, PS, PET *etc.*). There has been a plethora of research work and monographs on the feedstock recycling of plastic wastes,¹ new pathways in plastic recycling and the current status of plastics recycling,² pyrolysis of individual and mixed plastics such as PP/PE, PP/PS, PE/PS mixed with and without PVC plastics into liquid products by using various catalysts and sorbents.^{3–5} It is well known that the pyrolysis of mixed plastics containing PVC or PVDC produces inorganic (HCl) and subsequently organic chlorine compounds during pyrolysis.^{3,4} Halogenated (Cl, Br) compounds in the liquid products obviates its use as a feedstock in refinery or fuel oil. The oil fraction from pyrolysis can be used in the petrochemical plants, if the chlorine does not exceed 100 ppm. The liquefaction of halogenated mixed waste plastic requires a suitable dehalogenation catalyst or sorbent for the effective removal of halogenated compounds from the plastic derived oils (PDO). In our earlier publications, we have reported the development of novel calcium based sorbents for the dehalogenation process.⁶ However, the preparation of such sorbents and treatment after the pyrolysis process has to be processed in a safe and effective manner. One of the twelve green chemistry principles shows that it is better to prevent waste than to treat or clean up waste after it has been created. The use of plastics cannot be avoided but the formation of

toxic and corrosive compounds during recycling of halogenated mixed plastics can be.

In the present investigation, we report for the first time the pyrolysis of PVC or PVDC mixed plastics PE/PP/PS and prevent the formation of chlorinated hydrocarbons in pyrolysis. The TG/DTA analysis of sample plastics was performed to understand the decomposition behavior and temperature. In the detailed investigation on the distribution of degradation products, chlorine analysis in various degradation products was discussed with the analysis of gas chromatographs with the flame ionization detector and the atomic emission detector.

Results and discussion

The pyrolysis of 3P/PVC and 3P/PVDC was performed using the temperature profiles shown in Fig. 1. The mixture of PE, PP and PS (1 : 1 : 1 by weight) is abbreviated as 3P. The pyrolysis products were classified into three groups: gas, liquid, and solid residue. Table 1 shows the yield of degradation products from 3P/PVC and 3P/PVDC, and average carbon number (C_{np}) and density of liquid products. The pyrolysis of PVC⁷ produced *ca.* 4% of liquid products; PVDC⁸ could not produce any liquid products, and the major

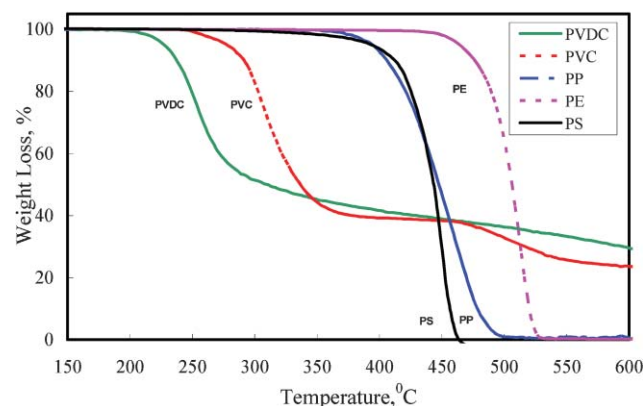


Fig. 1 TGA analysis of PVDC, PVC, PP, PE, and PS samples.

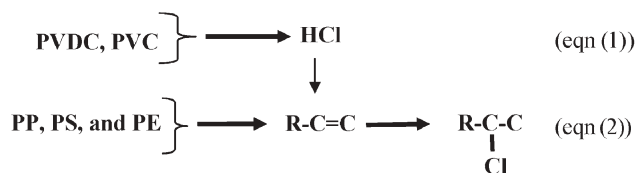
Department of Applied Chemistry, Graduate School of Natural Science and Technology, Okayama University, 3-1-1Tshushima Naka, 700-8530, Okayama, Japan. E-mail: bhaskar@cc.okayama-u.ac.jp; Fax: +81 86 251 8082; Tel: +81 86 251 8081

Table 1 Product yields and properties of liquid product from 3P/PVC and 3P/PVDC mixed plastics

Sample	Method	Yield of degradation products (wt%)			Liquid products	
		Liquid (L)	Gas ^a (G)	Residue (R)	C _{np} ^b	Density/g cm ⁻³
3P/PVC	Mode1	65.4	28.7	5.9	12.3	0.799
	Mode2	60.9	28.2	10.9	11.2	0.801
3P/PVDC	Mode3	64.1	28.4	7.5	11.2	0.801

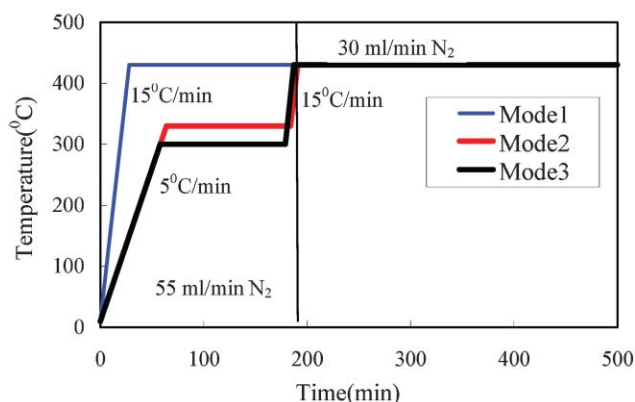
^a G = 100 - (L + R). ^b Average carbon number of liquid product.

portion was gas (68 wt%) and residue (32 wt%), due to the presence of high chlorine content in PVC (53.2 wt%) and PVDC (73.2 wt%). Pyrolysis of 3P/PVC produced a higher yield of liquid products in the single step rate of heating (mode 1) than the two step rate of heating (mode 2) to the pyrolysis temperature (430 °C). We have previously reported the thermal and catalytic degradation of PE/PVC, PP/PVC, and PS/PVC by silica–alumina catalysts and dechlorination by iron oxides (FeOOH and Fe₃O₄ sorbents).^{3,4} Bhaskar *et al.*^{6,9,10} reported the liquefaction of mixed plastics (PE/PP/PS) containing PVC and dechlorination of liquid products by calcium carbonate carbon composite (Ca–C) sorbent and optimized the reaction conditions with simulated HCl gas. In all the above reports, the single step rate of heating and different catalysts/sorbents were employed for the removal of halogenated hydrocarbons from PDO. It can be understood from TGA studies that the decomposition temperature of PVC, PVDC is much lower than for PE, PP, and PS which are main components in municipal waste plastics. There has been a plethora of research work on the decomposition behavior of PVC and PVDC by TG analysis and our TGA decomposition profiles are comparable^{11–14} (Fig. 2). The first decomposition step is the loss of HCl from either PVC or PVDC. The formation of chlorinated hydrocarbons during PVC, PVDC mixed plastics pyrolysis can be followed from Scheme 1. The HCl evolved from the PVC or PVDC reacts with the olefinic hydrocarbons produced from the commingled plastics such as PE, PP and PS. Based on the decomposition behavior of PVC and PVDC samples, the temperature profiles were modified from mode 1 (single step) to controlled pyrolysis (two step) to remove the HCl evolved from the PVC or PVDC from the

**Scheme 1** Plausible steps for the formation of chlorinated hydrocarbons during pyrolysis of PVC, PVDC mixed plastics.

reactor and avoid the formation of chlorinated hydrocarbons in the liquid products. In mode 1 pyrolysis (single step), the formation of chlorinated hydrocarbons due to the addition of HCl (evolved from PVC or PVDC) with the olefinic hydrocarbons (PE or PP or PS) is possible; however in mode 2 (two step) pyrolysis, by keeping at the low pyrolysis temperature (300 or 330 °C) for 2 h, the evolved HCl will be carried out from the reactor with the carrier gas (N₂) and the formation of chlorinated hydrocarbons is avoided. As can be seen from Scheme 1 and Fig. 2, the two step pyrolysis *i.e.*, decomposition of the PVC or PVDC plastics in the first stage (Scheme 1, eqn (1)) and removal of the HCl from the reactor environment and subsequently increasing the reactor temperature to the final pyrolysis temperature (Scheme 1, eqn(2)) was performed. In addition to the two step pyrolysis, the quantity of carrier gas flow was increased during step 1 pyrolysis for the complete removal of hydrogen chloride from the reactor. The initial PVDC decomposition temperature is lower than the PVC decomposition temperature and the step 2 temperature for PVDC was fixed at 300 °C and 330 °C for PVC.

The distribution of chlorine in different pyrolysis products from 3P/PVC and 3P/PVDC is summarized in Table 2. Table 2 shows that the pyrolysis of 3P/PVC with mode 1 produced the liquid hydrocarbons with 390 ppm of chlorine and gaseous products with 5890 ppm. The major organic chlorine compounds in liquid products were 2-chloro-2-methylpropane,

**Fig. 2** Temperature program(s) for the pyrolysis of 3P/PVC and 3P/PVDC.**Table 2** The distribution of chlorine content in various pyrolyses of products of 3P/PVC and 3P/PVDC

Sample 10 g	Temperature program	Chlorine		
		Liquid (ppm)	Gas (ppm)	Residue/mg
3P/PVC	Mode1	390	5890	25
	Mode2 STEP1 STEP2	— n.d.	6370 70	39
3P/PVDC	Mode3 STEP1 STEP2	— 15	6760 990	74

n.d.: not detected

2-chloro-2-methylpentane, α -chloroethylbenzene and 2-chloro-2-phenylpropane. The nature of chlorinated hydrocarbons formed with the PE, PP or PS mixed plastics with PVC was well described by Shiraga *et al.*³ and Uddin *et al.*⁴ Single step heating up to the pyrolysis temperature produced liquid hydrocarbons with chlorine, and chlorine in the residue is low. During the two step pyrolysis of 3P/PVC and 3P/PVDC (mode 2 and mode 3), there are no oil (liquid) products up to step 1 as the evolved gaseous product is HCl and the non-condensable hydrocarbons up to C₁–C₅. In step 2 for both 3P/PVC (330 °C for 2 h) and 3P/PVDC (300 °C for 2 h) pyrolysis, the major portion of chlorine (1 g PVC contains 524 mg of chlorine and PVDC contains 732 mg of chlorine) content in the mixed plastics samples has been removed in the form of HCl. It is clear from Table 2 that the two step pyrolysis produced the halogen free hydrocarbons from the 3P/PVC mixed plastics and pyrolysis of 3P/PVDC produced the liquid products with a concentration of 15 ppm chlorine. The plastic derived oil with less than 100 ppm of chlorine can be acceptable to use as a feedstock in refinery or fuel oil.

The liquid products were analyzed by gas chromatography equipped with an atomic emission detector (AED) for the quantitative analysis of chlorinated hydrocarbons. Fig. 3 illustrates the chromatograms of selective chlorine compounds in liquid products obtained from 3P/PVC (mode 1 and mode 2) and 3P/PVDC (mode 3). It is clear from Fig. 3 that the chlorinated hydrocarbons were completely removed by the two step pyrolysis of 3P/PVC and 3P/PVDC. The traces of chlorinated hydrocarbons found in 3P/PVDC liquid products were *ca.* 15 ppm.

Experimental

Materials

High-density polyethylene (PE) was obtained from Mitsui Chemical Co. Ltd., Japan; polypropylene (PP) from Ube

Chemical Industries Co. Ltd., Japan; polystyrene (PS) from Asahi Kasei Industries Co., Ltd., Japan; and poly(vinylidene chloride) (PVDC) from Geon Chemical Co. Ltd. The grain sizes of PP, PE, PS and PVC were about 3 mm \times 2 mm. The mixture of PP, PE, PS was abbreviated as 3P in the manuscript. The chlorine content in PVC was 52.4 wt% and PVDC was 73.2 wt%.

Pyrolysis procedure

Pyrolysis of 3P/PVC and 3P/PVDC where 3P is PE (3 g) + PP (3 g) + PS (3 g) was performed in a glass reactor (length: 350 mm; id 30 mm) under atmospheric pressure by batch operation with identical experimental conditions. Briefly, 10 g of mixed plastics were loaded into the reactor for thermal degradation and in the second reactor quartz grains (thermal) were charged and kept at 350 °C. The quartz grains were used to maintain the similar space velocities in the absence of catalyst/sorbent for dehalogenation. The rate of heating used in Mode 1 and step 2 of Mode 2 and Mode 3 was 15 °C min⁻¹; in step 1 of Mode 2 and Mode 3 it was 5 °C min⁻¹. For the pyrolysis of 3P/PVC (mode 1), the reactor temperature was increased from room temperature to the final temperature of 430 °C and kept till the end of pyrolysis experiment (nitrogen flow 30 ml min⁻¹). For the pyrolysis of 3P/PVC (mode 2), the reactor temperature was increased from room temperature to 330 °C (nitrogen flow 55 ml min⁻¹) and kept for 2 h at 330 °C (nitrogen flow 55 ml min⁻¹) and then subsequently increased to a final temperature of 430 °C and kept till the end of the pyrolysis experiment (nitrogen flow 30 ml min⁻¹). For pyrolysis of 3P/PVDC, the reactor temperature was increased from room temperature to 300 °C (nitrogen flow 55 ml min⁻¹) and kept for 2 h at 300 °C (nitrogen flow 55 ml min⁻¹) and then subsequently increased to a final temperature of 430 °C and kept till the end of the pyrolysis experiment (nitrogen flow 30 ml min⁻¹). A schematic experimental setup for the pyrolysis of mixed plastics and the detailed analysis procedure can be found elsewhere.^{6,8} The TG analysis was performed on Shimadzu TGA-51 instrument using approximately 20–30 mg of plastic sample in a nitrogen atmosphere (50 ml min⁻¹). The rate of heating was 5 °C min⁻¹ (from room temperature) and the maximum temperature was 800 °C.

Analysis procedure

The quantitative analysis of the liquid products (collected once at the end of the experiment) was performed using a gas chromatograph equipped with a flame ionization detector (FID; YANACO G6800) to obtain the quantity of hydrocarbons and carbon number distribution of the liquid products. The distribution of chlorine compounds and the quantity of chlorine content (organic) in liquid products was analyzed by a gas chromatograph equipped with atomic emission detector (AED; HP G2350A; HP-1; capillary column with cross-linked methyl siloxane; 25 m \times 0.32 mm \times 0.17 μ m). 1,2,4-Trichlorobenzene was used as internal standard for the quantitative determination of chlorine content in the GC-AED analysis. The amount of Cl content in the water trap was analyzed using an ion chromatograph (DIONEX, DX-120 Ion Chromatograph). The quantitative

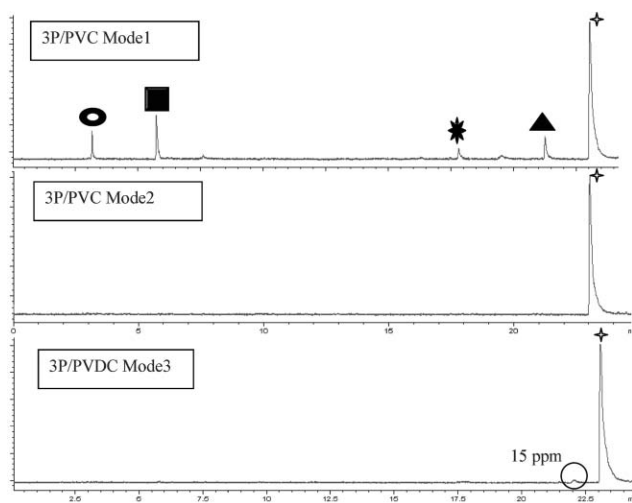


Fig. 3 GC-AED chromatograms for selective chlorine compounds. ☆ Internal standard for chlorine (1,2,4-trichloro benzene), ▲ 2-chloro-2-phenyl propane, ★ α -chloro ethyl benzene, ■ 2-chloro-2-methyl pentane, ○ 2-chloro-2-methyl propane.

determination of chlorine in the residue was measured using a combustion flask and then subjected to ion chromatography.

The gas chromatograph equipped with a mass selective detector analysis was performed [GC-MSD; HP 5973; column, HP-1; capillary column with cross-linked methyl siloxane, 25 m × 0.32 mm × 0.17 μm] for the identification of various chlorinated hydrocarbons in liquid products. The composition of the liquid products was characterized using C-NP grams (C stands for carbon and NP from normal paraffin) and Cl-NP gram (Cl stands for chlorine). The curves were obtained by plotting the weight percent of Cl, which was in the liquid products against the carbon number of the normal paraffin determined by comparing the retention times from GC analysis using a non-polar column. In brief, the NP gram is a carbon number distribution of hydrocarbons derived from the gas chromatogram based on boiling points of a series of normal paraffin. Further details on the NP gram can be found elsewhere.¹⁵

Conclusions

The pyrolysis of 3P/PVC, and 3P/PVDC was performed in a two step temperature program by keeping the final pyrolysis temperature as 430 °C at atmospheric pressure. The formation of chlorinated hydrocarbons in both 3P/PVC and 3P/PVDC was higher in single step pyrolysis. The two step temperature program eliminated the hydrogen chloride from the reactor (step 1) and avoided the formation of chlorinated hydrocarbons in the liquid products (step 2). The two step pyrolysis produced the plastic derived oils without halogenated hydrocarbons (less than 15 ppm). The optimization of pyrolysis parameters is crucial to avoid/decrease the formation of halogenated hydrocarbons, as proposed in Scheme 1.

Acknowledgements

The authors thank the Ministry of Education, Culture, Sports, Science and Technology, Japan and the Centre of Excellence Program for the 21st Century—Strategic Solid Waste Management for Sustainable Society at Okayama University for financial support to carry out the research.

References

- 1 J. Aguado and D. Serrano in, *RSC Clean Technology Monographs, on Feedstock Recycling of Waste Plastic*, ed. J. H. Clark, Royal Society of Chemistry, Cambridge, 1999.
- 2 W. Kaminsky, *Angew. Makromol. Chem.*, 1995, **232**, 151.
- 3 Y. Shiraga, M. A. Uddin, A. Muto, M. Narazaki, Y. Sakata and K. Murata, *Energy Fuels*, 1999, **13**, 2, 428.
- 4 M. A. Uddin, Y. Sakata, Y. Shiraga, A. Muto and K. Murata, *Ind. Eng. Chem. Res.*, 1999, **38**, 4, 1406.
- 5 Y. Sakata, M. A. Uddin, A. Muto, M. Narazaki, K. Koizumi, K. Murata and M. Kaji, *Ind. Eng. Chem. Res.*, 1998, **37**, 2889.
- 6 T. Bhaskar, T. Matsui, J. Kaneko, M. A. Uddin, A. Muto and Y. Sakata, *Green Chem.*, 2002, **4**, 372.
- 7 T. Bhaskar, M. A. Uddin, K. Kaneko, K. Kusaba, T. Matsui, A. Muto, Y. Sakata and K. Murata, *Energy Fuels*, 2003, **17**, 75.
- 8 Y. Sakata, M. A. Uddin, K. Koizumi and K. Murata, *Polym. Degrad. Stab.*, 1996, **53**, 111.
- 9 T. Bhaskar, M. Tanabe, A. Muto and Y. Sakata, *Polym. Degrad. Stab.*, 2005, **89**, 38.
- 10 T. Bhaskar, T. Matsui, K. Nitta, M. A. Uddin, A. Muto and Y. Sakata, *Energy Fuels*, 2002, **16**, 1533.
- 11 T. Akama, T. Yoshioka, T. Suzuki, M. Uchida and A. Okuwaki, *Chem. Lett.*, 2001, 540.
- 12 R. Knumann and H. Bockhorn, *Combust. Sci. Technol.*, 1994, **101**, 285.
- 13 I. C. McNeill, L. Memetea and W. J. Cole, *Polym. Degrad. Stab.*, 1995, **49**, 181.
- 14 M. Blazsó and E. Jakab, *J. Anal. Appl. Pyrolysis*, 1999, **49**, 125.
- 15 K. Murata, Y. Hirano, Y. Sakata and M. A. Uddin, *J. Anal. Appl. Pyrolysis*, 2002, **65**, 71.

A kinetic study on the decomposition of 5-hydroxymethylfurfural into levulinic acid

B. Girisuta, L. P. B. M. Janssen and H. J. Heeres*

Received 21st December 2005, Accepted 22nd May 2006

First published as an Advance Article on the web 22nd June 2006

DOI: 10.1039/b518176c

Levulinic acid (LA), accessible by the acid catalyzed degradation of biomass, is potentially a very versatile green intermediate chemical for the synthesis of various (bulk) chemicals for applications like fuel additives, polymers, and resin precursors. We report here a kinetic study on one of the key steps in the conversion of biomass to levulinic acid, *i.e.* the reaction of 5-hydroxymethylfurfural (HMF) to levulinic acid. The kinetic experiments were performed in a temperature window of 98–181 °C, acid concentrations between 0.05–1 M, and initial HMF concentrations between 0.1 and 1 M. The highest LA yield was 94% (mol/mol), obtained at an initial HMF concentration of 0.1 M and a sulfuric acid concentration of 1 M. The yield at full HMF conversion is independent of the temperature. An empirical rate expression for the main reaction as well as the side reaction to undesired humins was developed using the power law approach. Agreement between experimental and model data is good. The rate expressions were applied to gain insights into optimum process conditions for batch processing.

1. Introduction

Biomass has been identified as an important source for bio-fuels and chemical products.¹ Biomass is abundantly available, for instance in the form of waste from agricultural, forest and industrial activities (*e.g.* paper industry). A substantial amount of research activity is currently undertaken world-wide to identify attractive chemical transformations to convert biomass into organic (bulk) chemicals, and to develop economically feasible processes for these transformations on a commercial scale. An attractive option is the conversion of lignocellulosic biomass into levulinic acid (4-oxopentanoic acid) by acid treatment.^{2–6}

Levulinic acid is a very versatile building block for the synthesis of (bulk) chemicals for applications like fuel additives, polymers, and resin precursors.⁷ Several reviews have been published describing the properties and potential industrial applications of levulinic acid and its derivatives.^{8–12}

On a molecular level, the conversion of a typical lignocellulosic biomass like wood or straw to levulinic acid follows a complicated reaction pathway,¹³ involving several intermediate products (see Fig. 1). The simplified reaction scheme given in Fig. 1 does not explicitly show the reactions leading to undesired black insoluble polymeric materials also known as humins. As part of a larger project to develop efficient reactor configurations for the conversion of biomass to levulinic acid, we have initiated a study to determine the kinetics of all steps involved (Fig. 1). A stepwise approach was followed, starting with the conversion of 5-hydroxymethylfurfural (HMF) to levulinic acid (LA).

A number of experimental studies have been reported on the kinetics of the acid catalyzed HMF decomposition to levulinic acid. The first study was carried out by Teunissen in 1930.¹⁴ Reactions were carried out at 100 °C using various acid catalysts with acid concentrations ranging between 0.1 and 0.5 N. Heimlich and Martin¹⁵ studied the reaction in a temperature range of 100–140 °C using hydrochloric acid (0.35 N) as catalyst. McKibbins *et al.*¹⁶ investigated the influence of sulfuric acid concentration (0.025–0.4 N) and temperature (160–220 °C) on the decomposition rate of HMF to levulinic acid. In all these studies, the effect of the initial concentration of HMF was not determined and first order kinetics was assumed. Kuster and van der Baan¹⁷ studied the influence of the initial HMF concentration on the kinetics of HMF decomposition at 95 °C using various concentrations (0.5–2.0 N) of hydrochloric acid. The most recent kinetic study was reported by Baugh and McCarty,¹⁸ who used dilute acid as catalyst at variable pH (2–4) and temperature (170–230 °C). Table 1 summarizes the results from previous kinetic studies on the acid catalysed reaction of HMF to levulinic acid.

On the basis of these data, it may be concluded that a general kinetic expression for a broad range of temperatures,

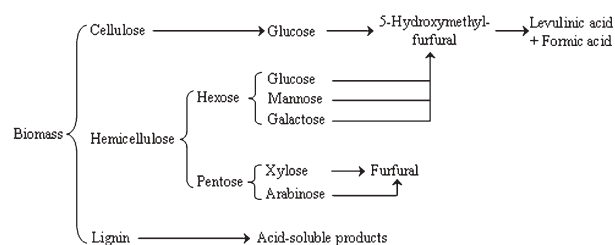


Fig. 1 Simplified reaction scheme for the conversion of lignocellulosic biomass into levulinic acid.

Department of Chemical Engineering, University of Groningen, Nijenborgh 4, Groningen, 9747 AG, Netherlands.
E-mail: H.J.Heeres@rug.nl; Fax: +31 50 363 4479; Tel: +31 50 363 4174

Table 1 Literature overview of rate of reaction for the acid catalysed decomposition of HMF

T	C_{acid}	$C_{\text{HMF},0}$	$R_{\text{HMF}}/\text{mol L}^{-1} \text{min}^{-1}$	Reference
100 °C	$C_{\text{H}_2\text{SO}_4} = 0.1\text{--}0.5 \text{ N}$ $C_{\text{HCl}} = 0.1\text{--}0.5 \text{ N}$	0.08–0.09 M	$R = 6.8 \times 10^{-3} C_{\text{H}^+} C_{\text{HMF}}$	14
100–140 °C	$C_{\text{HCl}} = 0.35 \text{ M}$	n.a.	$R = 1.1 \times 10^{11} \exp\left(-\frac{96000}{RT}\right) C_{\text{HMF}}$	15
160–220 °C	$C_{\text{H}_2\text{SO}_4} = 0.025\text{--}0.4 \text{ N}$	0.061–0.139 M	$R = 2.4 \times 10^{11} \alpha_{\text{H}} C_{\text{A}} \exp\left(-\frac{96800}{RT}\right) C_{\text{HMF}}^a$	16
95 °C	$C_{\text{HCl}} = 0.5\text{--}2.0 \text{ N}$	0.25–1 M	$R = 0.001(C_{\text{H}^+})^{1.2} C_{\text{HMF}}$	17
170–230 °C	pH = 2–4	0.024 M	$R = (1300 + 4.1 \times 10^6 C_{\text{H}^+}) \exp\left(-\frac{55900}{RT}\right) C_{\text{HMF}}$	18

^a α_{H} represents a correction factor given in the original paper and C_{A} is expressed in normality (N).

catalysts and initial HMF concentrations is lacking. In addition, all earlier studies focus on the overall decomposition of HMF without discriminating between the rates of the main reaction to LA and formic acid (FA) and the side reaction to humins. In this paper, the kinetics of the acid catalyzed decomposition of HMF in a broad range of process conditions will be reported, including the kinetics of the reactions leading to humin. The results will be applied to gain insights into the optimum process conditions to reduce humin formation and to achieve the highest LA yield. Furthermore, the results will also be used as input for a full kinetic model for the acid catalyzed hydrolysis of biomass to levulinic acid. These results will be reported in due course.

2. Experimental

2.1 Experimental procedure

All chemicals used in this study were of analytical grade and used without purification. HMF was obtained from Fisher Scientific BV (Netherlands). All acid catalysts were purchased from Merck GmbH (Darmstadt, Germany). Milli-Q water was used to prepare the various solutions.

The reactions were carried out in glass ampoules (inside diameter of 3 mm, wall thickness of 1.5 mm, and length of 15 cm). The ampoules were filled with approximately 0.5 cm³ of reaction mixture and sealed using a torch. The sealed ampoules were placed in a special rack that can hold up to 20 ampoules, and placed in a constant temperature oven (± 1 °C). At different reaction times, ampoules were taken from the oven and quenched into an ice-water bath (4 °C) to stop the reaction. The reaction mixture was taken out of the ampoule and diluted with water to 10 cm³. Insoluble humins were separated using a 0.2 μm cellulose acetate filter (Schleicher & Schuell MicroScience GmbH, Dassel, Germany). The particle-free solution was subsequently analyzed using High Performance Liquid Chromatography (HPLC).

2.2 Analytical methods

The composition of the liquid phase was determined using an HPLC system consisting of a Hewlett Packard 1050 pump, a Bio-Rad organic acid column Aminex HPX-87H, and a Waters 410 differential refractometer. The mobile phase consisted of an aqueous solution of sulfuric acid (5 mM) at

flow rate of 0.55 cm³ min⁻¹. The column was operated at 60 °C. The analysis for a sample was complete within 40 minutes. A typical chromatogram is shown in Fig. 2. The concentrations of each compound in the product mixture were determined using calibration curves obtained by analysing standard solutions with known concentrations.

The gas composition was analyzed with gas chromatography (Varian Micro GC CP-2003) equipped with a TCD cell using a Porapak Q column operated at 75 °C. Helium was used as the carrier gas. Humin particles were analyzed using Field Emission Scanning Electron Microscopy (FESEM) on a JEOL 6320F. C and H elemental analyses were performed at the Analytical Department of the University of Groningen using an automated Euro EA3000 CHNS analyser.

2.3 Heat transfer experiments

At the start of the reaction, the reaction takes place non-isothermally due to heating-up of the contents of the ampoule from room temperature to the oven temperature. To gain insights in the time required to heat up the reaction mixture and to compensate for this effect in the reaction modelling studies, the temperature inside the ampoules as a function of the time during the heat up process were determined experimentally. For this purpose, an ampoule equipped with

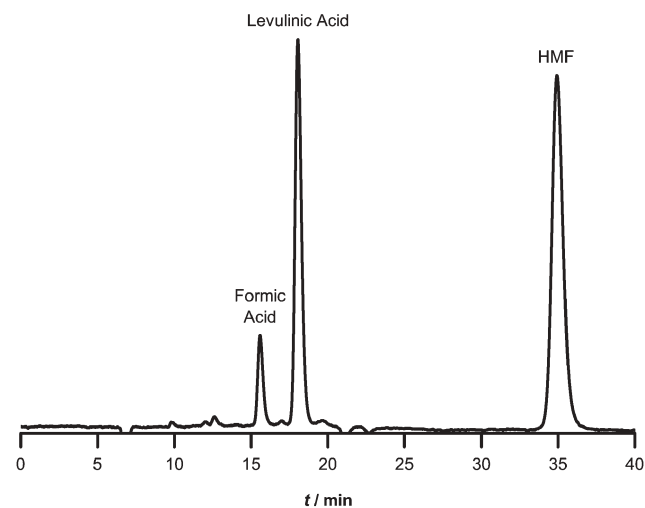


Fig. 2 HPLC chromatogram for HMF decomposition.

a thermocouple was filled with a representative reaction mixture (1 M HMF in water without acid). The ampoule was then closed tightly using a special bolt and screw system to prevent evaporation of the liquid. The ampoule was subsequently placed in the oven at a specified temperature and the temperature of the reaction mixture was followed in time. Before and after an experiment, the amount of liquid inside the ampoule was measured to ensure that evaporation of the liquid did not occur.

The experimental profiles at different temperatures were modelled using a heat balance for the contents in an ampoule:

$$\frac{d(MC_p T)}{dt} = UA_t(T_{\text{oven}} - T) \quad (1)$$

When assuming that the heat capacity of reaction mixture is constant and not a function of temperature, rearrangement of eqn (1) will give:

$$\frac{dT}{dt} = \frac{UA_t}{MC_p}(T_{\text{oven}} - T) = h(T_{\text{oven}} - T) \quad (2)$$

Solving the ordinary differential eqn (2) with the initial values $t = 0$, $T = T_i$ leads to:

$$T = T_{\text{oven}} - (T_{\text{oven}} - T_i)\exp^{-ht} \quad (3)$$

The value of h was determined by fitting all experimental data at different oven temperatures (100–160 °C) using a non-linear regression method, and was found to be 0.596 min⁻¹. Fig. 3 shows an experimental and modelled temperature profile performed at an oven temperature of 100 °C. Eqn (3) was incorporated in the kinetic model to describe the non-isothermal behaviour of the system at the start of the reaction.

The effect of the chemical reaction on the heating profiles was modelled using the mass and energy balance (eqn (1) with an additional term for the chemical reaction) for a batch reactor. The heating profiles did not change significantly when taking into account an additional term for chemical reaction. Therefore, the heating profiles were not compensated for the occurrence of chemical reaction.

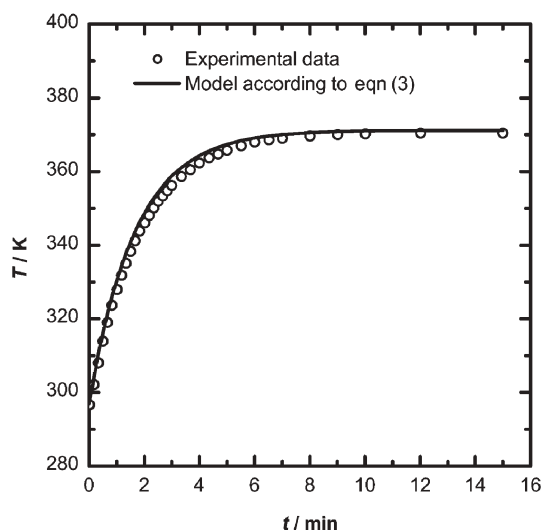


Fig. 3 Heating profile of the reaction mixture at $T_{\text{oven}} = 100$ °C.

2.4 Determination of the kinetic parameters

The kinetic parameters were estimated using a maximum likelihood approach, which is based on minimization of errors between the experimental data and the kinetic model. Details about this procedure can be found in the literature.^{19,20} Minimization of objective function is initiated by providing initial guesses for each kinetic parameter. The best estimates were obtained using the MATLAB toolbox `fminsearch`, which is based on the Nelder–Mead optimization method.

The concentrations of HMF and LA vary considerably from experiment to experiment and within an experimental run. As a result, the high concentrations will dominate the error calculation when minimizing the objective function. To solve this problem, the concentrations of HMF and LA were scaled and transformed to the HMF conversion and the LA yield, respectively. By definition,²¹ the HMF conversion (X_{HMF}) and LA yield (Y_{LA}) vary between 0–1, and are expressed as:

$$X_{\text{HMF}} = \frac{(C_{\text{HMF},0} - C_{\text{HMF}})}{C_{\text{HMF},0}} \quad (4)$$

$$Y_{\text{LA}} = \frac{(C_{\text{LA}} - C_{\text{LA},0})}{C_{\text{HMF},0}} \quad (5)$$

3. Results and discussion

3.1 Acid screening

At the start of the research, a number of acid catalysts were screened (H_3PO_4 , oxalic acid, HCl, H_2SO_4 , and HI) to determine the preferred acid for further studies. All screening experiments were conducted at 98 °C and 1 hour reaction time using a $C_{\text{HMF},0}$ of 0.1 M and acid concentrations of 1 M. The results are shown in Fig. 4. H_3PO_4 and oxalic acid gave very low HMF conversions (<25%). In addition, the LA yields were also very low (5–9%). The application of HI resulted in very high HMF conversion, unfortunately accompanied with very low LA yields. Major by-products were humins and some as yet unidentified soluble products. Of all acids screened, HCl and H_2SO_4 gave the best results. Conversions were between 52–57%, and the yields between 48–53%. H_2SO_4 showed a slightly better performance than HCl and was used in subsequent experiments.

3.2 Reaction products

The acid catalysed decomposition of 5-hydroxymethylfurfural (HMF, **1**) to levulinic acid (LA, **2**) and formic acid (FA, **3**) is schematically presented in Scheme 1.

A typical reaction profile of the acid catalysed HMF decomposition reaction is given in Fig. 5. In line with the reaction stoichiometry, the LA and FA co-product were always produced in a 1 : 1 molar ratio. This implies that both LA and FA are stable under the reaction conditions employed and do not decompose to other products (*vide infra*).

Possible by-products, other than FA, are insoluble dark-brown substances, known as humins, and gas-phase components due to thermal degradation of reactants/products. Humins were formed in all experiments. The elemental

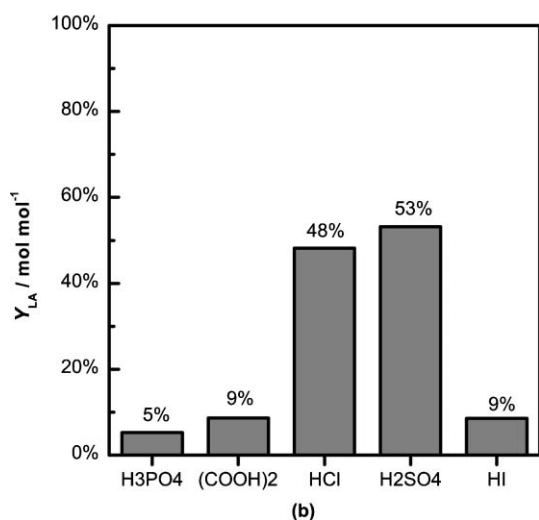
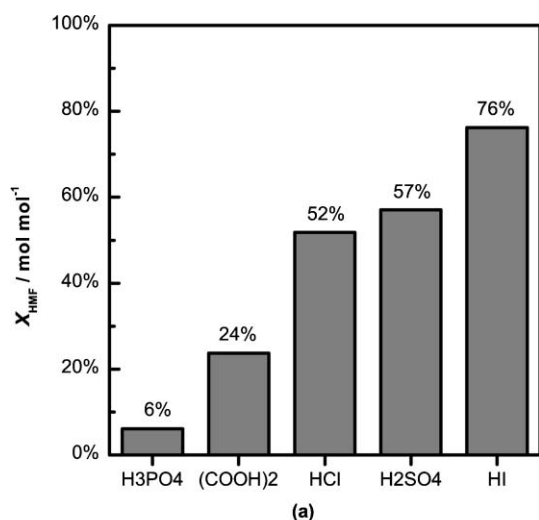
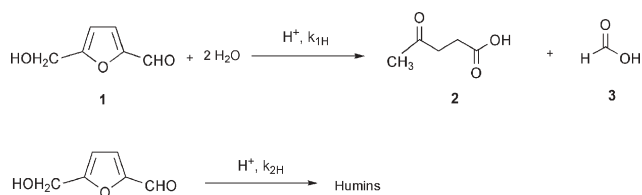


Fig. 4 Effects of acid type on (a) HMF conversion and (b) LA yield.



composition of a typical humin sample was determined and contained 61.2 wt% of carbon and 4.5 wt% of hydrogen. These values are close to the elemental composition given in the literature²² (C, 63.1; H, 4.2) for the humins obtained by reacting HMF with 0.3 wt% oxalic acid at 130 °C for 3 hours. To gain insights in the average particle size and particle morphology, a number of humin samples were analysed using SEM. A typical example is given in Fig. 6. The humins appear as round, agglomerated particles with a diameter between 5–10 μm.

The gas phase composition after reaction was analysed using GC. Only CO₂ could be detected. However, the amount of CO₂ formed was always less than 2 wt% of the HMF intake,

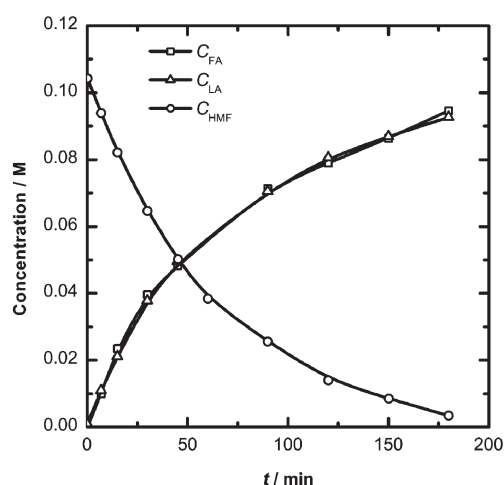


Fig. 5 Typical concentration profile of HMF decomposition reaction ($T = 98$ °C, $C_{\text{HMF},0} = 0.1$ M, $C_{\text{H}_2\text{SO}_4} = 1$ M).

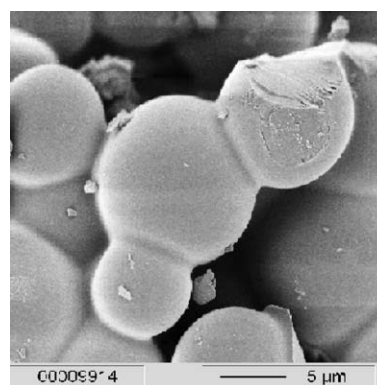


Fig. 6 Scanning electron microscope image of the insoluble humin product.

implying that this is only a minor reaction pathway under these conditions.

3.3 Effects of temperature, acid concentration and initial HMF concentration on HMF conversion and LA yield

A total of 11 batch experiments were performed in a broad range of process conditions ($T = 98$ – 181 °C, $C_{\text{HMF},0} = 0.1$ – 1 M) using sulfuric acid as the catalyst (0.05 – 1 M). The reaction rate is very sensitive to the temperature. For instance, essentially quantitative HMF conversion (X_{HMF}) can be achieved in 10 minutes at 181 °C ($C_{\text{H}_2\text{SO}_4} = 0.1$ M). However, the rate is reduced dramatically at lower temperatures, and a 10 h reaction time was required to obtain $X_{\text{HMF}} = 80\%$ at 98 °C ($C_{\text{H}_2\text{SO}_4} = 0.25$ M, see Fig. 7).

The effect of the $C_{\text{H}_2\text{SO}_4}$ on HMF conversion and LA yield is shown graphically in Fig. 8. Evidently, higher acid concentrations result in higher reaction rates (Fig. 8(a)). At 181 °C, the highest temperature in our study, only dilute solutions of sulfuric acid could be applied. Due to the occurrence of very fast reactions at this temperature, regular sampling to obtain concentration–time profiles proved not possible. At similar conversion levels, the LA yield is slightly improved when using higher acid concentrations (Fig. 8(b)).

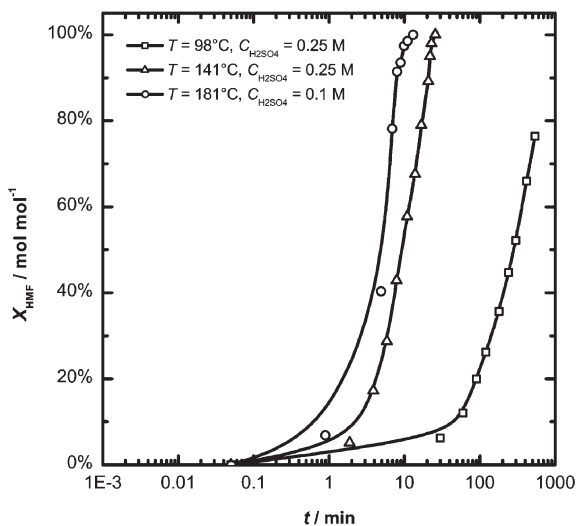


Fig. 7 Effect of temperature on HMF conversion ($C_{\text{HMF},0} = 0.1 \text{ M}$).

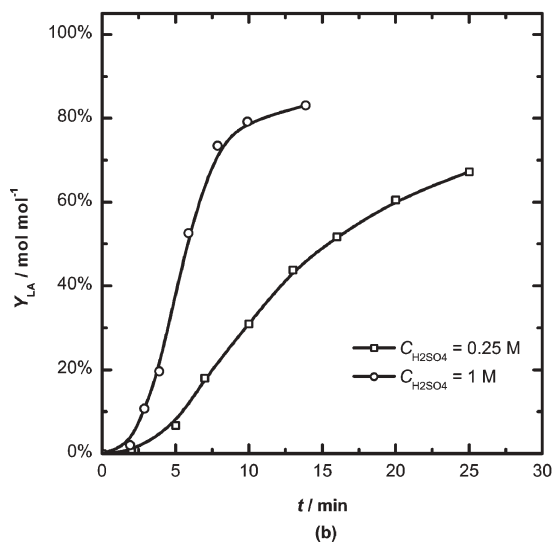
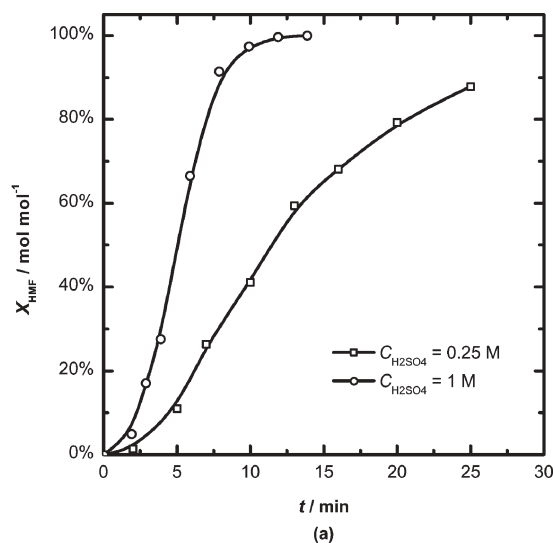


Fig. 8 Effect of acid concentration on (a) X_{HMF} and (b) Y_{LA} , at $T = 141 \text{ }^\circ\text{C}$ and $C_{\text{HMF},0} = 1 \text{ M}$.

A number of experiments were performed with variable initial concentrations of HMF (0.1–1.7 M) at $T = 98 \text{ }^\circ\text{C}$, and $C_{\text{H}_2\text{SO}_4} = 1 \text{ M}$. The conversion of HMF is only slightly dependent on the initial concentration of HMF (Fig. 9(a)), an indication that the reaction order in HMF is close to 1. The initial concentration of HMF has a dramatic effect on the LA yield (Fig. 9(b)). The LA yield was significantly higher when using a low initial concentration of HMF (84% vs. 50%).

3.4 Development of a kinetic model

The kinetic model is based on the equations given in Scheme 1. It is assumed that HMF decomposes to LA and humins in a parallel reaction mode.^{16,17} It cannot be excluded *a priori* that LA and FA are also a source for humins and decompose under the reaction conditions employed. A number of experiments were conducted using pure LA and FA (at $141 \text{ }^\circ\text{C}$ and $C_{\text{H}_2\text{SO}_4} = 1 \text{ M}$). Decomposition of both compounds did not occur under these conditions, implying that HMF is the sole source of humins.

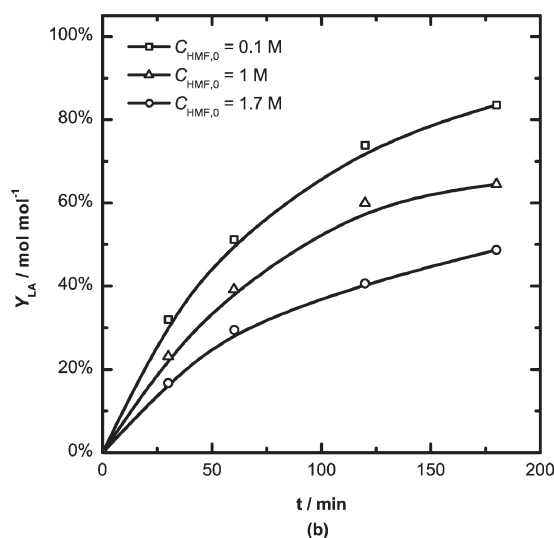
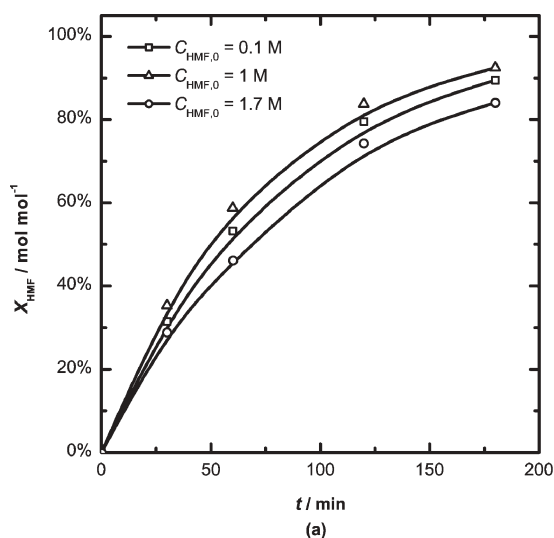


Fig. 9 Influence of initial concentration of HMF on (a) X_{HMF} and (b) Y_{LA} , at $T = 98 \text{ }^\circ\text{C}$ and $C_{\text{H}_2\text{SO}_4} = 1 \text{ M}$.

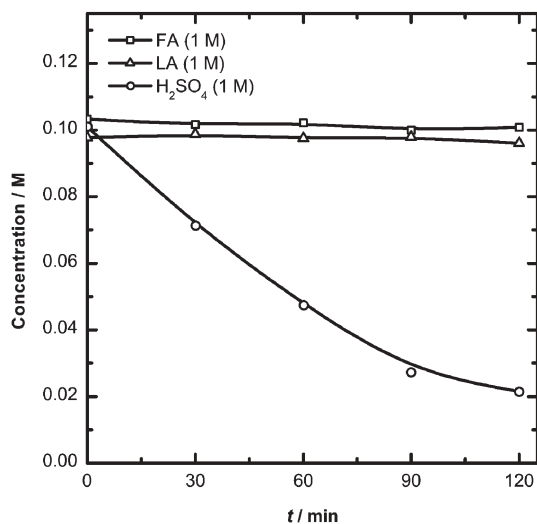


Fig. 10 HMF decomposition using FA, LA, and sulfuric acid as catalyst ($T = 98\text{ }^{\circ}\text{C}$ and $C_{\text{HMF},0} = 0.1\text{ M}$).

Both FA and LA are acidic compounds that potentially could also catalyse the decomposition of HMF. To investigate possible autocatalytic effects of the reaction products, a number of experiments were performed using FA or LA as catalysts ($C_{\text{acids}} = 1\text{ M}$) to probe this possibility. The results are given in Fig. 10. It may be concluded that both LA and FA do not catalyse the decomposition of HMF, excluding autocatalytic effects in the kinetic scheme. Apparently, the $\text{p}K_{\text{a}}$ values of both acids (FA = 3.74 and LA = 4.59) are too low to catalyse the reaction.

When applying the kinetic scheme as given in Scheme 1 and applying a power law approach instead of first-order reactions to express rate equations, the following relations hold:

$$R_1 = k_{1\text{H}}(C_{\text{HMF}})^{\alpha\text{H}}(C_{\text{H}^+})^{\alpha\text{H}} \quad (6)$$

$$R_2 = k_{2\text{H}}(C_{\text{HMF}})^{\beta\text{H}}(C_{\text{H}^+})^{\beta\text{H}} \quad (7)$$

The temperature dependencies of the kinetic rate constants are defined in terms of modified Arrhenius equations:

$$k_{1\text{H}} = k_{1\text{RH}} \exp \left[-\frac{E_{1\text{H}}}{R} \left(\frac{1}{T} - \frac{1}{T_{\text{R}}} \right) \right] \quad (8)$$

$$k_{2\text{H}} = k_{2\text{RH}} \exp \left[-\frac{E_{2\text{H}}}{R} \left(\frac{1}{T} - \frac{1}{T_{\text{R}}} \right) \right] \quad (9)$$

where T_{R} is the reference temperature, set at $140\text{ }^{\circ}\text{C}$.

In a batch system, the concentrations of HMF and LA as a function of time are represented by the following differential equations:

$$\frac{dC_{\text{HMF}}}{dt} = -(R_1 + R_2) \quad (10)$$

$$\frac{dC_{\text{LA}}}{dt} = R_1 \quad (11)$$

3.4.1 Modelling results. A total of 11 batch experiments gave 106 sets of experimental data, where each set consists of the

Table 2 Kinetic parameters of HMF decomposition using sulfuric acid as catalyst

Parameter	Estimate
$k_{1\text{RH}}/\text{M}^{1-\alpha\text{H}-\alpha\text{H}}\text{ min}^{-1}$ ^a	0.340 ± 0.010
$E_{1\text{H}}/\text{kJ mol}^{-1}$	110.5 ± 0.7
$k_{2\text{RH}}/\text{M}^{1-\beta\text{H}-\beta\text{H}}\text{ min}^{-1}$ ^a	0.117 ± 0.008
$E_{2\text{H}}/\text{kJ mol}^{-1}$	111 ± 2.0
αH	0.88 ± 0.01
βH	1.23 ± 0.03
αH	1.38 ± 0.02
βH	1.07 ± 0.04

^a $T_{\text{R}} = 140\text{ }^{\circ}\text{C}$

concentrations of HMF and LA at a certain reaction time. The best estimates of the kinetic parameters and their standard deviations were determined using a MATLAB optimization routine, and the results are given in Table 2. A good fit between experimental data and the kinetic model was observed, as shown in Fig. 11. This is confirmed by a parity plot (Fig. 12).

With the model available, it is possible to gain quantitative information on the effects of the process conditions and input variables on the selectivity of the reaction. For this purpose, it is convenient to use the rate selectivity parameter (S),²³ which is defined as the ratio between the rate of the desired reaction and the rate of undesired reaction.

$$S = \left(\frac{\text{rate of LA formation}}{\text{rate of humin formation}} \right) = \frac{R_1}{R_2} \quad (12)$$

Substitution of the rate expressions and kinetic constants equations as given in eqn (6)–(9) gives:

$$S = \frac{k_{1\text{RH}}}{k_{2\text{RH}}} \exp \left[-\frac{(E_{1\text{H}} - E_{2\text{H}})}{R} \left(\frac{1}{T} - \frac{1}{T_{\text{R}}} \right) \right] (C_{\text{HMF}})^{\alpha\text{H} - \beta\text{H}} (C_{\text{H}^+})^{\alpha\text{H} - \beta\text{H}} \quad (13)$$

Using eqn (13), it is possible to maximise S by selection of the C_{HMF} , $C_{\text{H}_2\text{SO}_4}$ and the temperature. The activation energies of the main reaction ($E_{1\text{H}} = 110.5\text{ kJ mol}^{-1}$) and the side reaction ($E_{2\text{H}} = 111\text{ kJ mol}^{-1}$) are similar (Table 2). This means that the selectivity of the reaction is independent on the temperature. Thus, to achieve high conversion rates in combination with high selectivity, it is attractive to perform the reaction at high temperatures.

Higher acid concentrations will speed up both the main and side reactions. The reaction order in acid of the main reaction ($\alpha\text{H} = 1.38$) is higher than that of the side reaction ($\beta\text{H} = 1.07$), which means that higher acid concentrations will have a positive effect on the selectivity of the reaction. Hence, both from a conversion and selectivity point of view, it is advantageous to work at high acid concentrations. Eqn (13) predicts that the selectivity will be higher when working at low C_{HMF} because the order in HMF is negative ($\alpha\text{H} - \beta\text{H} = -0.35$). Here, a compromise between a high reaction rate (high HMF concentration favoured) and a good selectivity (low HMF concentration favoured) needs to be established (*vide infra*).

3.4.2 Alternative models. We have applied the power-law approach to define the reaction rates of the two reactions

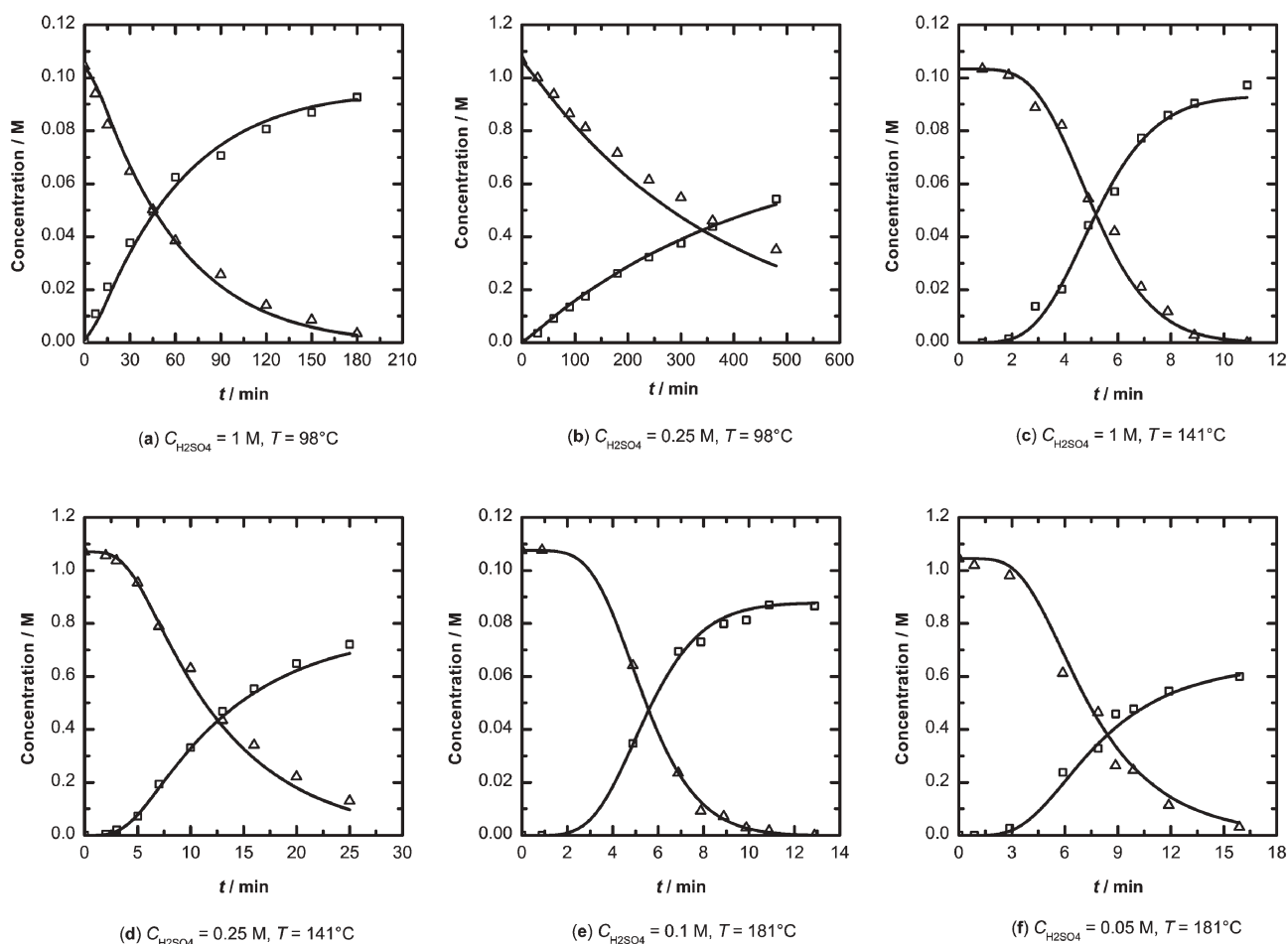


Fig. 11 Comparison of experimental data (\square : C_{LA} ; \triangle : C_{HMF}) and kinetic model (solid lines).

(Scheme 1). With the experimental data set available, it is also possible to test other reaction models and particularly those models where all reactant orders are set to 1. To compare the quality of the models, the goodness-of-fit approach was

applied. The goodness-of-fit for a response of a model can be represented by fit-percentages such as:

$$\%FIT_{HMF} = \left[1 - \frac{\text{norm}(C_{HMF} - \hat{C}_{HMF})}{\text{norm}(C_{HMF} - \bar{C}_{HMF})} \right] \times 100\% \quad (14)$$

$$\%FIT_{LA} = \left[1 - \frac{\text{norm}(C_{LA} - \hat{C}_{LA})}{\text{norm}(C_{LA} - \bar{C}_{LA})} \right] \times 100\% \quad (15)$$

Table 3 shows the results for a number of possible models. It is clear that the power law model described in this report including humin formation shows the highest goodness-of-fit.

4. Application of the kinetic model

4.1 Comparisons with literature models

Various kinetic models for the sulfuric acid catalysed decomposition of HMF have been reported in the literature (Table 1). To demonstrate the broad applicability of the model presented in this paper, the predicted HMF reaction rates according to this model were compared to the various literature models. For this purpose, a set of reaction conditions (T , $C_{H_2SO_4}$, and C_{HMF}) was selected within the validity range of our model ($100^\circ\text{C} < T < 180^\circ\text{C}$, $0.05\text{ M} < C_{H_2SO_4} < 1\text{ M}$,

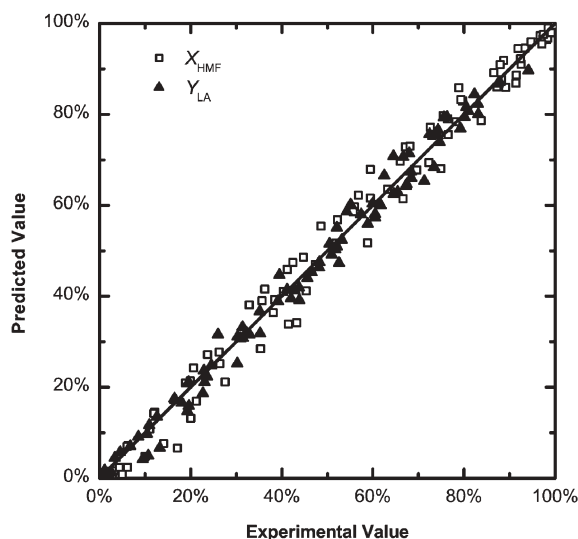


Fig. 12 Parity plot for all experimental and model points.

Table 3 Goodness-of-fit of several kinetic models

Main reaction	Side reaction	%FIT _{HMF}	%FIT _{LA}
$R_1 = k_{1H}C_{HMF}C_{H^+}$	—	53%	41%
$R_1 = k_{1H}(C_{HMF})^{0.97}(C_{H^+})^{1.33}$	—	58%	48%
$R_1 = k_{1H}C_{HMF}C_{H^+}$	$R_2 = k_{2H}C_{HMF}C_{H^+}$	70%	62%
$R_1 = k_{1H}(C_{HMF})^{0.88}(C_{H^+})^{1.38}$	$R_2 = k_{2H}(C_{HMF})^{1.23}(C_{H^+})^{1.07}$	89%	87%

0.1 M < $C_{HMF,0}$ < 1 M). The reaction rates of HMF ($R_{HMF,power}$) at various reaction conditions were calculated using eqn (6) and eqn (7), by taking into account that $R_{HMF,power} = R_1 + R_2$. Similarly, the R_{HMF} for the literature models ($R_{HMF,lit}$) were calculated using the data provided in Table 1. The $R_{HMF,lit}$ were compared with $R_{HMF,power}$ and the results are given in Fig. 13. A good fit between the $R_{HMF,lit}$ and $R_{HMF,power}$ was observed, indicating the broad applicability of our power law model.

4.2 Batch simulation and optimization

With the model available, it is possible to calculate the X_{HMF} and Y_{LA} as a function of the batch time and process conditions. As an example, the modelled batch time required for $X_{HMF} = 90\%$ at various temperatures and acid concentrations is given in Fig. 14.

The kinetic model also allows determination of the optimum reaction conditions to achieve the highest Y_{LA} . For this purpose, eqn (4) is differentiated to give:

$$dX_{HMF} = -\frac{dC_{HMF}}{C_{HMF,0}} \quad (16)$$

Combination of eqn (10), eqn (11) and eqn (16) leads to the following expressions:

$$\frac{dC_{HMF}}{dX_{HMF}} = -C_{HMF,0} \quad (17)$$

$$\frac{dC_{LA}}{dX_{HMF}} = \frac{R_1}{R_1 + R_2} C_{HMF,0} \quad (18)$$

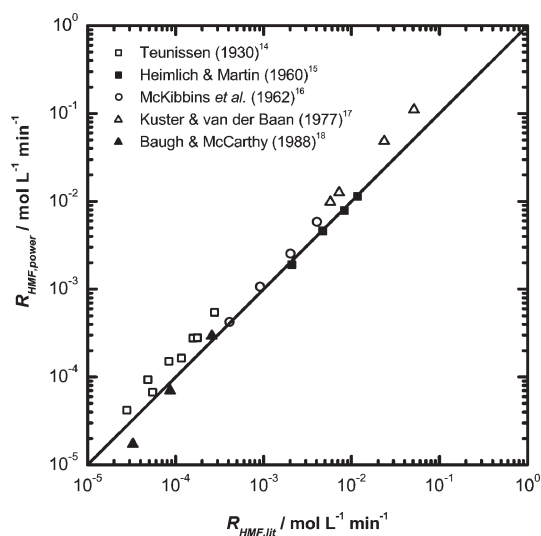


Fig. 13 Comparison between the kinetic model provided here and previous kinetic studies.

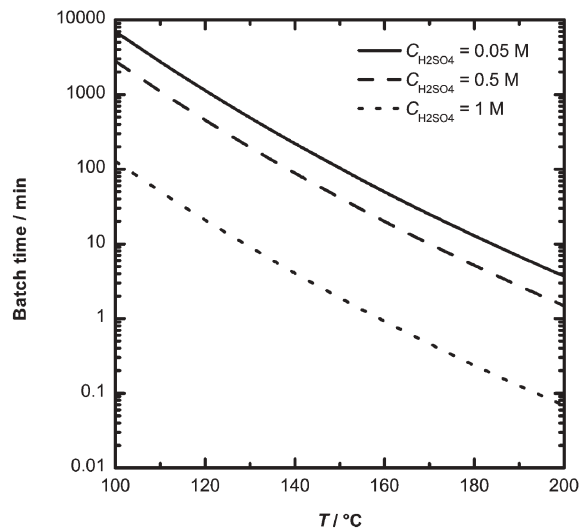


Fig. 14 Batch time for $X_{HMF} = 90\%$ as a function of temperature and acid concentration ($C_{HMF,0} = 0.1$ M).

Eqn (17) and eqn (18) were solved using the numerical integration toolbox ode45 in MATLAB software package from 0 to 90% HMF conversion. The LA yield was subsequently calculated using eqn (5). Fig. 15 shows the LA yield as a function of $C_{HMF,0}$ and C_{H^+} at $T = 180$ °C and 90% HMF conversion. It is evident that the LA yield is highest at high acid concentrations and low initial HMF concentrations, in line with the experimental results (*vide supra*).

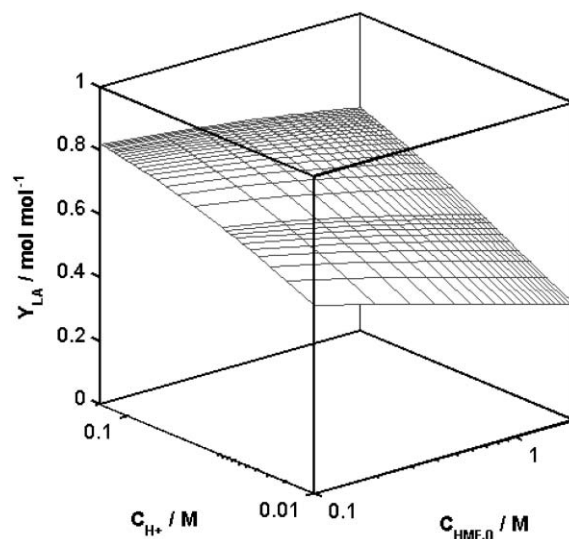


Fig. 15 Effects of $C_{HMF,0}$ and C_{H^+} on Y_{LA} ($T = 180$ °C and $X_{HMF} = 90\%$).

5. Conclusions

This study describes an in-depth experimental and modelling study on the acid catalysed decomposition of HMF into LA and FA and humins by-products in a batch reactor. Acid screening studies show that H_2SO_4 and HCl are the catalysts of choice with respect to LA yield. The LA yield is highest at high acid concentrations and low initial HMF concentrations and essentially independent of the temperature.

A broadly applicable kinetic model for the acid catalysed HMF decomposition at sulfuric acid concentrations between 0.05 and 1 M, initial concentrations of HMF between 0.1 and 1 M and a temperature window of 98–181 °C using a power law approach has been developed. The reaction rates for the main reaction to LA and FA and the side reaction to humins were modelled as a function of C_{HMF} , C_{H^+} and T . A maximum likelihood approach has been applied to estimate the kinetic parameters. A good fit between experimental data and modelling results was obtained. The highest LA yield at short batch times is obtained at high temperature, a low initial HMF concentration and a high acid concentration.

6. Nomenclature

a_{H}	Reaction order of HMF in the main reaction to LA and FA
α_{H}	Reaction order of H^+ in the main reaction to LA and FA
A_t	Heat transfer area (m^2)
b_{H}	Reaction order of HMF in the side reaction to humins
β_{H}	Reaction order of H^+ in the side reaction to humins
C_{H^+}	Concentration of H^+ (M)
C_{HMF}	Concentration of HMF (M)
$C_{\text{HMF},0}$	Initial concentration of HMF (M)
C_p	Heat capacity of reaction mixture ($\text{J g}^{-1} \text{K}^{-1}$)
C_{LA}	Concentration of levulinic acid (M)
$C_{\text{LA},0}$	Initial concentration of levulinic acid (M)
$E_{1\text{H}}$	Activation energy of the main reaction to LA and FA (kJ mol^{-1})
$E_{2\text{H}}$	Activation energy of the side reaction to humins (kJ mol^{-1})
h	Heat transfer coefficient from the oven to the reaction mixture (min^{-1})
$k_{1\text{H}}$	Reaction rate constant of HMF for the main reaction ($\text{M}^{1-\alpha_{\text{H}}-\alpha_{\text{H}}} \text{min}^{-1}$)
$k_{1\text{RH}}$	Reaction rate constant $k_{1\text{H}}$ at reference temperature ($\text{M}^{1-\alpha_{\text{H}}-\alpha_{\text{H}}} \text{min}^{-1}$)
$k_{2\text{H}}$	Reaction rate constant of HMF for the side reaction to humins ($\text{M}^{1-b_{\text{H}}-\beta_{\text{H}}} \text{min}^{-1}$)
$k_{2\text{RH}}$	Reaction rate constant $k_{2\text{H}}$ at reference temperature ($\text{M}^{1-b_{\text{H}}-\beta_{\text{H}}} \text{min}^{-1}$)
M	Mass of the reaction mixture (g)
R	Universal gas constant, $8.3144 \text{ J mol}^{-1} \text{ K}^{-1}$
R_1	Reaction rate of HMF to LA and FA ($\text{mol L}^{-1} \text{ min}^{-1}$)
R_2	Reaction rate of HMF to humins ($\text{mol L}^{-1} \text{ min}^{-1}$)
S	Rate selectivity parameter
t	Time (min)
T	Reaction temperature (K)

T_i	Temperature of reaction mixture at $t = 0$ (K)
T_{oven}	Temperature of oven (K)
T_{R}	Reference temperature (K)
U	Overall heat transfer coefficient ($\text{W m}^{-2} \text{ K}^{-1}$)
X_{HMF}	Conversion of HMF (mol mol^{-1})
Y_{LA}	Yield of levulinic acid (mol mol^{-1})
Special symbols	
\hat{C}_i	Estimated value of matrix C_i ($i = \text{HMF, LA}$)
\bar{C}_i	Average value of matrix C_i ($i = \text{HMF, LA}$)
norm(C)	Norm. of matrix C
%FIT $_i$	Fit percentage of the i th compound ($i = \text{HMF, LA}$)

Acknowledgements

The authors thank the University of Groningen (Netherlands) for financial support through an Ubbo Emmius Scholarship to B. Girisuta, and Mr H. Nijland for recording the SEM images.

References

- D. L. Klass, *Biomass for Renewable Energy, Fuels, and Chemicals*, Academic Press, New York, USA, 1998.
- S. W. Fitzpatrick, *US Pat.* 5 608 105, 1997.
- V. Ghorpade and M. A. Hanna, *US Pat.* 5 859 263, 1999.
- W. A. Farone and J. E. Cuzens, *US Pat.* 6 054 611, 2000.
- J. Y. Cha and M. A. Hanna, *Ind. Crops Prod.*, 2002, **16**, 109–118.
- Q. Fang and M. A. Hanna, *Bioresour. Technol.*, 2002, **81**, 187–192.
- J. J. Bozell, L. Moens, D. C. Elliott, Y. Wang, G. G. Neuenschwander, S. W. Fitzpatrick, R. J. Bilski and J. L. Jarnefeld, *Resour. Conserv. Recycl.*, 2000, **28**, 227–239.
- R. H. Leonard, *Ind. Eng. Chem.*, 1956, **48**, 1331–1341.
- M. Kitano, F. Tanimoto and M. Okabayashi, *Chem. Econ. Eng. Rev.*, 1975, **7**, 25–29.
- J. J. Thomas and G. R. Barile, *Proceedings of 8th Symposium on Energy from Biomass and Waste*, Lake Buena Vista, FL, 1984.
- V. Ghorpade and M. A. Hanna, in *Cereal Novel Uses and Processes*, ed. G. M. Campbell, C. Webb, and S. L. McKee, Plenum Press, New York, pp. 49–55.
- B. V. Timokhin, V. A. Baransky and G. D. Eliseeva, *Russ. Chem. Rev.*, 1999, **68**, 80–93.
- H. E. Grethlein, *J. Appl. Chem. Biotechnol.*, 1978, **28**, 296–308.
- H. P. Teunissen, *Recl. Trav. Chim. Pays-Bas*, 1930, **49**, 784–826.
- K. R. Heimlich and A. N. Martin, *J. Am. Pharm. Assoc.*, 1960, **49**, 592–597.
- S. Mckibbins, J. F. Harris, J. F. Saeman and W. K. Neill, *For. Prod. J.*, 1962, **12**, 17–23.
- B. F. M. Kuster and H. S. van der Baan, *Carbohydr. Res.*, 1977, **54**, 165–176.
- K. D. Baugh and P. L. McCarty, *Biotechnol. Bioeng.*, 1988, **31**, 50–61.
- Y. Bard, *Nonlinear Parameter Estimation*, Academic Press, New York, USA, 1974.
- C. D. Knightes and C. A. Peters, *Biotechnol. Bioeng.*, 20-7-2000, **69**, 160–170.
- K. R. Westerterp, W. P. M. van Swaaij and A. A. C. M. Beenackers, *Chemical Reactor Design and Operation*, John Wiley & Sons Ltd, Chichester, 1984.
- J. J. Blanksma and G. Egmond, *Recl. Trav. Chim. Pays-Bas*, 1946, **65**, 309–310.
- H. S. Fogler, *Elements of Chemical Reaction Engineering*, 3rd edn, Prentice Hall PTR, New Jersey, USA, 1999.

Facile and regioselective mono- or diesterification of glycerol derivatives over recyclable phosphazene organocatalyst†

Ghizlane Kharchafi,^a François Jérôme,^{*a} Jean-Paul Douliez^b and Joël Barrault^a

Received 28th February 2006, Accepted 30th May 2006

First published as an Advance Article on the web 22nd June 2006

DOI: 10.1039/b603091b

P1 phosphazene is a strong non-ionic base able to catalyze the esterification of various glycerol derivatives with fatty methyl esters at room temperature – properties responsible for the selectivity observed in this study. Indeed, when the reaction was conducted at room temperature in an organic solvent, and especially in acetonitrile, we showed that the different fatty glycerides produced could be trapped during the catalytic process as a pure product by simple precipitation. Using these experimental conditions, it was therefore possible to perfectly and selectively control the successive esterification steps of various glycerol derivatives and the regioselectivity of this reaction, affording a very competitive alternative to the enzymatic pathway. Moreover, the precipitation of the reaction products during the catalytic process affords a very facile purification work up, and allows the recycling of both the organic solvent and the organocatalyst, therefore limiting the environmental impact of the presented process.

Introduction

In the last thirty years, intense research has been devoted to the chemical potential of glycerol. Indeed, glycerol is the co-product of the biodiesel industry, and its chemical valorisation is one of the main keys for the industrial development of vegetable oils.¹ Its biocompatibility and its large availability make of this biomolecule an attractive and cheap organic building block. However, due to the presence of three hydroxyl groups, the chemical transformation of glycerol requires the development of selective catalytic routes in order to avoid many protection and deprotection steps, which increase the cost and the environmental impact of the resulting process.² The mono-, di- or polyesterification of glycerol and its derivatives such as diglycerol and triglycerol with fatty methyl esters is a very important industrial reaction for the synthesis of safer emulsifiers³ or “bio” organic building blocks for the production of polymers⁴ and pharmaceuticals.⁵ The control of the regioselectivity and the different esterification steps is the main key of the process, in order to selectively stop the reaction at one of the desired esters. Up to now, only methods involving enzymes were able to selectively stop this reaction to the mono- or diesterification step⁶ and even, in some cases, to control the regioselectivity of the reaction.⁷ However, the enzymatic chemical pathway still suffers from a complex purification work up. For this reason, studies were also directed towards the development of selective heterogeneous catalysts such as metal oxides,⁸ zeolites,⁹ basic or acid functionalized mesoporous silica¹⁰ or anion exchange resins.¹¹ However, although this approach allowed an easier

purification of the reaction products, this method was unfortunately much less selective than using enzymes. Many other examples of selective and catalytic acylation of primary alcohols were also reported in the literature.¹² However, in most cases, these chemical approaches involved transition metals which are air sensitive and transposable with difficulties to the acylation of glycerol with fatty methyl esters due to important hydrophilic–lipophilic interactions.

In this paper, we now report the first example of a recyclable metal-free catalytic process able to totally control, under air, the esterification degree of various glycerol derivatives, and the regioselectivity of this reaction without the assistance of protective groups. P1 phosphazene¹³ is a strong non-ionic base with a pK_a value higher than 27, and we show here that this strongly basic derivative is a very promising organocatalyst for the selective transesterification of fatty methyl esters with glycerol derivatives.

Catalysis in acetonitrile

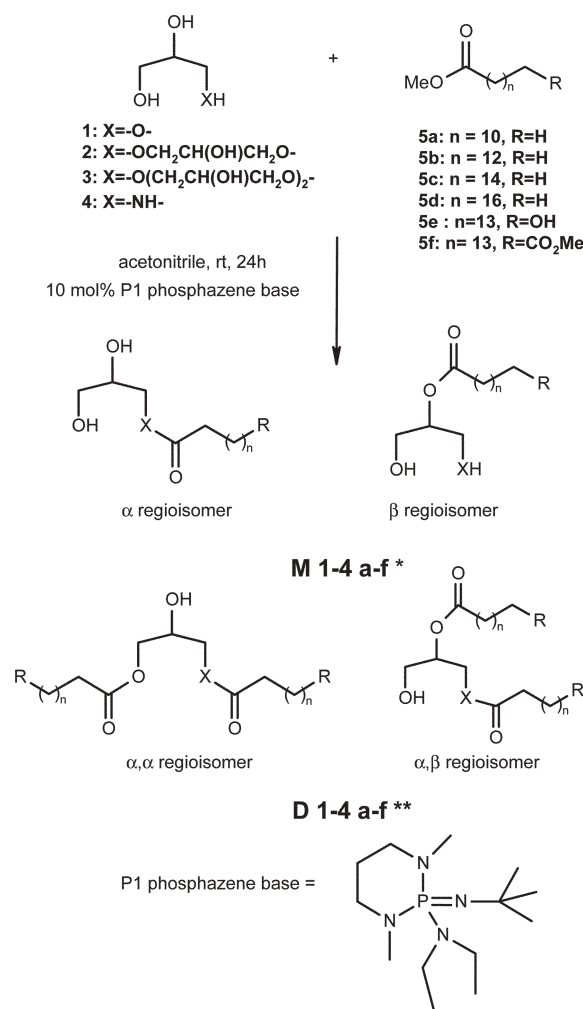
In the first experiments, all of the following catalytic tests were carried out starting from glycerol. In a typical procedure, glycerol **1** (25 mmol) and various fatty methyl esters **5a–f** (5 mmol) were mixed in the presence of 10 mol% of 2-terbutylamino-2-diethylamino-1,3-dimethylperhydropyridine-1,3,2-diazaphosphorine (P1 phosphazene) and stirred in 20 mL of acetonitrile. Thanks to the high basicity of the P1 phosphazene and its great stability, all catalytic reactions were performed under air and at room temperature, except for **5d–f** for which a minimum temperature of 35 °C was necessary in order to ensure their complete dissolution. In this work, we deliberately focussed our study towards fatty methyl esters **5a–f** since these are widely used to tune the lipophilic properties of the resulting esters (Scheme 1).

In the case of methyl dodecanoate **5a**, monoglycerides **M1a** were produced in low yield, since at room temperature it was impossible to remove methanol (produced *in situ*) from the

^aLaboratoire de Catalyse en Chimie Organique, UMR 6503, CNRS-Université de Poitiers, ESIP, 40 Avenue du Recteur Pineau, Poitiers Cedex, 86022, France. E-mail: francois.jerome@univ-poitiers.fr; Fax: +33 5 49 45 40 52; Tel: +33 5 49 45 33 49

^bINRA/BIA/ISD, Rue de la Géraudière, Nantes Cedex, 44316, France

† Electronic supplementary information (ESI) available: ¹³C NMR spectra and selected GC chromatograms. See DOI: 10.1039/b603091b



* **M 1-4**: product resulting from the monoesterification of polyols **1-4**

** **D 1-4**: product resulting from the diesterification of polyols **1-4**

Scheme 1 Catalytic and regioselective esterification of glycerol derivatives with functional fatty methyl esters.

reaction mixture. Consequently, a statistical thermodynamic equilibrium was reached, and only 45% of monoglycerides **M1a** were produced, as a mixture of two regioisomers α and β in a typical molar ratio of 85 : 15 (Table 1, entry 1).

In contrast, starting from methyl tetra-, hexa- and octadecanoate (**5b**, **5c**, **5d**, respectively), very high yields of **M1b-d** were obtained. Indeed, as reported in Table 1 (entries 2–4), monoglycerides **M1b-d** were produced in greater than 78% isolated yield, and remarkably no trace of di- and triesters were detected by GC or NMR spectroscopy, affording a process very highly selective towards monoesters. This very high selectivity observed at room temperature was the result of the poor solubility of the monoacylglycerol **M1b-d** in the reaction mixture. Indeed, at room temperature, the produced monoesters **M1b-d** precipitated as a white powder during the organocatalytic process, thus shifting the equilibrium towards the selective formation of monoesters. At the end of the reaction, the highly pure monoacylglycerols **M1b-d** were easily recovered by filtration and just washed with water, in order to

Table 1 Esterification of glycerol derivatives **1-4** over P1 phosphazene organocatalyst after 24 hours at room temperature

Entry	Fatty ester	Polyol	Polyol/ester molar ratio	% Isolated yield ^a	
				Product: % monoester (% α) ^b	Product: % diester (% α,α) ^b
1	5a	1	5	M1a : 45 (85) ^c	0
2	5b	1	5	M1b : 79 (100)	0
3	5c	1	5	M1c : 78 (100)	0
4	5d ^d	1	2	M1d : 86 (100)	0
5	5a ^e	1	5	M1a : 76 (100)	0
6	5d ^d	1	1.5	0	D1d : 81 (100)
7	5c	1	0.5	0	D1c : 80 (99)
8	5d ^d	1	0.5	0	D1d : 78 (100)
9	5e ^d	1	2	0	6 : 65 (100) ^f
10	5f ^d	1	2	M1f : 46 (88) ^c	0
11	5f ^d	1	5	7 : 65 (99) ^g	0
12	5d ^d	2	5 ^h	0	D2d : 65 (100)
13	5d ^d	3	5 ^h	M3d : 50 (100)	0
14	5d ^d	4	1	M4d : 90 (100)	0

^a Isolated yields of diesters were determined with respect to the starting fatty methyl esters: % diester = $[(2 \times n_{\text{diester}})/n_{\text{fatty ester}}] \times 100$. ^b The regioselectivity of the reaction was determined by ¹H NMR and GC analyses. 100% regioselectivity means that the second regioisomer was not observed by NMR or GC. ^c Yield and regioselectivity were determined by GC. ^d Reaction carried out at 35 °C. ^e Reaction carried out at 15 °C. ^f In this case two successive fatty chains are branched on one hydroxyl group of the glycerol moiety (see Scheme 2). ^g The structure of derivative **7** corresponds to two glycerol moieties branched to the two terminal ester groups of **5f** (see Scheme 2). ^h Mixture of acetonitrile–DMSO (19 : 1) was used as solvent.

get rid of traces of glycerol, affording a very facile purification work up.

Regioselectivity of the process

Remarkably, whereas all reported transesterification catalytic processes produced monoglycerides as a mixture of two regioisomers α and β in a typical molar ratio of 85 : 15, NMR investigations clearly showed that, in our case, **M1b-d** derivatives were formed as a unique α regioisomer *i.e.* with the ester moiety branched on the primary hydroxyl group (Scheme 1). Indeed, ¹³C NMR spectra of **M1b-d** exhibited only one single peak for the carbonyl group located at 174 ppm, and no split of any peak was observed in the ¹H NMR spectra, contrary to what was usually observed. As supplementary evidence, whereas the two regioisomers α and β of **M1a** appeared as a double peak in GC, only one single peak was detected for **M1b-d** confirming the great regioselectivity of the process (see Electronic Supplementary Information†). This unprecedented finding on the regioselectivity is directly linked to the precipitation of the monoester **M1b-d** during the catalytic process. Indeed, in basic solution, it is well known that the ester moiety can migrate from the primary to the secondary hydroxyl group explaining the presence of the two regioisomers α and β . However, in our case, as only the α regioisomer precipitates, the thermodynamic equilibrium between the α and β form was totally shifted toward the α regioisomers.

In the case of **5a**, it is interesting to note that when the reaction mixture was cooled down to 15 °C, monoester **M1a**

becomes insoluble in acetonitrile, and can also be obtained as a pure α -regioisomer with a yield higher than 76% (Table 1, entry 5).

The possibility to fully control the regioselectivity of the reaction is a very important parameter, since reported work showed that differences in surfactant properties can be observed depending on the position of the fatty chain on the polyol moiety.¹⁴

Influence of the glycerol/fatty methyl ester molar ratio

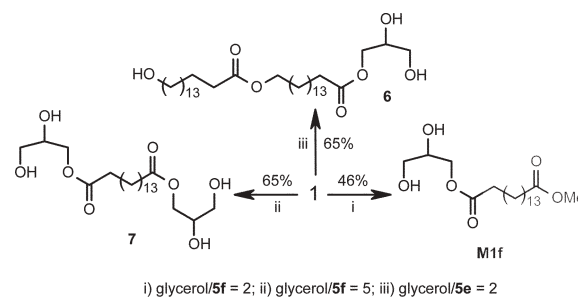
Whereas starting from **5a–c** it was necessary to use a glycerol/fatty methyl ester molar ratio of 5, we found that in the case of **5d**, it was possible to decrease this molar ratio to 2 without affecting the reaction selectivity (Table 1, entry 4). This particular behaviour of **5c** is closely related to its higher lipophilicity which makes the precipitation of the monoglyceride **M1d** from the reaction mixture easier.

Surprisingly, when the glycerol/fatty methyl ester **5d** molar ratio was dropped from 2 to 1.5 a total change of the selectivity was observed; diester **D1d** was now produced in greater than 81% yield, and curiously, in this case, no trace of monoester **M1d** was detected (Table 1, entry 6). We assume that this total change of selectivity was closely related to the solubility of glycerol in the reaction mixture. Indeed, GC analysis indicated that below 0.5 mol L⁻¹ of glycerol, the monoester **M1d** produced *in situ* can be dissolved in the reaction mixture and esterified a second time, leading to a small quantity of diester **D1d**. However, as **D1d** diester was insoluble in acetonitrile, this later precipitated, now shifting the thermodynamic equilibrium towards the formation of diester **D1d**. It is noteworthy that when the glycerol/fatty methyl ester molar ratio was dropped to 0.5, diesters **D1d** but also **D1c** were remarkably produced as pure white solids in greater than 80% yield (Table 1, entries 7,8). Moreover, as previously described for the synthesis of monoesters **M1b–d**, GC, ¹H and ¹³C NMR analyses showed that diesters **D1c,d** were also obtained with greater than 99% selectivity as α,α regioisomer whereas a statistic regioisomer distribution of $\alpha,\alpha/\alpha,\beta$ of 65 : 35 was usually obtained in all reported catalytic processes.^{8–10}

According to experimental conditions, it clearly appears from the above that, in acetonitrile, the catalytic process can be selectively driven either towards the production of α -monoglycerides or α,α -diglycerides affording a very versatile process.

Influence of polyfunctional fatty methyl esters on the reaction selectivity

Starting from polyfunctional fatty methyl ester **5e,f**, this organocatalytic pathway remains very selective. Indeed, using a glycerol/**5e** molar ratio of 2, diester **6** was selectively obtained in greater than 65% yield (Table 1, entry 9). Interestingly, in this case, thanks to lipophilic interactions, the second esterification only took place on the hydroxyl group of the fatty chain (Scheme 2). Indeed, ¹³C NMR clearly showed the dissymmetry of the molecule and the structure of the α -regioisomer. The structure of **6** was finally confirmed by electrospray mass spectrometry which indicated only one single peak located at 624 uma [MH⁺, Na⁺]. It is worth noting



Scheme 2 Regioselective esterification of glycerol with **5e,f**.

that an increase of the molar ratio from 2 to 5 did not affect the selectivity of the reaction.

In the case of **5f**, with a glycerol/**5f** molar ratio of 2, the catalytic process unfortunately stopped after 46% conversion, since, as observed for monoester **M1a**, monoester **M1f** was produced with only 46% yield as two regioisomers, α and β , in a molar ratio of 88 : 12 (Table 1, entry 10). However, when the glycerol/**5f** molar ratio was raised to 5, a total change of selectivity was observed since 1,16-diglycerol-hexadecanedioate, **7**, was now obtained as a pure α,α regioisomer in greater than 65% yield (Scheme 2; Table 1, entry 11). The catalytic transformation of the soluble monoester **M1f** into the insoluble derivative **7** require a lot of time explaining the non formation of **7** after 24 h when starting from a glycerol/**5f** molar ratio of 2.

To our knowledge, this reported chemical pathway is the only example of an organocatalytic route able to selectively control the esterification degree and the reaction regioselectivity of glycerol with polyfunctional fatty methyl esters, making this route a very competitive alternative to the enzymatic chemical pathway.

Transposition to glycerol derivatives

Based on these promising results, our organocatalytic process was extended to diglycerol **2** and triglycerol **3** in order to obtain a wider range of biosurfactants with different hydrophilic–lipophilic balance. However, as **2** and **3** were sparingly miscible in pure acetonitrile, their catalytic esterification with **5d** was carried out in a mixture of acetonitrile–DMSO (19 : 1). Due to the presence of DMSO, the monoester of diglycerol **M2d** was soluble in the reaction mixture and consequently the organocatalytic process afforded pure diester of diglycerol **D2d**, in greater than 65% yield (Table 1, entry 12). When diglycerol **2** was replaced by triglycerol **3**, the hydrophilicity of the polyol moiety was considerably increased, and the resulting monoesters **M3d** became insoluble in the reaction mixture and, in this case, were selectively produced as a pure white solid in greater than 50% yield (Table 1, entry 13). Remarkably, as previously obtained in the case of glycerol, GC and NMR investigations clearly showed that the diester of diglycerol **D2d** and monoesters of triglycerol **M3d** were also produced as only α,α and α regioisomers, respectively (see Electronic Supplementary Information†).

When an amino group replaced one hydroxyl group of glycerol, the selectivity of the catalytic process still remains

very high. Indeed, starting from an equimolar mixture of 1-amino-2,3-propanediol, **4**, and fatty methyl ester **5d**, only the amidation reaction occurred and the resulting fatty amide **M4d** was obtained in greater than 90% isolated yield (Table 1, entry 14). Interestingly, contrary to what was generally observed in the literature,¹⁵ in our case, no trace of esteramide was detected as secondary products, affording a new interesting pathway for the synthesis of β -blockers.^{5b}

Influence of the solvent

Even though satisfactory results were obtained in acetonitrile, the catalytic activity of P1 phosphazene was also explored in dimethylsulfoxide, which is a definitely more acceptable aprotic solvent than acetonitrile in terms of toxicity.

As shown in Table 2, starting from glycerol **1**, but with dimethylsulfoxide instead of acetonitrile, the catalytic process was selectively driven towards the production of diesters **D1b–d**. Indeed, at room temperature, monoacylglycerol **M1b–d** were soluble in DMSO, whereas it was not the case for diesters **D1b–d**. Consequently, in DMSO and at room temperature, diesters **D1b–d** precipitated from the reaction mixture, and despite the use of five times excess of glycerol, were always produced as only α,α regioisomers, with yields ranging from 72% to 95% (Table 2). However, as expected, the yield of diesters **D1b–d** closely depended on the lipophilicity of the starting fatty methyl ester. Indeed, starting from **5b** and **5c**, 24% and 9% of monoglyceride **M1b,c** were detected in the recovered DMSO, respectively (Table 2, entries 1–2), whereas starting from **5d** complete conversion into diester **D1d** was observed after 24 hours of reaction (Table 2, entry 3).

Other solvents such as diglyme, acetone, tetrahydrofuran, dichloromethane, diethyl ether and heptane were also tested, but they did not give satisfactory results at room temperature, mainly because of the poor miscibility of glycerol in these solvents (data not shown).

From this study, it clearly appears that acetonitrile is the most versatile organic solvent for the regioselective mono- or diesterification of glycerol with fatty derivatives. DMSO, less toxic than acetonitrile, unfortunately allows only the production of α,α -diglycerides.

Recycling experiments

In order to limit the environmental impact of the solvent, recycling experiments were carried out starting from glycerol

Table 2 Catalytic process in dimethylsulfoxide^a

Entry	Fatty Ester	Time/h	Isolated yield (%) ^b	
			Product: % monoester (% α) ^c	Product: % diester (% α,α) ^c
1	5b	24	M1b : 24 ^d (85)	D1b : 72 (100)
2	5c	24	M1c : 9 ^d (85)	D1c : 80 (100)
3	5d	24	0	D1d : 95 (100)

^a Glycerol 25 mmol, fatty methyl ester 5 mmol, 10 mol% P1 phosphazene, 35 °C. ^b Isolated yields of diesters were determined with respect to the starting fatty methyl ester: % diester = $[(2 \times n_{\text{diester}}) / n_{\text{fatty ester}}] \times 100$. ^c The regioselectivity of the reaction was determined by ¹H NMR and GC analyses. ^d Quantity of monoglyceride detected in the recovered DMSO, yield was determined by GC.

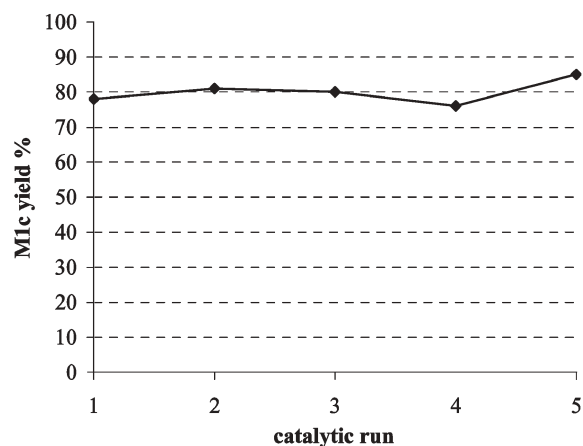


Fig. 1 Recycling experiments in acetonitrile carried out in the presence of 10 mol% of P1 phosphazene, at 35 °C and for 24 hours. As the excess of glycerol was recycled, after each catalytic run 5 mmol of glycerol and 5 mmol of **5c** were added in order to obtain a constant glycerol/**5c** molar ratio of 5

(25 mmol) and **5c** (5 mmol) in acetonitrile. After the first run, acetonitrile was collected at the end of the reaction by filtration. The recovered monoglyceride α -**M1c** was washed with 3 mL of acetonitrile in order to remove traces of glycerol. GC analysis revealed that the recovered acetonitrile contains more than 90% of the excess of glycerol (*i.e.* 18 mmol instead of the 20 mmol expected), and only traces of soluble **M1c** and unreacted fatty methyl ester **5c**. It is worth noting that no secondary products such as soap, polyglycerol or acrolein were detected in the filtrate confirming the great selectivity of the process. Moreover, titration of acetonitrile with an aqueous solution of chlorhydric acid (0.1 M), in the presence of phenolphthalein as indicator, revealed that 100% of the initial amount of catalyst remained dissolved in acetonitrile. Therefore, at the end of the reaction, after filtration of acetonitrile and addition of 1 eq. of glycerol and 1 eq. of fatty methyl ester **5c**, it was possible to reuse the reaction mixture for at least five more catalytic runs without any impact on the reaction selectivity (Fig. 1). Indeed, starting from **5c**, five successive catalytic runs were successfully performed affording pure α -monoglycerides **M1c**, with yields higher than 76%.

The high selectivity obtained in this study, combined with the possibility of recycling the organic solvent, the excess of glycerol and the organocatalyst, considerably limits the environmental impact of the process.

Conclusion

The above results show a novel and recyclable metal-free organocatalytic route able to closely control, under mild conditions, the esterification degree of various glycerol derivatives with functional fatty methyl esters and the regioselectivity of the reaction without assistance of protecting groups. The precipitation of the mono- or diglycerides in organic solvents is the main key to the selectivity obtained in this study.

The organocatalytic process presented here involves a strong non-ionic P1 phosphazene base able to catalyse the transesterification reaction at room temperature – properties

responsible for the selectivity observed. Among various organic solvents, we found that the association of the P1 phosphazene catalyst with acetonitrile was the best solution to perfectly control the selectivity of the transesterification reaction. Moreover, thanks to the precipitation of the different targeted fatty glycerides during the catalytic process, the purification work up was very facile, and we found that it was possible to recycle acetonitrile, the excess of glycerol and the organocatalyst, therefore limiting the environmental impact of the process.

This highly selective and recyclable process opens a new alternative to the enzymatic procedure for the mild and regioselective synthesis of various fatty derivatives with different hydrophilic–lipophilic balances, which are of great interest in many research fields.

Experimental section

Chemicals

Industrial glycerol (97%) **1** and fatty methyl esters **5a–d** (99%) were kindly provided by Stearinerie Dubois. Diglycerol **2** (95%) and triglycerol **3** (80%) were provided by Solvay. Acetonitrile, 1-amino-2,3-propanediol **4**, 2-tert-Butylimino-2-diethylamino-1,3-dimethyl-perhydro-1,3,2-diazaphosphorine (P1-phosphazene) were purchased from Sigma–Aldrich and used as received without further purification. 16-Methyl-hydroxyhexadecanoate **5e** and 1,16-methylhexadecanedioate **5f** were synthesized from 16-hydroxyhexadecanoic acid and 1,16-hexadecanedioic, respectively (purchased from Sigma–Aldrich), by reaction with 10 mol% of H₂SO₄ in methanol. The reaction mixture was stirred under reflux overnight before being diluted in water. The precipitated fatty methyl esters were recovered by filtration and washed with water until pH = 7. Fatty methyl esters **5e** and **5f** were obtained with 80% and 95% yield, respectively.

Physical methods

IR spectra were recorded on a FT-IR Perkin Elmer (spectrum one) using ATR technology over a diamond crystal. ¹H and ¹³C NMR spectra were recorded on a Bruker Avance 300 DPX 300. Chemical shifts are expressed in ppm relative to Me₄Si. Mass spectrometry was carried out on a thermo DK XP + ion max (electrospray) and on a GC/MS Varian 1200 Triple quadrupole equipped with a Factor Four VF5MS 30 m × 0.25 mm × 0.25 μm column (in this case, products were silylated before analysis). Microanalyses were measured on a NA 2100 instrument.

Chromatographic analyses

The reaction progress was monitored and quantified by external calibration on a Varian 3300 GPC equipped with a BPX5 column (12 m × 0.22 mm) supplied by SGE. Prior to analysis, products were silylated according to the Sahasrabudhe method described in ref. 16. This analytical technique allowed the quantification of glycerol derivatives **1–4**, fatty methyl esters **5a–f**, α and β-monoesters **M1–4a–f**, α,α- and α,β-diglycerides **D1–4a–f**, and triglycerides.

General catalytic procedure

Glycerol derivatives **1–4** (25 mmol) were mixed with fatty methyl esters **5a–f** (5 mmol) in 20 mL of acetonitrile or dimethylsulfoxide. 135 mg (10 mol% with respect to the fatty methyl ester) of P1 phosphazene was then added, and the reaction mixture was stirred under air for 24 hours at room temperature (or 35 °C for **5d–f**). During the catalytic process, all the different glycerides precipitated as a white powder. At the end of the reaction, all the precipitated glycerides were collected by filtration, and the reaction mixture containing the acetonitrile, the excess of glycerol and the organocatalyst was isolated for recycling experiments. The collected fatty glycerides were washed with pure water in order to remove traces of glycerol. All recovered fatty glycerides were dried under vacuum (10^{−2} mmHg) overnight before analysis.

Reactions carried out with a molar ratio of 2, 1.5 and 0.5 were always performed starting from 5 mmol of fatty methyl esters, 135 mg (10 mol%) of P1 phosphazene and 20 mL of acetonitrile. In all experiments, only the initial quantity of glycerol derivatives was tuned in order to obtain the desired molar ratio.

1-Monododecanoyl-*rac*-glycerol (M1a)

¹H NMR (300 MHz, CDCl₃) δ 0.88 (t, 3H, ³J_{HH} = 6.5 Hz, CH₃), 1.26 (m, 16H, CH₂), 1.62 (m, 2H, CH₂), 2.34 (t, 2H, CH₂, ³J_{HH} = 7.5 Hz), 3.13 (s, 2H, OH), 3.58 (dd, 1H, ²J_{HH} = 11.5 Hz, ³J_{HH} = 6.0 Hz, CH_aH_b), 3.69 (dd, 1H, ²J_{HH} = 11.5 Hz, ³J_{HH} = 6.4 Hz, CH_aH_b), 3.92 (m, 1H, CH), 4.13 (dd, 1H, ²J_{HH} = 11.6 Hz, ³J_{HH} = 5.8 Hz, CH_cH_d), 4.18 (dd, 1H, ²J_{HH} = 11.6 Hz, ³J_{HH} = 5.3 Hz, CH_cH_d); ¹³C NMR (75 MHz, CDCl₃) δ 14.1 (CH₃), 22.7 (CH₂), 24.9 (CH₂), 29.2–29.6 (6 CH₂), 31.9 (CH₂), 34.2 (CH₂), 63.4 (CH₂O), 65.1 (CH₂O), 70.3 (CHOH), 174.4 (C=O); IR (neat) ν 719 (w), 1046 (m), 1176 (m), 1469 (m), 1729 (s), 2850 (m), 2916 (s), 2957 (w), 3232 (large) cm^{−1}; Electrospray mass spectrometry: *m/z* = 275 [MH⁺]; Elemental analyses calcd for C₁₅H₃₀O₄: %C 65.66, %H 11.02, found: %C 66.17, %H 10.98

1-Monotetradecanoyl-*rac*-glycerol (M1b)

¹H NMR (300 MHz, CDCl₃) δ 0.88 (t, 3H, ³J_{HH} = 6.5 Hz, CH₃), 1.26 (m, 20H, CH₂), 1.60 (m, 2H, CH₂), 2.35 (t, 2H, CH₂, ³J_{HH} = 7.5 Hz), 2.88 (s, 2H, OH), 3.58 (dd, 1H, ²J_{HH} = 12.0 Hz, ³J_{HH} = 6.0 Hz, CH_aH_b), 3.69 (dd, 1H, ²J_{HH} = 12.0 Hz, ³J_{HH} = 6.0 Hz, CH_aH_b), 3.91 (m, 1H, CH), 4.15 (m, 2H, CH_cH_d); ¹³C NMR (75 MHz, CDCl₃) δ 14.1 (CH₃), 22.7 (CH₂), 24.9 (CH₂), 29.1–29.7 (8 CH₂), 31.9 (CH₂), 34.2 (CH₂), 63.4 (CH₂O), 65.1 (CH₂O), 70.3 (CHOH), 174.4 (C=O); IR (neat) ν 719 (w), 1046 (m), 1176 (m), 1469 (m), 1729 (s), 2850 (m), 2915 (s), 2957 (w), 3231 (large) cm^{−1}; Impact electronic mass spectrometry (silylated adduct): *m/z* = 431 [M⁺, −CH₃]; Elemental analyses calcd for C₁₇H₃₄O₄: %C 67.51, %H 11.33, found: %C 67.44, %H 11.38.

1-Monohexadecanoyl-*rac*-glycerol (M1c)

¹H NMR (300 MHz, CDCl₃) δ 0.88 (t, 3H, ³J_{HH} = 6.5 Hz, CH₃), 1.26 (m, 24H, CH₂), 1.63 (m, 2H, CH₂), 2.17 (s, 1H, OH), 2.35 (t, 2H, CH₂, ³J_{HH} = 7.5 Hz), 2.60 (s, 1H, OH), 3.71

(m, 2H, CH_aH_b), 3.93 (m, 1H, CH), 4.16 (m, 2H, CH_cH_d); ¹³C NMR (75 MHz, CDCl₃) δ 14.1 (CH₃), 22.7 (CH₂), 24.9 (CH₂), 29.1–29.7 (10 CH₂), 31.9 (CH₂), 34.2 (CH₂), 63.3 (CH₂O), 65.2 (CH₂O), 70.3 (CHOH), 174.4 (C=O); IR (neat) ν 719 (w), 1046 (m), 1176 (m), 1469 (m), 1729 (s), 2850 (m), 2915 (s), 2957 (w), 3231 (large) cm⁻¹; Impact electronic mass spectrometry (silylated adduct): *m/z* = 459 [M⁺, -CH₃]; Elemental analyses calcd for C₁₉H₃₈O₄: %C 69.05, %H 11.59, found: %C 68.79, %H 11.42.

1-Monooctadecanoyl-*rac*-glycerol (M1d)

¹H NMR (300 MHz, CDCl₃) δ 0.87 (t, 3H, CH₃), 1.26 (m, 28H, CH₂), 1.62 (m, 2H, CH₂), 2.36 (t, 2H, CH₂, ³J_{HH} = 7.5 Hz), 2.61 (s, 2H, OH), 3.60 (dd, 1H, ²J_{HH} = 9.0 Hz, ³J_{HH} = 6.0 Hz, CH_aH_b), 3.69 (dd, 1H, ²J_{HH} = 12.0 Hz, ³J_{HH} = 6.0 Hz, CH_aH_b), 3.93 (m, 1H, CH), 4.19 (m, 2H, CH_cH_d); ¹³C NMR (75 MHz, CDCl₃) δ 14.1 (CH₃), 22.7 (CH₂), 24.9 (CH₂), 29.1–29.7 (12 CH₂), 31.9 (CH₂), 34.2 (CH₂), 63.4 (CH₂O), 65.2 (CH₂O), 70.3 (CHOH), 174.4 (C=O); IR (neat) ν 719 (w), 1047 (m), 1177 (m), 1469 (m), 1729 (s), 2849 (s), 2915 (s), 2957 (w), 3298 (large) cm⁻¹; Electrospray mass spectrometry: *m/z* = 382 [MNa⁺]; Elemental analyses calcd for C₂₁H₄₂O₄: %C 70.35, %H 11.81, found: %C 70.32, %H 11.81

1-Monooctadecanoyl-*rac*-glycerol-16-methylacetate (M1f)

mixture of regioisomer α and β; ¹H NMR (300 MHz, CDCl₃) δ 1.25 (m, 20H, CH₂), 1.62 (m, 4H, CH₂), 2.32 (m, 4H, CH₂CO), 3.00 (broad peak, 2H, OH), 3.66 (s, 3H, OCH₃), 3.90 (m, 2H, CH₂O), 3.94 (m, 1H, CH-O), 4.17 (m, 2H, CH₂O); ¹³C NMR (75 MHz, CDCl₃) δ 25.0 (CH₃), 29.2–29.6 (12 CH₂), 34.1 (CH₂), 51.5 (CH₃O), 63.3 (CH₂O), 65.2 (CH₂O), 70.3 (CH-O), 174.38 (C=O, β regioisomer), 174.45 (C=O, α regioisomer); IR (neat) ν 719 (w), 1114 (w), 1168 (m), 1737 (s), 2849 (s), 2916 (s), 2949 (w), 3373 (large) cm⁻¹; Impact electronic mass spectrometry (silylated adduct): *m/z* = 488 [M⁺ - 2 CH₃]; Elemental analyses calcd for C₂₀H₃₈O₆: %C 64.14, %H 10.23, found: %C 63.92, %H 10.22

N-Octadecanoyl-*rac*-amidopropan-2,3-diol (M4d)

¹H NMR (300 MHz, pyridine d₅) δ 0.89 (t, 3H, ³J_{HH} = 6.9 Hz), 1.22 (m, 28H, CH₂), 1.82 (p, 2H, ³J_{HH} = 7.5 Hz, CH₂), 2.45 (t, 2H, ³J_{HH} = 7.4 Hz), 3.90 (dd, 1H, ²J_{HH} = 11.8 Hz, ³J_{HH} = 5.8 Hz, CHO), 3.92 (m, 1H, CHO), 3.96 (m, 3H, CH₂O and CH-O), 4.35 (s, 1H, OH), 6.67 (s, 1H, OH), 6.94 (s, 1H, NH); ¹³C NMR (75 MHz, pyridine d₅) δ 14.3 (CH₃), 22.9 (CH₂), 26.4 (CH₂), 29.6–30.0 (12 CH₂), 32.1 (CH₂), 36.7 (CH₂), 43.5 (CH₂N), 65.0 (CH₂O), 72.2 (CH-O), 174.5 (C=O); IR (neat) ν 724 (m), 1038 (m), 1550 (s), 1637 (s), 2849 (s), 2918 (s), 2954 (w), 3321 (large) cm⁻¹; Electrospray mass spectrometry: *m/z* = 381 [MNa⁺].

1,3-Dihexadecanoyl-*rac*-glycerol (D1c)

¹H NMR (300 MHz, CDCl₃) δ 0.88 (t, 6H, CH₃, ³J_{HH} = 6.5 Hz), 1.26 (m, 48H, CH₂), 1.65 (m, 4H, CH₂), 2.35 (t, 4H, CH₂, ³J_{HH} = 7.5 Hz), 2.46 (s, 1H, OH), 4.15 (m, 5H, CH); ¹³C NMR (75 MHz, CDCl₃) δ 14.1 (CH₃), 22.7 (CH₂), 24.9 (CH₂), 29.1–29.7 (10 CH₂), 31.9 (CH₂), 34.1 (CH₂), 65.1 (CH₂O), 68.4

(CHOH), 173.9 (C=O); IR (neat) ν 719 (w), 1047 (m), 1178 (m), 1470 (m), 1729 (s), 2849 (s), 2915 (s), 2957 (w), 3302 (large) cm⁻¹; Elemental analyses calcd for C₃₅H₆₈O₅: %C 73.89, %H 12.05, found: %C 73.43, %H 11.76

1,3-Dioctadecanoyl-*rac*-glycerol (D1d)

¹H NMR (300 MHz, CDCl₃) δ 0.88 (t, 6H, CH₃, ³J_{HH} = 6.5 Hz), 1.25 (m, 56H, CH₂), 1.61 (m, 4H, CH₂), 2.32 (t, 4H, CH₂, ³J_{HH} = 7.5 Hz), 2.46 (s, 1H, OH), 4.16 (m, 5H, CH).

¹³C NMR (75 MHz, CDCl₃) δ 14.1 (CH₃), 22.7 (CH₂), 24.9 (CH₂), 29.1–29.7 (12 CH₂), 31.9 (CH₂), 34.1 (CH₂), 65.1 (CH₂O), 68.4 (CHOH), 173.9 (C=O); IR (neat) ν 716 (w), 1047 (m), 1179 (m), 1470 (m), 1730 (s), 2849 (s), 2913 (s), 2956 (w), 3299 (large) cm⁻¹; Electrospray mass spectrometry: *m/z* = 644 [MH⁺, H₂O]; Elemental analyses calcd for C₃₉H₇₆O₅: %C 74.95, %H 12.26, found: %C 74.87, %H 12.28

1,7-Dioctadecanoyl-*rac*-diglycerol (D2d)

¹H NMR (300 MHz, CDCl₃) δ 0.88 (t, 6H, CH₃, ³J_{HH} = 6.6 Hz), 1.25 (m, 52H, CH₂), 1.62 (m, 4H, CH₂), 1.72 (m, 4H, CH₂), 2.34 (t, 4H, CH₂, ³J_{HH} = 7.5 Hz), 2.99 (s, 2H, OH), 3.58 (m, 4H, CH₂O), 4.01 (m, 2H, CHOH), 4.13 (m, 4H, CH₂O); ¹³C NMR (75 MHz, CDCl₃) δ 14.1 (CH₃), 22.7 (CH₂), 24.9 (CH₂), 29.1–29.7 (11 CH₂), 31.9 (CH₂), 34.2 (CH₂), 40.9 (CH₂), 65.2 (CH₂O), 68.9 (CHOH), 72.5 (CH₂O), 174.0 (C=O); IR (neat) ν 716 (m), 1147 (m), 1472 (m), 1736 (s), 2849 (s), 2916 (s), 2954 (w), 3420 (large) cm⁻¹; Electrospray mass spectrometry: *m/z* = 722 [MNa⁺]; Elemental analyses calcd for C₄₂H₈₂O₇: %C 72.16, %H 11.82, found: %C 71.95, %H 11.92

1-Monooctadecanoyl-*rac*-triglycerol (M3d)

¹H NMR (300 MHz, pyridine d₅) δ 0.87 (t, 3H, CH₃, ³J_{HH} = 6.0 Hz), 1.29 (m, 282H, CH₂), 1.65 (m, 2H, CH₂), 2.39 (t, 2H, CH₂, ³J_{HH} = 7.5 Hz), 3.64 (m, 9H), 4.08 (m, 2H), 4.55 (m, 2H), 5.16 (m, 2H), 6.43 (s, 1H, OH), 6.62 (s, 2H, OH), 6.78 (s, 1H, OH); ¹³C NMR (75 MHz, pyridine d₅) δ 14.3 (CH₃), 22.9 (CH₂), 25.3 (CH₂), 29.4–30.0 (12 CH₂), 32.2 (CH₂), 34.4 (CH₂), 64.7 (CH₂O), 66.7 (CH₂O), 68.8 (CH-O), 70.0 (CH-O), 72.0 (CH-O), 73.9 (CH₂O), 74.2 (CH₂O), 74.4 (2 CH₂O), 173.7 (C=O); IR (neat) ν 717 (m), 1119 (m), 1472 (m), 1736 (s), 2849 (s), 2914 (s), 2954 (w), 3321 (large) cm⁻¹; Electrospray mass spectrometry: *m/z* = 530 [MNa⁺]; Elemental analyses calcd for C₂₇H₅₄O₈: %C 64.00, %H 10.74, found: %C 63.88, %H 10.68

1-Monooctadecanoyl-*rac*-glycerol-16-hydroxyoctadecanoyl (6)

¹H NMR (300 MHz, pyridine d₅) δ 1.26 (m, 46H, CH₂), 1.52 (m, 4H, CH₂), 1.65 (m, 4H, CH₂), 1.75 (m, 4H, CH₂), 2.39 (m, 4H, CH₂), 3.90 (t, 2H, ³J_{HH} = 6.2 Hz, CH₂O), 4.16 (m, 2H, CH₂O), 4.20 (t, 2H, CH₂O), 4.47 (m, 1H, CH-O), 4.67 (m, 2H, CH₂O), 5.91 (broad s, OH), 6.58 (broad s, OH), 6.95 (broad s, OH); ¹³C NMR (75 MHz, pyridine d₅) δ 25.3 (CH₂), 25.4 (CH₂), 26.3 (CH₂), 26.6 (CH₂), 29.1–30.0 (22 CH₂), 33.8 (CH₂), 34.5 (CH₂), 62.2 (CH₂O), 64.3 (CH₂O), 64.4 (CH₂O), 66.8 (CH₂O), 70.9 (CH-O), 173.6 (C=O), 173.9 (C=O); IR (neat) ν 719 (w), 1045 (m), 1177 (m), 1458 (m), 1174 (m), 1462 (w), 1733 (s), 2849 (s), 2916 (s), 3322 (large) cm⁻¹; Electrospray mass spectrometry: *m/z* = 624 [MNa⁺]

1,16-Di-*rac*-glycerolhexadecanedioate (7)

^1H NMR (300 MHz, pyridine d_5) δ 1.21 (m, 20H, CH_2), 1.67 (m, 4H, CH_2), 2.37 (t, 4H, $^3J_{\text{HH}} = 7.3$ Hz, CH_2CO), 4.15 (m, 2H, CH_2O), 4.47 (m, 1H, CH-O), 4.67 (dd, 1H, $^2J_{\text{HH}} = 10.9$ Hz, $^3J_{\text{HH}} = 6.2$ Hz, CH_cO), 4.74 (dd, 1H, $^2J_{\text{HH}} = 10.9$ Hz, $^3J_{\text{HH}} = 4.4$ Hz, CH_dO) 5.09 (broad s, 2H, OH), 6.7 (broad s, 2H, OH); ^{13}C NMR (75 MHz, pyridine d_5) δ 25.3 (CH_3), 29.4–29.9 (12 CH_2), 34.4 (CH_2), 64.3 (CH_2O), 66.8 (CH_2O), 70.9 (CH-O), 173.8 (C=O); IR (neat) ν 718 (w), 1046 (m), 1171 (m), 1730 (s), 2849 (s), 2915 (s), 3229 (large) cm^{-1} ; Electrospray mass spectrometry: $m/z = 458$ [MNa^+]; Elemental analyses calcd for $\text{C}_{22}\text{H}_{42}\text{O}_8$: %C 60.81, %H 9.74, found: %C 60.40, %H 9.54

Acknowledgements

This work was supported by the CNRS and the Ministère de la Recherche. GK is grateful to the Moroccan government for her PhD grant.

References

- (a) M. Mittelbach and H. Junek, *Fr. Pat.* FR26003296, 1998; (b) H. Henkel, *Eur. Pat.* EP200982, 1986.
- (a) P. A. Anastas and J. C. Warner in *Green Chemistry: Theory and Practice*, Oxford University Press, Oxford, 1998; (b) J. M. Clark, *Green Chem.*, 1999, **1**, 1.
- E. Jungermann and N. O. V. Sonntag in *Glycerin: a Key Cosmetic Ingredient*, Marcel Dekker Inc. Ed., New York, 1991.
- (a) O. Saravari, P. Phapant and V. Pimpan, *J. Appl. Polym. Sci.*, 2005, **96**, 4, 1170; (b) J. Barrault, F. Jérôme and Y. Pouilloux, *Lipid Technol.*, 2005, **17**, 6, 131.
- (a) J. Falbe in *Surfactants in Consumer Products: Theory, Technology and Applications*, Springer-Verger, New York, 1998; (b) M. Kloosterman, V. H. M. Elferink, J. Van Lersel, J. H. Roskam, E. M. Meijer, L. A. Hulshof and R. Sheldon, *Trends Biotechnol.*, 1998, **6**, 251; (c) S. Takano, M. Yanase, Y. Sekiguchi and K. Ogasawara, *Tetrahedron Lett.*, 1987, **28**, 1784; (d) A. Legrand, *World Pat.* WO98/00120, 1998.
- (a) C. Otero, J. A. Arcos, M. Angeles Berrendero and C. Torres, *J. Mol. Catal. B: Enzym.*, 2001, **11**, 883; (b) J.-H. Xu, Y. Kato and Y. Asano, *Biotechnol. Bioeng.*, 2001, **73**, 493; (c) E. Santaniello, P. Ferraboschi and P. Grisenti, *Enzyme Microb. Technol.*, 1993, **15**, 367; (d) J. S. Dordick, *Enzyme Microb. Technol.*, 1989, **11**, 194.
- S. Wongsakul, P. Prasertan, U. T. Bornscheuer and A. H-Kittikun, *Eur. J. Lipid Sci. Technol.*, 2003, **105**, 68.
- (a) A. Corma, S. B. A. Hamid, S. Iborra and A. Velty, *J. Catal.*, 2005, **234**, 340; (b) S. Banquart, C. Vanhove, Y. Pouilloux and J. Barrault, *Appl. Catal., A*, 2001, **218**, 1.
- (a) M. da Silva-Machado, D. Cardoso, J. Perez-Pariente and E. Sastre, *Stud. Surf. Sci. Catal.*, 2000, **130**, 3417; (b) M. da Silva-Machado, J. Perez-Pariente, E. Sastre, D. Cardoso and A. M. de Guereu, *Appl. Catal., A*, 2000, **203**, 321.
- (a) G. Kharchafi, F. Jérôme, I. Adam, Y. Pouilloux and J. Barrault, *New J. Chem.*, 2005, **29**, 928; (b) W. D. Bossaert, D. E. De Vos, W. M. Van Rhijn, J. Bullen, P. J. Grobet and P. A. Jacobs, *J. Catal.*, 1999, **182**, 156; (c) J. Pérez-Pariente, I. Diaz, F. Mohino and E. Sastre, *Appl. Catal., A*, 2003, **254**, 173; (d) A. Corma, S. Iborra, S. Miquel and J. Primo, *J. Catal.*, 1998, **173**, 315; (e) J. Barrault, S. Banquart and Y. Pouilloux, *C. R. Chim.*, 2004, **7**, 593.
- (a) Y. Pouilloux, S. Abro, C. Vanhove and J. Barrault, *J. Mol. Catal. A: Chem.*, 1999, **149**, 243; (b) F. Jérôme, G. Kharchafi, I. Adam and J. Barrault, *Green Chem.*, 2004, 72.
- (a) R. Kluger, *J. Am. Chem. Soc.*, 2002, **124**, 3303; (b) L. L. Cameron, S. C. Wang and R. Kluger, *J. Am. Chem. Soc.*, **126**, 10721; (c) B. M. Trost and T. Mino, *J. Am. Chem. Soc.*, 2003, **125**, 2410.
- (a) B. Kovacevic, D. Baric and Z. B. Maksic, *New J. Chem.*, 2004, **28**, 284; (b) R. Schwesinger, H. Schlemper, C. Hasenfratz, J. Willaredt, T. Dambacher, T. Breuer, C. Ottaway, M. Fletschinger, J. Boele, H. Fritez, D. Putzas, H. W. Rotter, F. G. Borwell, A. V. Satish, G.-Z. Ji, E.-M. Peters, K. Peters, H. G. von Schnering and L. Walz, *Liebigs Ann.*, 1996, 1055.
- (a) V. Molinier, B. Fenet, J. Fitremann, A. Bouchu, G. Descotes and Y. Queneau, *Colloids Surf., A*, 2000, **172**, 125; (b) Y. Queneau, J. Gagnaire, J. J. West and J. W. Goodby, *J. Mater. Chem.*, 2001, **11**, 2839.
- (a) A. L. Kenna, in *Fatty Amides, Synthesis, Properties, Reactions and Applications*, Witco Chemical Corporation, Humko Chemical Division, Memphis, 1982, 111; (b) H. L. Sanders, *J. Am. Oil Chem. Soc.*, 1958, 548.
- M. R. Sahasrabudhe, *J. Am. Oil Chem. Soc.*, 1957, **44**, 376.

Functional monolithic resins for the development of enantioselective versatile catalytic minireactors with long-term stability: TADDOL supported systems

Belen Altava,* M. Isabel Burguete,* Eduardo García-Verdugo, Santiago V. Luis* and Maria J. Vicent

Received 7th March 2006, Accepted 9th June 2006

First published as an Advance Article on the web 23rd June 2006

DOI: 10.1039/b603494b

Polymeric monoliths containing TADDOL subunits have been prepared by polymerization of the corresponding functional monomers. Treatment with TiX_4 species affords Ti-TADDOLates, which can be used sequentially for two different reactions, namely the Diels–Alder reaction and the $ZnEt_2$ addition to benzaldehyde. These monolithic materials allow working either in batch or under flow conditions. The Diels–Alder reaction is carried out more efficiently in batch than under flow conditions, but the opposite is found for the $ZnEt_2$ addition.

Enantioselectivities obtained compare well with those for other related supported systems. In some cases ee values found for the polymer-bound system are higher than those for the homogeneous analogue. The supported Ti-catalysts show an extraordinary long-term stability, being active for at least one year.

Introduction

Catalysis is a key tool for green and sustainable chemistry,¹ and many examples of its successful application, in particular for bulk chemicals production are well known.² The practical application of enantioselective catalysis continues to be, however, an important challenge nowadays, and examples of its use at an industrial level are more limited.² This is despite the very high efficiency with which stereoselective syntheses can be carried out at the laboratory scale.³ The development of enantioselective heterogeneous catalysts represents one of the main approaches to this challenge. Immobilized catalysts are best suited, in principle, for practical applications, as they can be easily recycled and reused.^{4,5} Different kinds of supports have been used for the immobilization process, but polystyrene-divinylbenzene (PS-DVB) resins continue to be one of the most popular supporting materials for this purpose.^{4–6} Nevertheless, this kind of catalyst still faces important barriers to its general use.

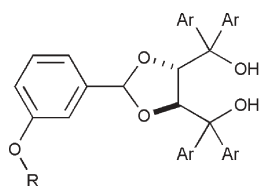
Supported systems very often show properties that greatly differ from those of the soluble analogues. The immobilization of a chiral auxiliary onto a polymeric matrix can be achieved by two alternative methodologies: grafting and copolymerization.^{4–7} The resulting functional polymers can have different physical and chemical properties.^{8a,c} Although the polymeric backbone has been considered for years as a truly inert component of the system, it is very important to realize that it plays an essential role in determining the overall performance of the supported species.^{4,8,9} Thus, the catalytic activity and the selectivity of a given supported species can be very much affected when the nature and the morphological characteristics

of the support are changed.^{7–10} Another important limitation of enantioselective heterogeneous catalysts, in terms of practical applications, is the need for developing a new catalyst for each individual process. In general, a single catalyst is prepared and used for a single reaction for one or several runs. An important goal, in this regard, should be the preparation of catalysts capable of being used, sequentially, for more than one single reaction. For this purpose, the development of heterogeneous systems with a capacity for scaling, with an outstanding long-term stability, being able to adapt to different solvents and reaction conditions and to automatic or simplified work-ups, is required.

The preparation of supported reagents and catalysts in the form of polymeric monoliths presents several distinct advantages that could overcome some of those limitations.¹¹ The corresponding monolithic materials, if properly designed, do not present the diffusional limitations that can be found in gel-type resins in the presence of non-swelling solvents, are very stable from a mechanical point of view and can be used advantageously under flow conditions.¹² Additionally, enantioselective polymer-bound catalysts prepared by polymerization in highly crosslinked networks have been reported to produce, in some cases, better asymmetric inductions than systems prepared by grafting.^{7–9} Accordingly, catalysts supported on polymeric monolithic materials have a great potential for developing catalytic minireactors.

Here we present data that reveal how monolithic catalysts functionalized with Ti-TADDOLate moieties can be active for different alternative reactions and present a very remarkable long-term stability so as to preserve the initial activity and selectivity for at least one year. The results obtained clearly highlight both the large influence of the polymeric matrix on the properties of these supported systems, including selectivity and stability, and the great potential of monolithic catalysts for practical applications.

Department of Inorganic and Organic Chemistry/Associated Unit for Advanced Organic Materials, University Jaume I/CSIC, E-12071 Castellón, Spain. E-mail: luiss@qio.uji.es; Fax: 34 964 728214; Tel: 34 964 728239



- 1 R=H
 2 R=CH₂Ph
 3 R=p-CH₂-C₆H₄-CHCH₂
 4 R=PS, grafting
 5 R=PS, polymerisation
- a, Ar=3,5-(CH₃)₂C₆H₃⁻
 b, Ar=2-Naphthyl
 c, Ar=1-Naphthyl

Chart 1 TADDOLs used in this work.

Results and discussion

Preparation of TADDOL derivatives

Since the seminal work by Seebach, Narasaka and others, Ti-TADDOLates have become an important and versatile class of chiral catalysts that have been used for a broad range of enantioselective organic transformations.^{13,14} In this regard, our group has been involved in the last years in the preparation of different resin-bound Ti-TADDOLates and related analogues, and in their study as Lewis acid catalysts for Diels–Alder reactions.^{10,15,20}

Homogeneous and supported TADDOL derivatives with the general structures **2**, **4** and **5** (Chart 1) were prepared and characterized according to the general procedure developed by our group.^{10,15,16} Compounds **2**, having the same structural features than functional moieties in polymers **4** and **5** are needed as reference compounds in solution. Comparisons made between homogeneous and supported species cannot rely

on species not having strictly the same structures, as even minor structural modifications can have significant effects on the performance of enantioselective catalysts.^{9a}

Monolithic polymers **5** were prepared by thermally induced radical solution polymerization of a monomeric mixture containing the corresponding vinylic derivative, styrene (ST) and divinylbenzene (DVB), using toluene/1-dodecanol as the precipitating porogenic mixture and AIBN as the radical initiator.¹¹ In order to take full advantage of the potential of those monolithic systems, polymerization was carried out within a stainless steel columnar mold, so that a simple connection through both end caps could allow us to use those columns as stable minireactors either in batch or under flow conditions. The resulting monolithic columns obtained are similar to those that have been used for chromatographic applications.^{11e,17}

Several experiments were designed to evaluate the influence of the different polymerization parameters on the appropriate mechanical and morphological properties. For the case of TADDOL **3a** (Ar = -3,5-(CH₃)₂C₆H₃-), the results of an initial set of experiments are shown in Table 1. In all cases, the amount and composition of the porogenic mixture was kept constant (*ca.* 60% of the total mixture: 20% of toluene, 40% of 1-dodecanol) and the effect of the variation in the composition of the monomeric mixture was analyzed. As can be seen in the table, very high backpressures were obtained in all cases. This can be ascribed to the formation of monolithic polymers with very low pore sizes as was evidenced by mercury intrusion porosimetry data. In the case for which a mixture of **3b**/ST/DVB was used as the monomeric mixture (entry 2 in Table 2) a

Table 1 Properties of monolithic columns prepared from **5b** using different monomeric compositions

Entry	Monomeric composition (wt%)			Toluene ^a (wt%)	Back pressure ^b /psi	Flow/mL min ⁻¹	D _{p,med} ^c /nm
	3a	DVB	ST				
1	20	80	—	20	435 (±35)	1	73
2	20	40	40	20	— ^d	— ^d	— ^d
3	30	70	—	20	617 (±12)	0.5	0
4	40	60	—	20	812 (±12)	1	61

^a The porogenic mixture was always toluene/1-dodecanol (1 : 2, w : w) and was used in a ratio 60 : 40 (w : w) porogens : monomers. ^b Measured on a pressure gauge. ^c Median pore diameter as determined by mercury intrusion porosimetry. ^d The polymer did not adhere to the walls of the columnar mold.

Table 2 Results obtained for the Diels–Alder reaction (Scheme 2) catalysed by Ti-TADDOLates considered in this work

Entry	Ligand ^a	R ^b	Ar	T/ ^o C	Conv. (%) ^{c,d}	endo : exo ^e	ee (%) ^f
1	2b	Bn	2-Naphthyl	0	96	74 : 26	61 (2 <i>S</i> ,3 <i>R</i>)
2	4b	PS-g	2-Naphthyl	0	50	83 : 17	40 (2 <i>S</i> ,3 <i>R</i>)
3	5b	PS-m	2-Naphthyl	0	90	83 : 17	37 (2 <i>S</i> ,3 <i>R</i>)
4	2a	Bn	3,5-(CH ₃) ₂ C ₆ H ₃	0	99	71 : 29	38 (2 <i>R</i> ,3 <i>S</i>)
5	5a	PS-m	3,5-(CH ₃) ₂ C ₆ H ₃	0	79	80 : 20	20 (2 <i>S</i> ,3 <i>R</i>)
6	4a	PS-g	3,5-(CH ₃) ₂ C ₆ H ₃	25	98	70 : 30	17 (2 <i>R</i> ,3 <i>S</i>)
7	5a	PS-m	3,5-(CH ₃) ₂ C ₆ H ₃	25	99	80 : 20	18 (2 <i>S</i> ,3 <i>R</i>)
8	2c	Bn	1-Naphthyl	0	99	83 : 17	20 (2 <i>R</i> ,3 <i>S</i>)
9	4c	PS-g	1-Naphthyl	0	35	80 : 20	13 (2 <i>R</i> ,3 <i>S</i>)
10	5c	PS-m	1-Naphthyl	0	55	85 : 15	43 (2 <i>R</i> ,3 <i>S</i>)
11	5c	PS-m	1-Naphthyl	-20	30	76 : 24	38 (2 <i>R</i> ,3 <i>S</i>)
12	5c	PS-m	1-Naphthyl	25	99	84 : 16	19 (2 <i>R</i> ,3 <i>S</i>)

^a 10% of catalyst was used in all cases relative to the amount of dienophile. Cyclopentadiene was always added 2.5 times in excess over dienophile. ^b PS-g: Polystyrene-divinylbenzene, attachment by grafting. PS-m: Polystyrene-divinylbenzene in monolithic form, attachment by polymerization. ^c Conversion of dienophile. ^d Determined by ¹H NMR. ^e Determined by ¹H NMR. ^f Determined by ¹H NMR using Eu(hfc)₃ on the major *endo* isomers.

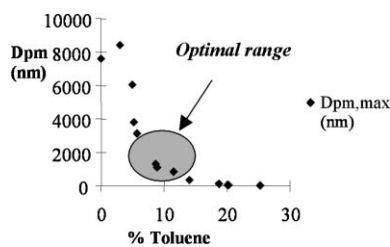


Fig. 1 Morphological properties for monolithic columns. $D_{p,med}$: median pore diameter as calculated from mercury intrusion porosimetry.

complete lack of adherence to the mold was observed for the resulting polymer. For all the monolithic columns in Table 2, the presence of a significant “wall effect” was observed, indicating that the eluent is mainly flowing through cracks in the monolith or between the wall of the mold and the polymer.

Taking into account the former results, a new series of experiments were carried out by using a fixed monomeric composition (the one shown in entry 4 of Table 1: 40% of **3a** and 60% of DVB) and studying the effect of the changes in the composition of the porogenic mixture on the morphological properties of the resulting monolithic polymers (**5a**). The results are gathered in Fig. 1 that show the variation in the $D_{p,med}$ (median pore diameter) calculated from mercury intrusion porosimetry, as a function of the amount of toluene used as porogen (the ratio monomers/porogens was kept always constant at a value of 40/60 w/w). In general, $D_{p,med}$ values considered appropriate for this kind of materials range from 1000 to 2000 nm. This roughly corresponds with the shadowed region in the graph. Accordingly, polymeric monoliths with the expected porosity and without “wall effects” were obtained using porogenic mixtures, for which toluene was about 10% in weight of the initial mixture.¹¹

The other monolithic polymers **5** were prepared using the same conditions optimized for resin **5a**. In all instances, yields were quantitative, with a complete incorporation of monomers into the polymeric monolith. Loadings ranged from 0.53 mmol g⁻¹ (**5a**) to 0.46 mmol g⁻¹ (**5c**). Both porosimetry data and the values of back pressures obtained for those resins indicated that a very similar porosity was present in all of them.

Study of resin-bound Ti-TADDOLates as Lewis acid catalysts for the Diels–Alder reaction

The corresponding monolithic Ti-TADDOLates were prepared, under an inert atmosphere, by treatment of **5** with an

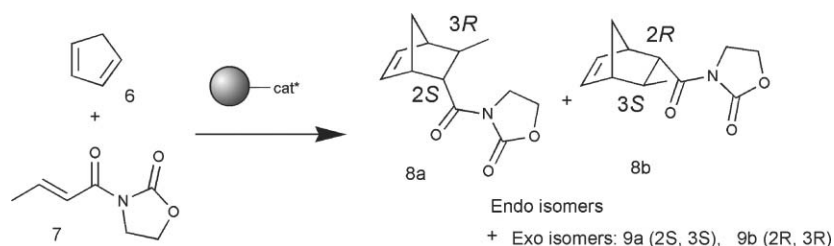
excess of a solution of Ti(OPrⁱ)₂Cl₂ previously prepared by mixing equimolar amounts of TiCl₄ and Ti(OPrⁱ)₄ in toluene.¹³ The corresponding solution was passed through the column using a syringe pump at a low flow rate. The Ti content in the resins was analyzed indirectly by titration of the solution resulting after the loading of the polymers. In all cases the uptake of Ti(OPrⁱ)₂Cl₂ was in the range expected for a quantitative transformation of the TADDOL fragment present. A semiquantitative analysis of Ti by electron microscopy (energy-disperse analysis by X-ray, EDAX) showed a uniform distribution of the metal, and the loadings calculated were in good agreement with those obtained by titration.¹⁸

The resulting Ti-TADDOLates were assayed as catalysts for the Diels–Alder reaction of cyclopentadiene **6** and 3-crotonoyl-1,3-oxazolidin-2-one **7** (see Scheme 1). Monolithic Ti-TADDOLates were used as the corresponding homogeneous analogues. Initial experiments were carried out in batch mode, loading the monolithic reactors with the reaction mixture in toluene, sealing both end-caps of the column and maintaining the appropriate temperature for the corresponding reaction time. Some results are gathered in Table 2.

In general, lower yields were obtained for heterogeneous systems **4** or **5** than for the homogeneous analogues **2**. The decrease in activity for supported reagents and catalysts has been often associated with limitations in the diffusion of reactants within the polymeric matrix.¹⁹ Monolithic systems were clearly superior to gel-type resins. Monolithic polymers are macroporous with good diffusion properties. Thus, higher conversions were always found for monolithic catalysts (compare, in particular, entries 2 and 3). Very similar *endo* : *exo* selectivities were observed for the different catalysts, homogeneous and heterogeneous, ranging from 71 : 29 (entry 4) to 85 : 15 (entry 10).

Regarding enantioselectivity, *ee* values obtained were, in general, below 60%. This is far from the excellent enantioselectivities reported earlier in solution for this reaction using simple TADDOL derivatives such as those derived from acetone.^{13d} This is related with the structural modifications needed to provide the linkage to the polymeric matrix. The presence of the benzyloxyphenyl substituent on the C-2 of the dioxolane ring, either for the homogeneous or for the related heterogeneous TADDOL analogues, has very large effects on the selectivities as has been demonstrated by different groups.^{13,14,20} However, the results achieved in this work clearly show the importance of the immobilization strategy to develop efficient supported catalysts.

At a first sight, the homogeneous catalysts seem to present higher enantioselectivities than the supported ones. This kind



Scheme 1

of behavior has been reported for different heterogenized systems, so that it has become usual to consider that heterogenization of enantioselective catalysts is normally accompanied by a significant decrease in selectivity (“*negative polymeric effect*”). Fortunately, this is not true and positive polymeric effects can be found in many cases, including effects on enantioselectivity.²¹

A comparison between the results obtained with gel-type resins and with monolithic polymers under the same experimental conditions (compare, for instance, entries 9 and 10) confirms that catalysts prepared by polymerization in a highly crosslinked matrix can provide better enantioselectivities than the ones prepared *via* grafting methodologies. Similar trends have been reported by us and other workers in different systems.^{8a,c,9} It is noteworthy, however, that, as shown in entries 8–10 of Table 2, the enantioselectivity obtained at 0 °C for the monolithic Ti-TADDOLate from **5c** (43% ee) is significantly higher than that for the homogeneous (from **2c**, 20% ee) and grafted (from **4c**, 13% ee) analogues, under the same conditions. This represents an additional example of the existence of “*positive polymeric effects*” of the matrix on selectivity, and clearly demonstrate how the nature of the active sites prepared by polymerization and grafting can be different.^{8b,9,10}

As could be expected, also for supported catalysts the activity increases with the temperature, whilst the enantioselectivity is higher at lower temperatures. Nevertheless, the effect was only significant for **5c** (entries 10 and 12) for which ee values experienced a two-fold increase from 25 °C to 0 °C. At the same time, a maximum in ee values seems to be reached at temperatures close to 0 °C, with no additional increase in enantioselectivity when the temperature is lowered up to –20 °C (entry 11).

In any case, it is important to note that enantioselectivities found with monolithic catalysts from **5b** and **5c** are within the higher reported for the use of supported Ti-TADDOLates as catalysts for the Diels–Alder reaction of 3-crotonoyl-1,3-oxazolidin-2-one and cyclopentadiene. A maximum value of 42% has been reported by Seebach *et al.* using polymeric Ti-TADDOLates obtained by suspension polymerization, having 1-naphthyl substituents.^{13d} Accordingly, the results here reported seem to represent the upper limit up to now achieved, in terms of enantioselectivity, for supported Ti-TADDOLates in this reaction. Other families of enantioselective polymer-supported catalysts have been, however, more successful for this reaction.²²

One of the more remarkable observations derived from data in Table 2 is that the major *endo* enantiomer obtained with the *endo* adducts in the case of monolithic catalyst from **5a**

(Ar = –3,5-(CH₃)₂–C₆H₃–) was the 2*S*,3*R* isomer instead of the 2*R*,3*S* isomer obtained with the homogeneous analogue from **2a** or with the catalyst from **4a** prepared by grafting (compare entries 5 and 7 with 6 in Table 3).²³

Clearly, *this reversal of topicity must be attributed to the polymeric matrix*. This result represents a first example of a polymer-bound enantioselective catalyst for which the topicity of the resulting products can be controlled through the appropriate design of the morphology of the matrix.^{8d} The role of the matrix could be ascribed to the generation of main-chain chirality/chiral cavities derived from the polymerization of a vinylic monomer containing chiral fragments.²⁴ Alternatively, it could be associated to the function of aromatic subunits at the groups bound to the C-2 position of the dioxolane ring. When those aromatic rings are present, π – π interactions with the α -substituent play a key role to determine both the nature of the most stable conformer and the relative stability of the possible transition states.^{13d,20} We have demonstrated that inhibiting the formation of such π – π interactions, introducing aliphatic spacers between C-2 and the aromatic unit, provides a way for decreasing the relative amount of the *endo*-2*R*,3*S* isomer formed.²⁰ Thus, polymerization of the corresponding vinylic TADDOL (**3a**) in a very rigid, highly crosslinked matrix might preclude the formation of those π – π interactions between the aromatic group at C-2 and one of the 3,5-dimethylphenyl substituents at the α -positions, precluding the formation of some of the expected conformers and modifying the relative energies of the participating transition states, favoring in this way the formation of the *endo*-2*S*,3*R* adduct.

Study of polymer-supported Ti-TADDOLates as catalysts under flow conditions

One of the most important practical advantages of the preparation of polymer-supported catalysts in the form of monolithic columns is the possibility of their use either in batch or under flow conditions.¹² Accordingly different experiments were carried out under flow conditions using the monolithic column **5a** with Ti-TADDOLate functionalities having 3,5-dimethylphenyl groups at the α -positions. Some results are shown in Table 3.

Two different kinds of experiments were carried out under flow conditions. For entry 2, the solution was continuously recirculated through the column, using an experimental set-up similar to the one formerly described for other monolithic systems (see Fig. 2).^{12a} For entries 3–5 no recirculation took place and the solution eluted from the column was analyzed directly.

Table 3 Results obtained for the Diels–Alder reaction of **6** and **7** under flow conditions, using monolithic Ti-TADDOLate from **5a**

Entry	dienophile/mol ⁻¹	dienophile/catalyst ^a	Flow/mL min ⁻¹	Yield (%)	<i>endo/exo</i>	ee ^e (%)
1	2	10	— ^b	99	4.0	18
2	0.06	6.1	0.25	55 ^c	3.1	23
3	0.18	2.0	0.04	20 ^d	3.3	6.5
4	0.11	3.4	0.04	25 ^d	2.8	19
5	0.11	3.4	0.1	25 ^d	2.3	25

^a Nominal ratio considering the total amount of catalyst in the column and the total amount of dienophile in the solution. ^b Reaction in batch, not under flow conditions. ^c Continuous recirculation of the solution through the column for 24 h. ^d No recirculation of the solution eluted from the column. ^e Determined by ¹H NMR using Eu(hfc)₃ on the major *endo* isomers, major *endo* isomer (2*S*,3*R*).

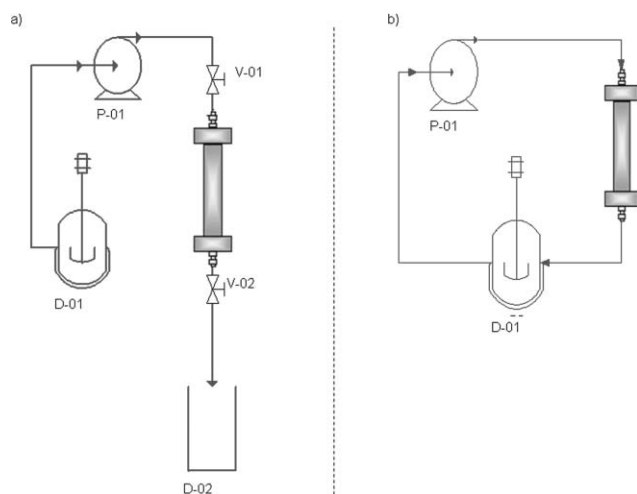


Fig. 2 Use of monolithic columns containing Ti-TADDOLates as catalytic minireactors under batch and flow conditions: (i) *Batch reaction*: the reaction mixture is pumped into the monolithic reactor (set-up a) the pump is stopped and the valves V-01 and V-02 closed during the reaction time. Products are washed out of the reactor by pumping dry solvent through. (ii) *Continuous flow reaction* (set-up a): the reaction mixture is pumped through the reactor and the products collected on reservoir D-02. (iii) *Recirculation* (set-up b). D-01, reagent feed vessel; P-01, reagent feed pump (HPLC Gilson Model 304, flow rate = 0.01–5 mL min⁻¹). Monolithic minireactors (1/4 in AISI 316 tubing 15 cm).

The data in Table 3 suggest that no significant advantages are found for this system with the use of flow conditions, in contrast to results obtained in other cases.¹² Under both conditions, the flow rate clearly affects the enantioselectivity of the reaction, the best ee values always being obtained for higher flow rates. The differences found between batch and flow systems have been often associated with the changes in the actual concentration of substrates at the active sites.^{12a,e} This should be particularly important for this reaction, for which this parameter has been demonstrated to be critical for the performance of Ti-TADDOLates in solution.^{13d,20c} The presence of two different kinds of catalytic active site with a different degree of accessibility, sites located at the surface and sites located at the crosslinked regions, could also be important if they present a different selectivity pattern. Access to the more hindered sites is likely to be diffusion controlled so that their participation is highly increased at lower flow rates. Similar experiments were carried out under flow conditions with Ti-TADDOLate from **5b** as the catalyst and the general patterns are similar to those shown in Table 3 for **5a**. Also in this case, best ee values (23%) were obtained for the higher flow rates studied.

Overall, a slight increase in enantioselectivity can be achieved, under flow conditions, with an appropriate design of the experiment, but this takes place at the expense of a significant reduction in yields.

Long-term stability studies

The very simple work-up needed in using the monolithic columns greatly facilitates their reuse and recycling. Simply by

connecting one end of the column to a pump and flushing the column with the appropriate anhydrous solvent the catalyst is ready for a new run. In this way, all the catalytic minireactors prepared were used for several runs without any appreciable loss of performance. This is now not unusual and many examples can be found in the literature in which the corresponding polymer-supported catalyst can be efficiently reused for 10–20 runs or even more.⁴ An important parameter, however, that needs to be analyzed for correctly assessing the potential practical applications of this kind of minireactor is the long-term stability.

Initial studies were carried out with the monolithic Ti-TADDOLate from **5a**, in order to analyze simultaneously its stability and to detect any modification in the reversal of topicity observed in the first runs. Some of the results obtained are shown in Fig. 3a. As can be seen, both the activity and the selectivity of this supported catalyst remain unchanged for a period of up to six months. No special care or work-up is needed to maintain the activity of the corresponding column, except to close both ends of the column after each run. Only when the column was left open to the air for a few days, after the sixth month of use, were some changes observed: the activity remained almost unchanged, but a decrease in the enantioselectivity was observed.

This behavior is indicative of an extraordinarily long-term stability for this kind of material and is common to other monolithic Ti-TADDOLates. Fig. 3b–c shows data corresponding to catalysts from **5b** (Ar = 2-naphthyl) and from **5c** (Ar = 1-naphthyl). The results confirm that no decrease in activity or selectivity can be detected after 6 or 8 months. Only when, after one year, the column is open to the air, was a significant decrease in activity and selectivity observed. In both cases, regeneration of the catalyst was attempted by a

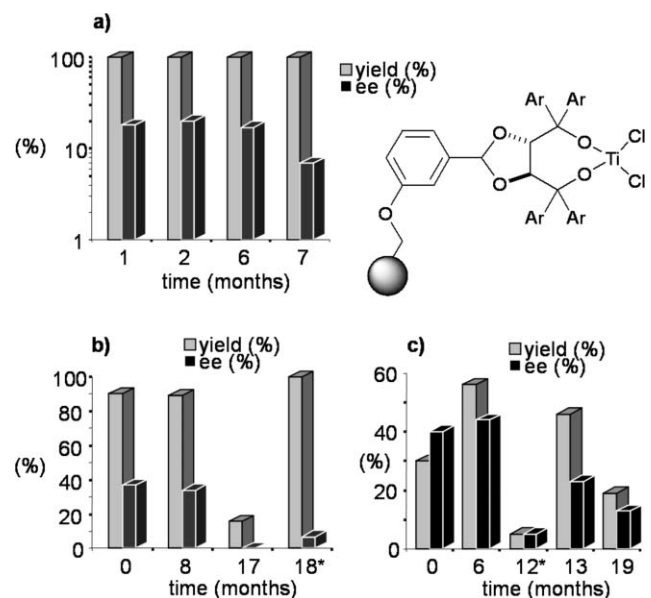


Fig. 3 Time-dependent activity and enantioselectivity of Ti-TADDOLates from **5** as catalysts for the Diels–Alder reaction between **6** and **7**. (a) Ar = 3,5-(CH₃)₂C₆H₃, (b) Ar = 2-naphthyl, (c) Ar = 1-naphthyl. The month for which regeneration of the catalyst was carried out is indicated by an asterisk.

thorough washing of the column, followed by drying and reloading with additional amounts of $\text{Ti}(\text{OPr})_2\text{Cl}_2$. The catalysts prepared in this way were assayed again for the same Diels–Alder reaction between **6** and **7**. As shown in Fig. 3, the activity was essentially recovered for the first run but not the enantioselectivity. On the other hand, the characteristic long-term stability of these columns is lost after regeneration and both activity and selectivity decrease sharply with use.

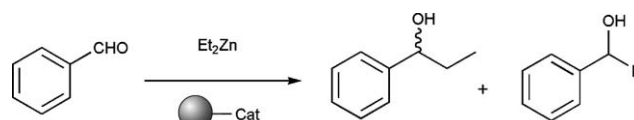
Monolithic Ti–TADDOLates as the basis of versatile catalysts

The lack of efficiency for the regeneration process of polymer-supported Ti–TADDOLates was, initially, rather surprising since very effective regeneration processes have been described by other authors for related resin-bound catalysts.¹³ In particular, regeneration is a critical step in the use of Ti–TADDOLates as catalysts in the addition of ZnEt_2 to benzaldehyde. In this case, Seebach and co-workers, for instance, have reported that the regenerated catalyst provides the same performance in terms of activity and selectivity and that regeneration can be performed for a large number of cycles.¹³

Nevertheless, this discrepancy in recyclability seems to be associated with the different reactions considered. Monolithic catalysts from **5** provided the same outputs, in this regard, as those reported by Seebach when the addition reaction using ZnEt_2 was studied as opposed to the Diels–Alder reaction. Thus, the Diels–Alder reaction seems to require a much more strict control of reaction parameters to be carried out successfully. In the case of supported Ti–TADDOLate catalysts we can consider that the presence of even minor amounts of residual Ti species not covalently bound to the ligand can interfere in catalysing the reaction in a non-selective way. The situation is different for the Et_2Zn addition, since it is known to be a ligand accelerated reaction, so that, in this case, the interference by non-ligand-bound Ti species should be much lower.

Those preliminary experiments are of great interest. However, a severe limitation for industrial applications of enantioselective catalysts is the need of a specific catalyst for each given reaction. The possibility of having a reusable catalyst capable of being applied efficiently for several reactions would greatly increase the potential for exploitation of these materials. Accordingly, different experiments were carried out using monolithic columns **5b**, having 2-naphthyl groups at the α -positions, for the addition reaction of ZnEt_2 to benzaldehyde. Some results are shown in Table 4.

The data in Table 4 show that monolithic Ti–TADDOLates do form versatile catalysts. The monolithic columns previously used in the study of the Diels–Alder reaction proved to be efficient catalysts for the ZnEt_2 addition to benzaldehyde (see entry 1), once the catalytic sites were regenerated by a thorough washing and further treatment with $\text{Ti}(\text{iPrO})_4$.¹³ As a matter of fact, the performance of this catalyst was comparable to that of a new column prepared, under the same conditions, but not used for any previous reaction (entry 2). In both cases, using a stoichiometric TiX_4 /ligand ratio, good conversions and selectivities were observed, but only moderate enantioselectivities. Even with the use of lower temperatures



Scheme 2

Table 4 Results obtained for the reaction between benzaldehyde and ZnEt_2 using monolithic catalyst from **5b**

Entry	Time/h	$T/^\circ\text{C}$	ZnEt_2 (eq.)	% cat. ^a	Yield (%)	Selectivity (%)	ee ^b (%)
1	24	5	1.4	40	88	78	33(1 <i>S</i>) ^{c,d}
2	19	5	1.4	40	84	88	39(1 <i>S</i>) ^d
3	20	−50	1.4	40	12	60	33(1 <i>S</i>) ^d
4	21	5	1.4	40	34	72	48(1 <i>S</i>) ^{d,e}
5	2.5	−30	1.8	20	60	100	99(1 <i>S</i>) ^{e,f}

^a Percentage of catalyst considering the total amount of catalyst in the column and the total amount of benzaldehyde in the solution.

^b Determined by chiral HPLC, using Chiralcel OD column.

^c Monolithic Ti–TADDOLate regenerated after its activity study in the Diels–Alder reaction. ^d Reaction in batch. ^e Using 1 eq. of $\text{Ti}(\text{iPrO})_4$. ^f Reaction under continuous flow (0.06 mL min^{-1}).

(entry 3) the enantioselectivity was no further improved. It has been reported that a stoichiometric TiX_4 /substrate ratio is convenient for the “*in situ*” regeneration of the catalytic species.¹³ Our results support this hypothesis and strongly suggest that only one single molecule of substrate is transformed, in a very selective way, by the catalytic site in agreement with the proposed mechanism.¹³ Taking this into consideration, and using a stoichiometric $\text{Ti}(\text{iPrO})_4$ /substrate ratio, a clear improvement was obtained. Even at 5°C , a 48% ee could be obtained (entry 4). Finally, an optimum outcome was achieved (entry 5) by carrying out the reaction, under those conditions, at $−30^\circ\text{C}$ and using a continuous flow system (0.06 mL min^{-1}). A 60% conversion was obtained along with a quantitative selectivity and enantioselectivity. It is noteworthy that the use of flow conditions allows one to work efficiently with lower catalyst/substrate ratios that in the case of batch experiments.

Conclusions

In summary, chiral functional monoliths prepared by polymerization of the corresponding chiral functional vinylic monomers have a great potential interest for the development of practical enantioselective catalysts and, accordingly, more environmentally friendly processes. These materials present some distinct advantages in this regard: (i) Optimization of the results obtained can be modulated by the appropriate adjustment of material preparation conditions such as composition of the monomeric mixture or amount and nature of the porogens. (ii) The corresponding catalytic reactions can be carried out either in batch or under flow (continuous or recirculation). (iii) Diffusional limitations inherent to many supported systems are avoided or severely reduced. (iv) Monoliths can be synthesized in different forms and shapes, including columnar molds as the ones here presented, which allows a significant simplification of the work up. (v) An outstanding long-term stability is observed. (vi) This

remarkable, chemical, mechanical and morphological stability allows their use as multipurpose catalysts, so that after a first reaction the monolith can be recovered and reused efficiently for a second, different reaction.

In the present work the same columnar polymeric monoliths containing Ti-TADDOLate functionalities have been used for two different reactions, namely the Diels–Alder reaction and the ZnEt₂ addition to benzaldehyde. The last reaction is clearly improved when the reaction is carried out under flow conditions but no significant advantages were found for the Diels–Alder reaction. In both cases, the optimized results obtained, either in batch or under flow, compare well with the best results reported for other supported Ti-TADDOLates. In the case of the Diels–Alder reaction, only moderate enantioselectivities can be obtained, but essentially quantitative enantioselectivities were achieved for the ZnEt₂ addition.

The results here presented highlight that heterogenization does not necessarily involve a decrease in the efficiency of the catalyst with regards to that of the corresponding homogeneous analogue. As a matter of fact, significant positive polymeric effects have been found in the present study. As an example, the ee values obtained for both of the studied reactions with TADDOLs containing naphthyl substituents at the α -position not only are comparable with the best values for related heterogeneous systems, but they are clearly superior to those obtained, under similar conditions, for the analogous soluble systems.

Experimental

General considerations

¹H and ¹³C NMR spectra were recorded on a Varian Mercury 300 spectrometer; chemical shifts are measured in ppm and coupling constants, *J*, in hertz. IR spectra were recorded on a Perkin-Elmer 2000 spectrometer, FT-IR spectra (cm⁻¹) were obtained from KBr pellets. Mass spectra were recorded on a Quattro LC (quadrupole-hexapole-quadrupole) mass spectrometer with an orthogonal Z-spray electrospray interface (Micromass). Elemental analysis were performed on an Elemental Carlo Erba 1108 apparatus. Optical rotations were measured on a JASCO DIP-1000 polarimeter; [α] values are given in units of 10⁻¹ deg cm² g⁻¹. HPLC analysis were carried out on a Merck liquid chromatograph with a Merck L-7400 detector and a Merck L-7200 autosampler. Toluene and tetrahydrofuran were distilled from sodium under an argon atmosphere. Acetone reagent grade, 99.5%, was used without further purification.

For the syntheses of **1a**, **1b** and **2a**, see ref. 15.

General procedure for the preparation of $\alpha,\alpha,\alpha',\alpha'$ -tetraaryl-1,3-dioxolane-4(*R*),5(*R*)-dimethanols (TADDOLs). Synthesis of **1c**

To a THF solution (30 mL) of 1-naphthylmagnesiumbromide (70 mmol), obtained from 1-bromonaphthalene (14.3 g, 70 mmol) and Mg (1.5 g, 70 mmol), was added carefully a solution of the ketal derived from *L*-diethyl tartrate and 3-hydroxybenzaldehyde (1.5 g, 5.3 mmol) in THF (20 mL). When addition was complete, the mixture was refluxed for

16 h. After cooling, a saturated solution of NH₄Cl was added to obtain a complete solubilization of the salts formed. The resulting solution was extracted with EtOAc, and the organic phase was dried (anhyd. MgSO₄) and vacuum evaporated. The crude product was purified by column chromatography (SiO₂, hexanes : AcOEt 9 : 1, 4 : 1, 3 : 2) to give TADDOL **1c** (72%) mp 165–173 °C; [α]_D²² +45.9 (*c* = 0.032 in CHCl₃); found: C 77.72, H 5.44; C₅₁H₃₈O₅·3H₂O requires C 78.04; H 5.65%; ν_{\max} /cm⁻¹: 3391, 1178 and 1103; δ_{H} (300 MHz; CDCl₃, 50 °C, Me₄Si): 3.7 (2H, s), 3.9 (2H, s), 5.6 (1H, s), 6.5–8.5 (32H, m); δ_{C} (300 MHz, CDCl₃, 25 °C, Me₄Si): 79.4, 80.4, 81.4, 81.6, 105.6, 113.3, 135.1, 141.9, 142.2, 156.2; EM (EI): *m/z*: 730 (M⁺).

General procedure for the preparation of $\alpha,\alpha,\alpha',\alpha'$ -tetraaryl-1,3-dioxolane-2-(*m*-benzyloxyphenyl)-4(*R*),5(*R*)-dimethanols. Synthesis of **2b**

A mixture of TADDOL **1b** (0.45 mmol), But₄Ni (0.045 mmol), K₂CO₃ (0.84 mmol) and a small amount of 18C6 and KI in dry acetone (10 mL) were stirred at rt for 30 min. After that period, benzyl bromide (0.45 mmol) was added, and the reaction was refluxed for 18 h. After cooling, a saturated solution of NH₄Cl was added until neutralization. The resulting solution was extracted with AcOEt, and the organic phase was dried (anhyd. MgSO₄) and vacuum evaporated. The crude product was purified by column chromatography (SiO₂, hexanes : AcOEt 10 : 1) to give **2b** (72%); mp 121–125 °C; [α]_D²⁰ +132.1 (*c* = 0.007 in CHCl₃); found: C 84.23, H 5.42; C₅₈H₄₄O₅ requires C, 84.85, H 5.40%; ν_{\max} /cm⁻¹: 3391, 1178 and 1103; δ_{H} (300 MHz, CDCl₃, 25 °C, Me₄Si): 4.6 (2H, d, *J*(H,H) = 4.3 Hz), 5.5 (2H, d, *J*(H,H) = 4.6 Hz), 5.6 (2H, d, *J*(H,H) = 4.3 Hz), 6.5–8.5 (37H, m); δ_{C} (300 MHz, CDCl₃): 76.9, 81.3, 105.5, 112.2, 115.9, 118.8, 124.5, 125.8–132.6 (6 peaks), 136.5, 139.1, 140.3, 141.3, 141.9, 158.6; EM (EI) *m/z*: 820 (M⁺).

Synthesis of **2c**

Prepared from TADDOL **1c** (0.45 mmol). Purified by column chromatography (SiO₂, hexanes : AcOEt 10 : 1) to give **2c** (79%); mp 165–173 °C; [α]_D²⁰ +65.4 (*c* = 0.032 in CHCl₃); found: C 84.70, H 5.31; C₅₈H₄₄O₅ requires C, 84.85, H 5.40. ν_{\max} /cm⁻¹: 3391, 1178 and 1103. δ_{H} (300 MHz, CDCl₃, 50 °C, Me₄Si): 3.7 (2H, s), 3.9 (2H, s), 5.6 (1H, s), 6.5–8.5 (37H, m); δ_{C} (300 MHz, CDCl₃): 79.4, 80.4, 81.4, 81.6, 105.6, 113.3, 116.5, 118.6, 121–130 (7 peaks), 131.0, 132.0, 135.1, 141.9, 142.2, 156.2; EM (EI) *m/z*: 820 (M⁺).

General procedure for the preparation of $\alpha,\alpha,\alpha',\alpha'$ -tetraaryl-1,3-dioxolane-2-(*m*-(*p*-vinylbenzyl)oxyphenyl)-4(*R*),5(*R*)-dimethanols. Synthesis of **3a**

A mixture of 4-vinylbenzene chloride (0.42 g, 2.5 mol), K₂CO₃ (0.53 g, 3.7 mmol), 18C6 (0.13 g, 0.5 mmol) and a catalytic amount of KI in dry acetone (50 mL) were stirred at rt for 30 min. After that period, TADDOL **1a** (1.6 g, 2.5 mmol) and acetone (15 mL) were added, and the reaction was refluxed for 45 h. After cooling, a saturated solution of NH₄Cl was added until neutralization. The resulting solution was extracted with

CH₂Cl₂, and the organic phase was dried (anhyd. MgSO₄) and vacuum evaporated. The crude was purified by column chromatography (SiO₂, hexanes : AcOEt 1 : 0, 10 : 0.25, 10 : 0.5, 10 : 1) to give **3a** (80.2%); mp 99–101 °C; [α]_D²² +59.2 (*c* = 0.032 in THF); found: C 82.11, H 7.30; C₅₂H₅₄O₅ requires C, 82.29, H 7.17; $\nu_{\max}/\text{cm}^{-1}$: 3545, 3100, 3050, 3010, 2920, 1629, 1602, 1510, 1480, 1379, 989, 900, 799 and 710; δ_{H} (300 MHz, CDCl₃, 50 °C, Me₄Si): 2.2–2.6 (24H, m), 4.6 (2H, m), 4.9–5.4 (4H, s + s + d + s), 5.7–5.75 (1H, dd, ¹²*J*(H,H) = 2.58 Hz, ²³*J*(H,H) = 17.58 Hz), 6.6–7.4 (21H, m); δ_{C} (300 MHz, CDCl₃, 50 °C): 21.7, 21.9, 22.0, 22.1, 73.0, 80.1, 81.6, 82.0, 105.1, 106.3, 112.1, 113.8, 114.5, 115.9, 117.0, 119.7, 120.1, 124.2, 124.3, 124.6, 124.8, 124.9, 129.9, 126.7, 128.1, 129.0, 129.2, 129.4, 129.5, 129.7, 136.8, 137.0, 137.2, 137.7, 138.0, 138.1. EM (TOF) *m/z*: 781.74 (M + Na⁺).

Synthesis of 3b

Prepared from TADDOL **1b** (2.5 mmol). The crude product was purified by crystallization from ether–hexanes to give **3b** (70.2%); mp 115 °C; [α]_D²² +139.94 (*c* = 0.055 in CHCl₃); found C, 84.92, H 5.40; C₆₀H₄₆O₅ requires C, 85.08, H 5.47; $\nu_{\max}/\text{cm}^{-1}$: 3545, 3100, 3047, 1699, 1596, 1508, 1485, 1460, 1395, 1352, 1266, 1230, 1174, 1093, 999 and 730; δ_{H} (300 MHz, CDCl₃, 25 °C, Me₄Si): 4.8 (2H, d, *J*(H,H) = 3 Hz), 5.3 (2H, d, *J*(H,H) = 6.7 Hz), 5.6 (1H, d, *J*(H,H) = 3 Hz), 5.7–5.8 (3H, s + d, *J*(H,H) = 6.7 Hz), 5.9 (1H, s), 6.5–8.5 (36H, m); δ_{C} (300 MHz, CDCl₃): 70, 81.3, 81.5, 105.0, 112.9, 114.2, 116.1, 119.8, 124.7, 125.8, 126.2, 127.5, 128.2, 128.4, 129.6, 132.6, 139.1, 140.5, 141.1, 141.4, 141.8, 155.4. EM (TOF) *m/z*: 870 (M + Na⁺).

Synthesis of 3c

Prepared from TADDOL **1c** (2.5 mmol). The crude product was purified by crystallization from ether–hexanes (79.2%); mp 103–107 °C; [α]_D²² +61.7 (*c* = 0.032 in THF); found: C 84.83, H 5.14; C₆₀H₄₆O₅ requires C, 85.08, H 5.47; $\nu_{\max}/\text{cm}^{-1}$: 3545, 3100, 3047, 1699, 1178, 1103; δ_{H} (300 MHz, CDCl₃, 25 °C, Me₄Si): 3.9 (1H, sa), 4.7 (2H, d, *J*(H,H) = 3.1 Hz), 5.2 (2H, d, *J*(H,H) = 6.3 Hz), 5.6 (2H, s + d, *J*(H,H) = 3.1 Hz), 5.8 (2H, d, *J*(H,H) = 6.3 Hz), 6.1 (1H, s), 6.9–8.6 (36H, m); δ_{C} (300 MHz, CDCl₃): 70, 81.3, 81.5, 105.0, 112.9, 114.2, 116.1, 119.8, 124.7, 125.8, 126.2, 127.5, 128.2, 128.4, 129.6, 132.6, 139.1, 140.5, 141.1, 141.4, 141.8, 155.4; EM (TOF) *m/z*: 870 (M + Na⁺);

General procedure for the preparation of polymer-supported TADDOLs 4. Synthesis of 4c

A mixture of TADDOL **1c** (0.314 g, 0.6 mmol), NaH (24 mg, 0.6 mmol), Bu₄Ni (23 mg, 0.06 mmol), and a small amount of 18C6 in dry THF (30 mL) were stirred at rt for 30 min. After that period, a chloromethylated resin (1 mmol Cl g⁻¹, 1% DVB, 200 mg, 0.2 mmol) was added, and the suspension was refluxed for 48 h. The polymer was filtered and washed with THF (3 ×), THF/H₂O (1 : 1) (3 ×), THF/MeOH (1 : 1) (3 ×), MeOH (3 ×), CH₂Cl₂ (3 ×), and acetone (3 ×) to give resin **4c** containing 0.59 mmol of functional groups g⁻¹ (DF = 0.11, 100% conversion); found: C 88.32, H 6.34.

[(C₁₀H₁₀)_{0.01}(C₈H₈)_{0.88}(C₆₂H₄₉O₅)_{0.11}] requires C, 88.71, H 6.63; $\nu_{\max}/\text{cm}^{-1}$: 3550, 1099, 1026.

Preparation of the monolithic polymer rods. Synthesis of 5

Chiral TADDOL derivative **3** (0.400 g) was dissolved in toluene (0.487 g, 20 wt% with respect to the polymerization mixture). Then DVB (0.600 g) and 1-dodecanol (1.012 g) together with AIBN (1 wt% with respect to the monomers) was added to obtain an homogeneous solution. The polymerization mixture was stirred and purged with nitrogen for 3 min and poured into a mold. The stainless steel tubular molds were sealed on the two ends, and placed in a vertical position into a water bath. The polymerization was allowed to proceed for 24 h at 70 °C. The seals were then removed, the tube was provided with fittings, attached to a high pressure pump, and THF was pumped through the column at a flow rate of 1 mL min⁻¹ to remove the porogenic solvents and any other soluble compounds.

General procedure for the Diels–Alder reactions with polymeric catalysts derived from 5, obtained by polymerization

A solution of TiCl₂(OⁱPr)₂ (0.25 M in toluene) was inserted in a syringe pump and passed with a continuous flow (0.6 mL h⁻¹, *V* = 9 mL) through the monolithic column previously washed with dry toluene for 1 h at 20 mL h⁻¹. Then the column was washed with dry toluene (3 h, 20 mL h⁻¹) to remove the excess of titanium.

A solution of 3-crotonoyl-1,3-oxazolidin-2-one (220 mg, 1.4 mmol) and cyclopentadiene (2.8 mol, 1.4 mL) in dry toluene (0.9 mL) was loaded into the monolithic column and the reaction mixture was maintained inside the column for 24 h. Then, the column was washed with dry toluene to remove the products obtained. The solvent was eliminated under reduced pressure, and the conversion and selectivities were determined by ¹H NMR spectroscopy (for methylene groups: **7** 1.94, **8** 1.10 ppm, **9** 0.83 ppm) and the enantioselectivities by ¹H NMR using Eu(hfc)₆ (lanthanide/adduct = 0.3; for vinyl protons: **8a** 6.32 ppm and 6.25 ppm, **8b** 6.5 ppm and 6.23 ppm) and chiral HPLC using Chiralcel OD column (hexanes–PrⁱOH: 99 : 1, flow 1 mL min⁻¹, temperature 30 °C, λ = 210 nm, **8a** 46.1 min; **8b** 50.8 min)

General procedure for the Diels–Alder reaction between 6 and 7 with polymeric catalyst derived from 5, obtained by polymerization, under continuous flow conditions

A 0.3 M solution of TiCl₂(ⁱPrO)₂ in toluene was pumped in continuous flow (20 mL h⁻¹, 5 mL) through the monolithic column, then the column was washed with dry toluene (20 mL h⁻¹, 3 h) to remove the excess of titanium. A solution of 3-crotonoyl-1,3-oxazolidin-2-one (543 mg, 3.5 mmol) and cyclopentadiene (6.2 mL, 95 mmol) in dry toluene (50 mL) was pumped through the monolithic column. The solvent fractions obtained from recirculated and no recirculated systems were vacuum evaporated to obtain the product. The conversion and selectivities were determined by ¹H NMR spectroscopy and the enantioselectivity by ¹H NMR and chiral HPLC using the Chiralcel OD column.

General procedure for the addition of diethylzinc to benzaldehyde using the polymeric catalysts derived from 5b

A 0.3 M solution of $\text{Ti}(\text{iPrO})_4$ in toluene was pumped in continuous flow (0.2 mL min^{-1} , 5 mL) through the monolithic column, then the column was washed with dry toluene (0.2 mL min^{-1} , 10 mL) to remove the excess of titanium. An 1.1 M solution of ZnEt_2 in toluene (4.1 mL, 4.5 mmol) was poured in a flask and cooled to *ca.* -30°C , benzaldehyde (328 μL , 3.2 mmol) and $\text{Ti}(\text{iPrO})_4$ (1.1 mL, 3.2 mmol) were added to the flask and the resulting solution was pumped through the monolithic column (0.8 mL , 0.3 mL min^{-1}). The reaction was maintained within the column at 5°C . After this, toluene and 0.1 M HCl/THF were allowed to pass through the system in order to remove and wash the product remaining in the reactor. The mixture was quenched with 2 M HCl and extracted with ether. The organic phase was washed with a solution of NaHCO_3 and brine, dried and vacuum evaporated to give the reaction crude that was analyzed by ^1H NMR to determine the yield and the selectivity: 10.15 ppm, (s, 1H) benzaldehyde; 1-phenylmethanol 4.77 ppm (s, 2H), 1-phenyl-1-ethanol 4.65 ppm, (t, 1H). The enantioselectivity was determined by chiral HPLC using a Chiralcel OD column (hexanes- Pr^iOH : 95 : 5, temperature 25°C , flow 1 mL min^{-1} , $\lambda = 210 \text{ nm}$, *R*-enantiomer: 10.48 min; *S*-enantiomer: 12.64 min).

General procedure for the addition of diethylzinc to benzaldehyde using the polymeric catalysts derived from 5b, under flow conditions

A 0.15 M solution of $\text{Ti}(\text{iPrO})_4$ in toluene was pumped in continuous flow (0.2 mL min^{-1} , 8 mL) through the monolithic column, then the column was washed with dry toluene (0.2 mL min^{-1} , 8 mL) to remove the excess of titanium. A 1.1 M solution of ZnEt_2 in toluene (2 mL, 2.2 mmol) and 15 mL of dry toluene were poured in a flask. This solution was cooled to *ca.* -30°C and $\text{Ti}(\text{iOPr})_4$ (0.4 mL, 1.2 mmol) and benzaldehyde (122 μL , 1.2 mmol) were added to the flask. All the system was maintained at -30°C . The resulting solution was pumped through the column, with the help of a HPLC pump (0.06 mL min^{-1}) and collected in a flask. After 2.5 h pumping, toluene (3 mL) and HCl (2M)/THF (8 mL) were pumped through the column. The solution obtained was extracted with Et_2O (20 mL). The organic phase was washed with a solution of NaHCO_3 and brine, dried and vacuum evaporated to give the reaction crude that was analyzed by ^1H NMR to determine the yield and the selectivity. The enantioselectivity was determined by chiral HPLC using a Chiralcel OD column.

Acknowledgements

Financial support has been provided by projects CTQ2005-08016 (MEC) and P1 1B2004-13 (Bancaja). E. G.-V. thanks MEC for a Ramon y Cajal fellowship.

References

- (a) P. T. Anastas and J. C. Warner, *Green Chemistry: Theory and Practice*, Oxford University Press, Oxford, 1998; (b) P. T. Anastas and M. M. Kirchhoff, *Acc. Chem. Res.*, 2002, **35**, 686–694; (c) A. Corma and H. Garcia, *Chem. Rev.*, 2003, **103**, 4307–4365.
- (a) R. Noyori, *Asymmetric Catalysis in Organic Synthesis*, Wiley, New York, 1994; (b) , *Comprehensive Asymmetric Catalysis*, ed. E. N. Jacobsen, A. Pfaltz and H. Yamamoto, Springer-Verlag, Berlin–Heidelberg, 1999 (first supplement, 2004); (c) *Asymmetric Catalysis on Industrial Scale*, ed. H. U. Blaser and E. Schmidt, Wiley-VCH, Weinheim, 2004.
- (a) C. Brown, *Chirality in Drug Design and Synthesis*, Academic Press, New York, 1990; (b) J. M. Brown, *Tetrahedron: Asymmetry*, 1991, **2**, 481–732; (c) L. Guo-Qiang, L. Yue-Ming and A. S. C. Chan, *Principles and Application of Asymmetric Synthesis*, Springer, Heidelberg, 2001.
- (a) See thematic issue: ed. J. A. Gladysz, Recoverable Catalysts and Reagents, *Chem. Rev.*, 2002, **102**, 3215–3892; (b) S. Brase, F. Lauterwasser and R. E. Ziegert, *Adv. Synth. Catal.*, 2003, **345**, 869–929; (c) M. Benaglia, A. Puglisi and F. Cozzi, *Chem. Rev.*, 2003, **103**, 3401–3429; (d) M. R. Buchmeiser, *Polymeric Materials in Organic Synthesis and Catalysis*, Wiley-VCH, Weinheim, 2003; (e) P. McMorn and G. J. Hutchings, *Chem. Rev.*, 2004, **33**, 108–122.
- (a) R. Drake, D. C. Sherrington and S. J. Thomson, *Reac. Funct. Polym.*, 2004, **60**, 65–75; (b) G. C. H. Chiang and T. Olsson, *Org. Lett.*, 2004, **6**, 3079–3082; (c) H. S. Eriksen, S. C. Oyaga, D. C. Sherrington and C. L. Gibson, *Synlett*, 2005, 1235–1238.
- For recent examples, see thematic issue: ed. P. Toy and M. Shi, Polymer-Supported Reagents and Catalysts: Increasingly Important Tools for Organic Synthesis, *Tetrahedron*, 2005, **61**, 12026–12192.
- (a) B. Altava, M. I. Burguete, E. García-Verdugo, S. V. Luis, R. V. Salvador and M. J. Vicent, *Tetrahedron*, 1999, **55**, 12897–12906; (b) M. I. Burguete, J. M. Fraile, J. I. García, E. García-Verdugo, C. I. Herreras, S. V. Luis and J. A. Mayoral, *J. Org. Chem.*, 2001, **66**, 8893–8901; (c) A. Cornejo, J. M. Fraile, J. I. García, M. J. Gil, S. V. Luis, V. Martínez-Merino and J. A. Mayoral, *J. Org. Chem.*, 2005, **70**, 5536–5544.
- (a) S. Itsuno, Y. Sakurai, K. Ito, T. Maruyama, S. Nakahama and J. M. J. Fréchet, *J. Org. Chem.*, 1990, **55**, 304–310; (b) S. Itsuno, K. Kamahori, K. Watanabe, T. Koizumi and K. Ito, *Tetrahedron: Asymmetry*, 1994, **5**, 523–526; (c) K. Kamahori, S. Tada, K. Ito and S. Itsuno, *Tetrahedron: Asymmetry*, 1995, **6**, 2547–2555; (d) For related studies on polysiloxanes, see M. Reggelin, *Nachr. Chem., Tech. Lab.*, 1997, **45**, 1196–1201.
- (a) B. Altava, M. I. Burguete, E. García-Verdugo, S. V. Luis and M. J. Vicent, *React. Funct. Polym.*, 2001, **48**, 25–35; (b) M. I. Burguete, J. M. Fraile, E. García-Verdugo, S. V. Luis, V. Martínez-Merino and J. A. Mayoral, *Ind. Eng. Chem. Res.*, 2005, **44**, 8580–8587.
- B. Altava, M. I. Burguete, J. M. Fraile, J. I. García, S. V. Luis, J. A. Mayoral and M. J. Vicent, *Angew. Chem., Int. Ed.*, 2000, **39**, 1503–1506.
- (a) F. Svec and J. M. J. Fréchet, *Chem. Mater.*, 1995, **7**, 707–715; (b) F. Svec and J. M. J. Fréchet, *Science*, 1996, **273**, 205–211; (c) S. Xie, F. Svec and J. M. J. Fréchet, *Chem. Mater.*, 1998, **10**, 4072–4078; (d) F. Svec and J. M. J. Fréchet, *Ind. Eng. Chem. Res.*, 1999, **38**, 34–48; (e) E. C. Peters, F. Svec and J. M. J. Fréchet, *Adv. Mater.*, 1999, **11**, 1169–1181; (f) F. Svec, T. B. Tennikova and Z. Deyl, *Monolithic Materials*, Elsevier, Amsterdam, 2003.
- (a) M. I. Burguete, E. García-Verdugo, M. J. Vicent, S. V. Luis, H. Pennemann, N. G. von Keyserling and J. Martens, *Org. Lett.*, 2002, **4**, 3947–3950; (b) P. Hodge, *Curr. Opin. Chem. Biol.*, 2003, **7**, 362–373; (c) U. Jas and A. Kirschning, *Chem.–Eur. J.*, 2003, **9**, 5708–5723; (d) A. Kirschning, U. Jas and G. Kunz, Chemistry in flow—new continuous flow reactors in organic synthesis, in *Innovation and Perspectives in Solid Phase Synthesis and Combinatorial Libraries*, ed. R. Epton, MPG Books Ltd, Kingswindford, UK, 2004; (e) P. Hodge, *Ind. Eng. Chem. Res.*, 2005, **44**, 8542–8553; (f) N. T. S. Phan, J. Khan and P. Styring, *Tetrahedron*, 2005, **61**, 12065–12073; (g) F. Bonfils, I. Cazaux, P. Hodge and C. Caze, *Org. Biomol. Chem.*, 2006, **4**, 493–497.
- (a) D. Seebach, A. K. Beck, R. Imwinkelried, S. Roggo and A. Wonnacott, *Helv. Chim. Acta*, 1987, **70**, 954–974; (b) D. Seebach, R. F. Marti and T. Hintermann, *Helv. Chim. Acta*, 1996, **79**, 1710–1740; (c) P. B. Rheiner and D. Seebach, *Chem.–Eur. J.*, 1999, **5**, 3221–3236; (d) D. Seebach, A. K. Beck and A. Heckel,

- Angew. Chem., Int. Ed.*, 2001, **40**, 92–138; (e) H. Sellner, P. B. Rheiner and D. Seebach, *Helv. Chim. Acta*, 2002, **85**, 352–387; (f) A. Heckel and D. Seebach, *Chem.–Eur. J.*, 2002, **8**, 559–572.
- 14 (a) K. Narasaka, N. Iwasawa, M. Inoue, T. Yamada, M. Nakashima and J. Sugimori, *J. Am. Chem. Soc.*, 1989, **111**, 5340–5345; (b) K. Narasaka, Y. Hayashi, H. Shimadzu and S. Niihata, *J. Am. Chem. Soc.*, 1992, **114**, 8869–8885; (c) K. V. Gothelf, I. Thomsen and K. A. Jørgensen, *J. Am. Chem. Soc.*, 1996, **118**, 59–64; (d) J. Irurre, A. Fernandez-Serrat and F. Rosanas, *Chirality*, 1997, **9**, 191–197; (e) S. Degni, C-E. Wilén and R. Leino, *Org. Lett.*, 2001, **16**, 2551–2554; (f) R. Imbos, A. J. Minnaard and B. L. Feringa, *J. Am. Chem. Soc.*, 2002, **124**, 184–185; (g) L. Hintermann, D. Broggini, A. Togni and K. Gothelf, *Helv. Chim. Acta*, 2002, **85**, 1597–1612; (h) H. F. Du, D. B. Zhao and K. L. Ding, *Chem.–Eur. J.*, 2004, **23**, 5964–5970.
- 15 B. Altava, M. I. Burguete, B. Escuder, S. V. Luis and R. V. Salvador, *J. Org. Chem.*, 1997, **62**, 3126–3134.
- 16 (a) B. Altava, M. I. Burguete, E. García-Verdugo, S. V. Luis and M. J. Vicent, *Tetrahedron Lett.*, 2001, **42**, 8459–8462; (b) B. Altava, M. I. Burguete, E. García-Verdugo, S. V. Luis and M. J. Vicent, *Tetrahedron*, 2001, **57**, 8675–8683.
- 17 M. I. Burguete, J. M. J. Fréchet, E. García-Verdugo, M. Janco, S. V. Luis, F. Svec, M. J. Vicent and M. C. Xu, *Polym. Bull.*, 2002, **48**, 9–15.
- 18 B. Altava, M. I. Burguete, J. C. Frias, E. García-España, S. V. Luis and J. F. Miravet, *Ind. Eng. Chem. Res.*, 2000, **39**, 3589–3595.
- 19 K. Hallman and C. Moberg, *Tetrahedron: Asymmetry*, 2001, **12**, 1475–1478.
- 20 (a) B. Altava, M. I. Burguete, J. M. Fraile, J. I. García, S. V. Luis, J. A. Mayoral, A. J. Royo and M. J. Vicent, *Tetrahedron: Asymmetry*, 1997, **8**, 2561–2570; (b) B. Altava, M. I. Burguete, E. García-Verdugo, S. V. Luis, J. F. Miravet and M. J. Vicent, *Tetrahedron: Asymmetry*, 2000, **11**, 4885–4893; (c) B. Altava, M. I. Burguete, J. I. García, S. V. Luis, J. A. Mayoral and M. J. Vicent, *Tetrahedron: Asymmetry*, 2001, **12**, 1829–1835.
- 21 (a) E. N. Jacobsen, *J. Am. Chem. Soc.*, 1999, **121**, 4147–4154; (b) J. Hu, G. Zhai, G. Yang and Z. Ding, *J. Org. Chem.*, 2001, **66**, 303–304; (c) Q.H. Fan, R. Wang and A. S. C. Chan, *Bioorg. Med. Chem. Lett.*, 2002, **12**, 1867–1871.
- 22 (a) D. Rechavi and M. Lemaire, *J. Mol. Catal. A: Chem.*, 2002, **182–183**, 239–247; (b) H. Nakano, K. Takahashi and R. Fujita, *Tetrahedron: Asymmetry*, 2005, **16**, 2133–2140.
- 23 In solution, formation as the major isomer of the *endo*-2*S*,3*R* instead of the usual *endo*-2*S*,3*R* is always associated with very bulky α -substituents, in particular 3,5-dimethylphenyl and 1-naphthyl, but not with 2-naphthyl. This experiment was reproduced several times with the same results, using different monolithic columns and starting from tartaric acid derivatives of different batches. All starting materials were checked to be pure and to have the expected configuration according to its $[\alpha]_D$ value. When the same kind of experiments were carried out starting from *D*-tartaric derivatives, the opposite results were obtained with the prevalence of the *endo*-2*S*,3*R* isomer for homogeneous and grafted catalysts and that of the *endo*-2*R*,3*S* isomer for the monolithic system.
- 24 (a) G. Wulff, *Angew. Chem., Int. Ed. Engl.*, 1995, **34**, 1812–1832; (b) G. Wulff, *Chem. Rev.*, 2002, **102**, 1–28; (c) J. J. Becker and M.-R. Gagné, *Acc. Chem. Res.*, 2004, **37**, 798–804; (d) E. Burri, M. Ohm, C. Dagueneu and K. Severin, *Chem.–Eur. J.*, 2005, **11**, 5055–5061.

Solvent and catalyst-free synthesis of polyphosphates†

Smaranda Iliescu, Gheorghe Ilia,* Nicoleta Plesu, Adriana Popa and Aurelia Pascariu

Received 17th February 2006, Accepted 13th June 2006

First published as an Advance Article on the web 27th June 2006

DOI: 10.1039/b602462a

Direct, efficient, solvent and catalyst-free synthesis of a series of polyphosphates was accomplished. The reaction involved a gas–liquid interfacial polycondensation between alkyl(aryl)phosphoric dichlorides and aromatic diols. The polyphosphates were characterized by IR, ^1H NMR, inherent viscosity, thermal analysis, X-ray diffractions and molar mass. Yields in the range 75–90% and inherent viscosities in the range 0.24–0.45 dl g $^{-1}$ were obtained. Polyphosphates were stable up to 170–250 °C, depending on phosphoric dichloride type. The X-ray diffraction patterns revealed that almost all the polymers were amorphous.

Introduction

Polymer chemistry has contributed in various ways to the present progress in industry, biology, biochemistry and medicine, providing new methods for preparing and studying macromolecules as well as providing new, highly specified materials. Phosphorus-containing polymers, respectively polyphosphonates and polyphosphates are of interest because they confer low flammability, plasticity, thermal stability and lubrication properties on polymers.¹ Much attention has been drawn in recent years towards a new class of biodegradable polymers belonging to polyphosphates. These polymers have been investigated as biomaterials in drug delivery, gene delivery, tissue engineering and agriculture.^{2–6} For this reason, research workers have developed several methods for industrial uses. The most important method which generates polyphosphates and polyphosphonates is polycondensation of phosphonic (phosphoric) dichlorides with diols. This procedure includes melt,⁷ solution,⁸ ultrasound solid-phase⁹ and interfacial polycondensation.¹⁰ The disadvantages of classical methods (corrosion, many noxious secondary products) are avoided using multiphase reaction systems. The phase transfer catalysis technologies are the most convenient due to the facts that the reaction conditions are mild, *i.e.* low temperature, one of the solvents is usually water, and there few secondary reactions.

In the previous paper we presented the synthesis of polyphosphonates by liquid–liquid interfacial polycondensation.¹¹ More attention has been recently paid on both environmental protection and ecological balance. Green chemistry plays an important role in reducing and eventually eliminating the impact of chemical industries on the environment.

This paper will offer new knowledge in environmental technologies for the reduction of ecological risks in the production of the new compounds with major impact on the environment. It is known that the best solvent is no solvent but

if a solvent is needed then water has a lot to recommend it and catalysis in aqueous biphasic systems is an industrially attractive methodology which has found broad application.¹² Therefore, we developed a new and efficient solvent and catalyst-free synthesis method, namely the gas–liquid reaction of phosphorus compounds.^{13,14} Organic reactions in aqueous media is a significant branch of green chemistry.

We are particularly interested in synthesis of new phosphorus polymers, structurally related to the biopolymers with polyphosphates in main chains. The purpose of this work was to continue the solvent catalyst-free synthesis of biodegradable polyphosphates, by a green synthetic methodology, namely the gas–liquid technique.

Experimental

Chemicals

The following phosphoric dichlorides (PD) were used as received from Aldrich Chemical Company: methylphosphoric dichloride (MPD), ethylphosphoric dichloride (EPD), propylphosphoric dichloride (PrPD), cyclohexylphosphoric dichloride (CDP), phenylphosphoric dichloride (PPD). The diols (D): bisphenol A (BA), 4,4'-biphenol (BP), tetrachlorobiphenol A (CIBA) were recrystallized before use.

Instruments

The IR spectra were recorded on a SPECORD M80 spectrophotometer and ^1H NMR spectra on a JEOL C-60 MHz spectrometer, respectively (CDCl_3 , 50 °C, 60 MHz). The polymers were characterized by viscosity, on an Ubbelohde suspended level viscometer, at 30 °C and by gel permeation chromatography, on an evaporative light scattering detector, PL-EMD 950" (2 × PL gel MIXEDC 300 × 7.5 mm columns; $T = 25$ °C; DMF as solvent; flow rate marker: PS 580). Thermogravimetric analyses were carried out on a TGA/SDTA 851-LF1100 Mettler apparatus, by heating in air (5 mg) from initial temperature of 20 to 1100 °C with a rate of 10 °C min $^{-1}$. Wide-angle X-ray diffractions were obtained using the powder method on a TUR M62 diffractometer apparatus with nickel-filtered Cu K α radiation (30 kV, 20 mA).

Institute of Chemistry, Romanian Academy, 24 Mihai Viteazul Bvd., 300223 Timisoara, Romania. E-mail: ilia@acad-icht.tm.edu.ro

† Electronic supplementary information (ESI) available: IR spectra of polymers P₂, P₃ and P₅ (Fig. S1); Representative ^1H NMR spectra of P₁ and P₅ (Fig. S2); and X-ray diffraction patterns of P₅, P₆ and P₇ (Fig. S3). See DOI: 10.1039/b602462a

General procedure

Gas-liquid polycondensation utilizes pairs of highly reactive monomers with one of the monomers in the gaseous state and the other in solution. A typical gas-liquid polycondensation procedure is presented in previous papers.^{13,14} Since phosphoric dichlorides are more volatile than diols they are preferentially employed in the gas phase. The appropriate phosphoric dichloride was heated (80–90 °C) and carried by a stream of nitrogen into a flask which contained aqueous 1M sodium hydroxide solution and the diol. The solvent used for the diols is water since it readily dissolves the phenolate formed. The nitrogen stream acts as a carrier gas for the phosphoric dichloride, protects the reaction mixture from atmospheric oxygen and agitates the reaction mixture. The reaction rate can be controlled by the nitrogen flow rate. In order to prevent the possibility of condensation of the vapor on the apparatus walls, the vapor mixture is overheated or diluted so that the partial pressure of the vapor reagent in the gas mixture is lower than its saturation vapor pressure. The carrier gas flow, which produced bubbles in the formed product that expanded and burst at the top of the reaction flask, was continued 15 min after the entire quantity of phosphoric dichloride is used. Polymer separates after 30 min from solution as a tacky, coherent mass, adhering to the container surface. The solid polymer was washed with distilled water until free of chloride ion and dried at 50 °C in vacuum. The obtained polymer shows wide ranges of consistency and softening.

The infrared (IR) spectrum (film) exhibited absorptions at:

P₁: 1280 cm⁻¹ (P=O), 1190, 920 cm⁻¹ (P–O–C_{arom}), 980 cm⁻¹ (P–O–C_{alif}), 3010, 1600, 1430, 740 cm⁻¹ (Ph). P₂: 1250 cm⁻¹ (P=O), 1200, 980 cm⁻¹ (P–O–C_{arom}), 1050 cm⁻¹ (P–O–C_{alif}), 2950, 1670, 1520, 810 cm⁻¹ (Ph). P₃: 1230 cm⁻¹ (P=O), 1190, 980 cm⁻¹ (P–O–C_{arom}), 1010 cm⁻¹ (P–O–C_{alif}), 2900, 1600, 1510, 820 cm⁻¹ (Ph). P₄: 1290 cm⁻¹ (P=O), 1150, 930 cm⁻¹ (P–O–C_{arom}), 1120 cm⁻¹ (P–O–C_{alif}), 3030, 1640, 1400, 750 cm⁻¹ (Ph). P₅: 1220 cm⁻¹ (P=O), 1190, 970 cm⁻¹ (P–O–C_{arom}), 3000, 1650, 1550, 750 cm⁻¹ (Ph). P₆: 1280 cm⁻¹ (P=O), 1180, 930 cm⁻¹ (P–O–C_{arom}), 2960, 1670, 1560, 800 cm⁻¹ (Ph), 510 (P–Cl). P₇: 1260 cm⁻¹ (P=O), 1170, 965 cm⁻¹ (P–O–C_{arom}), 3020, 1680, 1500, 700 cm⁻¹ (Ph).

The nuclear magnetic resonance (¹H NMR) spectrum in CDCl₃, showed signals (δ) at:

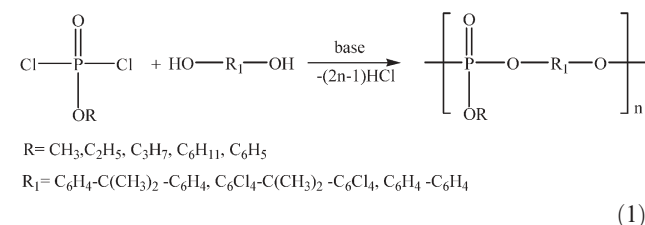
P₁: 1.6 ppm (s, C(CH₃)₂), 7.1 ppm (s, aromatic hydrogen in main chain), 3.7 ppm (d, hydrogen in side chain (P–O–R)), 6.5–7.0 ppm (m, phenol end group). P₂: 1.6 ppm (s, C(CH₃)₂), 7.1 ppm (s, aromatic hydrogen in main chain), 4.2 ppm (m) and 1.4 ppm (t), hydrogen in side chain (P–O–R), 6.5–7.0 ppm (m, phenol end group). P₃: 1.6 ppm (s, C(CH₃)₂), 7.1 ppm (s, aromatic hydrogen in main chain), 3.8 ppm (m) and 1–2 ppm (m), hydrogen in side chain (P–O–R), 6.5–7.0 ppm (m, phenol end group). P₄: 1.5 ppm (s, C(CH₃)₂), 7.1 ppm (s, aromatic hydrogen in main chain), 1.1–2.4 ppm (m, hydrogen in side chain (P–O–R)), 6.5–7.0 ppm (m, phenol end group). P₅: 1.6 ppm (s, C(CH₃)₂), 6.2–7.5 ppm (m, aromatic hydrogen in main chain, hydrogen in side chain (P–O–R) and phenol end group). P₆: 1.6 ppm (s, C(CH₃)₂), 7.4 ppm (m, hydrogen in side chain (P–O–R)), 6.5–7.0 ppm (m, phenol end group).

P₇: 7.0–7.8 ppm (m, aromatic hydrogen in main chain, hydrogen in side chain (P–O–R) and phenol end group).

Results and discussion

The aim of this work was to apply the gas-liquid methodology as an eco-friendly and economical procedure for green chemistry. In this paper we report the synthesis of polyphosphate by the gas-liquid polycondensation of alkylphosphoric dichlorides: methylphosphoric dichloride (MPD), ethylphosphoric dichloride (EPD), propylphosphoric dichloride (PrPD) and cyclohexylphosphoric dichloride (CDP); arylphosphoric dichlorides: phenylphosphoric dichloride (PPD); and with diols: bisphenol A (BA), 4,4'-biphenol (BP) and tetrachlorobisphenol A (CIBA).

Polyphosphates were synthesized by reacting phosphoric dichloride (vapor) with sodium salts of the diphenol compounds in a gas-liquid system (reaction 1)



(1)

The method does not require an organic solvent or catalyst, and the reaction takes place in water. For these reasons the auxiliary procedures in gas-liquid interfacial polycondensation are simplified considerably. The possible environmental benefits are obvious with no concerns over solvent emissions or any byproducts derived from the solvent. Therefore, only ionic impurities (*i.e.* NaCl) need to be washed from the polymer. After a definite time of reaction (usually 30 min) the polymers were filtered from the liquid phase and washed. The products obtained by the gas-liquid technique contain strongly adsorbed water which should be removed prior to further polymer characterization or processing. This can be achieved by means of effective drying, for example, under vacuum.

The yields, inherent viscosities, molecular weights and phosphorus content for the obtained polyphosphates are presented in Table 1.

The most appropriate conditions for the synthesis of these polymers by this method are as follows: reaction temperature 40 °C, molar ratio PD : D = 2.5 : 1; 1M NaOH_{aq}. Yields in the range 75–90% were obtained. Inherent viscosities measurements varied between 0.24–0.40 dl g⁻¹.

The high molecular weights of these polyphosphates might be explained by the hydrolytic stability of the monomers used.

The polyphosphates obtained from arylphosphoric dichlorides present higher molecular weights than the polyphosphates obtained from alkylphosphoric dichlorides. The aromatic character of the phosphate bond in arylphosphoric dichloride rendered it more stable than the alkylphosphoric dichloride in an alkaline environment.

The structure of the polyphosphates synthesized was elucidated by IR and ¹H NMR spectroscopy. The IR spectra of all these polymers were similar and confirm the structure of the obtained polyphosphates.

Table 1 Results of gas–liquid interfacial polycondensation of phosphoric dichlorides (PD) with diphenols (D)^a

Polymer	PD	D	Yield (%)	$\eta_{inh}^b/dl\ g^{-1}$	Mn ^c	Mw ^c	Mw/Mn	%P ^d calc.	Exp.
P ₁	MPD	BA	80	0.22	10500	18375	1.75	10.19	9.85
P ₂	EPD	BA	82	0.23	11250	21150	1.88	9.74	9.60
P ₃	PrPD	BA	85	0.24	11480	22041	1.92	9.33	9.28
P ₄	CPD	BA	88	0.28	25480	50960	2.00	8.33	8.12
P ₅	PPD	BA	92	0.38	42570	76626	1.8	8.45	8.34
P ₆	PPD	CIBA	75	0.31	34580	65702	1.9	4.82	4.30
P ₇	PPD	BP	90	0.45	57606	117808	2.045	9.56	9.43

^a Reaction conditions: 0.10 mol PD, 0.040 mol D, 0.090 mol 1M NaOH, 50 min, reaction temperature 40 °C. Temperature of phosphoric dichloride was maintained by an oil bath at 80–90 °C. ^b The inherent viscosities η_{inh} were determined for solutions of 0.5 g per 100 mL in tetrachlorethane, at 30 °C. ^c Mn–number average molecular weight, Mw–weight average molecular weight; molecular weights (for example, the molecular weight distribution for the polyphosphate P₇ is presented in Fig. 1) measured by GPC in chloroform, with polystyrene used as the standard. ^d Determined by the Schöniger method.

For all polyphosphates the disappearance of the broad O–H stretch of diol was observed. Because the P(O)–OH and P(O)–Cl bands were missing, it was believed that the end groups of the polyphosphates chains consisted of phenol end groups. The $\nu_{(P-OH)}$ band at 2700–2500 cm^{-1} which indicates the presence of a phosphonate linkage and the band at 2400 cm^{-1} for $\nu_{(P-H)}$ are both absent and this confirms the existence of the polyphosphate.

The ¹H NMR spectra for all polyphosphates showed no signals at values higher than 12 ppm which indicate the presence of phosphate [P(O)–OH] and no peaks for phosphonates (P–H). So, this suggests that there was no significant cleavage of the ester bond of the polyphosphates during reaction.

The thermal behavior of the polyphosphates was evaluated by means of TGA. Fig. 2 shows an example of polyphosphates P₅, P₆ and P₇ with a heating rate 10 °C min⁻¹ in nitrogen. The TGA results of all the polyphosphates are summarized in Table 2.

The polyphosphates obtained from alkylphosphoric dichlorides, P₁, P₂, P₃ and P₄, respectively, are stable up to

170–190 °C and start degrading between 170–220 °C, and exhibit residual masses of 12–20% at 700 °C in nitrogen.

The polyphosphates obtained from arylphosphoric dichlorides, P₅, P₆ and P₇, respectively, start to degrade between

Table 2 Thermal properties of polyphosphates

Polym.	$T_d^{10\%/^{\circ}C}$	Inception of fast degradation/ ^o C	$T_d^{50\%/^{\circ}C}$	Residue at 700 °C (%)
P ₁	170	210	300	12
P ₂	170	220	290	13
P ₃	180	220	310	15
P ₄	190	230	330	20
P ₅	250	340	480	40
P ₆	230	300	420	22
P ₇	260	450	700	48

^a Where $T_d^{10\%}$ is the temperature at which 10% mass loss was observed and $T_d^{50\%}$ is the temperature at which 50% mass loss was observed.

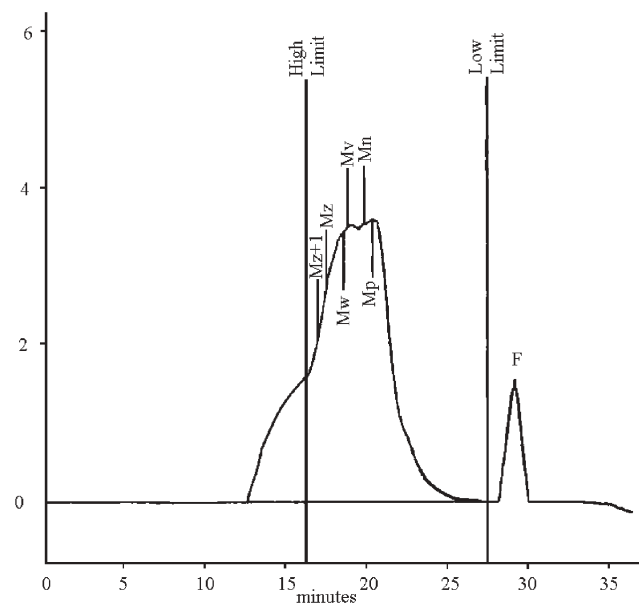


Fig. 1 Molecular weight averages for polyphosphate P₇. Mp = 44 243; Mz = 227 369; Mn = 57 606; Mz+1 = 323 200; Mw = 117 808; Mv = 99 972; Polydispersity = 2.045; peak area = 213 797 mV min.

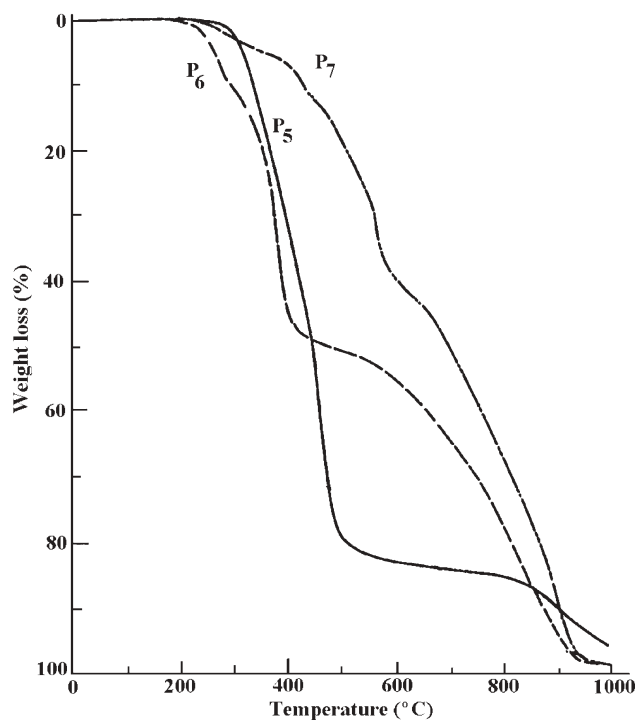


Fig. 2 Thermogravimetric data for polyphosphates P₅–P₇.

230–290 °C. The polyphosphate P₆, having chlorine atoms, had a lower temperature of thermal degradation than P₅ and P₇. This result may be explained by the fact that hydrogen chloride is easily evolved from chloride-containing polymers during the thermal degradation process.

Polyphosphates were analyzed by X-ray diffraction in terms of intensity versus 2θ , where θ is the angle of diffraction (Bragg angle). The percent crystallinity of the polyphosphates was determined from ratio between the area of the crystalline region and the area of the crystalline region + area of the amorphous region. The percent crystallinity is found to be: 37.7% for P₇ and 16.2% for P₅. All other polyphosphates (P₁, P₂, P₃, P₄ and P₆) are amorphous.

Conclusions

This paper provides a simple and green synthetic methodology for the reaction of alkyl(aryl)phosphoric dichlorides with aromatic diols in an aqueous medium, without the use of other solvents or a catalyst. This method requires no reagent purification and affords the desired polymers in high yields and acceptable molecular weights, without the formation of unwanted side products. The simplification of reaction protocols is an important concept in designing new clean methodologies.

A series of seven polyphosphates were synthesized by gas–liquid interfacial polycondensation. Optimum conditions for this process included a reaction temperature of 40 °C, 1M

NaOH solution, and an excess of phosphoric dichloride. The reactions did not require a long reaction time (approx. 30 min). The structures of these polymers were confirmed by IR and ¹H NMR.

Due to the advantages of this method, such as the use of an aqueous medium in organic synthesis and the absence of the solvent and catalyst, it is expected to be developed further.

References

- 1 S. Minegishi, S. Komatsu, A. Kameyama and T. Nishikubo, *J. Polym. Sci., Part A: Polym. Chem.*, 1999, **37**, 959.
- 2 M. Chabal, A. S. Gupta, S. Lapina and D. F. Bruley, *Crit. Rev. Ther. Drug Carrier Syst.*, 2003, **20**, 4, 295.
- 3 Z. Zhao, J. Wang, H. Q. Mao and K. W. Leong, *Adv. Drug Delivery Rev.*, 2003, **55**, 483.
- 4 A. Gupta and S. Lopina, *Polymer*, 2004, **45**, 14, 4653.
- 5 G. L. Kortstee, K. J. Appeldoorn, C. F. Bouting and E. W. van Niel, *Biochemistry*, 2004, **65**, 3, 332.
- 6 A. Akelah, *Mater. Sci. Eng., C*, 1996, **C4**, 83.
- 7 H. Shoba, H. Johnson, M. Saukarapandian, Y. S. Kim, P. Raugarajan, D. C. Baird and J. E. Mc Grath, *J. Polym. Sci., Part A: Polym. Chem.*, 2001, **39**, 17, 2904.
- 8 P. Sakthiel and P. Kannan, *Polymer*, 2005, **46**, 23, 9821.
- 9 L. E. Elizalde, N. P. Torres and J. G. Rodriguez, *Macromol. Rep.*, 1993, **A30**, 295.
- 10 S. Roy and S. Maiti, *J. Polym. Mater.*, 2004, **21**, 1, 39.
- 11 S. Iliescu, G. Iliia, A. Popa, G. Dehelean, G. Macarie and L. Pacureanu, *Rev. Roum. Chim.*, 2001, **46**, 9, 115.
- 12 R. A. Sheldon, *Green Chem.*, 2005, **7**, 5, 267.
- 13 S. Iliescu, G. Iliia, A. Popa, G. Dehelean, L. Macarie and L. Pacureanu, *Polym. Bull.*, 2001, **46**, 165.
- 14 G. Iliia, S. Iliescu and A. Popa, *Green Chem.*, 2005, **7**, 4, 217.

Ruthenium hydroxide on magnetite as a magnetically separable heterogeneous catalyst for liquid-phase oxidation and reduction†

Miyuki Kotani,^a Takeshi Koike,^b Kazuya Yamaguchi^{ab} and Noritaka Mizuno^{*ab}

Received 2nd March 2006, Accepted 19th June 2006

First published as an Advance Article on the web 5th July 2006

DOI: 10.1039/b603204d

Three kinds of reactions, (i) aerobic oxidation of alcohols, (ii) aerobic oxidation of amines, and (iii) reduction of carbonyl compounds to alcohols using 2-propanol as a hydrogen donor, could efficiently be promoted by an easily prepared ruthenium hydroxide catalyst on magnetite ($\text{Ru}(\text{OH})_x/\text{Fe}_3\text{O}_4$). A wide variety of substrates including aromatic, aliphatic, and heterocyclic ones could be converted to the desired products in high to excellent yields without any additives such as bases and electron transfer mediators. After the reaction, the catalyst/product(s) separation could be easily achieved with a permanent magnet and more than 99% of $\text{Ru}(\text{OH})_x/\text{Fe}_3\text{O}_4$ catalyst could usually be recovered for each reaction. The catalysis for these reactions was intrinsically heterogeneous, and $\text{Ru}(\text{OH})_x/\text{Fe}_3\text{O}_4$ recovered after these reactions could be reused without appreciable loss of the catalytic performance.

Introduction

Oxidation of alcohols and amines is of paramount importance in organic synthesis as well as in industry because of the wide use of the products as important intermediates for medicines, agricultural chemicals, and fragrances.¹ Traditionally, they have been oxidized in non-catalytic ways with stoichiometric oxidants such as chromium(VI) and manganese compounds in the presence of strong mineral acids, which produce enormous amounts of toxic metal salts as waste. Due to the increasing environmental concerns, many efforts have been made to develop the oxidation systems using environmentally-benign molecular oxygen as a sole oxidant. However, most systems can be applicable for the oxidations of only activated substrates or large quantities of additives such as bases and electron transfer mediators are needed.² Therefore, little is known of widely usable oxidations of alcohols and amines with molecular oxygen alone.³

The reduction of carbonyl compounds to the corresponding alcohols is also a fundamental functional transformation. The transition-metal-catalyzed Meerwein–Ponndorf–Verley-type reduction is convenient for the larger-scale production because it is not necessary to use high-pressure molecular hydrogen or hazardous reduction reagents such as LiAlH_4 and NaBH_4 . Enantioselective reductions have also been achieved in extremely high enantiomeric excesses using transition metal catalysts with chiral ligands.⁴

Until now, many soluble transition metal-based homogeneous catalysts have been developed for the above-mentioned reactions. They are usually dissolved in reaction solutions making all catalytic sites accessible to substrates and show high catalytic activity and selectivity. Despite these advantages, homogeneous catalysts have a share of only *ca.* 20% in industrial processes^{5,6} because catalyst/product(s) separation (problem of product contamination) and reuse of (expensive) catalysts are very difficult. Therefore, the development of easily recoverable and recyclable heterogeneous catalysts with filtration or centrifugation have received a particular research interest especially for fine chemicals syntheses.⁶ The immobilization of catalytically active species on insoluble materials such as metal oxides and polymers is a solution. Separation and recovery of the immobilized catalysts are usually performed by filtration (or centrifugation), of which the efficiency of recovery of the catalysts is somewhat reduced during repeated use in some cases due to the catalyst pulverization and/or degradation.⁷

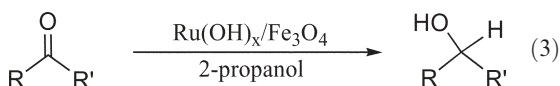
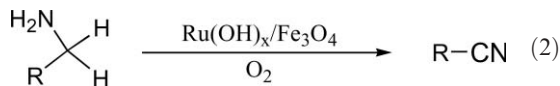
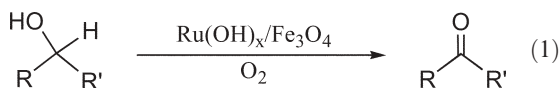
Recently, magnetic materials have attracted much attention because of their wide applications⁸ to supports of catalysts and enzymes, drug delivery, and biosensors. Especially, the magnetic properties make possible the complete recovery of the catalyst by means of an external magnetic field, which is an important advantage of the use of a magnetically separable catalyst. In this paper, we demonstrated the immobilization of ruthenium hydroxide, which is an active catalyst for selective oxidation with molecular oxygen in the liquid phase,⁹ on magnetic particles ($\text{Ru}(\text{OH})_x/\text{Fe}_3\text{O}_4$). The $\text{Ru}(\text{OH})_x/\text{Fe}_3\text{O}_4$ could act as an efficient heterogeneous catalyst for the aerobic oxidations of alcohols and amines [eqn (1) and (2)], and reductions of carbonyl compounds to alcohols with 2-propanol [eqn (3)]. The catalyst/product(s) separation could be easily achieved with a permanent magnet and more than 99% of $\text{Ru}(\text{OH})_x/\text{Fe}_3\text{O}_4$ catalyst could usually be recovered for each reaction. The catalyst was easily separated with an

^aCore Research for Evolutional Science and Technology (CREST), Japan Science and Technology Agency (JST), 4-1-8 Honcho, Kawaguchi, Saitama, 332-0012, Japan

^bDepartment of Applied Chemistry, School of Engineering, The University of Tokyo, 7-3-1 Hongo, Bunkyo-ku, Tokyo, 113-8656, Japan. E-mail: nmizuno@mail.ecc.u-tokyo.ac.jp; Fax: 81 3 5841 7220; Tel: 81 3 5841 7272

† Electronic supplementary information (ESI) available: Fig. S1 and S2. See DOI: 10.1039/b603204d

external magnet and the recovered catalyst was reusable without significant loss of the catalytic performance.



Results and discussion

The $\text{Ru(OH)}_x/\text{Fe}_3\text{O}_4$ catalyst was prepared according to the following procedures.⁹ An aqueous solution containing RuCl_3 (8.3×10^{-3} M, 120 mL) and Fe_3O_4 (4 g) was vigorously stirred at room temperature for a few minutes. Then, the pH of the solution was quickly adjusted to 13 by the addition of an aqueous solution of NaOH (1 M) and the resulting slurry was stirred for 24 h. The solid was then filtered off, washed with a large amount of water, and air-dried to afford $\text{Ru(OH)}_x/\text{Fe}_3\text{O}_4$ (Ru content; 2.6 wt%, BET surface area; $11.0 \text{ m}^2 \text{ g}^{-1}$). The X-ray photoelectron spectrum of $\text{Ru(OH)}_x/\text{Fe}_3\text{O}_4$ showed the signals of $3d_{5/2}$ and $3p_{3/2}$ at 281.2 and 463.0 eV, respectively, showing that ruthenium species on $\text{Ru(OH)}_x/\text{Fe}_3\text{O}_4$ is $+3$.^{9,10} The X-ray diffraction spectrum of $\text{Ru(OH)}_x/\text{Fe}_3\text{O}_4$ showed the intense signals at $d = 2.9569, 2.5198, 2.0924, 1.6117,$ and 1.4806 \AA . The signal positions and intensities almost agreed with those of the parent Fe_3O_4 . The signals of ruthenium metal and ruthenium oxide were not detected, showing that Ru species is highly dispersed on Fe_3O_4 .

A typical procedure for the reaction was as follows. Into a glass reactor were successively placed $\text{Ru(OH)}_x/\text{Fe}_3\text{O}_4$, a substrate, and a solvent. The reaction mixture was shaken (800 rev min^{-1}) at the reaction temperature under 1 atm of molecular oxygen (for oxidation) or argon (for reduction). The conversion and product selectivity were periodically

determined by GC analysis. After the reaction, a permanent magnet was attached on an outside wall of the glass reactor in order to place the $\text{Ru(OH)}_x/\text{Fe}_3\text{O}_4$ catalyst (Fig. 1b) and the reaction solution was removed off. Thus, the catalyst/product(s) separation was extremely simple. More than 99% of $\text{Ru(OH)}_x/\text{Fe}_3\text{O}_4$ could usually be recovered.

The use of solid catalysts can make the workup very simple; catalysts can easily be recovered after the reaction and can be reused without the significant loss of the catalytic activity and selectivity. However, leaching and/or deactivation problems of the heterogeneous catalysts are responsible for severe drawbacks and are frequently observed in many cases. First of all, the aerobic oxidation of 1-phenylethanol as a model substrate was carried out with $\text{Ru(OH)}_x/\text{Fe}_3\text{O}_4$ under the conditions of Table 1 in order to verify whether the observed catalysis is truly heterogeneous or not. The catalyst was magnetically separated around 50% conversion at the reaction temperature and the reaction was again carried out with the filtrate under the same conditions. As shown in Fig. 2, the oxidation was completely stopped by the removal of the catalyst. Further, it was confirmed by ICP-AES analysis that no ruthenium and iron species were found in the filtrate (Ru: $<0.0019 \text{ wt}\%$, Fe: $<0.0023 \text{ wt}\%$). Therefore, we conclude that the nature of the observed catalysis is truly heterogeneous.¹¹

The present $\text{Ru(OH)}_x/\text{Fe}_3\text{O}_4$ showed high catalytic activity for liquid-phase aerobic oxidation of alcohols and amines, and reduction of carbonyl compounds to alcohols in the presence of 2-propanol (Tables 1–3). The reaction conditions were optimized by changing the reaction temperature, solvent, and scale. Under the present reaction conditions, no oxidation or reduction proceeded in the absence of the catalyst or in the presence of Fe_3O_4 . In the case of the reactions of alcohols with the catalyst precursor of $\text{RuCl}_3 \cdot n\text{H}_2\text{O}$, Friedel–Crafts-type reactions of alcohols with toluene (solvent) and dehydrative condensations of alcohols proceeded, and no oxidation of alcohols was observed.

Table 1 shows the results of $\text{Ru(OH)}_x/\text{Fe}_3\text{O}_4$ -catalyzed oxidation of various alcohols with 1 atm of molecular oxygen. All primary and secondary benzylic alcohols were converted into the corresponding aldehydes and ketones, respectively, in almost quantitative yields (entries 1–6). The α,β -unsaturated cinnamyl alcohol afforded the corresponding α,β -unsaturated aldehyde without the intramolecular hydrogen transfer and geometrical isomerization (entry 7). The present system could also oxidize sulfur containing and secondary aliphatic alcohols in high yields (entries 8–10). The oxidation of radical clock substrate of cyclopropylphenyl carbinol exclusively produced cyclopropylphenyl ketone without the ring-opened products (entry 3).

The present $\text{Ru(OH)}_x/\text{Fe}_3\text{O}_4$ was also active for the aerobic oxidations of various amines. The results are summarized in Table 2. Primary aromatic amines as well as aliphatic ones were converted into the corresponding nitriles in high yields with small amounts of *N*-alkylimines as byproducts (entries 1–5). Not only primary amines but also secondary and heterocyclic ones were selectively oxidized (entries 6 and 8). The $\text{Ru(OH)}_x/\text{Fe}_3\text{O}_4$ could also act as an efficient heterogeneous catalyst for the aerobic oxidation of alkylarenes. For example, xanthene was quantitatively oxidized to the

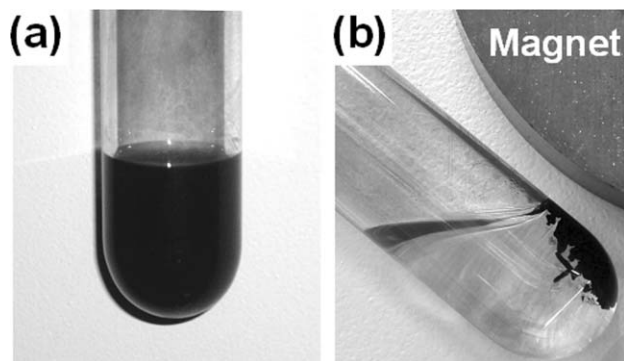
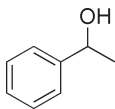
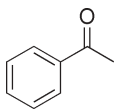
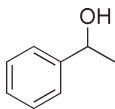
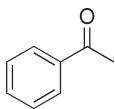
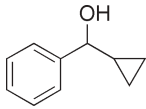
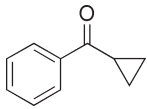
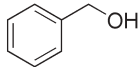
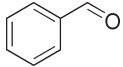
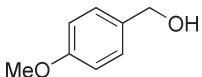
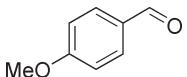
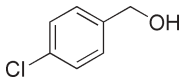
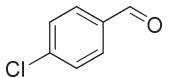
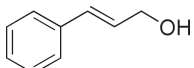
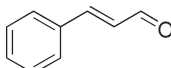
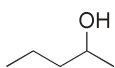
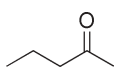
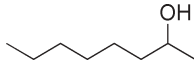
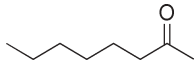
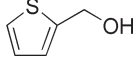
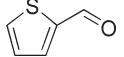


Fig. 1 Aerobic oxidation with $\text{Ru(OH)}_x/\text{Fe}_3\text{O}_4$. The pictures (a) and (b) show the reaction mixture and the response of $\text{Ru(OH)}_x/\text{Fe}_3\text{O}_4$ to a magnet, respectively.

Table 1 Aerobic oxidation of various alcohols catalyzed by Ru(OH)_x/Fe₃O₄^a

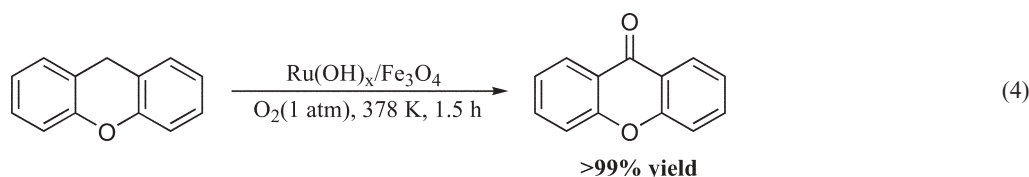
Entry	Substrate	Product	Time/h	Conversion (%)	Selectivity (%)
1			2	>99	>99
2 ^b			2	93	>99
3			1	>99	>99
4			1	>99	>99
5			1	>99	>99
6			1	>99	>99
7			1.5	95	>99
8			5	80	>99
9			5	83	>99
10			1.5	>99	>99

^a Reaction conditions: substrate (1 mmol), Ru(OH)_x/Fe₃O₄ (Ru: 3.8 mol%), toluene (3 mL), 378 K, under 1 atm of molecular oxygen. The conversion and selectivity were determined by GC using an internal standard (naphthalene or diphenyl). ^b Reuse experiment. The initial rate was almost the same as that for the first run with the fresh catalyst.

corresponding ketone of 9-xanthenone (>99% yield) within 1.5 h under the same conditions in Table 1 [eqn (4)].

The addition of radical scavengers such as 2,6-di-*tert*-butyl-4-methylphenol did not affect the reaction rates as well as the product selectivity for the oxidation of 1-phenylethanol. Further, the oxidations of radical clock, *e.g.*, cyclopropylphenyl carbinol, exclusively produced cyclopropylphenyl ketone. These results show that free-radical intermediates are

not involved in the present alcohol oxidation. The oxidation of primary alcohols proceeded faster than secondary ones for their mixture (competitive oxidations). For example, an equimolar mixture of benzyl alcohol and 1-phenylethanol gave a mixture of benzaldehyde and acetophenone in 95% and 12% yields, respectively, at 378 K for 70 min. The ratio of the oxidation rate of benzyl alcohol to that of 1-phenylethanol was 14.7. The faster oxidation of primary alcohols support the



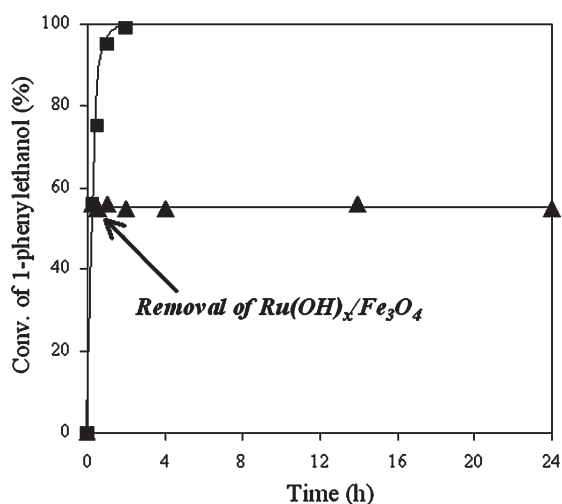


Fig. 2 Effect of removal of $\text{Ru(OH)}_x/\text{Fe}_3\text{O}_4$ on the aerobic oxidation of 1-phenylethanol. Without removal of $\text{Ru(OH)}_x/\text{Fe}_3\text{O}_4$ (■); the arrow indicates the removal of $\text{Ru(OH)}_x/\text{Fe}_3\text{O}_4$ (▲).

formation of ruthenium-alkoxide *via* the ligand exchange of ruthenium-hydroxide species on $\text{Ru(OH)}_x/\text{Fe}_3\text{O}_4$ with an alcohol. The formation of metal-alkoxide species is well known for the selective oxidation of the primary hydroxyl group.¹²

On the basis of the above results, the present alcohol oxidation includes the formation of ruthenium-alkoxide

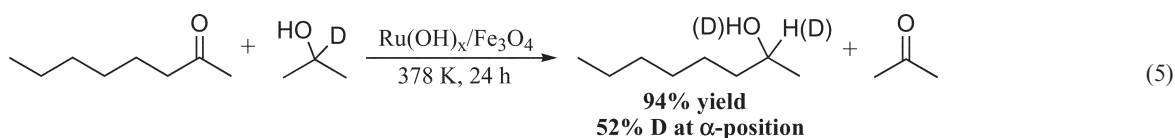
species, followed by the typical β -hydrogen elimination to afford the corresponding carbonyl compound and ruthenium-hydride species. The hydride species is then reoxidized by molecular oxygen. Monitoring the O_2 uptake for the oxidation of benzylalcohol revealed that the amount of O_2 consumption was *ca.* half that of benzaldehyde produced (see electronic supplementary information (ESI), Fig. S1†). The 1 : 2 (O_2 : product) stoichiometry shows that the simple dehydrogenation does not proceed and support the reaction mechanism above described. The kinetic isotope effect ($k_{\text{H}}/k_{\text{D}}$) at 378 K was 4.7 ± 0.2 for the intramolecular competitive oxidation of α -deuterio-*p*-methylbenzyl alcohol, showing that the β -hydrogen elimination is the rate-determining step. Amine oxidation would proceed in a similar way as reported for $\text{Ru(OH)}_x/\text{Al}_2\text{O}_3$.⁹

Various kinds of ketones could be reduced to the corresponding alcohols in high yields using 2-propanol as a hydrogen donor (Table 3). Acetophenones were efficiently converted to the corresponding 1-phenylethanols in excellent yields (entries 1–3). Not only aromatic ketones but also aliphatic ones such as 3-pentanone, 2-octanone, 3-octanone, and cyclohexanone could be reduced to the corresponding aliphatic secondary alcohols in high yields (entries 4 and 7–9). When the reduction of 2-octanone was carried out using 2-deuterio-2-propanol under the conditions in Table 3 with 7.6 mol% of $\text{Ru(OH)}_x/\text{Fe}_3\text{O}_4$, 2-octanol was obtained in 94% yield for 24 h. The deuterium content at the α -position of

Table 2 Aerobic oxidations of various amines catalyzed by $\text{Ru(OH)}_x/\text{Fe}_3\text{O}_4$ ^a

Entry	Substrate	Product	Time/h	Conversion (%)	Selectivity (%)
1			7	96	82 ^b
2			4	>99	94 ^b
3			5	98	94 ^b
4	$\text{CH}_3(\text{CH}_2)_7\text{NH}_2$	$\text{CH}_3(\text{CH}_2)_6\text{CN}$	24	85	97 ^b
5	$\text{CH}_3(\text{CH}_2)_{11}\text{NH}_2$	$\text{CH}_3(\text{CH}_2)_{10}\text{CN}$	24	53	97 ^b
6			1.5	>99	>99
7 ^c			1.5	>99	>99
8 ^d			24	85	88 ^e

^a Reaction conditions: substrate (1 mmol), $\text{Ru(OH)}_x/\text{Fe}_3\text{O}_4$ (Ru: 3.8 mol%), toluene (3 mL), 378 K, under 1 atm of molecular oxygen. The conversion and selectivity were determined by GC using an internal standard (naphthalene or diphenyl). ^b *N*-Alkylimines were formed as byproducts (~18% selectivity). ^c Reuse experiment. The initial rate was almost the same as that for the first run with the fresh catalyst. ^d The reaction was carried out in *o*-xylene (3 mL) at 423 K. ^e Benzonitrile, benzaldehyde, and benzoic acid were formed as byproducts (~10% selectivity).



2-octanol was 52%, suggesting the formation of ruthenium dihydride species during the reaction [eqn (5)].^{13,14}

The $\text{Ru(OH)}_x/\text{Fe}_3\text{O}_4$ could be attached on the outside wall of the reactor after the reaction and the reaction solution could be easily separated off. The XRD patterns of the catalyst recovered after the oxidation and reduction were the same as that of the fresh $\text{Ru(OH)}_x/\text{Fe}_3\text{O}_4$ catalyst (ESI, Fig. S2),[†] showing that the ruthenium species and Fe_3O_4 support keep the original structure during the reaction. The catalyst could be reused without a significant loss of the catalytic activity and selectivity for both the oxidations and reductions (entry 2 in Table 1, entry 7 in Table 2, and entries 5 and 6 in Table 3). Furthermore, $\text{Ru(OH)}_x/\text{Fe}_3\text{O}_4$ has been reused for different types of reactions sequentially (Table 4). The catalyst was first used for the oxidation of 1-phenylethanol (alcohol oxidation, entry 1). After the alcohol oxidation, the recovered catalyst

was reused for the oxidation of 2,3-dihydroindole (amine oxidation, entry 2), followed by the reuse for the reduction of 3-pentanone with 2-propanol (reduction, entry 3). As shown in Table 4, the catalyst could be reused without a significant loss of the activity and selectivity in the sequential reuse reactions.

Conclusion

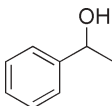
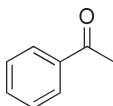
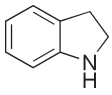
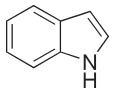
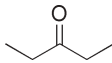
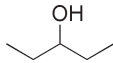
In summary, we have successfully developed a magnetically separable heterogeneous catalyst for aerobic oxidations and reductions with 2-propanol. The catalyst/product(s) separation could be easily achieved with a permanent magnet while the catalytic activities of $\text{Ru(OH)}_x/\text{Fe}_3\text{O}_4$ were comparable to or lower than that of $\text{Ru(OH)}_x/\text{Al}_2\text{O}_3$.⁹ The catalyst recovered after the reaction was reusable without a significant loss of the catalytic performance.

Table 3 Reduction of various ketones using 2-propanol as a hydrogen donor catalyzed by $\text{Ru(OH)}_x/\text{Fe}_3\text{O}_4$ ^a

Entry	Substrate	Product	Time/h	Conversion (%)	Selectivity (%)
1			1	90	97 ^b
2			2	98	>99
3			2	89	>99
4			1	95	>99
5 ^c			1	96	>99
6 ^c			1	95	>99
7			1	95	>99
8			1	95	>99
9			1	99	99

^a Reaction conditions: substrate (1 mmol), $\text{Ru(OH)}_x/\text{Fe}_3\text{O}_4$ (Ru: 3.8 mol%), 2-propanol (3 mL), 378 K, under 1 atm of argon. The conversion and selectivity were determined by GC using an internal standard (naphthalene or diphenyl). ^b Styrene was formed as a byproduct (~3% selectivity). ^c Reuse experiments: 1st reuse (entry 5) and 2nd reuse (entry 6). Initial rates were almost the same as that for the first run with the fresh catalyst.

Table 4 Reuse of Ru(OH)_x/Fe₃O₄ for different types of the reactions sequentially^a

Entry	Substrate	Product	Time/h	Conversion (%)	Selectivity (%)
1			2	>99	>99
2			1.5	>99	>99
3			1	83	>99

^a The reaction conditions were the same as those in Tables 1 and 2. The conversion and selectivity were determined by GC using an internal standard (naphthalene or diphenyl).

Experimental

General

GC analyses were performed on Shimadzu GC-17A with a flame ionization detector equipped with a DB-WAX or TC-1 capillary column (internal diameter = 0.25 mm, length = 30 m). Mass spectra were recorded on Shimadzu GCMS-QP2010 at an ionization voltage of 70 eV equipped with a DB-WAX capillary column (internal diameter = 0.25 mm, length = 30 m). NMR spectra were recorded on JEOL JNM-EX-270. ¹H and ¹³C NMR spectra were measured at 270 and 67.8 MHz, respectively, with TMS as an internal standard. ²H NMR spectra were measured at 41.25 MHz using benzene-*d*₆ as an external standard. XPS measurements were carried out on JEOL JPS-90 using monochromated Al K α radiation ($h\nu = 1486.6$ eV). The X-ray anode was run at 200 W and the voltage was kept at 10 kV. The pass energy was fixed at 20.0 eV to ensure sufficient resolution to determine peak positions accurately. The XRD patterns were measured with Rigaku Multiflex (Cu K α radiation, 40 kV–50 mA). Substrates and solvents (except for 2-propanol) were commercially obtained from Tokyo Kasei, Aldrich, and Fluka (reagent grade) and used without further purification. 2-Propanol was in particular carefully purified (degassed). Fe₃O₄ was purchased from Aldrich (Cat. No. 310069, CAS 1317-61-9, BET surface area: 6.8 m² g⁻¹).

Preparation of Ru(OH)_x/Fe₃O₄

Fe₃O₄ (4 g) was vigorously stirred with an aqueous solution of RuCl₃ (120 mL, 8.3 × 10⁻³ M) at room temperature for 10 min. Then, the pH of the solution was slowly adjusted to 13 by the addition of an aqueous solution of NaOH (1 M) and the resulting slurry was stirred for additional 24 h. The solid was then filtered off, washed with a large amount of water, and air-dried to afford Ru(OH)_x/Fe₃O₄ as a black powder (4.0 g). The content of ruthenium was 2.6 wt%. The BET surface area was 11.0 m² g⁻¹. The X-ray photoelectron spectrum of Ru(OH)_x/Fe₃O₄ showed the peaks of 3d_{5/2} and 3p_{3/2} at 281.2 and 463.0 eV, respectively, showing that ruthenium species on Ru(OH)_x/Fe₃O₄ is +3. The X-ray diffraction spectrum of

Ru(OH)_x/Fe₃O₄ showed the intense signals at $d = 2.9569$, 2.5198, 2.0924, 1.6117, and 1.4806 Å. The signal positions and intensities were very close to those of the parent Fe₃O₄. Diffraction signals due to ruthenium metal and ruthenium oxide were not detected, showing that Ru species is highly dispersed on Fe₃O₄.

Procedures for Ru(OH)_x/Fe₃O₄-catalyzed reactions

Into a glass reactor were successively placed Ru(OH)_x/Fe₃O₄, a substrate, and toluene (*o*-xylene for dibenzylamine). The reaction mixture was shaken (800 rev min⁻¹) at 378 K (423 K for dibenzylamine) under 1 atm of molecular oxygen (equipped with a balloon). The conversion and product selectivity were periodically determined by GC analysis. All products have been identified by comparison of their ¹H and ¹³C NMR signals with the literature data.

All operations were carried in the glove box under argon for the reduction of carbonyl compounds. Into a glass reactor were successively placed Ru(OH)_x/Fe₃O₄, a substrate, and 2-propanol. The reaction mixture was shaken (800 rev min⁻¹) at reaction temperature under 1 atm of argon. The conversion and product selectivity were periodically determined by GC analysis. All products have been identified by comparison of their ¹H and ¹³C NMR signals with the literature data.

Recycling of Ru(OH)_x/Fe₃O₄

After the reaction, a permanent magnet was externally applied in order to place the Ru(OH)_x/Fe₃O₄ catalyst on the side wall of the reactor and the reaction solution was removed off. More than 99% of Ru(OH)_x/Fe₃O₄ could usually be recovered. In the case of alcohol and amine oxidation, the catalyst was recovered, washed with toluene and an aqueous solution of NaOH (pH = 13), and air-dried before reuse. In the case of reduction, the catalyst was used directly for the next run.

Acknowledgements

This work was supported by the Core Research for Evolutional Science and Technology (CREST) program of

the Japan Science and Technology Agency (JST) and the Grants-in-Aid for Scientific Research from Ministry of Education, Culture, Sports, Science and Technology.

References

- R. A. Sheldon and J. K. Kochi, *Metal Catalyzed Oxidations of Organic Compounds*, Academic Press, New York, 1981; C. L. Hill, in *Advances in Oxygenated Processes*, ed. A. L. Baumstark, JAI Press, Inc., London, 1988, vol. 1, p. 1; M. Hudlucky, *Oxidations in Organic Chemistry*, ACS Monograph Series, American Chemical Society, Washington DC, 1990; A. Madin, in *Comprehensive Organic Synthesis*, ed. B. M. Trost, I. Fleming and S. V. Ley, Pergamon Press, Oxford, 1991, vol. 7, p. 251.
- T. Mallat and A. Baiker, *Chem. Rev.*, 2004, **104**, 3037; I. W. C. E. Arends and R. A. Sheldon, in *Modern Oxidation Methods*, ed. J.-E. Bäckvall, Wiley-VCH, Weinheim, 2004, pp. 83–118, and references cited therein.
- Examples of aerobic alcohol and amine oxidation: R. Lenz and S. V. Ley, *J. Chem. Soc., Perkin Trans. 1*, 1997, 3291; A. Hanyu, E. Takezaki, S. Sakaguchi and Y. Ishii, *Tetrahedron Lett.*, 1998, **39**, 5557; A. Dijkman, A. Marino-González, A. Mairata i Payeras, I. W. C. E. Arends and R. A. Sheldon, *J. Am. Chem. Soc.*, 2001, **123**, 6826; G. Csajnyik, A. H. Ell, L. Fadini, B. Pugin and J.-E. Bäckvall, *J. Org. Chem.*, 2002, **67**, 1657; T. Nishimura, T. Onoue, K. Ohe and S. Uemura, *J. Org. Chem.*, 1999, **64**, 6750; G.-J. ten Brink, I. W. C. E. Arends and R. A. Sheldon, *Science*, 2000, **287**, 1636; I. E. Markó, P. R. Giles, M. Tsukazaki, S. M. Brown and C. J. Urch, *Science*, 1996, **274**, 2044; I. E. Markó, P. R. Giles, M. Tsukazaki, I. Chellé-Regnaut, C. J. Urch and S. M. Brown, *J. Am. Chem. Soc.*, 1997, **119**, 12661; K. Yamaguchi, K. Mori, T. Mizugaki, K. Ebitani and K. Kaneda, *J. Am. Chem. Soc.*, 2000, **122**, 7144; K. Mori, K. Yamaguchi, T. Mizugaki, K. Ebitani and K. Kaneda, *Chem. Commun.*, 2001, 461; K. Mori, K. Yamaguchi, T. Mizugaki, K. Ebitani and K. Kaneda, *J. Am. Chem. Soc.*, 2002, **124**, 11573; I. E. Markó, A. Gautier, R. Dumeunier, K. Doda, F. Philippart, S. M. Brown and C. J. Urch, *Angew. Chem., Int. Ed.*, 2005, **43**, 1588; J. S. M. Samec, A. H. Ell and J.-E. Bäckvall, *Chem.–Eur. J.*, 2005, **11**, 2327; A. J. Bailey and B. R. James, *Chem. Commun.*, 1996, 2343; S. Cenini, F. Porta and M. Pizzotto, *J. Mol. Catal.*, 1982, **15**, 297; R. Tang, S. E. Diamond, N. Neary and F. Mares, *J. Chem. Soc., Chem. Commun.*, 1978, 562; Y. Maeda, T. Nishimura and S. Uemura, *Bull. Chem. Soc. Jpn.*, 2003, **76**, 2399 and references cited therein.
- G. Zassinovich, G. Mestroni and S. Gladiali, *Chem. Rev.*, 1992, **92**, 1051; T. Naota, H. Takaya and S.-I. Murahashi, *Chem. Rev.*, 1998, **98**, 2599; R. Noyori, *Chem. Soc. Rev.*, 1989, **18**, 187; R. Noyori, *Science*, 1990, **248**, 1194; R. Noyori and S. Hashiguchi, *Acc. Chem. Res.*, 1997, **30**, 97; M. J. Palmer and M. Will, *Tetrahedron: Asymmetry*, 1999, **10**, 2045 and references cited therein.
- J. Hagen, *Industrial Catalysis: A Practical Approach*, Wiley-VCH, Weinheim, 1999.
- R. A. Sheldon and H. van Bekkum, *Fine Chemical through Heterogeneous Catalysis*, Wiley, Weinheim, 2001; P. T. Anastas and J. C. Warner, *Green Chemistry: Theory and Practice*, Oxford University Press, London, 1998; R. A. Sheldon, *Green Chem.*, 2000, **2**, G1; P. T. Anastas, L. B. Bartlett, M. M. Kirchhoff and T. C. Williamson, *Catal. Today*, 2000, **55**, 11.
- In the case of Ru(OH)_x/Al₂O₃, ca. 95% of the catalyst could be recovered by filtration.
- J. Zhang, Y. Wang, H. Ji, Y. Wei, N. Wu, B. Zuo and Q. Wang, *J. Catal.*, 2005, **229**, 114; H. M. R. Gardimalla, D. Mandal, P. D. Stevens, M. Yen and Y. Gao, *Chem. Commun.*, 2005, 4432; P. D. Stevens, G. Li, J. Fan, M. Yen and Y. Gao, *Chem. Commun.*, 2005, 4435; J. Lee, D. Lee, E. Oh, J. Kim, Y.-P. Kim, S. Jin, H.-S. Kim, Y. Hwang, J. H. Kwak, J.-G. Park, C.-H. Shin, J. Kim and T. Hyeon, *Angew. Chem., Int. Ed.*, 2005, **44**, 7432; T.-J. Yoon, J. S. Kim, B. G. Kim, K. N. Yu, M.-H. Cho and J.-K. Lee, *Angew. Chem., Int. Ed.*, 2005, **44**, 1068.
- K. Yamaguchi and N. Mizuno, *Angew. Chem., Int. Ed.*, 2002, **41**, 4538; K. Yamaguchi and N. Mizuno, *Angew. Chem., Int. Ed.*, 2003, **42**, 1480; K. Yamaguchi and N. Mizuno, *Chem.–Eur. J.*, 2003, **9**, 4353; K. Kamata, J. Kasai, K. Yamaguchi and N. Mizuno, *Org. Lett.*, 2004, **6**, 3577; M. Matsushita, K. Kamata, K. Yamaguchi and N. Mizuno, *J. Am. Chem. Soc.*, 2005, **127**, 6632.
- S. Murata and K. Aika, *J. Catal.*, 1992, **136**, 110; G. P. Williams, in *CRC Handbook of Chemistry and Physics*, ed. D. R. Lida, CRC Press, Washington DC, 82nd edn, 2001, section 10, pp. 200–205.
- R. A. Sheldon, M. Wallau, I. W. C. E. Arends and U. Schuchardt, *Acc. Chem. Res.*, 1998, **31**, 485.
- K. B. Sharpless, K. Akashi and K. Oshima, *Tetrahedron Lett.*, 1976, **17**, 2503; S. Kanemoto, S. Matsubara, K. Takai, K. Oshima, K. Utimoto and H. Nozaki, *Bull. Chem. Soc. Jpn.*, 1988, **61**, 3607.
- In the case of the reduction of acetophenone using 2-deuterio-2-propanol with Ru(OH)_x/Al₂O₃ at 363 K, the α-deuterium of 2-deuterio-2-propanol was selectively transferred to the carbonyl carbon of acetophenone to give 1-deuterio-1-phenylethanol as a major product (88% yield, 91% deuterium content at the α-position). See: K. Yamaguchi, T. Koike, M. Kotani, M. Matsushita, S. Shinachi and N. Mizuno, *Chem.–Eur. J.*, 2005, **11**, 6574.
- O. Pàmies and J.-E. Bäckvall, *Chem.–Eur. J.*, 2001, **7**, 5052.

[Hmim][NO₃]⁺—an efficient solvent and promoter in the oxidative aromatic chlorination[†]

Cinzia Chiappe,* Elsa Leandri and Marianna Tebano

Received 4th May 2006, Accepted 21st June 2006

First published as an Advance Article on the web 6th July 2006

DOI: 10.1039/b606258j

Brønsted acidic ionic liquid [Hmim][NO₃] has been used as a cosolvent and “promoter” for oxidative halogenation of aromatic compounds with aqueous halohydric acids. This method is characterized by a high atom economy. Potentiality and limits are presented.

Introduction

Halogenated organic compounds constitute an important class of intermediates as they can be converted into other functionalities by simple chemical transformation. Aryl halides are the starting materials for the preparation of organometallic reagents, numerous bulk and fine chemicals, and pharmaceuticals.¹ The classical synthetic procedure based on the use of molecular halogens,² although generally efficient, utilizes only 50% of the starting reagent, with the other half forming HBr or HCl waste. For deactivated compounds, this reaction also requires stoichiometric amounts of Lewis acids (e.g. AlCl₃), increasing the volumes of waste streams. Transportation/storage of large quantities of molecular bromine or chlorine may be further complications. These problems enhance the appeal of halogenation protocols based on halide salt oxidation with hydrogen peroxide,³ often envisaged in a manner similar to the biohalogenations performed by haloperoxidase enzymes. Analogously to the enzymatic processes however, these reactions require the presence of V or Mo salts as catalysts⁴ and drastically depend on the presence of stoichiometric amounts of acid.⁵ The requirement for stoichiometric acid as a reagent raises reagent prices and increases waste by-products. Therefore, some doubts have been raised about the possibility of applying peroxide-mediated bromide salt oxidation for large-scale bromination. Finally, although the use of halogenating enzymes (haloperoxidases, FADH₂-dependent halogenase, perhydrolases)⁶ could be the most effective from an environmental point of view, large-scale halogenations using enzymes have not been commercialized: one of the reasons for this is that these reactions need to be performed in dilute solutions, rendering them less attractive from an economic point of view.⁷

Recently, to at least partially overcome these problems, the halogenation of aromatic compounds was investigated in ionic liquids (ILs). Halogenated arenes have been obtained using N-halosuccinimides in [bmim][PF₆] and in [bmim][BF₄]⁸ or trihalide based ILs.^{9,10} In particular, the use of the Brønsted

acidic ionic liquid 3-methylimidazolium tribromide ([Hmim][Br₃]) as reagent and solvent avoids toxic chlorinated solvents and gives, as the sole by-product of the reaction, 3-methylimidazolium bromohydrogenate; another IL which can be isolated and used as reagent–solvent for other reactions.¹¹ However, in this case the atom economy of the bromination process is again quite low (55%).

The oxidative approach is probably the sole method able to give a higher atom economy. In contrast to other aromatic electrophilic substitution reactions, which have been extensively investigated in ionic liquids, with the exception of a recent patent¹² only one example of chlorination of benzene, using HCl in [bmim][NO₃], has been reported.¹³ In order to obtain information about limits and possibilities of the oxidative approach for halogenations of aromatic compounds we have investigated the chlorination of some arenes using Brønsted acidic [Hmim]⁺ ionic liquids, bearing NO₃[−] or Cl[−] as the counteranion.

Results and discussion

Brønsted acidic [Hmim][NO₃] and [Hmim][Cl] can be obtained simply by neutralization. The combination of 1-methylimidazole with HNO₃ (67%) in a 1 : 1 molar ratio produces, after water removal, a white solid (mp 67 °C) identified as 3-methylimidazolium nitrate ([Hmim][NO₃]), whereas the same reaction with HCl (37%) gives 3-methylimidazolium chloride ([Hmim][Cl]), a liquid compound at room temperature.

Initially, the efficiency of the three potential chlorinating systems, [Hmim][NO₃]-HCl (37%), [Hmim][Cl]-HNO₃ (67%) and [Hmim][NO₃]-[Hmim][Cl] was evaluated using mesitylene (**1**) as substrate (Fig. 1). The experiments were carried out at 80 °C and 100 °C. The [Hmim][NO₃]-[Hmim][Cl] mixture (1 : 2) gave only the unreacted substrate, showing that the oxidative process required the presence of an aqueous acid. Therefore, the optimal ratio among the reagents was evaluated by mixing the IL ([Hmim][Cl] or [Hmim][NO₃]), the substrate and the appropriate aqueous acid in the ratios reported in Table 1. The reaction mixtures were heated at 80 °C in the presence of air for 24 or 48 h, as reported in Table 1. Products were extracted with hexane (6 × 3 mL) and analyzed by GC-MS and NMR. The data reported in Table 1 show that, although in all the examined conditions the species present in solution were always water, [Hmim]⁺, Cl[−], NO₃[−], and H⁺, the

Dipartimento di Chimica Bioorganica e Biofarmacia, vis Bonanno 33, Pisa, 56126, Italy. E-mail: cinziac@farm.unipi.it; Fax: +39 050 2219660; Tel: +39 050 2219669

[†] Electronic supplementary information (ESI) available: GC-MS chromatograms of all investigated compounds. See DOI: 10.1039/b606258j

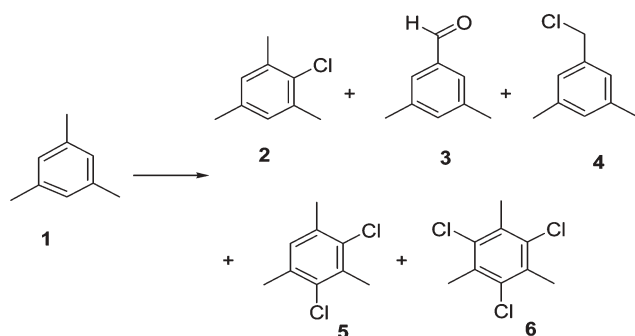


Fig. 1 Oxidative chlorination of mesitylene **1**.

system [Hmim][NO₃]-HCl provided the highest selectivity toward the mono-chloro derivative **2**.

Moreover, the ESI-MS analysis of the ionic liquid recovered at the end of the reaction performed in the 2 : 1 [Hmim][NO₃]-HCl mixture (after products extraction) showed the exclusive presence of the starting IL, [Hmim][NO₃]. This result suggested: (1) the involvement of another oxidant and (2) that the halogenating system [Hmim][NO₃]-HCl might be re-used, simply by re-adding substrate and HCl after product extraction. Generally, in the recycling experiments water was removed by evaporation before the addition of reagents to avoid an excessive increase of the water concentration in the reaction mixture. Recycling experiments (represented in Table 2) show that for at least four cycles there is no significant decrease in activity; the fourth cycle was conducted seven days after the preceding one.

Finally, it is worth noting that, for this system, the higher conversion, associated with the higher selectivity, was obtained working with a substrate:[Hmim][NO₃]:HCl ratio of 1 : 2 : 1. Data reported in Table 3 indeed show that the selectivity towards **2** decreases significantly with decreasing percentage of [Hmim][NO₃] (compare runs 4 and 5). On the other hand, selectivity and yields are unaffected by the reaction scale (compare runs 1, 5 and 6).

The efficacy of [Hmim][NO₃]-HCl as a chlorinating system was also ascertained with other aromatic substrates (Fig. 2). The reaction mixtures (substrate-[Hmim][NO₃]-HCl (37%), 1 : 2 : 1) were heated at 80 °C for 48 h. Products were extracted with hexane (6 × 3 mL) and analyzed by GC-MS and NMR. As shown in Fig. 2, the halogenation of activated substrates is achieved with high to excellent conversions and yields; almost exclusively the mono-substituted adduct can be isolated. The system is also active with sterically hindered tri- and tetrasubstituted benzenes (**1,7**) and with naphthalene,

Table 2 Recycle experiments for oxidative chlorination of mesitylene, **1**

Recycle	Conversion (%)	Products (%)		
		2	3	4
1	94	96	1	3
2	90	96	1	3
3	95	96	1	3
4 ^a	98	97	1	2

^a Carried out after a week.

Table 3 Dependence of the product distribution for chlorination of **1** on the ratio substrate, [Hmim][NO₃] and HCl

	1/mmol	IL/mmol	HCl/mmol	Conversion (%)	Products (%)				
					2	3	4	5	6
1	1.0	2.00	1.00	99	96	1	3	—	—
2	2.0	2.00	2.00	100	76	3	5	16	—
3	3.0	2.00	3.00	80	68	2	10	17	3
4	5.0	2.00	5.00	80	60	4	14	15	7
5	5.0	10.0	5.0	93	97	1	2	—	—
6	10	20	10	93	96	1	3	—	—

which is halogenated exclusively at C-1. The higher reactivity of compound **1** with respect to **7** suggests that the reaction occurs through a polar mechanism, involving an ionic intermediate (σ -complex) and an ionic transition state in the rate determining step.¹⁴ Anisole gives preferentially, but not exclusively, the *para*-derivative **26**. It is worth noting that no phenol was detected in the halogenation of this substrate. On the other hand, chlorobenzene was completely non-reactive. No product arising from chlorobenzene was detected in the reaction mixture, even after longer reaction times (data not reported in table). Moreover, in this case, the GC-MS analyses evidenced the formation of a significant amount of the product arising from the exhaustive halogenation of the imidazolium ring. As the formation of this compound was observed exclusively in the reaction of chlorobenzene, it is probable that in the absence of a good substrate the halogenation of the cation of the IL may become a competitive process. Finally, it is worthy of note that the chlorination of **13** does not occur on the aromatic ring but exclusively on the methyl group, whereas substrates bearing the formyl group (**15** and **22**) give practically only the corresponding carboxylic acids.

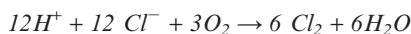
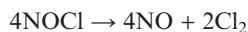
On the basis of all the above reported data, in particular considering that only [Hmim][NO₃] has been detected at the end of the reactions, we propose an oxidative mechanism of the type shown below; the compounds arising from NO₃⁻ reduction (NOCl or NO) being oxidized in the reaction

Table 1 Product distribution for oxidative chlorination of mesitylene **1**^a

1/mmol	IL/mmol [Hmim][NO ₃]	Acid/mmol HCl	Time/h	Conversion (%)	Products (%)				
					2	3	4	5	6
1	2	1	24	62	96	1	3	—	—
1	2	1	48	99	96	1	3	—	—
	[Hmim][Cl]	HNO ₃							
1	2	1	24	84	85	1	3	11	—
1	1	2	24	83	71	2	3	19	5

^a Yields of the isolated products >90%.

mixture by the atmospheric oxygen. The NO_3^- anion is fundamental for the oxidation of chloride, but being reformed during the course the reaction it can be considered a stoichiometric catalyst, defined here as a “promoter”.



Oxygen is, after all, the true oxidant of this process, which gives water as the sole reaction by-product; H^+ is consumed during the course of the reaction and $[\text{Hmim}][\text{NO}_3]$ may be recycled.

Aromatic chlorination in $[\text{Hmim}][\text{NO}_3]\text{-HCl}$ can therefore be considered a “green” oxidative process, characterized by a very high atom economy (99%).

Finally, attempts to perform the bromination of mesitylene under comparable conditions (80 °C, 24 h) using the system $[\text{Hmim}][\text{NO}_3]\text{-HBr}$ (48%) yielded selectively the mono-bromo derivative; however, the conversion was significantly lower (30%) than for chlorination (62%).

Conclusions

In conclusion, $[\text{Hmim}][\text{NO}_3]$ may be considered an interesting alternative solvent–“promoter” (or catalyst) for synthesis of aryl halides starting from non-activated or sterically hindered arenes. This IL is air stable, easy to prepare and handle and is able to oxidize hydrohalic acids, being at the same time re-oxidized by oxygen. The total atom economy of this process makes it particularly attractive from an environmental point of view. The potentiality and limits of this method applied to the electrophilic chlorination of aromatic compounds and ketones have been demonstrated.

Experimental

GC-MS analyses were performed with a gas-chromatograph equipped with a DB-5 capillary column (30 m × 0.25 mm; coating thickness 0.25 μm) and an ion trap mass detector. Analytical conditions: injector and transfer line temperatures 220 and 240 °C, respectively; oven temperature programmed from 60 °C to 240 °C at 3 °C min⁻¹; carrier gas helium at 1 ml min⁻¹; injection of 0.2 μl (10% hexane solution); split ratio 1 : 30. Identification of the constituents was based on comparison of the retention times with those of authentic samples, and computer matching against commercial (NIST 98 and ADAMS) and home-made mass spectra library built up from pure substances and MS literature data. The ¹H and ¹³C NMR spectra were obtained in CDCl₃ with a 200 MHz instrument using TMS as the internal reference. ESI-MS spectra were obtained using an electrospray (ESI-MS) spectrometer equipped with Xcalibur software. Mesitylene, acetophenone, imidazole, anisole, durene, *o*-tolylaldehyde,

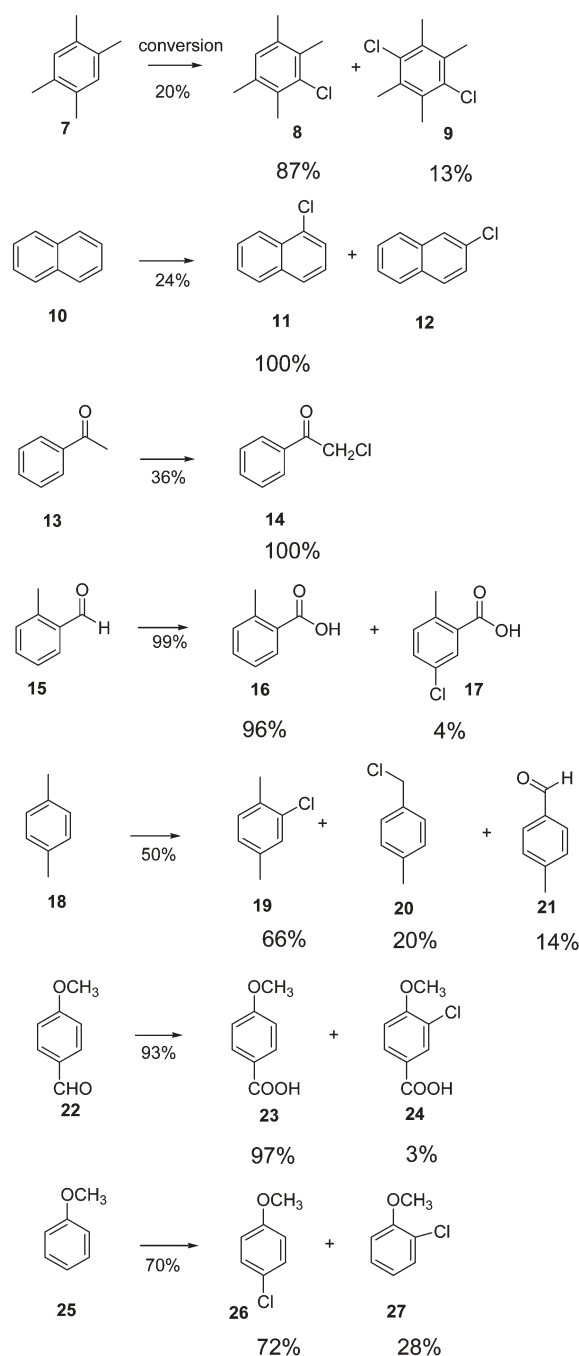


Fig. 2 Examined aromatic substrates.

p-anisaldehyde, *p*-xylene, HCl (37%) and HNO₃ (65%) were commercial products (>95% pure). $[\text{Hmim}][\text{Cl}]$ and $[\text{Hmim}][\text{NO}_3]$ were obtained by neutralization of 1-methylimidazole with HCl or HNO₃. Aqueous HCl or HNO₃ were mixed with an equimolar amount of 1-methylimidazole at 0 °C, and the pure ILs (NMR, ESI-MS) were obtained by water evaporation under reduced pressure.

General procedure for oxidative chlorination of aromatic compounds

Oxidative chlorination of mesitylene is described as a representative example: 1.0 mmol (120 mg) of mesitylene was

added to a mixture containing 2 mmol (290.0 mg) of [Hmim][NO₃] and 1 mmol (36.5 mg) of HCl (37%). The reaction was heated at 80 °C for 48 h then, after cooling at room temperature, extracted with hexane (6 × 3 mL). The combined extracts were analyzed by GC-MS or by NMR.

Recycling procedure

After product extraction, traces of organic solvents and water were eliminated at reduce pressure. Substrate and HCl were added and the mixture was heated again at the indicated temperature.

Acknowledgements

We thank MIUR and the University of Pisa for the financial support.

References

- 1 (a) *Ullmann's Encyclopedia of Industrial Chemistry*, 6th edn, Wiley-VCH, Weinheim, 2002; (b) S. G. Davis, *Organotransition Metal Chemistry: Application to Organic Synthesis*; Pergamon Press, Oxford, 1982.
- 2 P. B. De La Mare, *Electrophilic Halogenation*, Cambridge University Press, Cambridge, 1976, ch. 5.
- 3 N. B. Barhate, A. S. Gasare, R. D. Wakharakar and A. V. Bedekar, *Tetrahedron*, 1999, **55**, 11127–11142.
- 4 (a) M. Bhattacharjee, *Polyhedron*, 1992, **11**, 2817; (b) V. Conte, F. Di Furia and S. Moro, *Tetrahedron Lett.*, 1994, **35**, 7429; (c) V. Conte, F. Di Furia and S. Moro, *Tetrahedron Lett.*, 1996, **37**, 8609; (d) R. C. Larock, *Comprehensive Organic Transformations*, VCH, New York, 1989, 315.
- 5 G. Rothenberg and J. H. Clark, *Green Chem.*, 2000, **2**, 248–251.
- 6 (a) K. H. Van Pée and S. Unversucht, *Chemosphere*, 2003, **52**, 299–312; (b) C. D. Murphy, *J. Appl. Microbiol.*, 2003, **94**, 539–548.
- 7 G. Rothenberg and J. H. Clark, *Org. Process Res. Dev.*, 2000, **4**, 270–274.
- 8 J. S. Yadav, B. V. S. Reddy, P. S. R. Reddy, A. K. Basak and A. V. Narsaiah, *Adv. Synth. Catal.*, 2004, **346**, 77–82.
- 9 J. Salzar and D. Romano, *Synlett*, 2004, **7**, 1318–1320.
- 10 C. Chiappe, E. Leandri and D. Pieraccini, *Chem. Commun.*, 2004, 2536–2537.
- 11 G. Driver and K. E. Johnson, *Green Chem.*, 2003, **5**, 163–169.
- 12 M. J. Earle and S. P. Katdare, *World Pat. WO 02/30852*, 2002.
- 13 M. J. Earle, S. P. Katdare and K. R. Seddon, *Org. Lett.*, 2004, **6**, 707–710.
- 14 (a) K. K. Laali and G. I. Borodkin, *J. Chem. Soc., Perkin Trans. 2*, 2002, 953–957; (b) C. Chiappe and D. Pieraccini, *ARKIVOC*, 2002, 249–255.

Preparation of terminal oxygenates from renewable natural oils by a one-pot metathesis–isomerisation–methoxycarbonylation–transesterification reaction sequence

Yulei Zhu,^{ab} Jim Patel,^a Selma Mujcinovic,^a W. Roy Jackson^{*a} and Andrea J. Robinson^a

Received 3rd April 2006, Accepted 13th June 2006

First published as an Advance Article on the web 7th July 2006

DOI: 10.1039/b604767j

Renewable natural oils can be converted into potentially high value terminal oxygenates by a single-pot, high yielding metathesis–isomerisation–methoxycarbonylation–transesterification reaction sequence.

Introduction

Generation of fine chemicals from natural oils is becoming increasingly important as the price of crude petroleum continues to rise.¹ Reactions of triglycerides can be used to prepare a wide range of useful products such as detergents, lubricants, surface coatings and biofuels.^{2,3} However, the range of potential applications is somewhat limited by the length of the fatty acid chains present in natural oils which are predominantly C₁₂–C₂₄. Recently there has been considerable interest in the use of olefin metathesis chemistry to convert long-chain unsaturated fatty acid esters into shorter chain olefins and unsaturated esters.^{4,5} Towards this end, we have reported a high yielding, highly selective method involving the cross-metathesis of natural oils with 2-butene.^{6,7} In this paper we describe a one-pot metathesis–isomerisation–methoxycarbonylation–transesterification reaction sequence which extends this methodology to the conversion of natural oils into commercially significant terminal oxygenates.

Results and discussion

Cross-metathesis of 2-butene with unsaturated fatty acid esters

Mixtures of unsaturated esters and alkenes were generated from the cross-metathesis of 2-butene with methyl oleate, high oleic sunflower oil, and linseed oil using the procedure described previously by us in this journal.⁷ The unsaturated esters present in these natural products provide esters of 9-undecenoic acid (**1**) and a range of 2-alkenes (**2–5**), as shown in Scheme 1. Thus compounds containing esters of oleic acid give 9-undecenoate (**1**) and 2-undecene (**2**), esters of linoleic acid give (**1**) plus hepta-2,5-diene (**3**) and 2-octene (**4**), and esters of linolenic acid give (**1**) plus two molecules of (**3**) and 2-pentene (**5**). Pure samples of 2-undecene (**2**) and methyl 9-undecenoate (**6**) were obtained by distillation of the products from a butenolysis reaction of high oleic sunflower seed oil.⁷

^aCentre for Green Chemistry, School of Chemistry, P.O. Box 23, Monash University, Victoria 3800, Australia.
E-mail: william.roy.jackson@sci.monash.edu.au; Fax: +61399054597;
Tel: +61399054552

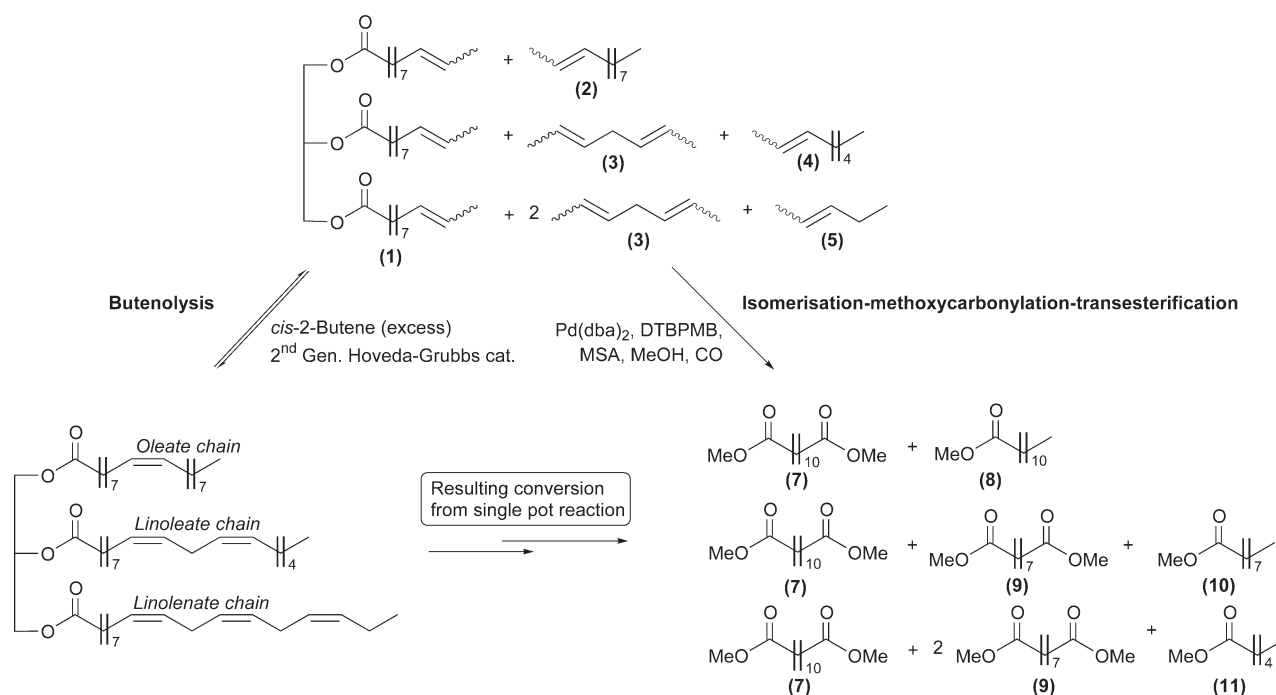
^bState Key Laboratory of Coal Chemistry, Institute of Coal Chemistry, Chinese Academy of Sciences, P.O. Box 165, Taiyuan 030001, Shanxi, P.R. China. Fax: +863514124899; Tel: +863514174341

Isomerisation–methoxycarbonylation

Recent papers by the Cole-Hamilton group have described the application of a highly selective and high yielding palladium catalysed isomerization–methoxycarbonylation sequence to a range of internal alkenes⁸ and unsaturated acids and esters, some of which can be derived from natural oils.⁹ We have applied this reaction to the internal alkenes and unsaturated esters obtained from the butenolysis reactions described above. Isomerisation–methoxycarbonylation reactions of methyl 9-undecenoate (**6**) and 2-undecene (**2**) with the catalyst system of 1,2-bis(di-*tert*-butylphosphinomethyl)benzene (DTBPMB), bis(dibenzylideneacetone)palladium(0), methanesulfonic acid (MSA) and methanol are summarised in Table 1. High yields and selectivity were obtained under the same conditions for both substrates to give dimethyl dodecanedioate (**7**) and methyl dodecanoate (**8**) respectively. The conditions used were analogous to those suggested by the Cole-Hamilton group.^{8,9} The product from the butenolysis of high oleic sunflower seed oil was stripped of volatile alkenes and the remaining triglycerides, containing predominantly 9-undecenoate esters with some saturated fatty acid esters (12%), were used to develop reaction conditions suitable for triglyceride substrates. In order to achieve analogous % conversion with natural oils, it was necessary to operate at higher pressure, a higher catalyst loading and longer reaction times (Table 1). Under these conditions, high selectivity for the terminal ester was achieved with complete ester exchange resulting in conversion to dimethyl esters, principally dimethyl dodecanedioate (**7**). The products were analysed by GC and compared with authentic samples; GC-MS was used in instances where product standards were not available. Complete conversion to the methyl ester derivatives was confirmed by ¹H NMR spectroscopy.

One-pot metathesis–isomerisation–methoxycarbonylation–transesterification reactions

In order to test the potential for vegetable oils to undergo a single pot metathesis–isomerisation–methoxycarbonylation–transesterification reaction sequence a simpler substrate, methyl oleate, was first tested in a simpler metathesis–isomerisation–methoxycarbonylation sequence using the conditions designed for triglycerides. Butenolysis was carried out in an autoclave following the conditions described previously



Scheme 1 The one-pot metathesis–isomerisation–methoxycarbonylation–transesterification reaction sequence for a triglyceride molecule containing oleic, linoleic and linolenic acids.

using second-generation Hoveyda–Grubbs catalyst.⁵ The reaction was terminated by the addition of a small amount of ethyl vinyl ether once high conversion had been achieved, as indicated by the *trans* : *cis* ratio of the 2-undecene (2) approaching the equilibrium value of *ca.* 80 : 20.⁷ The unreacted butene was then evaporated and the autoclave was charged with DTBPMB, bis(dibenzylideneacetone)palladium(0) (Pd(dba)₂), MSA and methanol. The autoclave was then pressurised to 400 psi with carbon monoxide and heated at 80 °C for 20 h. Chromatographic analysis of the product mixture showed very high conversion of 2-undecene (2) to methyl dodecanoate (8) and of methyl 9-undecenoate (6) to dimethyl dodecanedioate (7). Small amounts of dimethyl nonadecanedioate (<4%) derived from the methoxycarbonylation of unreacted methyl oleate, and methyl nonadecanoate (<2%) derived from the methoxycarbonylation of 9-octadecene (a self-metathesis product of methyl oleate), were characterised by GC-MS.

Table 1 Isomerisation–methoxycarbonylation of butenolysis products

Substrate	Conversion (%)	Selectivity for terminal esters (%)
2-Undecene (2) ^a	100	97
Methyl 9-undecenoate (6) ^a	99	97
Triglyceride of 9-undecenoic acid (<i>ca.</i> 88%) and saturated fatty acids (<i>ca.</i> 12%) ^b	99	97

^a 50 psi, 80 °C, 14 h. Molar ratio of C=C in substrate : MSA : DTBPMB : Pd(dba)₂ = 200 : 10 : 5 : 2. ^b 400 psi, 80 °C, 20 h. Molar ratio of C=C in substrate : MSA : DTBPMB : Pd(dba)₂ = 100 : 10 : 5 : 2.

Traces of methyl palmitate and methyl stearate, impurities in the original methyl oleate, were also observed.

Two vegetable oils were chosen for study based on their widely different unsaturated fatty acid composition. High oleic sunflower seed oil contains a high proportion of mono-unsaturated oleic acid esters (81%) together with the dieneic linoleic esters (10%) and saturated esters (9%). In contrast, linseed oil contains a much higher percentage of the polyunsaturated fatty acid esters, linoleic esters (13%) and linolenic esters (53%), with a smaller amount of oleic acid esters (22%) and saturated esters (12%).

Application of the one-pot reaction sequence to high oleic sunflower seed oil gave a product mixture very similar in composition to that obtained from the reaction of methyl oleate, demonstrating high conversion to the two major products (7) and (8) with very high regioselectivity (Table 2). The sunflower seed oil containing 10% of linoleic acid esters could be expected to give similar proportions of the diene (3) and consequently *ca.* 10% of the dimethyl azelate (9). A significantly reduced amount of (9) was initially observed (<5%) and it was later established that without careful fractionation of the product mixture, the heptadiene (3) co-distilled during the removal of the 2-butene.

The co-distillation of 2-butene and heptadiene (3) was found to be a more significant problem when isolating the products of the butenolysis of linseed oil. Accordingly, the total product mixture was methoxycarbonylated *without* the removal of 2-butene. The resultant product mixture accurately reflected the fatty acid composition of the parent oil showing (in order of increasing GC retention time) methyl pentanoate (from unreacted 2-butene), methyl hexanoate (10), methyl nonanoate (11), methyl dodecanoate (8), dimethyl nonanedioate (9),

Table 2 One-pot reactions

Substrate	Butenolysis ^a		Isomerisation–methoxycarbonylation–(transesterification) ^b		
	<i>Trans</i> : <i>cis</i> isomers for 2-undecene		Conversion (%)		Selectivity for terminal esters (%)
			(2) to (8)	(1) to (7)	Methyl dodecanoate
Methyl oleate	80 : 20	99	99	96	95
Sunflower seed oil	81 : 19	98	98	97	97
Linseed oil ^c	79 : 21	98	99	96	96
Linseed oil ^d	81 : 19	99	99	95	95

^a Molar ratio of C=C in substrate : *cis*-2-butene : second-generation Hoveyda–Grubbs catalyst = 1 : 10 : 0.0001. ^b Molar ratio of C=C in butenolysis product : MSA : DTBPMB : Pd(dba)₂ = 100 : 10 : 5 : 2. ^c 2-Butene removed before methoxycarbonylation. ^d 2-Butene retained for methoxycarbonylation.

dimethyl dodecandioate (7), methyl palmitate and methyl stearate. Quantification using the Ackman method¹⁰ indicated molar ratios of (11, 5%), (10, 21%), (8, 11%), (9, 21%) and (7, 36%). The ratio of unsaturated acids in the linseed oil would predict a distribution of (11, 4%), (10, 17%), (8, 7%), (9, 39%) and (7, 29%) respectively. The product distribution obtained was found to be similar to that predicted although the amount of the diester (9) was somewhat lower than expected. The saturated palmitate and stearate esters represented ca. 5% of the esters in agreement with the linseed oil composition (4% expected).

Conclusion

In conclusion this paper describes the conversion of natural oils into terminal oxygenates by a butenolysis–isomerization–methoxycarbonylation–transesterification reaction sequence. The method is complimentary to direct ozonolysis of these materials.³ In contrast to ozonolysis, however, the method described offers the potential to fractionate the olefinic products at the intermediate stage to facilitate selective methoxycarbonylation and economical production of target esters.

Experimental

General

All reactions and manipulations of organometallic compounds were carried out under an argon atmosphere using Schlenk techniques. Solvents were purified and dried according to standard procedures and stored under an argon atmosphere. Methyl 9-undecenoate and 2-undecene were prepared as described previously,⁷ degassed by 3 freeze–pump–thaw cycles and stored under argon. Commercial samples of triolein and vegetable oils were degassed and passed through a short plug of activated alumina under argon immediately prior to use. Similarly, liquid *cis*-2-butene was passed through a short alumina plug at –5 °C under argon. The second-generation Hoveyda–Grubbs catalyst was prepared according to a literature procedure.¹¹ All other reagents were purchased and used without further purification. GC analyses were performed on a Varian Model 3700 gas chromatograph equipped with a 30 m × 0.53 mm 30QC51-BPX5 column (1 μm film thickness, He at 4 × 10² kPa). GC-MS analyses were performed using a Hewlett Packard gas chromatograph equipped with an Agilent MSD and a 30 m × 0.25 mm HP5S column (0.25 μm film thickness) using He as a carrier gas. NMR spectra were

recorded with a Bruker 400 MHz spectrometer (¹H NMR, 400.130 MHz).

Standard procedure for methoxycarbonylation reactions

A stainless steel autoclave equipped with a glass-liner and stirrer bar was placed under an argon atmosphere and charged with an alkene (or mixture of alkenes), 1,2-bis(di-*tert*-butylphosphinomethyl)benzene, bis(dibenzylideneacetone) palladium(0), methanesulfonic acid and methanol. The autoclave was then charged to the desired pressure with carbon monoxide then sealed and heated at 80 °C with stirring for the desired time. After this time the autoclave was cooled to ambient temperature and then the pressure slowly released. The product mixture was analysed by GC and GC-MS and in the case of triglycerides by ¹H NMR spectroscopy.

One-pot butenolysis–isomerisation–methoxycarbonylation reactions

A stainless steel autoclave equipped with a glass-liner and stirrer bar was placed under an argon atmosphere and cooled to –5 °C in a low-temperature methanol bath. The autoclave was charged with a vegetable oil or methyl oleate (equivalent to 3.39 mmol of C=C bonds) and *cis*-2-butene (1.90 g, 33.9 mmol) and stirring was started. The reaction was initiated by the addition of a freshly prepared solution of second-generation Hoveyda–Grubbs catalyst (0.21 mg, 0.33 μmol) in dichloromethane (20 μL) and the autoclave was sealed. The reaction mixture was monitored by removal of 50 μL samples using a pre-cooled gas-tight syringe. Each sample was quenched by addition to a solution of ethyl vinyl ether (100 μL) in dichloromethane (1 mL). The reaction mixture was analysed by GC and the conversion was estimated from the ratio of the *trans* : *cis* isomers for the 2-undecene.⁷ A *trans* : *cis* ratio of ~80 : 20 was considered to indicate maximum conversion. Once maximum conversion was achieved (1 h) the reaction was quenched with ethyl vinyl ether (10 μL) and the autoclave was either warmed to room temperature to remove the butene or kept at –5 °C to retain the 2-butene. The autoclave was then charged with 1,2-bis(di-*tert*-butylphosphinomethyl)benzene, bis(dibenzylideneacetone)palladium(0), methanesulfonic acid, and methanol (10 mL). The autoclave was pressurised to 400 psi with carbon monoxide, sealed and heated at 80 °C with stirring for 20 h. After this time the autoclave was cooled to ambient temperature and then the

pressure slowly released. The product mixture was analysed by GC, GC-MS and ^1H NMR spectroscopy.

Acknowledgements

We thank Orica Pty Ltd for provision of funds through their Strategic Research Initiative, and Johnson Matthey for a loan of precious metals.

References

- 1 J. F. Jenck, F. Agterberg and M. J. Droscher, *Green Chem.*, 2004, **6**, 544.
- 2 *Oleochemical Manufacture and Applications*, ed. F. D. Gunstone and R. J. Hamilton, Sheffield Academic Press, 2001.
- 3 U. Biermann, W. Friedt, S. Lang, W. Lühs, G. Machmüller, J. O. Metzger, M. Rüschen, Klaas, H. J. Schäfer and M. Schneider, *Angew. Chem., Int. Ed.*, 2000, **39**, 2206.
- 4 J. C. Mol, *Green Chem.*, 2002, **4**, 5.
- 5 K. A. Burdett, L. D. Harris, P. Margl, B. R. Maughon, T. Mokhtar-Zadeh, P. C. Saucier and E. P. Wasserman, *Organometallics*, 2004, **23**, 2027.
- 6 J. Patel, J. Elaridi, W. R. Jackson, A. J. Robinson, A. K. Serelis and C. Such, *Chem. Commun.*, 2005, 44, 5546.
- 7 J. Patel, S. Mujcinovic, W. R. Jackson, A. J. Robinson, A. K. Serelis and C. Such, *Green Chem.*, 2006, **8**, 450.
- 8 C. J. Rodriguez, D. F. Foster, G. R. Eastman and D. J. Cole-Hamilton, *Chem. Commun.*, 2004, 15, 1720.
- 9 C. Jiménez-Rodríguez, G. R. Eastman and D. J. Cole-Hamilton, *Inorg. Chem. Commun.*, 2005, **8**, 878.
- 10 R. G. Ackman, *J. Gas Chromatogr.*, 1964, **2**, 173.
- 11 S. B. Garber, J. S. Kingsbury, B. L. Gray and A. H. Hoveyda, *J. Am. Chem. Soc.*, 2000, **122**, 8168.

Chemical Technology

A well-received news supplement showcasing the latest developments in applied and technological aspects of the chemical sciences



Free online and in print issues of selected RSC journals!*

- **Application Highlights** – newsworthy articles and significant technological advances
- **Essential Elements** – latest developments from RSC publications
- **Free access** to the original research paper from every online article

*A separately issued print subscription is also available

RSC Publishing

www.rsc.org/chemicaltechnology

0300020



Journal of Environmental Monitoring

Comprehensive, high quality coverage of multidisciplinary, international research relating to the measurement, pathways, impact and management of contaminants in all environments.

- Dedicated to the analytical measurement of environmental pollution
- Assessing exposure and associated health risks
- Fast times to publication
- Impact factor: 1.578
- High visibility - cited in MEDLINE



Environmental Science Books

Issues in Environmental Science & Technology

Series Editors:

R E Hester and R M Harrison

Format: **Hardback**

Price: **£45.00**

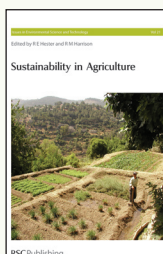
RSC Member Price: **£29.25**

Written by leading experts, this series presents a multidisciplinary approach to pollution and the environment. Focussing on the science and broader issues including economic, legal and political considerations.

Sustainability in Agriculture Vol. No. 21

Discusses the key factors impacting on global agricultural practices including fair trade, the use of pesticides, GM products and government policy.

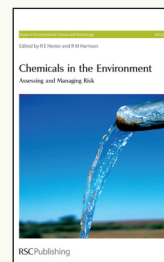
2005 | xiv+130 pages | ISBN-10: 0 85404 201 6
ISBN-13: 978 0 85404 201 2



Chemicals in the Environment Assessing and Managing Risk Vol. No. 22

Beginning with a review of the current legislation, the book goes on to discuss scientific and technical issues relating to chemicals in the environment and future developments.

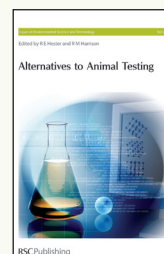
2006 | xvi+158 pages | ISBN-10: 0 85404 206 7
ISBN-13: 978 0 85404 206 7



Alternatives to Animal Testing Vol. No. 23

Provides an up-to-date discussion on the development of alternatives to animal testing including; international validation, safety evaluation, alternative tests and the regulatory framework.

2006 | xii+118 pages | ISBN-10: 0 85404 211 3
ISBN-13: 978 0 85404 211 1



Practical Environmental Analysis 2nd Edition

By *M Radojevic and V N Bashkin*

A new edition textbook providing an up-to-date guide to practical environmental analysis. Ideal for students and technicians as well as lecturers wishing to teach the subject.

Hardback | 2006 | xxiv+458 pages | £39.95 | RSC member price
£25.75 | ISBN-10: 0 85404 679 8 | ISBN-13: 978 0 85404 679 9



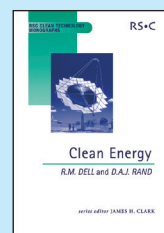
Clean Energy (RSC Clean Technology Monographs)

By *R M Dell and D A J Rand*

Series Editor *J H Clark*

Covering a broad spectrum of energy problems, this highly accessible book discusses in detail strategies for the world's future energy supply.

Hardback | 2004 | xxxvi+322 pages | £89.95 | RSC Member Price
£58.25 | ISBN-10: 0 85404 546 5 | ISBN-13: 978 0 85404 546 4



An Introduction to Pollution Science

By *R M Harrison*

A student textbook looking at pollution and its impact on human health and the environment. Covering a wide range of topics including pollution in the atmosphere, water and soil, and strategies for pollution management.

Hardback | 2006 | ca xii+322 pages | £24.95 | RSC Member Price
£16.50 | ISBN-10: 0 85404 829 4 | ISBN-13: 978 0 85404 829 8

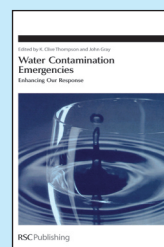


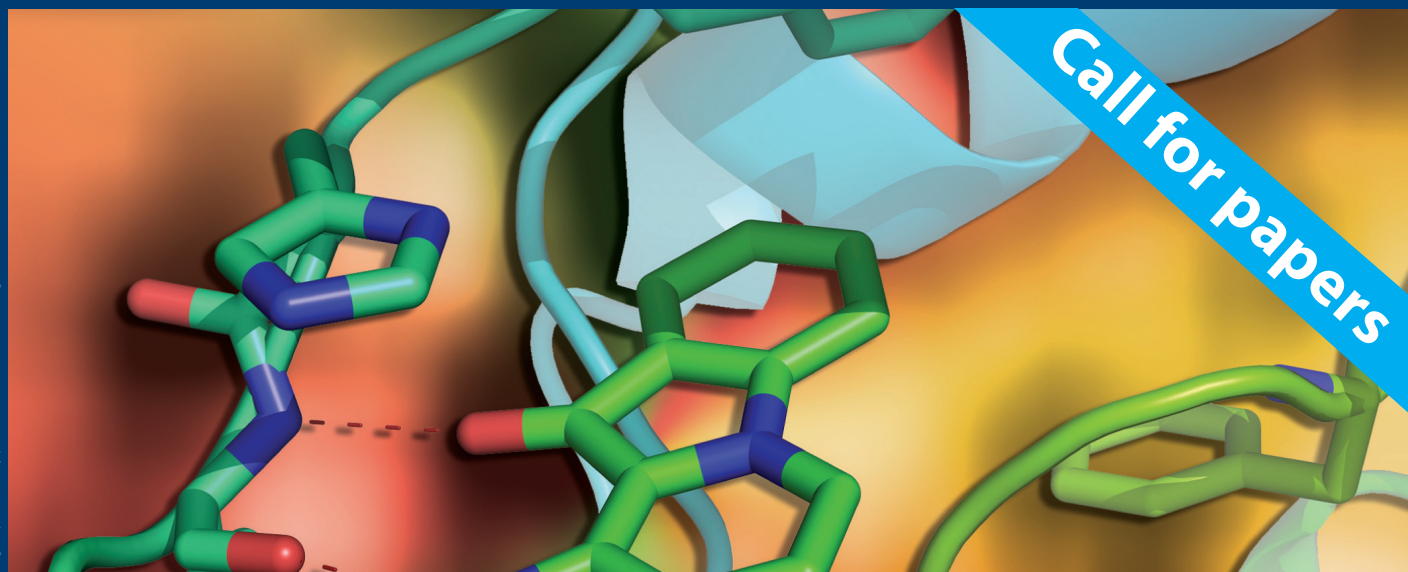
Water Contamination Emergencies Enhancing Our Response

By *J Gray and K C Thompson*

A look at the impact and response of contaminated water supplies including the threat of chemical, biological, radiological and nuclear (CBRN) events.

Hardback | 2006 | x+372 pages | £99.95 | RSC Member Price
£64.75 | ISBN-10: 0 85404 658 5 | ISBN-13: 978 0 85404 658 4





Organic & Biomolecular Chemistry

A major peer-reviewed international, high quality journal covering the full breadth of synthetic, physical and biomolecular organic chemistry.

Publish your review, article, or communication in OBC and benefit from:

- The fastest times to publication (as little as 14 days for communications and 30 days from receipt for papers)
- High visibility (OBC is indexed in MEDLINE)
- Impact factor 2.547
- Free colour (where scientifically justified)
- Electronic submission and manuscript tracking via ReSource (www.rsc.org/ReSource)
- A first class professional service
- No page charges



Submit today!

RSC Publishing

www.rsc.org/obc